Targeting the Cause, affecting the Course

de Raaf, M.A.

2016

document version
Publisher's PDF, also known as Version of record

Pulmonary Arterial Hypertension is a progressive and devastating disease characterized by dysfunction and remodeling of the pulmonary vasculature, leading to increased pulmonary vascular resistance, compensatory right ventricular remodeling and eventually dilatation and heart failure. To find an effective treatment for Pulmonary Arterial Hypertension, animal models are used to simulate the disease.
In this thesis, Michiel Alexander de Raaf and colleagues describe and characterize the disease progression of such animal model; the Sugen Hypoxia model. Several treatments were tested and evaluated on their efficacy. As both lungs and heart use mutual pathways for disease progression as well as for compensatory remodeling against the disease, the treatment paradox 'what might be beneficial for the lungs, could harm the right ventricle' was evaluated.

Targeting the cause affecting the course
Characterization and Optimization of Experimental Models for Pulmonary Arterial Hypertension
M.A. De Raaf

Targeting the cause affecting the course

Characterization and Optimization of Experimental Models for Pulmonary Arterial Hypertension

Michiel Alexander de Raaf

Targeting the cause affecting the course

Characterization and Optimization of Experimental Models for Pulmonary Arterial Hypertension

"The real voyage of discovery is not in seeking new landscapes,
but in having new eyes."
M. Proust 1871-1922

cover design 'the landscape': modified from microscopy photo
of an advanced Sugen Hypoxia lung

ISBN: 978-94-6233-267-6
Awesome cover and thesis design: Pascal Vleugels
Printed by: Gildeprint

VRIJE UNIVERSITEIT

TARGETING THE CAUSE, AFFECTING THE COURSE
Characterization and Optimization of Experimental Models for Pulmonary Arterial Hypertension

ACADEMISCH PROEFSCHRIFT

ter verkrijging van de graad Doctor aan
de Vrije Universiteit Amsterdam,
op gezag van de rector magnificus
prof.dr. V. Subramaniam,
in het openbaar te verdedigen
ten overstaan van de promotiecommissie
van de Faculteit der Geneeskunde
op dinsdag 24 mei 2016 om 9.45 uur
in de aula van de universiteit,
De Boelelaan 1105

door

Michiel Alexander de Raaf

geboren te Breda

promotor : prof.dr. A. Vonk Noordegraaf
copromotor : dr. H.J. Bogaard

Cordially dedicated to
Paola Ballario
la mamma scientifica

Overige leden Promotiecommissie:

prof.dr. R. Berger
prof.dr. N.F. Voelkel
prof.dr. W. Mooi
dr. J. Aman
dr. M. Kool
dr. D. Merkus

Financial funding:
Grant support was received from PAH patient association "Live Life Max"
the Dutch Lung Foundation (Longfonds #3.3.12.036),
European Respiratory Society Long Term FellowShip grant 2015
Contract research with Boehringer Ingelheim GmbH
We acknowledge cordially "Stichting PHA Nederland" for their financial support to print this thesis. Please visit http://www.pha-nl.nl/ for their dedicated work to Dutch P(A)H patients.

We acknowledge "DataSciences International" for their financial support to print this thesis.

We acknowledge Mieke van Schaik-Verlee and the late Cor van Schaik for their financial support to print this thesis.

The research conducted was performed at:
VU University & VU University medical center, Amsterdam, The Netherlands
Radboud University medical center, Nijmegen, The Netherlands
University Medical Center, Groningen, The Netherlands
Virginia Commonwealth University, Richmond, Virginia, USA
INSERM UMR_S999, Centre Chirugical Marie Lannelongue, Le Plessis-Robinson/Paris, France

"We choose to go to the moon. We choose to go to the moon in this decade and do the other things, not because they are easy, but because they are hard, because that goal will serve to organize and measure the best of our energies and skills, because that challenge is one that we are willing to accept, one we are unwilling to postpone, and one which we intend to win, and the others, too."

John F. Kennedy, September 12, 1962,
Rice University, Houston, TX, USA.

Table of contents

Chapter 1:
Advances in understanding of pulmonary arterial hypertension and the evolution of experimental pulmonary hypertension models.

Michiel Alexander de Raaf[1,2], Norbert F. Voelkel[3], Harm Jan Bogaard[1,2]

Parts of this chapter were published as: PVRI Chronicle 2015; vol2, issue 2, p55-61

Affiliation:
Departments of [1]Pulmonology and [2]Physiology, VU University Medical Center / Institute for Cardiovascular Research, Amsterdam, The Netherlands. [3]Pulmonary and Critical Care Medicine Division, Virginia Commonwealth University, Richmond, Virginia, USA.

"Primary Pulmonary Hypertension has been called the cardiologist's cancer"

Greg Elliott in personal conversation with Norbert Voelkel, early 80's

Pulmonary Arterial Hypertension (PAH) can be a rapidly progressive and devastating disease characterized by dysfunction and remodeling of the pulmonary vasculature, leading to increased pulmonary vascular resistance. The increased vascular resistance pushes the right ventricle (RV) into adaptive compensatory remodeling by hypertrophy, but eventually RV dilatation, heart failure and death of the patient become inevitable [1, 2]. Today, 3 pathways are targeted in PAH treatment: the nitric oxide-cyclic guanosine monophosphate pathway, the endothelin pathway and the prostacyclin pathway [3]. Although treatments affecting these pathways delay disease progression and increase survival rates [3, 4], they do not cure PAH [3]. The pathogenic paradigm of PAH has shifted from pulmonary vasoconstriction driven by smooth muscle cells to vascular remodeling affecting all vessel wall layers. In this chapter, a brief overview will be given of how PAH research has converged on the role of the endothelial cell (EC). Due to the appreciation of the central role of the EC in both pathogenesis and pathobiology, animal models, like the Sugen hypoxia (SuHx) rat model, resembling EC vascular remodeling were developed. However, the SuHx rat model was not characterized and formed the basis for this thesis. In respect to the intima remodeling observed in the SuHx model, several treatments targeting endothelial proliferation were tested in the model.

The first WHO classification of Pulmonary Hypertension took place in 1972, following on the first attempts of morphologic characterizations of the pulmonary hypertensive lung, for example by Wagenvoort et al. [5, 6], followed by the first WHO classification of Pulmonary Hypertension in 1972. In this classification, the pathological focus in PAH, then called Primary Pulmonary Hypertension, was on the vascular media of the pulmonary arterioles, featuring hypertrophied and hyperplastic pulmonary artery smooth muscle cells (PASMC) [1, 2, 7]. The "vascular media paradigm" of PAH ascribed a major pathogenic role to sustained pulmonary vasoconstriction and was fueled by two PAH outbreaks related to the use of the appetite suppressants Aminorex (Menocil®) and fenfluramine (Ponderal®) in the late 60's and 80's. Both drugs are serotonin transporter substrates acting on the PASMC and promote vasoconstriction and PASMC hypertrophy and proliferation. At that time, the signature plexiform lesion was regarded as an epiphenomenon. Attempts to understand these lesions better and to correlate these with for example blood flow were made at that time, but the lack of scientific methodology and gaps in knowledge on endothelial biology hampered progress in this direction.

The description of idiopathic PAH as 'the cardiologist's cancer' in the early 80's meant at that time that PAH and cancer shared a common clinical and scientific context. Both conditions were untreatable due to a profound lack of understanding and absence of technologies to study pathogenesis and pathobiology. As dedicated research did not lead to a medical cure for PAH, the idea that other vascular wall cells than smooth muscle cells were also involved in the disease was gradually accepted. For a better understanding of PAH, it was necessary to study the cellular and molecular aspects of the disease. An expanding research effort revealed the mechanisms by which PAH is characterized today: endothelial dysfunction, PASMC hypertrophy and hyperplasia, persistent inflammation and dysimmunity and dysregulated intra- and extracellular cell signaling in the cells of all layers of the pulmonary vessel bed, leading to pulmonary vessel remodeling [8–10]. Endothelial dysfunction is reflected in increased activity of contractive vasoactive agents as endothelin-1, serotonin, angiotensin II and decreased activity of dilative vasoactive agents as nitric oxide and prostacyclin, shifting the balance to persistent vasoconstriction. The hyperproliferative endothelium in PAH disobeys the "law-of-the-monolayer" and has a monoclonal origin in plexiform lesions [11–13]. This hyperproliferation is mediated by increased activity of growth factors as fibroblast growth factor-2, platelet derived

growth factor and epidermal growth factor and is accompanied by apoptopic resistance [14–17]. Also in the PASMC the increased activity of growth factors and apoptosis resistance are observed. As in the EC, hyperproliferation of PASMC is connected to deregulated BMPRII signaling, for example due to the germline BMPRII-mutation, which has a penetrance of approximately 75% in hereditary familial PAH [10, 14, 15] and is also present in other forms of PAH. Another germline mutation in PAH is found in the KNCK3 gene, which decreases the activity of TWIK-related acid-sensitive K+ channel-1 [15]. KNCK3 mutations and alterations in other ion channels (the voltage-gated K+ channel, transient receptor potential 1 and 6 and calcium sensing receptor) contribute to the hyperpolarization, contraction and proliferation of the PASMC [9, 18, 19]. Moreover, the PASMC in PAH goes through an energetic shift to glycolysis [20], also found in fibroblasts of the pulmonary vascular adventitia [21], which is also referred to as the Warburg effect. These, and other, dysregulated mechanisms contribute to the abnormal cell signaling leading to disordered angiogenesis [16, 17, 23]. These mechanisms in the pulmonary vasculature perhaps recruit inflammatory cells which can release cytokines and chemokines as for example interleukin 1 and 6 [11, 15, 24–26]. It is now recognized that all layers of the vessel wall contribute to pulmonary vascular remodeling in PAH; including the hyperproliferative endothelium, and the plexiform lesion is no longer neglected as a hallmark of PAH [27, 28]. Many of the observations made during the study of pulmonary vascular remodeling in PAH, echoed the description of the hallmarks of cancer as described by Hanahan and Weinberg [28–31]. This expansion in knowledge gave rise to the exploration of potential treatment targets, which were already studied for their efficacy in cancer, such as Histone DeACetylase inhibitors (HDACis) and Tyrosine Kinase Inhibitors (TKIs) [32].

Experimental models to resemble pulmonary arterial hypertension.

Translational research on the development of pulmonary hypertension and potential treatments of the disease has relied on animal models that replicate one or more important aspects of the disease [33–36]. Reeves and Grover were the first to use hypoxia induced pulmonary hypertension as a model of the human condition when they studied Brisket disease in cattle kept at high altitude [37, 38]. Exposure to hypoxia was soon also used to study pulmonary hypertension in rats. In addition, an animal model based on the administration of monocrotaline

was first used in 1967 [39, 40]. The monocrotaline and chronic hypoxia animal models of pulmonary hypertension both exhibit profound remodeling of the vascular media and hypertrophy of PASMC. Because these phenomena were considered singularly important in human pulmonary hypertension, and scientific methodology was lacking to create endothelial focussed animal models, there was no progress to develop alternative animal models.

The expansion in pathobiological knowledge of PAH has coincided with the establishment of new animal models of the disease. When in 2001 the Sugen Hypoxia model (SuHx) of PAH was discovered [41], the striking resemblance was appreciated between the pathological changes in the SuHx rat and the human PAH lung. More specifically, it was noted that the intima remodeling and obliterative vascular remodeling that is typical of human PAH, was mimicked by the lung vascular changes found in the SuHx rat [35, 41, 42]. The SuHx model also brought the understanding that the emergence of a proliferative endothelium could require an initial phase of endothelial apoptosis, as it could be prevented by a broad spectrum caspase inhibitor [41, 43].

Despite increasing popularity, the SuHx model has not (yet) become a 'gold standard' for animal research in PAH. In comparison to the classic animal models, the SuHx model is more complex, has not been thoroughly characterized and is more difficult to implement and harmonize among laboratories. In addition, a vast amount of translational studies has been performed with the chronic hypoxia and monocrotaline models and this body of work is a heritage of historical literature to which new data is conveniently compared. Therefore, many translational studies are still performed using the traditional animal models. Remarkably, many potential treatments adopted from the cancer field, are still explored in the classic animal models that do not represent the pathobiology of angio-obliterative PAH nor offer a hyperproliferative endothelium as a treatment target. This might explain why therapeutic interventions seem curative in animal studies whereas human PAH remains refractory to treatment [44, 45].

Conclusion

Due to the ineffectiveness of vasodilating drugs and aided by many cellular and molecular findings, the pathogenic paradigm of PAH has shifted from vasoconstriction towards vessel remodeling with resemblances to malignancy. Concurrently, novel animal models have evolved, which feature the human hallmark of PAH, a hyperproliferative endothelium, that is not found in more traditional animal models. Therefore, when these traditional animal models are used to assess anti-proliferative drug targets of the endothelium, they become unpredictable in their translational value. Of course, due to the unknown pathogenesis of PAH, it is paradoxically true that no animal model can resemble PAH completely. However, with the increasing realization and evaluation of the different pathobiologies resembled by animal models [33–35], the selection of the used animal model should be explicitly motivated.

The thesis part I: Characterization

The need for characterization and harmonization of the SuHx rat model formed the basis for this thesis and this work is reported in **Chapter 2** [42]. The main finding of the characterization study described in this chapter is that media changes, consisting of hypertrophic and/or hyperplastic PASMCs, may play a minor role in late disease progression in the SuHx model [42]. This is in accordance to the morphologic characterization of lungs from end-stage PAH patients performed by Stacher et al., who showed that vascular remodeling in end-stage PAH consists mostly of intima thickening, not medial remodeling [46]. Minor changes in the media in advanced PAH may explain why current treatments acting on PASMCs are unable to cure PAH. At the same time, it is well known that the onset of PAH may be triggered by changes in the media. For example, PAH can develop after the use of appetite suppressing drugs, which are serotonin transporter inhibitors, acting on the PASMC. We tested the hypothesis that an intact serotonin pathway is not only sufficient, but also required for the development of intima remodeling in **Chapter 3**. By exposing a knock-out rat with an impaired serotonin pathway to the SuHx intervention, we showed that an intact serotonin pathway is not required for the development of severe angio-obliterative experimental PH.

Several animal models are available to induce angioobliterative lesions. In addition to the SuHx model, models are available based on the combined exposure to increased blood flow and monocrotaline (for example monocrotaline plus aortic-caval shunt and monocrotaline plus pneumonectomy) [47, 48]. Moreover, rats also develop such lesions after their combined exposure to ovalbumin and sugen [49]. To test the hypothesis that hypoxic media remodeling is not required to generate angio-obliterive PH, we combined Sugen administration with pneumonectomy to induce pulmonary hypertension. In **Chapter 4** we report that using this intervention, severe pulmonary hypertension with similar angio-obliterative lesions develops, again without a major contribution of changes in the medial wall.

The thesis part II: Treatments

Similar signaling pathways are involved in the functional and structural changes in the right ventricle and lungs in PAH [50]. Medication hampering remodeling in the pulmonary vasculature may at the same time worsen right ventricular adaptation [51–55]. As cardiac function is the most prognostic parameter

in human PAH [4, 56], meticulous care should be given in PAH to improve, or at least conserve, cardiac function. We evaluated the potential cardiotoxicity as well beneficial treatment effects in the pulmonary vasculature of different treatments. In **Chapter 5** we evaluated the treatment outcome of Histone Deacetylase Inhibitors (HDACis) in experimental PH [50] and tested the treatment of trichostatin A (TSA), a HDACi, in the SuHx model, which appeared to be not effective. The tyrosine Kinase Inhibitor (TKI) BIBF1000 was evaluated for potential cardiotoxicity in the isolated cardiac pressure-overload pulmonary artery banding PAB model and for the potential treatment response in the pulmonary vasculature in the SuHx model in **Chapter 6**. BIBF1000 showed mild beneficial treatment effects in both lungs as heart. To improve the observed therapeutic effect, the study was repeated with the related TKI Nintedanib, which has an increased specificity and sensitivity in comparison to BIBF1000. In **Chapter 7**, we evaluated the treatment potential of nintedanib, and showed again a mild therapeutic effect, and functional cardiac improvement. In **Chapter 8**, the use of Endothelin-1 Receptor Antagonists (ERA's) was reviewed. ERA's hamper pathological remodeling of the pulmonary vasculature and as such exert beneficial effects in PAH. However, they also disturb fetal development of cardiopulmonary tissues, which may affect RV adaptation to the increased pulmonary vascular resistance. Finally, in **Chapter 9**, the collected results and conclusions of the studies described in this thesis are discussed.

References

1. Simonneau G, Robbins IM, Beghetti M, Channick RN, Delcroix M, Denton CP, Elliott CG, Gaine SP, Gladwin MT, Jing Z-C, Krowka MJ, Langleben D, Nakanishi N, Souza R. Updated clinical classification of pulmonary hypertension. *J. Am. Coll. Cardiol.* 2009; 54: S43–S54.
2. Simonneau G, Gatzoulis MA, Adatia I, Celermajer D, Denton C, Ghofrani A, Gomez Sanchez MA, Krishna Kumar R, Landzberg M, Machado RF, Olschewski H, Robbins IM, Souza R. Updated clinical classification of pulmonary hypertension. *J. Am. Coll. Cardiol.* 2013; 62: D34–D41.
3. Humbert M, Sitbon O, Simonneau G. Treatment of pulmonary arterial hypertension. *N. Engl. J. Med.* 2004; 351: 1425–1436.
4. D'Alonzo GE, Barst RJ, Ayres SM, Bergofsky EH, Brundage BH, Detre KM, Fishman AP, Goldring RM, Groves BM, Kernis JT, others. Survival in patients with primary pulmonary hypertension. *Ann. Intern. Med.* 1991; 115: 343–349.

5. Wagenvoort CA, Wagenvoort N. Primary Pulmonary Hypertension A Pathologic Study of the Lung Vessels in 156 Clinically Diagnosed Cases. *Circulation* 1970; 42: 1163–1184.
6. Wagenvoort CA. Vasoconstrictive primary pulmonary hypertension and pulmonary veno-occlusive disease. *Cardiovasc. Clin.* 1972; 4: 97–113.
7. Simonneau G, Galiè N, Rubin LJ, Langleben D, Seeger W, Domenighetti G, Gibbs S, Lebrec D, Speich R, Beghetti M, Rich S, Fishman A. Clinical classification of pulmonary hypertension. *J. Am. Coll. Cardiol.* 2004; 43: 5S – 12S.
8. Guignabert C, Tu L, Girerd B, Ricard N, Huertas A, Montani D, Humbert M. New molecular targets of pulmonary vascular remodeling in pulmonary arterial hypertension: importance of endothelial communication. *Chest* 2015; 147: 529–537.
9. Rabinovitch M. Molecular pathogenesis of pulmonary arterial hypertension. *J. Clin. Invest.* 2012; 122: 4306–4313.
10. Voelkel NF, Gomez-Arroyo J, Abbate A, Bogaard HJ, Nicolls MR. Pathobiology of pulmonary arterial hypertension and right ventricular failure. *Eur. Respir. J.* 2012; 40: 1555–1565.
11. Tuder RM, Groves B, Badesch DB, Voelkel NF. Exuberant endothelial cell growth and elements of inflammation are present in plexiform lesions of pulmonary hypertension. *Am. J. Pathol.* 1994; 144: 275.
12. Voelkel NF, Cool C, Lee SD, Wright L, Geraci MW, Tuder RM. Primary pulmonary hypertension between inflammation and cancer. *Chest* 1998; 114: 225S – 230S.
13. Lee SD, Shroyer KR, Markham NE, Cool CD, Voelkel NF, Tuder RM. Monoclonal endothelial cell proliferation is present in primary but not secondary pulmonary hypertension. *J. Clin. Invest.* 1998; 101: 927–934.
14. Deng Z, Morse JH, Slager SL, Cuervo N, Moore KJ, Venetos G, Kalachikov S, Cayanis E, Fischer SG, Barst RJ, Hodge SE, Knowles JA. Familial primary pulmonary hypertension (gene PPH1) is caused by mutations in the bone morphogenetic protein receptor-II gene. *Am. J. Hum. Genet.* 2000; 67: 737–744.
15. Guignabert C, Tu L, Girerd B, Ricard N, Huertas A, Montani D, Humbert M. New molecular targets of pulmonary vascular remodeling in pulmonary arterial hypertension: importance of endothelial communication. *Chest* 2015; 147: 529–537.
16. Tu L, Dewachter L, Gore B, Fadel E, Dartevelle P, Simonneau G, Humbert M, Eddahibi S, Guignabert C. Autocrine fibroblast growth factor-2 signaling contributes to altered endothelial phenotype in pulmonary hypertension.

Am. J. Respir. Cell Mol. Biol. 2011; 45: 311–322.
17. Schermuly RT. Reversal of experimental pulmonary hypertension by PDGF inhibition. *J. Clin. Invest.* 2005; 115: 2811–2821.
18. Bonnet S, Michelakis ED, Porter CJ, Andrade-Navarro MA, Thébaud B, Bonnet S, Haromy A, Harry G, Moudgil R, McMurtry MS, Weir EK, Archer SL. An abnormal mitochondrial-hypoxia inducible factor-1alpha-Kv channel pathway disrupts oxygen sensing and triggers pulmonary arterial hypertension in fawn hooded rats: similarities to human pulmonary arterial hypertension. *Circulation* 2006; 113: 2630–2641.
19. Michelakis ED, McMurtry MS, Wu X-C, Dyck JRB, Moudgil R, Hopkins TA, Lopaschuk GD, Puttagunta L, Waite R, Archer SL. Dichloroacetate, a metabolic modulator, prevents and reverses chronic hypoxic pulmonary hypertension in rats: role of increased expression and activity of voltage-gated potassium channels. *Circulation* 2002; 105: 244–250.
20. Xu W, Koeck T, Lara AR, Neumann D, DiFilippo FP, Koo M, Janocha AJ, Masri FA, Arroliga AC, Jennings C, Dweik RA, Tuder RM, Stuehr DJ, Erzurum SC. Alterations of cellular bioenergetics in pulmonary artery endothelial cells. *Proc. Natl. Acad. Sci. U. S. A.* 2007; 104: 1342–1347.
21. Stenmark KR, Tuder RM, El Kasmi KC. Metabolic Reprogramming and Inflammation Act in Concert to Control Vascular Remodeling in Hypoxic Pulmonary Hypertension. *J. Appl. Physiol. Bethesda Md 1985* 2015; : jap.00283.2015.
22. Jones PL, Cowan KN, Rabinovitch M. Tenascin-C, proliferation and subendothelial fibronectin in progressive pulmonary vascular disease. *Am. J. Pathol.* 1997; 150: 1349–1360.
23. Tuder RM, Chacon M, Alger L, Wang J, Taraseviciene-Stewart L, Kasahara Y, Cool CD, Bishop AE, Geraci M, Semenza GL, Yacoub M, Polak JM, Voelkel NF. Expression of angiogenesis-related molecules in plexiform lesions in severe pulmonary hypertension: evidence for a process of disordered angiogenesis. *J. Pathol.* 2001; 195: 367–374.
24. Huertas A, Perros F, Tu L, Cohen-Kaminsky S, Montani D, Dorfmüller P, Guignabert C, Humbert M. Immune dysregulation and endothelial dysfunction in pulmonary arterial hypertension: a complex interplay. *Circulation* 2014; 129: 1332–1340.
25. Molossi S, Clausell N, Rabinovitch M. Reciprocal induction of tumor necrosis factor-alpha and interleukin-1 beta activity mediates fibronectin synthesis in coronary artery smooth muscle cells. *J. Cell. Physiol.* 1995; 163: 19–29.

26. Steiner MK, Syrkina OL, Kolliputi N, Mark EJ, Hales CA, Waxman AB. Interleukin-6 overexpression induces pulmonary hypertension. *Circ. Res.* 2009; 104: 236–244, 28p following 244.
27. Adnot S, Eddahibi S. Lessons from oncology to understand and treat pulmonary hypertension. *Int. J. Clin. Pract. Suppl.* 2007; : 19–25.
28. Guignabert C, Tu L, Le Hiress M, Ricard N, Sattler C, Seferian A, Huertas A, Humbert M, Montani D. Pathogenesis of pulmonary arterial hypertension: lessons from cancer. *Eur. Respir. Rev. Off. J. Eur. Respir. Soc.* 2013; 22: 543–551.
29. Hanahan D, Weinberg RA. The hallmarks of cancer. *Cell* 2000; 100: 57–70.
30. Hanahan D, Weinberg RA. Hallmarks of cancer: the next generation. *Cell* 2011; 144: 646–674.
31. Rai PR, Cool CD, King JAC, Stevens T, Burns N, Winn RA, Kasper M, Voelkel NF. The cancer paradigm of severe pulmonary arterial hypertension. *Am. J. Respir. Crit. Care Med.* 2008; 178: 558–564.
32. Stenmark KR, Rabinovitch M. Emerging therapies for the treatment of pulmonary hypertension. *Pediatr. Crit. Care Med. J. Soc. Crit. Care Med. World Fed. Pediatr. Intensive Crit. Care Soc.* 2010; 11: S85–S90.
33. Ryan J, Bloch K, Archer SL. Rodent models of pulmonary hypertension: harmonisation with the world health organisation's categorisation of human PH. *Int. J. Clin. Pract. Suppl.* 2011; : 15–34.
34. Stenmark KR, Meyrick B, Galie N, Mooi WJ, McMurtry IF. Animal models of pulmonary arterial hypertension: the hope for etiological discovery and pharmacological cure. *Am. J. Physiol. Lung Cell. Mol. Physiol.* 2009; 297: L1013–L1032.
35. Nicolls MR, Mizuno S, Taraseviciene-Stewart L, Farkas L, Drake JI, Al Husseini A, Gomez-Arroyo JG, Voelkel NF, Bogaard HJ. New models of pulmonary hypertension based on VEGF receptor blockade-induced endothelial cell apoptosis. *Pulm. Circ.* 2012; 2: 434–442.
36. Voelkel NF, Schranz D, editors. The Right Ventricle in Health and Disease [Internet]. New York, NY: Springer New York; 2015 [cited 2015 May 18]. Available from: http://link.springer.com/10.1007/978-1-4939-1065-6.
37. Reeves JT, Leathers JE. Hypoxic pulmonary hypertension of the calf with denervation of the lungs. *J. Appl. Physiol.* 1964; 19: 976–980.
38. Will DH, Alexander AF, Reeves JT, Grover RF. High Altitude-Induced Pulmonary Hypertension in Normal Cattle. *Circ. Res.* 1962; 10: 172–177.
39. Kay JM, Harris P, Heath D. Pulmonary hypertension produced in rats by ingestion of Crotalaria spectabilis seeds. *Thorax* 1967; 22: 176–179.

40. Rosenberg HC, Rabinovitch M. Endothelial injury and vascular reactivity in monocrotaline pulmonary hypertension. *Am. J. Physiol. - Heart Circ. Physiol.* 1988; 255: H1484–H1491.
41. Taraseviciene-Stewart L, Kasahara Y, Alger L, Hirth P, Mc Mahon G, Waltenberger J, Voelkel NF, Tuder RM. Inhibition of the VEGF receptor 2 combined with chronic hypoxia causes cell death-dependent pulmonary endothelial cell proliferation and severe pulmonary hypertension. *FASEB J. Off. Publ. Fed. Am. Soc. Exp. Biol.* 2001; 15: 427–438.
42. De Raaf MA, Schalij I, Gomez-Arroyo J, Rol N, Happé C, de Man FS, Vonk-Noordegraaf A, Westerhof N, Voelkel NF, Bogaard HJ. SuHx rat model: partly reversible pulmonary hypertension and progressive intima obstruction. *Eur. Respir. J.* 2014; 44: 160–168.
43. Sakao S, Taraseviciene-Stewart L, Lee JD, Wood K, Cool CD, Voelkel NF. Initial apoptosis is followed by increased proliferation of apoptosis-resistant endothelial cells. *FASEB J. Off. Publ. Fed. Am. Soc. Exp. Biol.* 2005; 19: 1178–1180.
44. Voelkel NF, Mizuno S, Bogaard HJ. The role of hypoxia in pulmonary vascular diseases: a perspective. *Am. J. Physiol. Lung Cell. Mol. Physiol.* 2013; 304: L457–L465.
45. Gomez-Arroyo JG, Farkas L, Alhussaini AA, Farkas D, Kraskauskas D, Voelkel NF, Bogaard HJ. The monocrotaline model of pulmonary hypertension in perspective. *Am. J. Physiol. Lung Cell. Mol. Physiol.* 2012; 302: L363–L369.
46. Stacher E, Graham BB, Hunt JM, Gandjeva A, Groshong SD, McLaughlin VV, Jessup M, Grizzle WE, Aldred MA, Cool CD, Tuder RM. Modern age pathology of pulmonary arterial hypertension. *Am. J. Respir. Crit. Care Med.* 2012; 186: 261–272.
47. Balogun J, Hailey VH. Exploring Strategic Change. Pearson Education; 2004.
48. Okada K, Tanaka Y, Bernstein M, Zhang W, Patterson GA, Botney MD. Pulmonary hemodynamics modify the rat pulmonary artery response to injury. A neointimal model of pulmonary hypertension. *Am. J. Pathol.* 1997; 151: 1019–1025.
49. Van Albada ME, Schoemaker RG, Kemna MS, Cromme-Dijkhuis AH, van Veghel R, Berger RMF. The role of increased pulmonary blood flow in pulmonary arterial hypertension. *Eur. Respir. J.* 2005; 26: 487–493.
50. De Raaf MA, Hussaini AA, Gomez-Arroyo J, Kraskaukas D, Farkas D, Happé C, Voelkel NF, Bogaard HJ. Histone deacetylase inhibition with trichostatin A does not reverse severe angioproliferative pulmonary hypertension in rats (2013 Grover Conference series). *Pulm. Circ.* 2014; 4: 237–243.

51. Zhao L, Chen C-N, Hajji N, Oliver E, Cotroneo E, Wharton J, Wang D, Li M, McKinsey TA, Stenmark KR, Wilkins MR. Histone deacetylation inhibition in pulmonary hypertension: therapeutic potential of valproic acid and suberoylanilide hydroxamic acid. *Circulation* 2012; 126: 455–467.
52. Cavasin MA, Demos-Davies K, Horn TR, Walker LA, Lemon DD, Birdsey N, Weiser-Evans MCM, Harral J, Irwin DC, Anwar A, Yeager ME, Li M, Watson PA, Nemenoff RA, Buttrick PM, Stenmark KR, McKinsey TA. Selective class I histone deacetylase inhibition suppresses hypoxia-induced cardiopulmonary remodeling through an antiproliferative mechanism. *Circ. Res.* 2012; 110: 739–748.
53. Bogaard HJ, Mizuno S, Voelkel NF. Letter by bogaard et Al regarding article, "histone deacetylation inhibition in pulmonary hypertension: therapeutic potential of valproic Acid and suberoylanilide hydroxamic Acid." *Circulation* 2013; 127: e539.
54. Bogaard HJ, Mizuno S, Hussaini AAA, Toldo S, Abbate A, Kraskauskas D, Kasper M, Natarajan R, Voelkel NF. Suppression of Histone Deacetylases Worsens Right Ventricular Dysfunction after Pulmonary Artery Banding in Rats. *Am. J. Respir. Crit. Care Med.* 2011; 183: 1402–1410.
55. Kong Y, Tannous P, Lu G, Berenji K, Rothermel BA, Olson EN, Hill JA. Suppression of class I and II histone deacetylases blunts pressure-overload cardiac hypertrophy. *Circulation* 2006; 113: 2579–2588.
56. Mauritz G-J, Kind T, Marcus JT, Bogaard H-J, van de Veerdonk M, Postmus PE, Boonstra A, Westerhof N, Vonk-Noordegraaf A. Progressive changes in right ventricular geometric shortening and long-term survival in pulmonary arterial hypertension. *Chest* 2012; 141: 935–943.

CHAPTER 1

Chapter 2:
SuHx rat model: partly reversible pulmonary hypertension, progressive intima obstruction.

Michiel Alexander de Raaf[1], Ingrid Schalij[1], Jose G. Gomez-Arroyo[2], Nina Rol1, Chris Happé[1], Frances S. de Man[1,3], Anton Vonk-Noordegraaf[1], Nico Westerhof[1,3], Norbert F. Voelkel[2], Harm Jan Bogaard[1].

Adapted from European Respiratory Journal. 2014 Jul;44(1):160-8.

Affiliation:
Departments of [1]Pulmonology and [3]Physiology, VU University Medical Center / Institute for Cardiovascular Research, Amsterdam, The Netherlands. [2]Pulmonary and Critical Care Medicine Division, Virginia Commonwealth University, Richmond, Virginia, USA.

Abstract:

The SU5416 combined with hypoxia (SuHx) rat model features angio-obliterative pulmonary hypertension resembling human pulmonary arterial hypertension (PAH). Despite increasing use of this model, a comprehensive hemodynamic characterization in conscious rats has not been reported. We used telemetry to characterize hemodynamic responses in SuHx-rats and associated these with serial histology.

Right Ventricular Systolic Pressure (RVSP) increased to 106±7 mmHg in response to SuHx and decreased but remained elevated at 72±8 mmHg upon return to normoxia. Hypoxia-only exposed rats showed a similar initial increase in RVSP, a lower maximum RVSP and near-normalization of RVSP during subsequent normoxia. Progressive vascular remodeling consisted of a fourfold increase in intima thickness, while only minimal changes in media thickness were found. The circadian range in RVSP provided an accurate longitudinal estimate of vascular remodeling.

In conclusion, in SuHx-rats re-exposure to normoxia leads to a partial decrease in pulmonary artery pressure in SuHx-rats, with persisting hypertension and pulmonary vascular remodeling characterized by progressive intima obstruction.

Introduction

Pulmonary Arterial Hypertension (PAH) is a progressive and fatal disease characterized by remodeling of the lung vessels, increased pulmonary vascular resistance and, ultimately, dysfunction of the right ventricle (RV)[1]. Animal models of pulmonary hypertension have provided critical insights that help to explain the pathobiology of the disease and have served as a platform for drug development[2]"container-title":"American journal of physiology. Lung cellular and molecular physiology","page":"L1013-1032","volume":"297","issue":"6","source":"NCBI PubMed","abstract":"At present, six groups of chronic pulmonary hypertension (PH. Traditionally, two animal models have been popular for preclinical testing of new PAH pharmacotherapies: the chronic hypoxia-induced pulmonary hypertension and the monocrotaline-lung injury model[2]"container-title":"American journal of physiology. Lung cellular and molecular physiology","page":"L1013-1032","volume":"297","issue":"6","source":"NCBI PubMed","abstract":"At present, six groups of chronic pulmonary hypertension (PH. More recently, new animal models based on vascular endothelial growth factor receptor (VEGF-R) blockade with the tyrosine kinase inhibitor SU5416 have been introduced and the SU5416 plus chronic hypoxia (hereafter SuHx) model is now being extensively used [3, 4]. Indeed, several investigators have demonstrated that the SuHx model represents many salient features of human PAH, such as severe pulmonary hypertension obliterative vascular lesions, RV dysfunction, decreased exercise endurance and treatment refractoriness [5–7]dramatic right ventricular hypertrophy, and pericardial effusion. Our recently published rat model of SPH recapitulates major components of the human disease. We used this model to develop new treatment strategies for SPH. SPH in rats was induced using VEGF receptor blockade in combination with chronic hypoxia. A large variety of drugs used in this study, including anticancer drugs (cyclophosphamide and paclitaxel. Plexiform-like lesions emerge in the pulmonary vasculature of SuHx rats when the normoxic re-exposure protocol is extended to 10 weeks or longer [4, 8].. Whereas histological changes in the lungs and RV of SuHx-rats have been described in much detail [8–10], a hemodynamic characterization of the model has been restricted to RV catheterizations in groups of anesthetized rats at different time-points [11]. Longitudinal hemodynamic measurements in conscious rats, as can be obtained using telemetry, are important to provide a context for the histological changes and to ascertain the value of the model for preclinical drug testing. Therefore the aim of this study is to characterize the hemodynamic

responses in conscious SuHx-rats and to associate these with morphological data obtained by serial histology. We show the feasibility of a longitudinal characterization of the hemodynamic changes in conscious and freely moving SuHx-rats and rats exposed to hypoxia alone, by measuring RV systolic pressure (RVSP) nearly continuously by means of an implanted telemetry device. Our study reveals a previously unappreciated but only partial reversibility of pulmonary hypertension in SuHx-rats, which may interfere with the interpretation of preclinical drug studies. Despite this partial reversibility in pulmonary hypertension, serial histology showed a progressive remodeling of the pulmonary vascular wall, in particular the intima layer.

Material and methods

Animal model

Ten male Sprague Dawley rats (Crl:CD(SD), Charles River, Sulzfeld, Germany) underwent implantation of a telemetric pressure sensor in the RV as described before [12]. To prepare SU5416 solution, 5 mg SU5416 was dissolved in 0.5 mL 0.5% cmc (carboxymethylcellulose). Subsequently, the tube was placed on a plate shaker for ~2 hours to dissolve and homogenize the solution. Within 3 hours after preparation of the SU5416 solution, it was administered in a dose of 25mg/kg subcutaneously in the neck. Five rats were exposed to hypoxia only (Hx) and 5 rats to SuHx. Eight additional groups of 4 SuHx-rats were used for serial measurements of RV hypertrophy, histology and hematocrit at baseline and after every subsequent week. SuHx mediated pulmonary hypertension was induced according to the protocol published previously [4, 13]. SU5416 (Tocris Bioscience, Bristol, UK) was administered to rats weighing <200 grams as a single subcutaneous injection (25 mg/kg) [14], 5-7 days after sensor implantation. SuHx (at day of injection) and Hx-rats were housed for four weeks in 10% oxygen (Biospherix Ltd. New York, USA) maintained by a nitrogen generator (Avilo, Dirksland, The Netherlands) and subsequently re-exposed to normoxia for three weeks. The study was approved by the local Animal Welfare committee (VU-Fys 11-16).

Telemetry

Telemetry implantation

Implantation surgery was performed as described previously [12]; a telemetry transmitter TA11PA-C40, (DSI, St. Paul, MN) was implanted by a transdiaphragmatic approach allowing insertion of the tip of the catheter into the RV, while the transmitter body was placed in the abdomen (survival rate was ~90%). Animals were allowed to recover for one week prior the induction of SuHx (**Figure 1**).

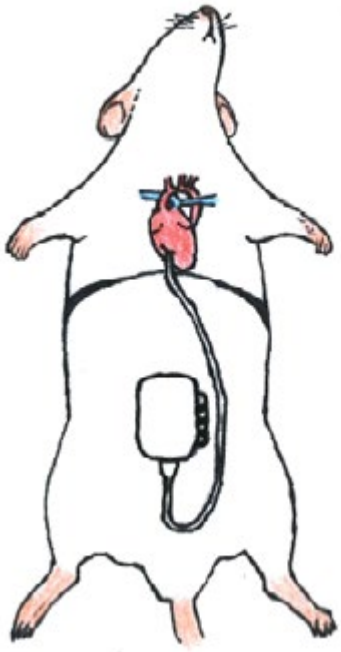

Figure 1: *A schematic drawing of the telemetry implantation. The tip of the catheter is inserted in the right ventricle, while the transmitter device is placed in the abdominal cavity (drawing perform by Ingrid Schalij).*

Telemetry acquisition and analyses

Telemetry data acquisition consisted of averaged recordings of one minute duration recorded every hour. The analysis was based on the RVSP at 10pm at baseline and at the end of every subsequent week. At the same time points, the circadian range in the RVSP ($\Delta RVSP_{max\text{-}min}$) was determined. In addition, acute changes in RVSP upon a four minute exposure to hyperoxia were recorded weekly.

Technical methodology of telemetry acquisition and analyses

The transmitter emits data to a receiver which is connected to the acquisition computer. Throughout the entire study, 1-minute acquisition bins of ~200-400 cardiac beats were collected every hour (DSI, St. Paul, MN). Every data bin used underwent a quality assessment before averaging. The morphology of the blood

pressure waveforms was visually assessed (**Figure 1**). Signals were only used when clear from technical deviations, which can be induced by electrical interference, (e.g. spikes derived from electromagnetic fields from the surroundings), signal dampening (e.g. due to clot formation on the tip of the catheter) and unexpected offset changes (e.g. due to kinking of the fluid filled catheter). When the signal did not meet the quality criteria, data from that time point onwards was excluded from further analysis, as recommended [17, 25, 26]. Parameters derived from telemetric monitoring were RVSP and Heart Rate (HR). Due to the sensitivity to gravity of the system, which may cause a pressure deviation of maximally four mmHg, RV diastolic pressure is not reported.
To account for circadian rhythm-induced changes, the 10PM bin of RVSP data was used for daily RVSP representation. Animals are active at this time and not affected by the possible stress due to biotechnical handlings. For assessing the reversible component of the RVSP increase, every week animals were briefly (5 minutes) exposed to 60% oxygen plus anesthesia in a small single-rat anesthesia induction chamber. 1% isoflurane was given for animal welfare reasons. The 4 subsequent 1 minute acquisition bins during the hyperoxic exposure were compared with the last RVSP acquisition bin measured prior to hyperoxia exposure (measured in the conscious animal in his 'home cage'). To assess daily circadian ranges in RVSP, maximum and minimum one-minute RVSP averages were determined and their difference, defined as delta RVSP ($\Delta RVSP_{max\text{-}min}$), was averaged over a week. RVSP did not show a clear sinusoid day/night rhythm (7AM to 7PM light/dark cycle), but multiple fluctuations in pressure throughout the day. The incidence of fluctuations was not different between groups (control (**Figure 6A**), hypoxia (**Figure 6B**) and SuHx (**Figure 6C**)) or between time point (before hypoxia, at end of hypoxia and at end of study). However, the magnitude of the fluctuations was significantly different between groups and time points.

Echocardiography

To measure RV end diastolic diameter (RVEDD) and tricuspid annular plane systolic excursion (TAPSE), animals underwent weekly echocardiographic assessments (Prosound SSD-4000 & UST-5542, Aloka, Tokyo, Japan), as published before[12].

Histological and morphometric analyses

Four µm slides of lung tissue were prepared and stained with Elastica van Gie-

son, for specific coloration of the elastic laminae, and scanned (3DHISTECH, Budapest, Hungary). A field of ~ 5 billion µm2 on every slide was fully evaluated. Because media hypertrophy and neo-muscularisation manifest during the development of PAH, small arteries and arterioles were divided into three classes, based on external diameters. The ranges of these classes were chosen to allow distinction of effect size and generation diameters of the pulmonary arteries in rats, as described by Hislop et al. [15]: <30 µm vessels represent pre-capillaries (intra-acinar, neomuscularisation and intima remodeling), 30-60 µm vessels represent alveolar duct or respiratory bronchiole arteries (intra-acinar, medial hypertrophy and intima remodeling) and 60-100 µm vessels represent terminal bronchiole (axial, pre-acinar) arteries. Concordant to human PAH, we hypothesized no changes in the latter class of vessels [18]. Only vessels with an approximate circular profile were included. Media and intima wall thickness were measured as described previously [4, 9, 16]. In each vessel, the diameter of the external elastic lamina, the diameter of the internal elastic lamina and the diameter of the lumen were determined. These values were used to calculate the relative medial wall thickness and intima thickness. Media thickness was measured in duplo by calculating (100*(diameter external elastic lamina– diameter internal elastic lamina))/(diameter external elastic lamina)[16]. Intima thickness was measured twice in each vessel by calculating (100*(diameter internal elastic lamina - diameter lumen)/(diameter external elastic lamina)). Hence, media and intima thickness are represented as averages. Completely obliterated vessels were also observed and included in the analyses. Representative images (**supplemental figure 3**) show vascular lesions in rows during wk0 through wk7.

Necropsy

Animals were exsanguinated under anesthesia after blood was taken to measure hematocrit. Lungs and hearts were weighed after separation of the heart into RV and left ventricle plus septum (LV+S). Tissues were fixed in formalin and embedded in paraffin. To preserve the integrity of the telemetry catheter, it was not possible to determine the RV/(LV+S) of the animals with a telemetry catheter inserted. From the non-telemetry animals, RVSP was measured using a Millar pressure catheter (Millar,Houston,TX, USA), as published before [12] (**supplemental figure 4**). The left lung lobe was inflated with low-melt 0.5% agarose on 25 cm H2O pressure, fixed in formalin and embedded in paraffin. Four µm slides of lung tissue were prepared and stained with H&E and EvG and scanned

(3DHISTECH, Budapest, Hungary).

Statistical analyses

Parametric variables were compared between groups using appropriate ANOVA with Bonferroni post-hoc tests. Correlations were determined using Pearson correlation tests (Graphpad, La Jolla, CA). Data is presented as mean ± SD.

Results

Telemetric RVSP and RV hypertrophy measurements

Telemetry was feasible for the measurement of RVSP in conscious rats up to, at least, 8 weeks (**Figure 2A-B**). The RVSP remained constant in a control rat, which confirms the accuracy of the telemetric method. There was no peri-operative or post-operative mortality. However, recordings in one Hx-rat did not meet quality criteria and were therefore excluded from the analyses [17].

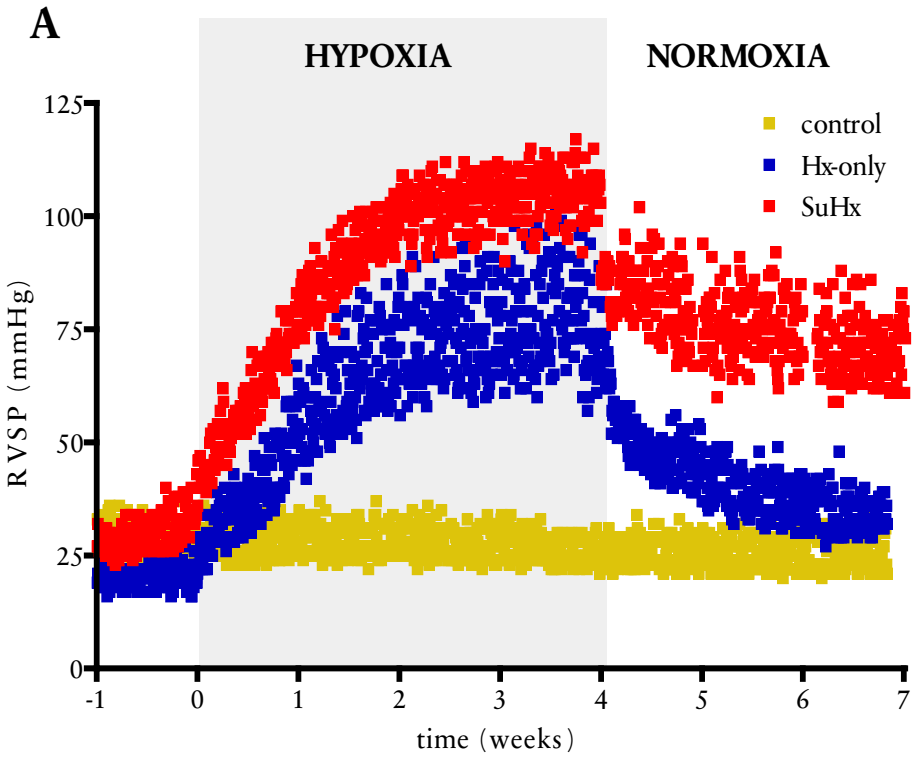

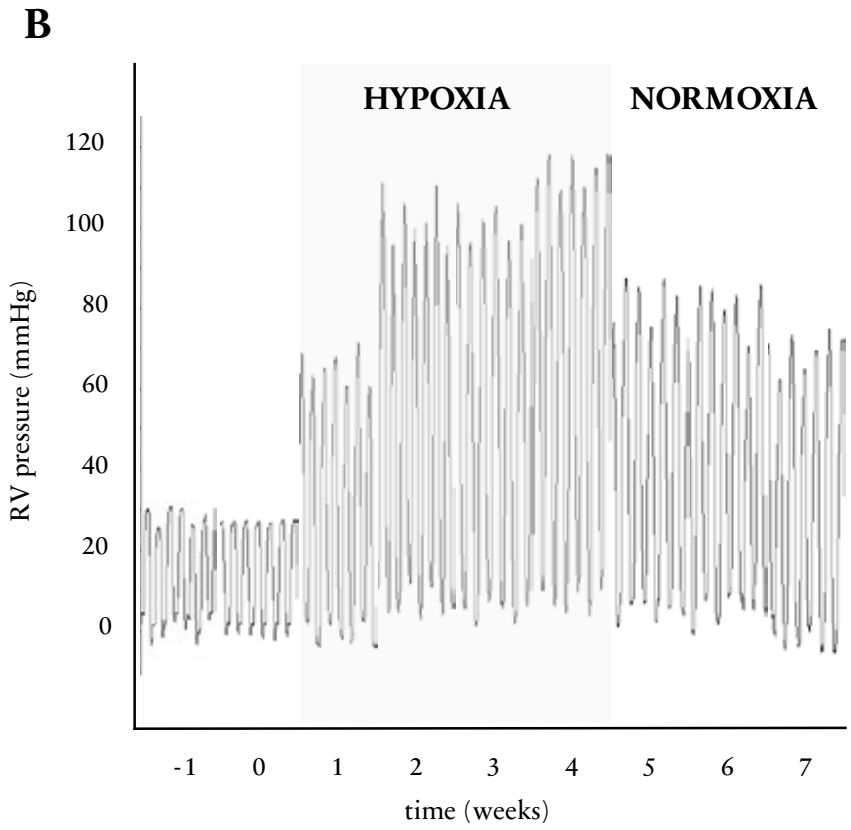

Figure 2: *Panel A shows a representative tracing of the telemetic RVSP acquisition. Panel B shows all pressure recordings (one minute average for every hour of acquisition) in one representative rat exposed to hypoxia only (Hx; blue) and one rat exposed to SU5416 and hypoxia (SuHx; red). Every square represents one hour of data acquisition. The data of one control rat (normal range of RVSP) is depicted in gray.*

The RVSP increased upon exposure to hypoxia in Hx-rats and SuHx-rats and both groups showed a comparable rise during the first 2 weeks of hypoxia (**Figure 3A**). Subsequently, SuHx-rats showed a trend to a progressively greater increase in RVSP to values above 100 mmHg, while Hx-rats showed an increase to about maximally 80 mmHg. Immediately upon re-exposure to normoxia, a rapid 20% decrease in RVSP was observed (**Figure 3B**). Hx-rats showed a significant but less

pronounced decrease in RVSP (**Figure 3C**). After this decrease, a mild reduction of pressure followed in both groups and at 6 and 7 weeks RVSP stabilized. At stabilization, RVSP in the SuHx-rat remained elevated and significantly higher as compared to Hx-rats. Echocardiography in SuHx-rats showed an increase in RVEDD and decrease in TAPSE during the hypoxic period, followed by a partial recovery during in the first two weeks of normoxic re-exposure and a subsequent further worsening in the last week of the protocol (**Figure 3D**). RVEDD was temporarily increased in Hx-only rats, whereas TAPSE was unaffected by hypoxia (**Figure 3E**).

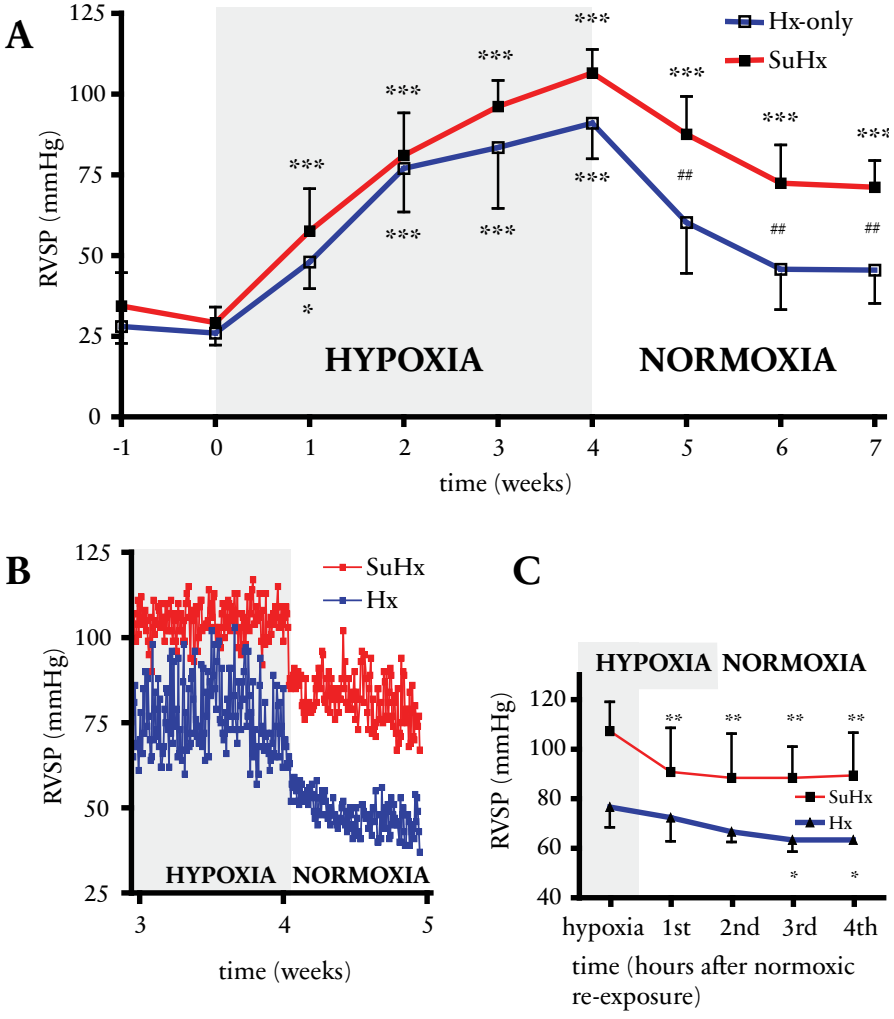

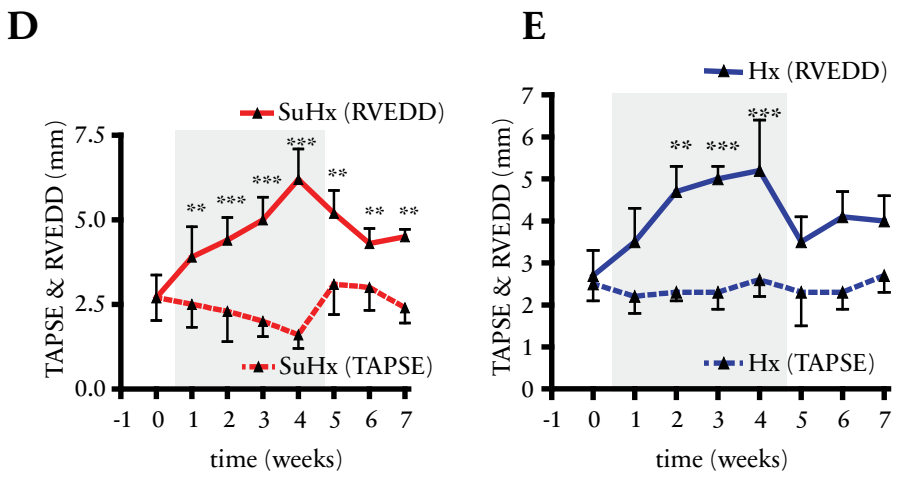

Figure 3: *A. Mean right ventricular systolic pressure (RVSP) throughout the entire study period in rats exposed to hypoxia only (n=4, Hx; blue) and exposed to SU5416 and hypoxia (n=5, SuHx; red). Significant differences from baseline are shown at different time-points (* = p<0.05, *** = p<0.001), as well as the differences between Hx and SuHx-rats (# = p<0.05). Panel B shows that re-exposure to normoxia results in an acute 20% decrease in RVSP within one hour in a representative SuHx-animal (data points each hour). To visualize the acute decrease in RVSP upon normoxic re-exposure, panel C shows significant differences between the mean RVSP measured during the last day of hypoxia and the first four normoxia time points in SuHx and Hx-rats (* = p<0.05, ** = p<0.01). Echocardiographic measurements of RV end-diastolic diameter (RVEDD) and tricuspid annular plane systolic excursion (TAPSE) are shown in panels D and E.*

In Hx- and SuHx-rats alike, brief exposure to hyperoxic conditions revealed an acute reversibility in pressure (**Figure 4A**). This finding was confirmed by catheterizations in the non-telemetry animals (histology groups) during termination, which showed lower RVSP values than those obtained in telemetry rats (**Figure 4B**). The acute decrease in pressure equaled the pressure increase over the first week. With continuous re-exposure to normoxia, this vasoreactive response to hyperoxia disappeared.

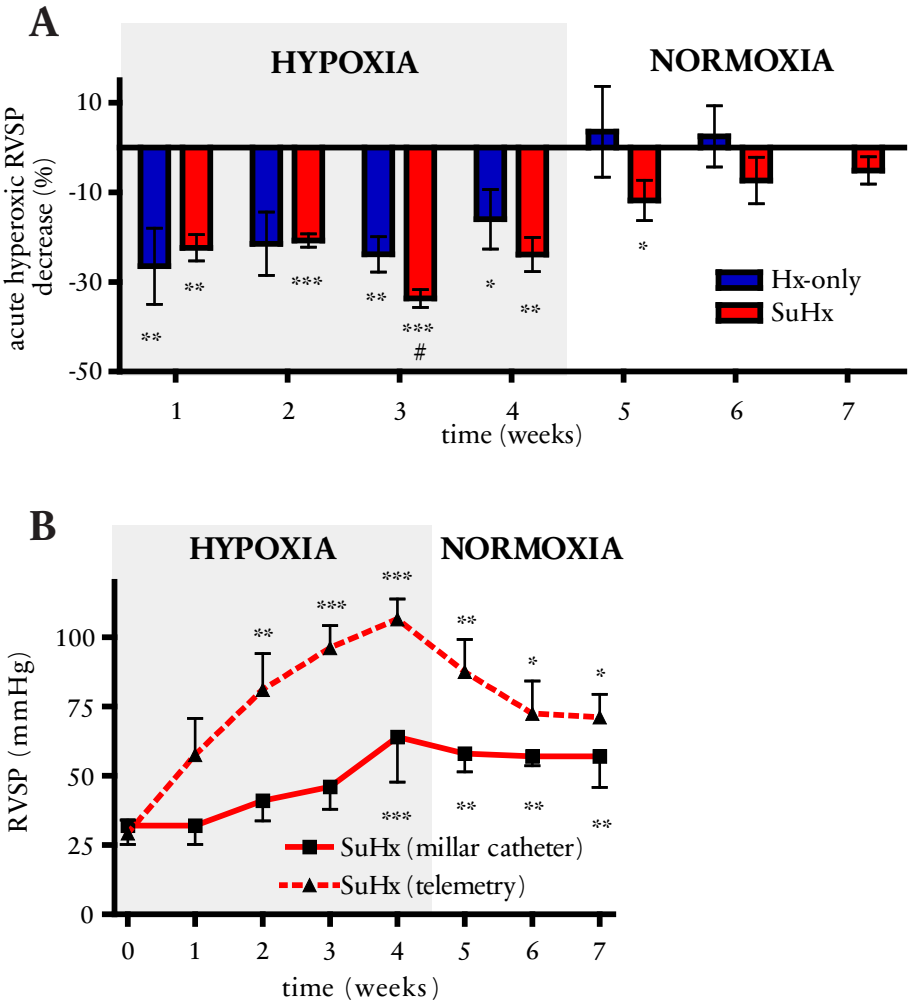

Figure 4: *Panel A: Right ventricular systolic pressure (RVSP) changes following an acute hyperoxic challenge in rats exposed to hypoxia only (Hx; blue) and rats exposed to SU5416 and hypoxia (SuHx; red). * = p <0.05, ** p<0.01, *** p <0.001. The RVSP change in week 3 was significantly different between Hx and SuHx-rats (# = p<0.05). The telemetric measured RVSP of conscious animals was compared with non-telemetric RV catheterizations in panel B.*

RV hypertrophy (RV/(LV+S)) in the SuHx-group increased progressively during hypoxia and partially decreased upon normoxic re-exposure (**Figure 5A**). The RV/(LV+S) correlated with the RVSP throughout the entire study period (**Figure 5B**). The hematocrit in SuHx-rats increased significantly during the hypoxic period and normalized within one week after re-exposure to normoxic conditions (**Figure 5C**). Hematocrit correlated with RVSP during the hypoxic period only (**Figure 5D**).

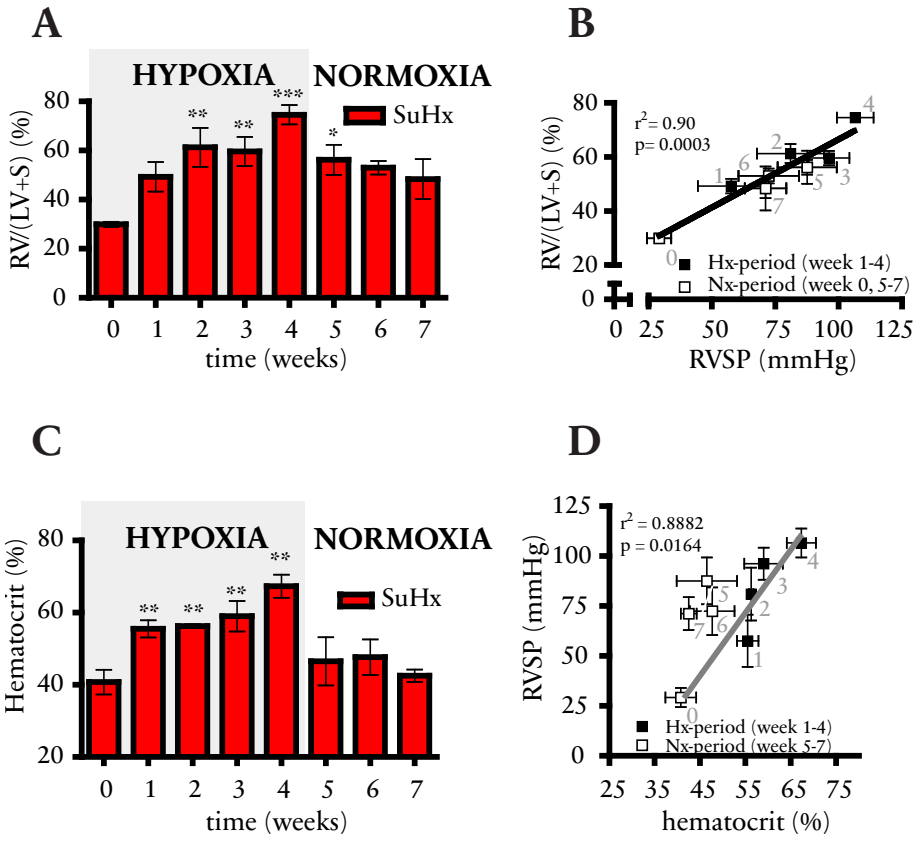

Figure 5: *Panel A shows weekly progression of right ventricular (RV) hypertrophy (expressed as RV weight over left ventricular plus septal weight, or RV/(LV+S)) in rats exposed to SU5416 and hypoxia (SuHx). Panel B shows a strong correlation, between RV/(LV+S) in hypoxia and after normoxic re-exposure, determined in 32 rats from 8 consecutive histology groups) and right ventricular systolic pressure (RVSP) (n=5; telemetry)*

at corresponding time-points (as indicated by study week number). Panel C shows the hematocrit of SuHx-rats. Panel D shows the correlation, during the hypoxic period only, between hematocrit and RVSP (telemetry) at corresponding time points (as indicated by study week number). Hypoxic period is shown by black squares and normoxic period by open squares. RVSP and hematocrit were not related during the normoxic re-exposure.

Circadian range in RVSP ($\Delta RVSP_{max\text{-}min}$)

During their hypoxic exposure, both groups showed a progressive increase in $\Delta RVSP_{max\text{-}min}$, while upon normoxic re-exposure the $\Delta RVSP_{max\text{-}min}$ decreased in Hx-rats but continued to increase in SuHx-rats (**Figure 6**).

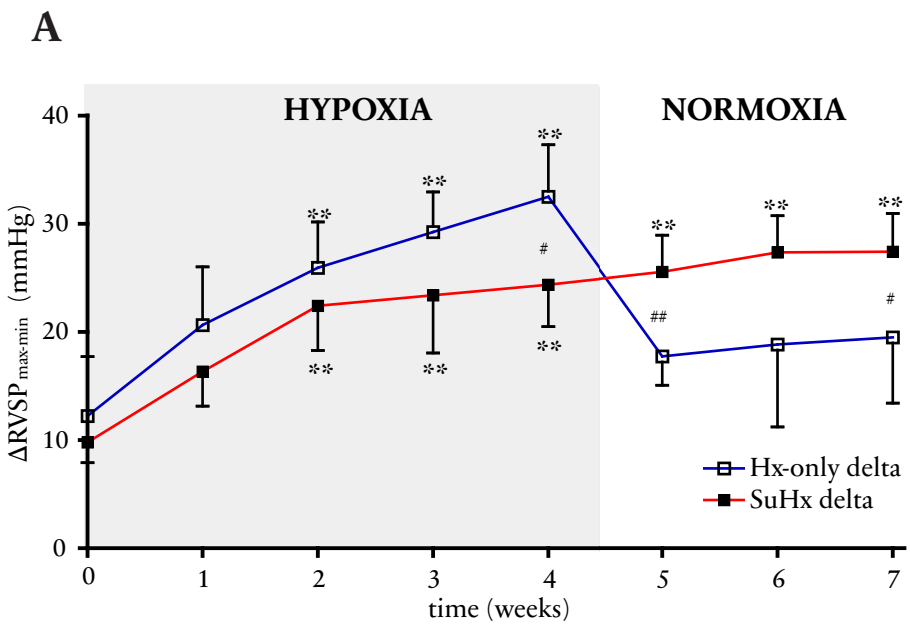

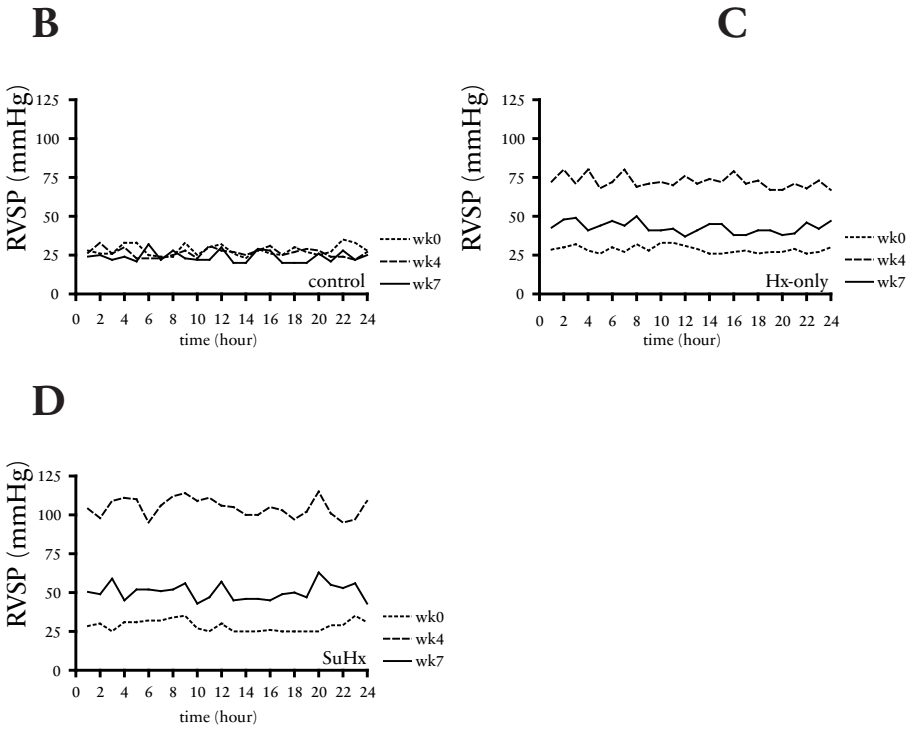

Figure 6: *Panel A: Daily ranges in right ventricular systolic pressure ($\Delta RVSP_{max-min}$) during the course of the experimental period in rats exposed to hypoxia only (Hx, blue) and rats exposed to SU5416 and hypoxia (SuHx, red). $\Delta RVSP_{max-min}$ increased significantly during the hypoxic period in Hx and SuHx-rats alike, but after return to normoxia decreased in Hx-rats and continued to increase in SuHx-rats. Significant differences are shown for the comparisons between baseline and subsequent weeks (* = p<0.05 and ** = p<0.01) and between Hx-rats and SuHx-rats (# = p<0.05 and ## = p <0.01. Panel B-D shows representative tracings of week 0, 4 and 7; baseline, end of the hypoxic exposure and after 3 weeks of normoxia, respectively.*

Vessel morphology

In **Figure 7A** representative examples are shown of changes in ~40µm vessels in SuHx-rats (**Figure 7A**). No changes in intima thickness were seen in arteries of 60-100 µm (**Figure 7B**), in contrast to an increase in intima thickness in smaller vessels (30-60 µm vessels in **Figure 7C** and <30 µm vessels in **Figure 7D**)). Upon return to normoxia, the intima remained thickened in vessels with a diameter up to 60 µm, resulting in a progressive narrowing of the lumen. Media thickness increased during the first week of hypoxia in <30 and 60-100 vessels, but decreased upon return to normoxia. A very strong correlation was observed between relative wall thickness (intima plus media) of <30 µm vessels and $\Delta RVSP_{max\text{-}min}$ (**Figure 8**).

A

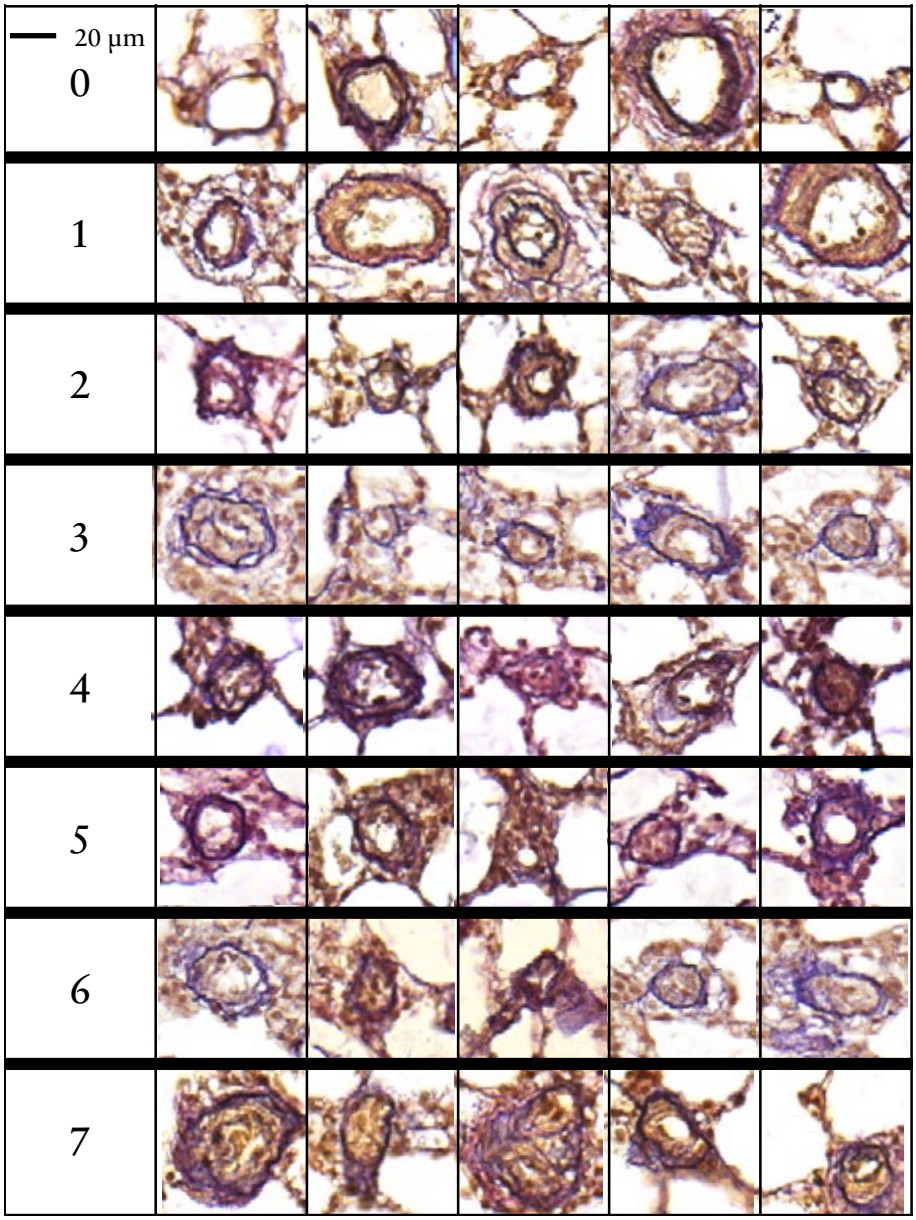

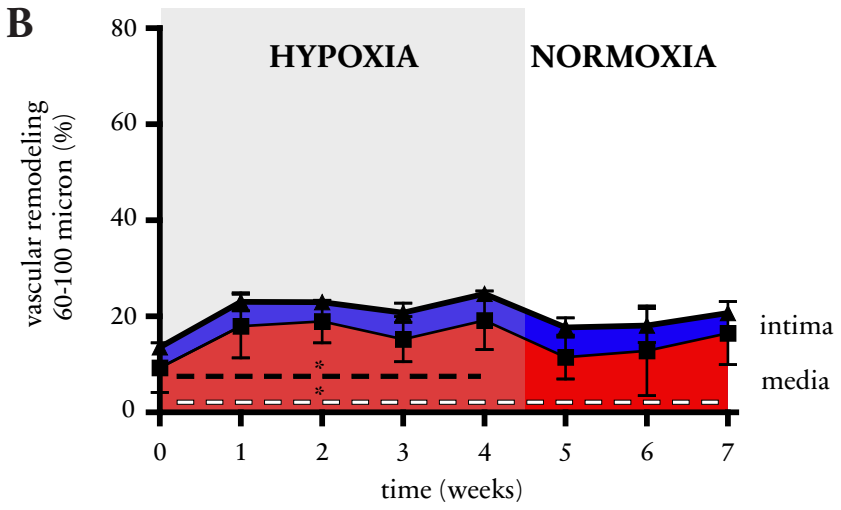
B
HYPOXIA
NORMOXIA
vascular remodeling
60-100 micron (%)
80
60
40
20
0
0
1
2
3
4
5
6
7
time (weeks)
intima
media
*
*

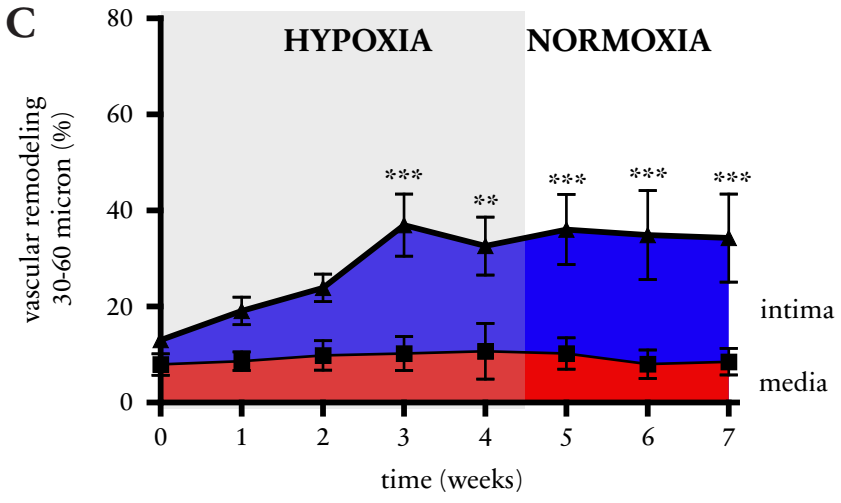
C
HYPOXIA
NORMOXIA
vascular remodeling
30-60 micron (%)
80
60
40
20
0
0
1
2
3
4
5
6
7
time (weeks)
intima
media
***
**
***
***
***

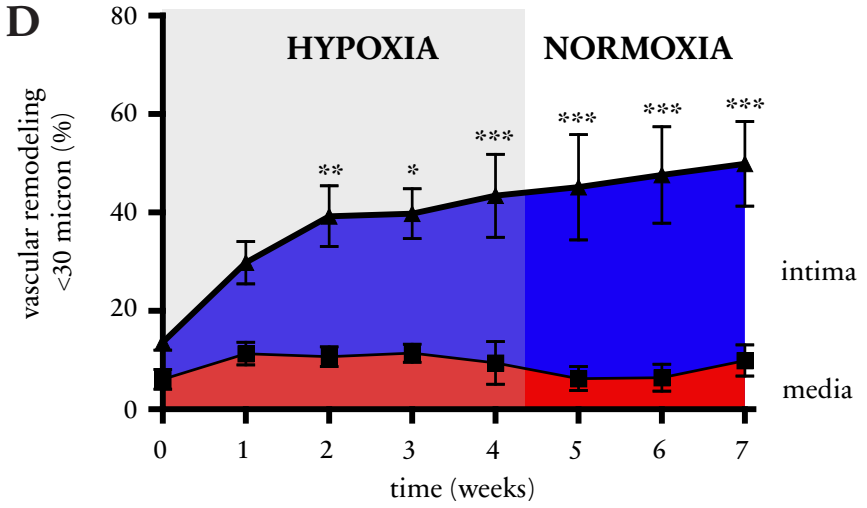

Figure 7: *Histology of pulmonary vessels in rats exposed to SU5416 and hypoxia (SUHx). Panel A shows representative Elastica van Giesson stains of small pulmonary arteries (~40 um) at different time-points. Cumulative time courses of the thickening of the intima (orange) and media (red) were expressed as percentage of the diameter of the external elastic lamina and calculated per vessel class. Panel B shows 60-100 µm vessels, panel C 30-60 µm vessels and panel D <30 µm vessels. The medial layer was significantly thickened ($p < 0.05$) during hypoxia and at week 7. Media and intima thickness are represented as averages; completely obliterated vessels were also observed and included in the analyses. Statistical significance from baseline, using repeated ANOVA, are denoted by: * = $p < 0.05$, ** = $p < 0.01$, *** $p = <0.001$. The media thickness of 60-100 µm vessels was significantly different between baseline and week 1(** = $p<0.01$).*

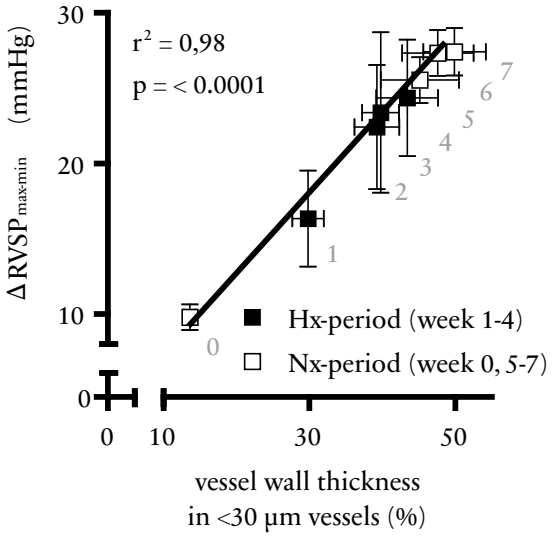

Figure 8: *Pearson correlation between the relative vessel wall thickness (intima plus media) of the smallest vessel class (<30 µm) and the daily range in right ventricular systolic pressure (ΔRVSP$_{max-min}$). Average values were taken from the histology and telemetry groups at corresponding time points. The grey numbers indicate the week of data collection.*

Discussion

The SuHx model is a model in which the combined exposure of rats to hypoxia and a VEGF-R antagonist induces angio-obliterative pulmonary hypertension [3]. By intima thickening mainly in the small arteries and limited neomuscularization, the SuHx model reproduces many aspects of the pathobiology of human PAH [18]. Here, we evaluated the time-course of vascular remodeling by histology and the evolution of hemodynamic changes using telemetry. Telemetry allowed several important observations in SuHx-rats. First and surprisingly, the RVSP was higher than anticipated in conscious, freely moving Hx animals. Second, we showed that after return to normoxia the SuHx-model regresses to a milder but persistent form of pulmonary hypertension. Third, while acutely reversible hypoxic vasoconstriction is an important component of pulmonary hypertension during the first phase of the model, the second phase is characterized by intima remodeling, which was progressive even after return to normoxic conditions. Fourth, we found a progressive increase in the circadian RVSP range in SuHx-rats, which can be used as a surrogate marker for the severity of vascular remodeling.

Serial Hemodynamic and histological characterization

Serial pressure measurements revealed an RVSP of 80 mmHg in Hx-rats (and even higher in SuHx-rats), which was higher than expected. Telemetry allowed measurements without anesthesia, during physical activity and without the need of removing rats from their hypoxic environment. Although the *in vitro* induction of endothelial proliferation by SU5416 starts within 3 days [19], a trend to significant hemodynamic differences between SuHx and Hx-rats did not become apparent until after two weeks of hypoxic exposure. The development in SuHx-rats of a RVSP that exceeded the pressure in Hx-rats was paralleled by the emergence of intima remodeling and a decrease in vasoreactivity in week 4. Together, these findings suggest the emergence of vascular remodeling in SuHx-rats three weeks after the administration of SU5416. As expected, RVSP in Hx-rats decreased further, but not completely, to normal values in the successive weeks after return to normoxia. The RVSP also decreased in SuHx-rats upon return to normoxia, but stabilized at a new plateau (**Figure 3A**). This up-and-partially-down pressure response in the SuHx model was not previously appreciated and contrasts with the findings of Toba et al., who showed persistent pulmonary hypertension in SuHx rats after return to normoxia [11]. This difference is likely explained by the

use of anesthesia, because we also found much lower RVSPs in separate groups of anesthesized SuHx rats prior to termination for tissue harvesting. Other than by the use of anesthesia, differences in pressure responses between our study and the study by Toba may be explained by differences in husbanding, animal handling and diet, including dietary copper content [20]. It is unlikely that technical complications of the telemetry method would explain differences in pressure responses, as the quality of all signals was carefully checked and signals in normal rats were stable. Clots at the site of telemetry implantation, which could possibly interfere with pressure recordings, were not observed. Abe et al. followed SuHx-rats, without telemetry, up to 14 weeks after the initial SU5416 administration and showed that vascular remodeling was driven by vessel obliteration [8]. This suggests that SuHx induced pulmonary hypertension is not fully reversible and that a longer telemetric follow-up of our rats would have likely revealed stable or progressive pulmonary hypertension. The major implication of partial and temporal reversibility of pulmonary hypertension in SuHx rats is the fact that treatment studies need to be carefully planned and require sufficient numbers of animals to avoid any false positive results.

RVSP in SuHx rats with telemetry showed a linear correlation with RV/(LV+S) in SuHx rats without telemetry (**Figure 5B**). This confirms that telemetry implantation does not affect the development of experimental pulmonary hypertension [4, 12]. The hematocrit in SuHx-rats increased significantly during the hypoxic period, which has been reported to be related to a combined effect of diuresis and intensified erythropoiesis [21]. The correlation between hematocrit and RVSP during the exposure to hypoxia suggests that some of the pressure increase in SuHx-rats is related to an increase in blood viscosity. It is interesting that, despite the progressive increase in pulmonary vascular remodeling, RV function, e.g. TAPSE, improves upon normoxic re-exposure. This suggests that hypoxic vasoconstriction and erythrocytosis significantly contribute to RV remodeling in the initial stages of the model.

During the hypoxic exposure, Hx- and SuHx-rats exhibited a progressively greater circadian range in RVSP (**Figure 6A**). Upon normoxic re-exposure, $\Delta RVSP_{max\text{-}min}$ recovered in Hx-rats but not in SuHx-rats. Interestingly, we demonstrated a strong correlation between $\Delta RVSP_{max\text{-}min}$ and wall thickness of <30μm vessels, which suggests that $\Delta RVSP_{max\text{-}min}$ could be used as a marker of remodeling of resistance vessels. In this setting, the lung circulation fails to accommodate a temporary

elevation in blood flow (which occurs during activity or stress), and as this class of vessels plays a major role in pulmonary vascular resistance [22, 23], RVSP increases substantially. This is in keeping with the previously published correlation between RVSP and the percentage of obliterative vessels [10, 14]. Further studies to understand the mechanism of this hemodynamic phenomenon and its response to treatment are warranted.

Comparison to human PAH

Although the hyperproliferative characteristics of the pulmonary endothelium in the SuHx-rat resembles similar changes in the human PAH lung, the mechanisms of action of SU5416 and hypoxia in this model have not been precisely identified. Therefore, potential treatment responses in this model may not be reproduced in human PAH. Unlike PAH patients and despite severe pulmonary vascular remodeling and RV dysfunction, SuHx rats exhibit low mortality rates. Serial histology of SuHx-rats showed vascular remodeling predominantly of vessels up to 60 μm. Moreover, the tunica media was relatively unaffected. This reflects the findings in human PAH provided by Stacher *et al*., who showed a large overlap between the media thickness of healthy controls and patients with end-stage human PAH [18]. As such, end stage human PAH and the SuHx model share features of fixed pulmonary hypertension and a histological pattern dominated by intima thickening. These changes may occur after an initial phase of vasoconstriction and media hypertrophy and may explain why PAH targeting treatments have varying degrees of success during distinct phases of the evolution of the pulmonary vascular disease in SuHx-rats and PAH patients.

Use of telemetry

Telemetry has become the 'gold standard' for blood pressure measurements in conscious, freely moving animals [24, 25], as continuous hemodynamic parameters can be acquired unaffected by the use of anesthesia or mechanical ventilation. Here we show that telemetry is highly informative for the longitudinal tracking of the RVSP in SuHx-rats. Having established the natural history of the development of PAH in this model, it is now feasible to monitor the RVSP during treatment interventions. The magnitude of the circadian range in RVSP, as revealed by telemetry, underscores the importance of meticulous attention to measurement protocols when using animals for cardiovascular research. A disad-

vantage of the method is that reliable measurements could not be obtained past 8 weeks after the implantation of the transmitter, when ~70% of its battery life is consumed. When telemetric pressure measurement could be combined with cardiac output measurements, this would strengthen the benefit of this method for assessing treatment responses.

Conclusion:

The SuHx-rat model is a unique experimental model reproducing a significant number of pathobiologically important features of human PAH. The present study shows that in the model, an initial phase of partially reversible hypoxic vasoconstriction and polycythemia, is followed by severe pulmonary hypertension developing in association with progressive remodeling of the intima. Withdrawal from hypoxia is associated with rapid reversal of polycythemia and a less rapid decrease in pressure, while pulmonary vascular remodeling progresses. Careful observation of the different phases of the SuHx model will now permit the testing of drugs during different stages of disease development. Telemetry studies as described here in this animal model of severe PAH can facilitate the design of preclinical studies to further improve our understanding of drug actions in PAH.

Acknowledgements

We would like to acknowledge A.J. Bak (AMC, Amsterdam, The Netherlands), D. Kraskauskas (VCU, Virginia, USA), Dr. K. Grünberg, Ing. H. Ketelaars, Dr. K. Kramer, R. Schutte (VU/VUMC, Amsterdam, The Netherlands) and Dr. G. Langenbach (ACTA, Amsterdam, The Netherlands) for their contribution to this study by sharing their knowledge and expertise.

References

1. Simonneau G, Robbins IM, Beghetti M, Channick RN, Delcroix M, Denton CP, Elliott CG, Gaine SP, Gladwin MT, Jing Z-C, Krowka MJ, Langleben D, Nakanishi N, Souza R. Updated clinical classification of pulmonary hypertension. *J. Am. Coll. Cardiol.* 2009; 54: S43–54.
2. Stenmark KR, Meyrick B, Galie N, Mooi WJ, McMurtry IF. Animal models of pulmonary arterial hypertension: the hope for etiological discovery and pharmacological cure. *Am. J. Physiol. Lung Cell Mol. Physiol.* 2009; 297: L1013–1032.
3. Nicolls MR, Mizuno S, Taraseviciene-Stewart L, Farkas L, Drake JI, Al Husseini A, Gomez-Arroyo JG, Voelkel NF, Bogaard HJ. New models of pulmonary hypertension based on VEGF receptor blockade-induced endothelial cell apoptosis. *Pulm Circ* 2012; 2: 434–442.
4. Taraseviciene-Stewart L, Kasahara Y, Alger L, Hirth P, Mc Mahon G, Waltenberger J, Voelkel NF, Tuder RM. Inhibition of the VEGF receptor 2 combined with chronic hypoxia causes cell death-dependent pulmonary endothelial cell proliferation and severe pulmonary hypertension. *FASEB J.* 2001; 15: 427–438.
5. Taraseviciene-Stewart L, Scerbavicius R, Choe K-H, Cool C, Wood K, Tuder RM, Burns N, Kasper M, Voelkel NF. Simvastatin causes endothelial cell apoptosis and attenuates severe pulmonary hypertension. *Am. J. Physiol. Lung Cell Mol. Physiol.* 2006; 291: L668–676.
6. Gomez-Arroyo J, Saleem SJ, Mizuno S, Syed AA, Bogaard HJ, Abbate A, Taraseviciene-Stewart L, Sung Y, Kraskauskas D, Farkas D, Conrad DH, Nicolls MR, Voelkel NF. A brief overview of mouse models of pulmonary arterial hypertension: problems and prospects. *Am. J. Physiol. Lung Cell Mol. Physiol.* 2012; 302: L977–991.
7. Bogaard HJ, Natarajan R, Mizuno S, Abbate A, Chang PJ, Chau VQ, Hoke NN, Kraskauskas D, Kasper M, Salloum FN, Voelkel NF. Adrenergic receptor blockade reverses right heart remodeling and dysfunction in pulmonary hypertensive rats. *Am. J. Respir. Crit. Care Med.* 2010; 182: 652–660.
8. Abe K, Toba M, Alzoubi A, Ito M, Fagan KA, Cool CD, Voelkel NF, McMurtry IF, Oka M. Formation of plexiform lesions in experimental severe pulmonary arterial hypertension. *Circulation* 2010; 121: 2747–2754.
9. Okada K, Tanaka Y, Bernstein M, Zhang W, Patterson GA, Botney MD. Pulmonary hemodynamics modify the rat pulmonary artery response to injury.

A neointimal model of pulmonary hypertension. *Am. J. Pathol.* 1997; 151: 1019–1025.

10. Oka M, Homma N, Taraseviciene-Stewart L, Morris KG, Kraskauskas D, Burns N, Voelkel NF, McMurtry IF. Rho kinase-mediated vasoconstriction is important in severe occlusive pulmonary arterial hypertension in rats. *Circ. Res.* 2007; 100: 923–929.
11. Toba M, Alzoubi A, O'Neill KD, Gairhe S, Matsumoto Y, Oshima K, Abe K, Oka M, McMurtry IF. Temporal hemodynamic and histological progression in Sugen5416/hypoxia/normoxia-exposed pulmonary arterial hypertensive rats. *Am. J. Physiol. Heart Circ. Physiol.* 2013; .
12. Handoko ML, Schalij I, Kramer K, Sebkhi A, Postmus PE, van der Laarse WJ, Paulus WJ, Vonk-Noordegraaf A. A refined radio-telemetry technique to monitor right ventricle or pulmonary artery pressures in rats: a useful tool in pulmonary hypertension research. *Pflugers Arch.* 2008; 455: 951–959.
13. Bogaard HJ, Natarajan R, Henderson SC, Long CS, Kraskauskas D, Smithson L, Ockaili R, McCord JM, Voelkel NF. Chronic Pulmonary Artery Pressure Elevation Is Insufficient to Explain Right Heart Failure. *Circulation* 2009; 120: 1951–1960.
14. Al Husseini A, Bagnato G, Farkas L, Gomez-Arroyo J, Farkas D, Mizuno S, Kraskauskas D, Abbate A, Van Tassel B, Voelkel NF, Bogaard HJ. Thyroid hormone is highly permissive in angioproliferative pulmonary hypertension in rats. *Eur. Respir. J.* 2013; 41: 104–114.
15. Hislop A, Reid L. Normal structure and dimensions of the pulmonary arteries in the rat. *J. Anat.* 1978; 125: 71–83.
16. McMurtry MS, Bonnet S, Wu X, Dyck JRB, Haromy A, Hashimoto K, Michelakis ED. Dichloroacetate prevents and reverses pulmonary hypertension by inducing pulmonary artery smooth muscle cell apoptosis. *Circ. Res.* 2004; 95: 830–840.
17. De Raaf MA. Usergroup course EMKA Technologies Paris Nov 2006 and Oct 2007. Usergroup meeting DSI, Paris Jan 2008 and Mrt 2011, Berlin Mrt 2013. 2006.
18. Stacher E, Graham BB, Hunt JM, Gandjeva A, Groshong SD, McLaughlin VV, Jessup M, Grizzle WE, Aldred MA, Cool CD, Tuder RM. Modern age pathology of pulmonary arterial hypertension. *Am. J. Respir. Crit. Care Med.* 2012; 186: 261–272.
19. Sakao S. Initial apoptosis is followed by increased proliferation of apoptosis-resistant endothelial cells. *The FASEB Journal* [Internet] 2005 [cited 2012

Aug 27]; Available from: http://www.fasebj.org/cgi/doi/10.1096/fj.04-3261fje.
20. Bogaard HJ, Mizuno S, Guignabert C, Al Hussaini AA, Farkas D, Ruiter G, Kraskauskas D, Fadel E, Allegood JC, Humbert M, Noordegraaf AV, Spiegel S, Farkas L, Voelkel NF. Copper Dependence of Angioproliferation in Pulmonary Arterial Hypertension in Rats and Humans. *American Journal of Respiratory Cell and Molecular Biology* 2011; 46: 582–591.
21. Kim N, Voicu L, Hare GMT, Cheema-Dhadli S, Chong CK, Chan SKW, Bichet DG, Halperin ML, Mazer CD. Response of the Renal Inner Medulla to Hypoxia: Possible Defense Mechanisms. *Nephron Physiology* 2012; 121: p1–p7.
22. Saouti N, Westerhof N, Postmus PE, Vonk-Noordegraaf A. The arterial load in pulmonary hypertension. *European Respiratory Review* 2010; 19: 197–203.
23. 23. Peacock AJ, Naeije R, Rubin LJ. Pulmonary Circulation, 3rd edition. 3rd ed. CRC Press; 2011.
24. Kurtz TW, Griffin KA, Bidani AK, Davisson RL, Hall JE, AHA Council on High Blood Pressure Research, Professional and Public Education Subcommittee. Recommendations for blood pressure measurement in animals: summary of an AHA scientific statement from the Council on High Blood Pressure Research, Professional and Public Education Subcommittee. *Arterioscler. Thromb. Vasc. Biol.* 2005; 25: 478–479.
25. Morton DB, Hawkins P, Bevan R, Heath K, Kirkwood J, Pearce P, Scott L, Whelan G, Webb A, British Veterinary Association Animal Welfare Foundation, Fund for Replacement of Animals in Medical Experiments, Royal Society for the Prevention of Cruelty to Animals, Universities Federation for Animal Welfare. Refinements in telemetry procedures. Seventh report of the BVAAWF/FRAME/RSPCA/UFAW Joint Working Group on Refinement, Part A. *Lab. Anim.* 2003; 37: 261–299.
26. Hawkins P, Morton DB, Bevan R, Heath K, Kirkwood J, Pearce P, Scott L, Whelan G, Webb A, Joint Working Group on Refinement. Husbandry refinements for rats, mice, dogs and non-human primates used in telemetry procedures. Seventh report of the BVAAWF/FRAME/RSPCA/UFAW Joint Working Group on Refinement, Part B. *Lab. Anim.* 2004; 38: 1–10.

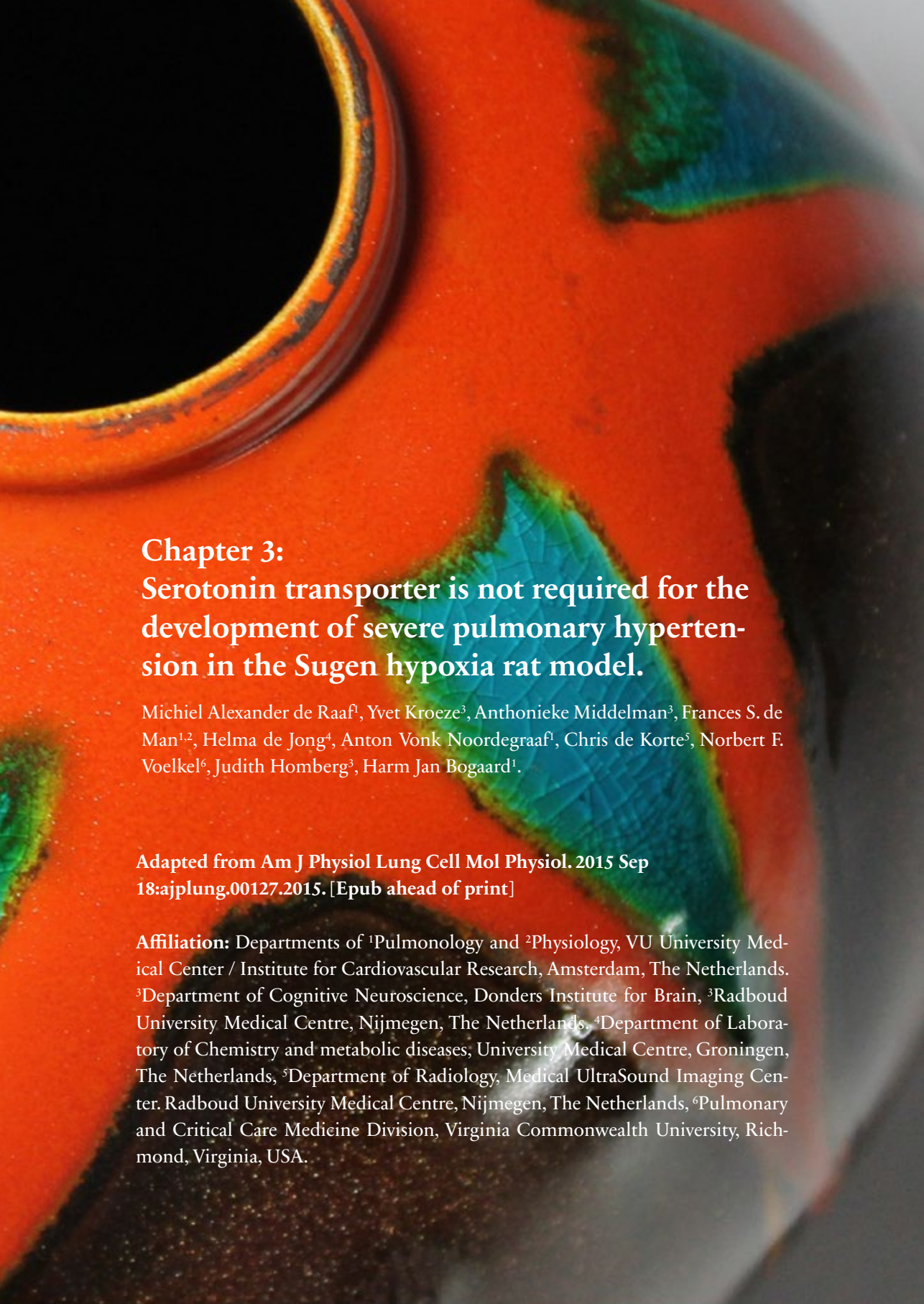

Chapter 3:
Serotonin transporter is not required for the development of severe pulmonary hypertension in the Sugen hypoxia rat model.

Michiel Alexander de Raaf[1], Yvet Kroeze[3], Anthonieke Middelman[3], Frances S. de Man[1,2], Helma de Jong[4], Anton Vonk Noordegraaf[1], Chris de Korte[5], Norbert F. Voelkel[6], Judith Homberg[3], Harm Jan Bogaard[1].

Adapted from Am J Physiol Lung Cell Mol Physiol. 2015 Sep 18:ajplung.00127.2015. [Epub ahead of print]

Affiliation: Departments of [1]Pulmonology and [2]Physiology, VU University Medical Center / Institute for Cardiovascular Research, Amsterdam, The Netherlands. [3]Department of Cognitive Neuroscience, Donders Institute for Brain, [3]Radboud University Medical Centre, Nijmegen, The Netherlands. [4]Department of Laboratory of Chemistry and metabolic diseases, University Medical Centre, Groningen, The Netherlands, [5]Department of Radiology, Medical UltraSound Imaging Center. Radboud University Medical Centre, Nijmegen, The Netherlands, [6]Pulmonary and Critical Care Medicine Division, Virginia Commonwealth University, Richmond, Virginia, USA.

Abstract:

Increased serotonin serum levels have been proposed to play a key role in Pulmonary Arterial Hypertension (PAH) by regulating vessel tone and vascular smooth muscle cell proliferation. An intact serotonin system, which critically depends on a normal function of the serotonin transporter (SERT), is required for the development of experimental pulmonary hypertension in rodents exposed to hypoxia or monocrotaline. While these animal models resemble human PAH only with respect to vascular media remodeling, we hypothesized that SERT is likewise required for the presence of lumen-obliterating intima remodeling, a hallmark of human PAH reproduced in the Sugen/hypoxia (SuHx) rat model of severe angioproliferative pulmonary hypertension. Therefore, SERT wild type (WT) and knock-out (KO) rats were exposed to the SuHx-protocol.

SERT-KO rats, while completely lacking SERT, were hemodynamically indistinguishable from WT rats. After exposure to SuHx, similar degrees of severe angioproliferative pulmonary hypertension and right ventricular hypertrophy developed in WT and KO rats (right ventricular systolic pressure 60 vs 55 mmHg, intima thickness 38 vs 30%, respectively).

In conclusion, despite its implicated importance in PAH, SERT does not play an essential role in the pathogenesis of severe angio-obliterative pulmonary hypertension in rats exposed to SuHx.

Introduction

Pulmonary Arterial Hypertension (PAH) is characterized by progressive remodeling of the pulmonary vessels, increased vascular resistance and, eventually, fatal dysfunction of the right ventricle (RV) [1]. Since the outbreaks of PAH caused by the administration of the appetite suppressants fenfluramine (Ponderal®) and Aminorex (Menocil®), which are serotonin transporter (SERT) substrates and indirect serotonergic agonists, the serotonin pathway has been attributed a key role in the pathogenesis of PAH [2–4]. Disturbances in the serotonin pathway in PAH patients include increased expression of SERT [2, 5, 6] and tryptophan hydroxase-1 (TPH1: the protein responsible for serotonin synthesis), increased extracellular serotonin levels [7, 8] and increased expression of the serotonin receptor 5-HT1B [6, 9]. Serotonin causes pulmonary vasoconstriction and pulmonary artery smooth muscle cell proliferation [9]. The many clinical associations between PAH and the serotonin system have been investigated in preclinical studies of rats exposed to monocrotaline and hypoxia. These animal models, however, only resemble PAH with respect to remodeling of the medial layer of the small pulmonary vessels (**Table 1**) [10]. Therefore, they provide no insight into the role of the serotonin pathway in intima proliferation, which is another critical characteristic of PAH [11–14]. *In-vivo* studies of models which display angioproliferation would address the question whether the serotonin pathway is essential in the pathogenesis of endothelial cell disease in PAH. We hypothesized that (increased) presence of SERT is required in the pathogenesis of severe angioproliferative pulmonary hypertension in the Sugen Hypoxia (SuHx) rat model of pulmonary hypertension. The SuHx-model is based on the combined exposure of rats to the vascular endothelial growth factor (VEGF)-inhibitor Sugen and chronic hypoxia [15–17]. The SuHx rat model develops angioproliferative remodeling of the intima with the formation of plexiform like angio-obstructive lesions and leads to RV dysfunction [15, 18–21]. Here, we used Slc6a41Hubr^{+} (SERT wildtype, WT) and Slc6a41Hubr^{-} SERT knock out (KO) rats to study the impact of a functional impairment of the serotonin system on the development of angioproliferative pulmonary vascular remodeling induced by Sugen plus hypoxia [22]. Our study reveals that SERT KO does not prohibit the development of progressive intima remodeling and pulmonary hypertension in SuHx rats. While an overactive serotonin system may be *sufficient* to induce pulmonary vascular muscularization, our findings suggest that intact serotonin signaling is not *required* for the development of angioobliterative pulmonary arterial disease.

Table 1: *Experimental models of pulmonary hypertension.*

Species	animal model			PH stimulus	RVSP in mmHg (WT/control → GMO/treatment)	
	5-HT synthesis	SERT	5-HT receptor			
Mouse	Tph1-/-			Hypoxia	20 → 14	[23]
				SuHx	47 → 38	[24]
		SERT-/-		Hypoxia	45 → 35	[25]
		SERT-/-			unchanged %	[26]
		Overexpression			35	[27, 28]
		Overexpression		Hypoxia	31→46 ♀	[29]
	Inhibitor (LP533401)	Overexpression			35→27	[27]
		Inhibitor(citalopram)		Hypoxia	36→33	[27]
		inhibitor(citalopram)		Hypoxia	32→28	[30]
		inhibitor (fluoxetine)		Hypoxia	32→26	[30]
	Inhibitor (LP533401)			Hypoxia	36→32	[27]
			5-HT2B-/-	Hypoxia	42→25 ♀♂	[6]
			5-HT1B-/-	Hypoxia	21→18	[31]
Rat		Inhibitor (fluoxetine)		MCT	60→30*	[32]
			5-HT2B inhibitor (C-122)	MCT	42→28	[33]
			5-HT2A inhibitor (sarpogrelate)	MCT	55→21*	[34]
			5-HT1B inhibitor (GR127935)	Hypoxia	66→54*	[31]
(FHR#)		Increased	Increased		susceptible	[35, 36]

**PA pressures have been calculated to RVSP [37], % data was not shown, # FHR= Fawn Hooded Rat ♀ = study was performed in female animals, ♂♀ = study was performed in both genders.*

The SERT KO rat

The full SERT KO rat was generated by N-ethyl-N-nitrosurea (ENU)-driven target-selected mutagenesis, by which method the DNA of spermatogonial stem cells was subjected to a point mutation and, by subsequent mating, a full knock-out was bred [38, 39]. By sequencing, it was found that a codon in the third exon was transferred from encoding cysteine to a stop codon [22]. This stop codon served as a full knock-out of the SERT assembly in the SERT KO rat. The lack of SERT and the absence of serotonin uptake in tissues were confirmed by the absence of SERT expression in tissues, the absence of d-fenfluramine induced hypothermia, absence of citalopram binding in the brain and by the increased bleeding times due to the absence of serotonin in blood platelets, which are fully dependent on SERT for the uptake of serotonin [22, 40, 41]. Matondo et al. measured that the serotonin level in the blood of the SERT KO rat is about 1-6% of that in the wild type [41].Homberg *et al.* phenotyped the SERT KO rat for neuroscientific use [22]. In the brain, due to the lack of SERT, intracellular serotonin level was decreased and extracellular serotonin was increased. No changes in TPH2 expression were found. Changes in compensatory systems for the serotonin system, such as dopamine and noradrenaline were not observed, which led to the conclusion that in respect to neurobiology, the phenotypic alterations were limited to serotonin alone [22]. The SERT KO rat has impaired object memory [42]. The systolic blood pressure was not altered in SERT KO rats [40]. The female SERT KO rat has more abdominal fat in comparison to the male [43].

Material and methods

Animal model

12 male Slc6a4^{1Hubr} – WT rats (SERT WT) and 12 (Slc6a4^{1Hubr} – KO) (SERT KO) male rats (Radboudumc, Nijmegen, The Netherlands) were allocated to 2 different groups: naïve control and SuHx exposed animals. SuHx mediated pulmonary hypertension was induced according to the protocol published previously [15, 17, 44]. Sugen (SU5416; Tocris Bioscience, Bristol, UK) was administered to rats weighing <200 grams as a single subcutaneous injection (25 mg/kg) [17, 45]. SuHx rats were housed from the day of injection and during the next three weeks in 10% oxygen (Biospherix Ltd. New York, USA) maintained by a nitrogen generator (Avilo, Dirksland, The Netherlands). SuHx-rats were subsequently re-exposed to normoxia for three weeks [17]. The study was approved by the local Animal Welfare committee (VU-Fys 12-15).

Echocardiography and hemodynamics

On the day of necropsy, all animals underwent echocardiographic assessments to measure RV wall thickness (RVWT) , RV end diastolic diameter (RVEDD), tricuspid annular plane systolic excursion (TAPSE), stroke volume (SV), heart rate (HR), cardiac output (CO), pulmonary artery acceleration time (PAAT) and cycle length (cl) (Philips Sonos 7500 with a S12 phased array transducer, Andover, MA, USA), as published previously [17, 46]. On the day of necropsy, RV systolic pressure (RVSP), mean pulmonary artery pressure (mPAP), end systolic elastance (Ees) and arterial elastance (Ea) (Millar Instruments, Houston, Texas) were measured, as published previously [47]. Total pulmonary resistance (TPR) was calculated as mPAP/CO and arterial ventricular coupling was derived as Ees/Ea.

Histological and morphometric analyses

After necropsy, the hematocrit was measured and heart and lungs were weighed before processing for histology. Following examination of stained histological sections, small pulmonary arteries were divided into three classes, based on external diameters: <30 µm, 30-60 µm and 60-100 µm [17, 48]. Media and intima wall thickness and percent of obliteration were measured and recorded according to previously published protocols [15, 17, 49, 50], in which closed vessels are >80% obliterated and open vessels are unaffected. Lungs were homogenized and

supernatants were extracted. According to the supplier's manual, a Western blot was performed to quantify cell proliferation (proliferating cell nuclear antigen, PCNA (FL-261): sc-7907, 1:1000 (Santa Cruz Biotechnology, Dallas, Texas), 2nd antibody HRP Anti-goat, 1:5000 (DAKO, Glostrup, Denmark)). Novex ECL chemiluminescent (Invitrogen, Carlsbad, California) was used for protein detection. Optical densities were measured and standardized with β-actin (A3854, 1:20000, Sigma, St. Louis, Missouri).

Serotonin, SERT and serotonin receptor measurements

Blood was centrifuged for 5 minutes at 1500 g to obtain plasma. Serotonin was determined in plasma and in lung tissue by using a serotonin ELISA kit (Abcam, Cambridge, UK), according to the instruction manual. ELISA measurements of plasma serotonin were confirmed by HPLC with electrochemical detection. Reagents, calibrators and internal standard (n-methylserotonin) were obtained from Chromsystems (Gräfelfing, Germany). The inter-assay variation was 5% at a level of 0.82 µmol/L. The lower limit of quantification was 0.06 µmol/L. 5-HIAA level was measured by LC-MS/MS (Waters Xevo TQ-MS, Milford, MA, USA). The expression of SERT in lungs was determined by Western blot; ST(C-20):sc-1458 (Santa Cruz Biotechnology, Dallas, Texas), 2nd antibody HRP Anti-goat, 1:5000 (DAKO, Glostrup, Denmark)). Novex ECL chemiluminescent (Invitrogen, Carlsbad, California) was used for protein detection. Optical densities were measured and standardized with β-actin (A3854, 1:20000, Sigma, St. Louis, Missouri). Presence of SERT in pulmonary vasculature was determined by immunofluorescence; ST(C-20):sc-1458 (Santa Cruz Biotechnology, Dallas, TX USA), 2nd antibody Alexa Fluor 488 anti-goat, 1:100 (ThermoFisher Scientific, Waltham, MA, USA), monoclonal anti-actin anti-smooth muscle – Cy3 antibody (Sigma Aldrich, St. Louis, MO, USA) and Slowfade Gold Antifade Mountant with DAPI (ThermoFisher Scientific, Waltham, MA, USA).

The expression of tryptophane hydroxylase 1 (TPH1, responsible for serotonin synthesis) and the receptors 5HT1B and 5HT2A were determined by QPCR (GoTaq® qPCR Master Mix (Promega Benelux b.v. Leiden, The Netherlands). Primers were designed using Primer3 online software (http://frodo.wi.mit.edu). QPCR reactions were performed on a 7500 Fast Real Time PCR System (Applied Biosystems, Foster City, CA, U.S.A) using the SYBR Green fluorescence quantification system. Using reference genes Ywhaz and Hprt, the cDNA content of the samples was normalized.

Statistical analyses

After confirmation of a normal distribution, parametric variables were compared between groups using appropriate two-way ANOVA with Bonferroni post-hoc tests. Data is presented as mean ± SEM (Graphpad, La Jolla, CA, USA).

Results

Animal strain

Clinical observation of the animals throughout the study protocol did not reveal obvious differences between WT and KO rats. Body weight was about 5-10% lower in all KO animals during the entire study. SERT expression was not present in lung tissue nor SERT was present in the pulmonary vasculature (**Figure 1A,B**), which confirms, in line with the conclusions by Smits et al. and Homberg et al. [22, 38], the full knock out of this strain. Using HPLC or ELISA, serotonin could not be detected in the plasma of SERT KO rats, while ELISA did not show presence of serotonin in lung tissue (**Figure 2A-C**). 5-HIAA levels were similar in KO and WT rats and were not altered by the SuHx protocol (**Figure2D**). WT rats, but not KO rats, showed a trend of increased TPH1 expression after SuHx exposure (**Figure 2E**). Receptor densities of 5HTR1B and 5HTR2A in the lung were not altered (**Figure 2F,G**).

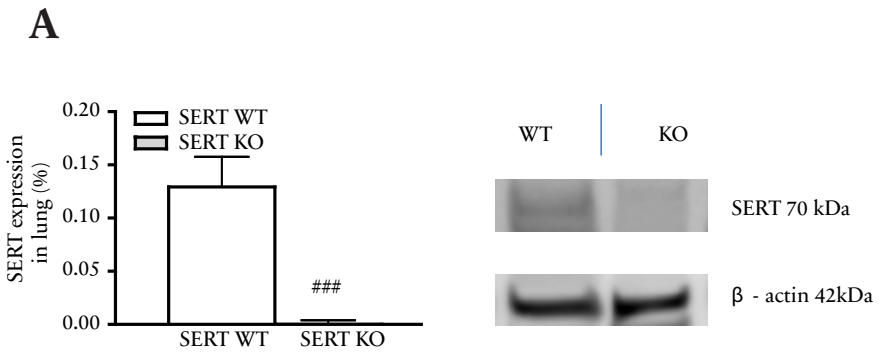

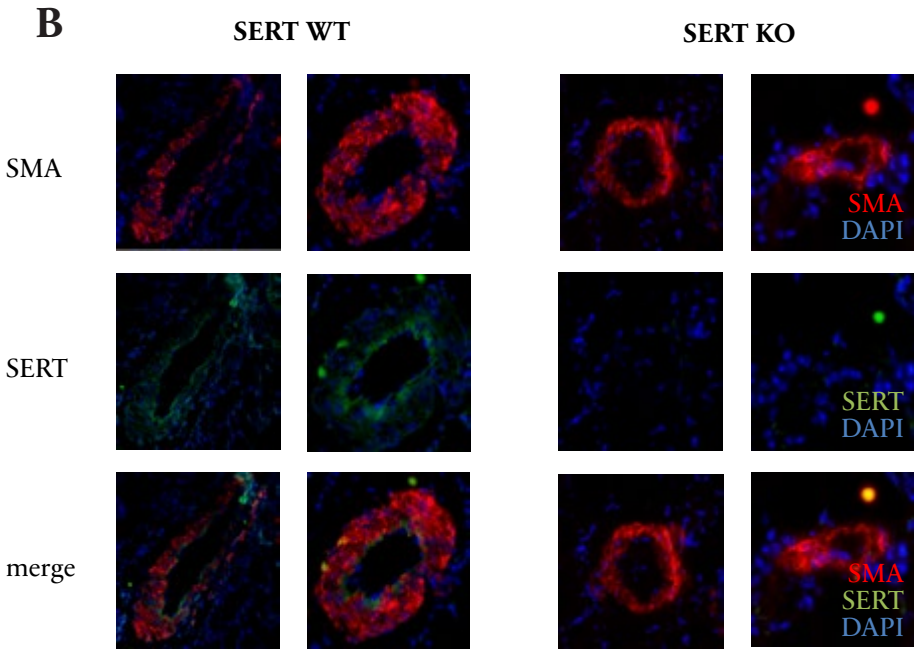

Figure 1: *Serotonin transporter expression in lungs (panel 1A) and presence of the Serotonin transporter in pulmonary vasculature (panel 1B, approximate vessel diameter is 40 micron) of wild type (WT) and knock-out (KO) rats, in naïve condition. Green (FITC) = SERT, Red (CY3) = Smooth muscle actin (SMA), Blue (DAPI) = nuclei. ### = p<0.001 for comparison between WT vs. KO; n = 6/group*

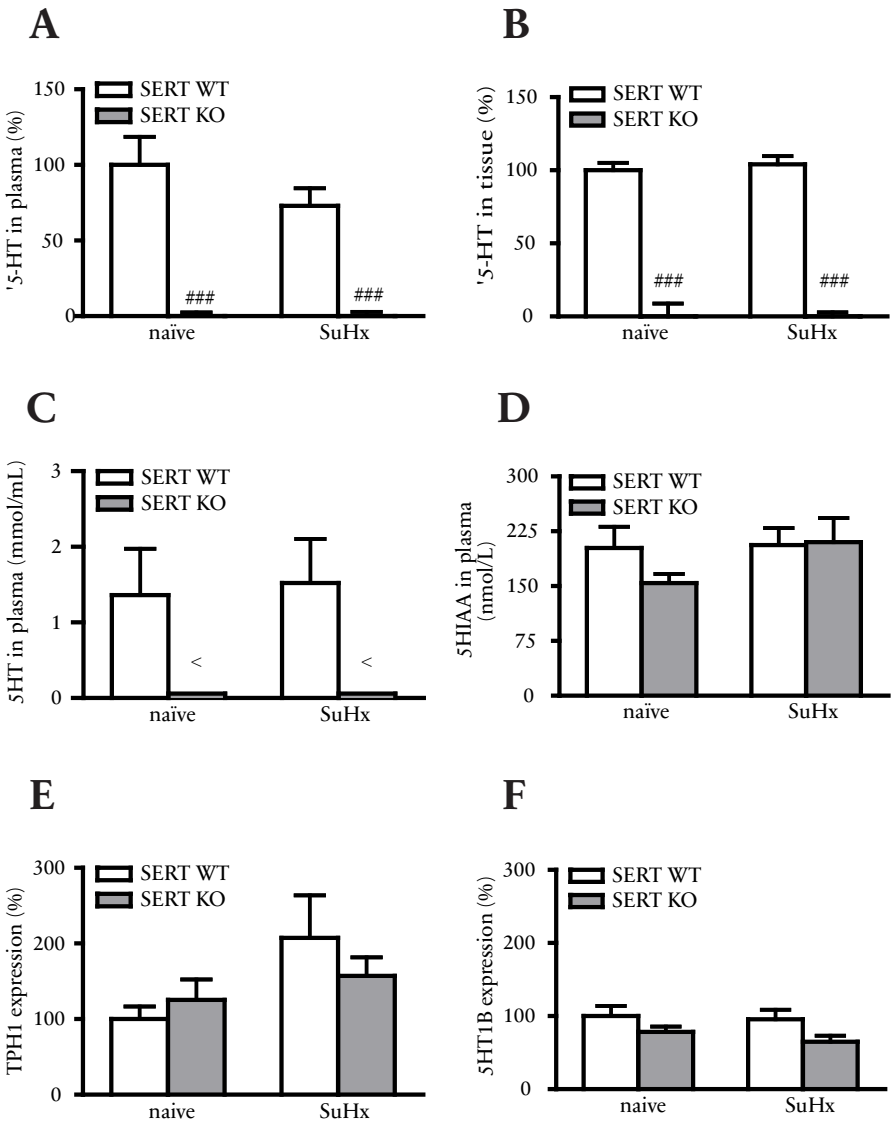
A
'5-HT in plasma (%)
150
100
50
0
SERT WT
SERT KO
###
###
naïve
SuHx
B
'5-HT in tissue (%)
150
100
50
0
SERT WT
SERT KO
###
###
naïve
SuHx
C
5HT in plasma (mmol/mL)
3
2
1
0
SERT WT
SERT KO
<
<
naïve
SuHx
D
5HIAA in plasma (nmol/L)
300
225
150
75
0
SERT WT
SERT KO
naïve
SuHx
E
TPH1 expression (%)
300
200
100
0
SERT WT
SERT KO
naive
SuHx
F
5HT1B expression (%)
300
200
100
0
SERT WT
SERT KO
naive
SuHx

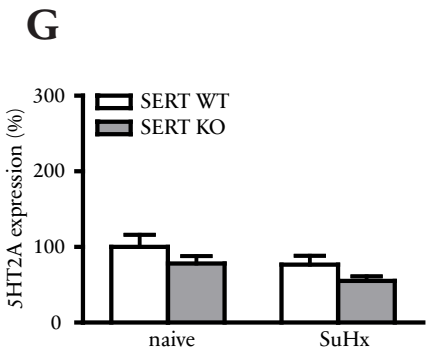

Figure 2: *Serotonin plasma levels measured by ELISA (panel 2A) and in lung tissue (panel 2B) of wild type (WT) and knock-out (KO) rats, in naïve condition and after exposure to Sugen Hypoxia (SuHx). Serotonin plasma levels were confirmed by HPLC (panel 2C), while 5-HIAA plasma levels were confirmed by GCMS (panel 2D). mRNA expression of TPH1 (panel 2E), receptor 5HT1B (panel 2F) and receptor 5HT2A (panel 2G). ### = p<0.001 for comparison between WT vs. KO; n = 6/group.*

Echocardiography and hemodynamics

Right heart remodeling after SuHx exposure was similar in WT and KO rats. All the animals showed an increase in RVWT and RVEDD and a trend towards a decrease in TAPSE (**Figure 3A-C**). PAAT/cl was decreased after SuHx exposure, but there were no differences between rat strains (**Figure 3D**). The CO was significantly lower in the SERT KO when exposed to SuHx, which was caused by a significantly lower HR (**Figure 4A-B**). SV was not different between WT and KO rats (**Figure 4C**). SuHx exposure resulted in a significant increases in RVSP, measured by right heart catheterization, in comparison to naïve control conditions (**Figure 5A**), but the RVSP was not different between SERT WT and SERT KO rats. TPR was increased in SuHx rats, WT and KO rats alike (**Figure 5B**).

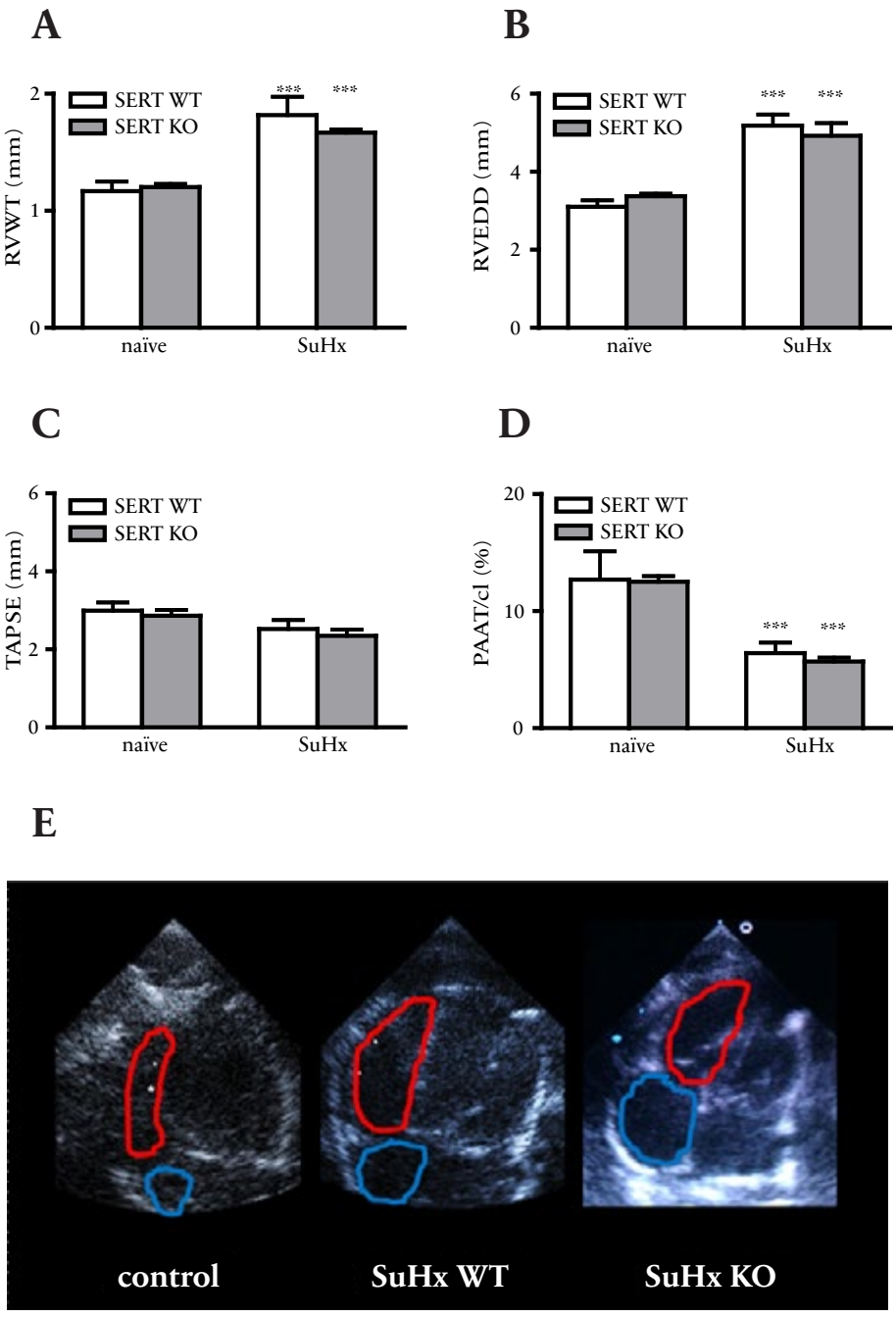
A
RVWT (mm)
SERT WT
SERT KO
naïve
SuHx
B
RVEDD (mm)
C
TAPSE (mm)
D
PAAT/cl (%)
E
control
SuHx WT
SuHx KO

Figure 3: *Echocardiographic parameters in wild type (WT) and knock-out (KO) rats, in naïve condition and after exposure to Sugen Hypoxia (SuHx). Right Ventricular Wall Thickness (RVWT, panel A), Right Ventricular End Diastolic Diameter (RVEDD, panel B), Tricuspid Annular Plane Systolic Excursion (TAPSE, panel C) and Pulmonary Artery Accelaration Time corrected for RR-cycle length (PAAT/cl, panel D) are not different between WT and KO rats, whereas significant differences were observed between naïve rats and SUHx rats. Panel E shows representative echocardiographic images of control, SuHx WT and SuHx KO rats. *** = p<0.001 for comparison between naïve vs. SuHx; n = 6/group.*

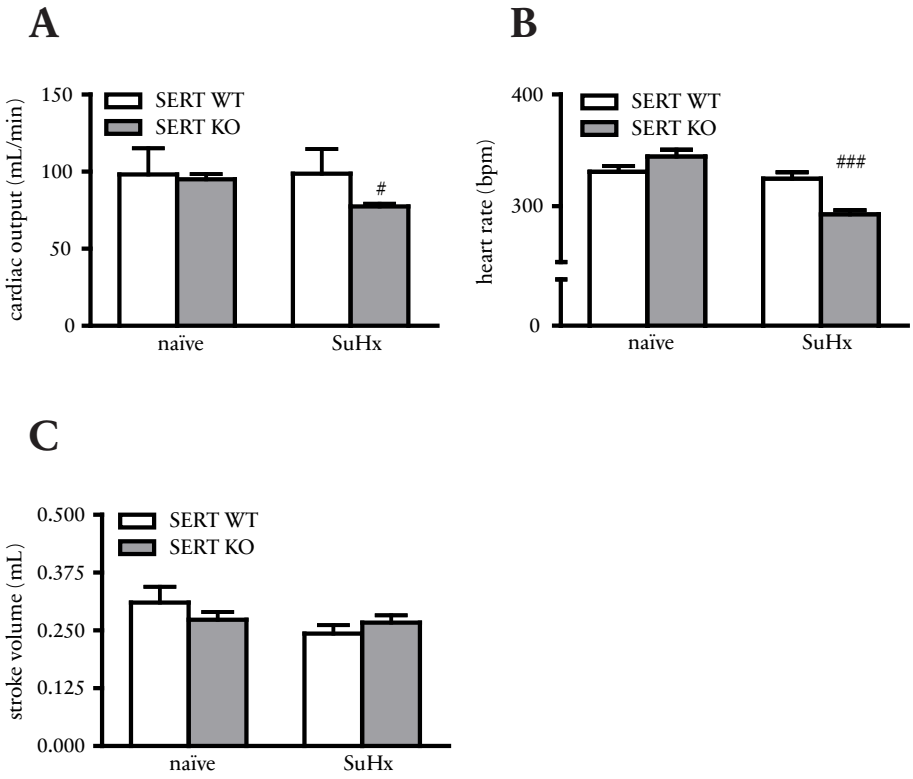

Figure 4: *Cardiac Output (CO, panel A), Stroke Volume (SV, panel B) and Heart Rate (HR, panel C) measured by echocardiography in wild type (WT) and knock-out (KO) rats, in naïve condition and after exposure to Sugen Hypoxia (SuHx). # = p<0.05 and ### = p<0.001 for comparison between WT vs. KO; n = 6/group.*

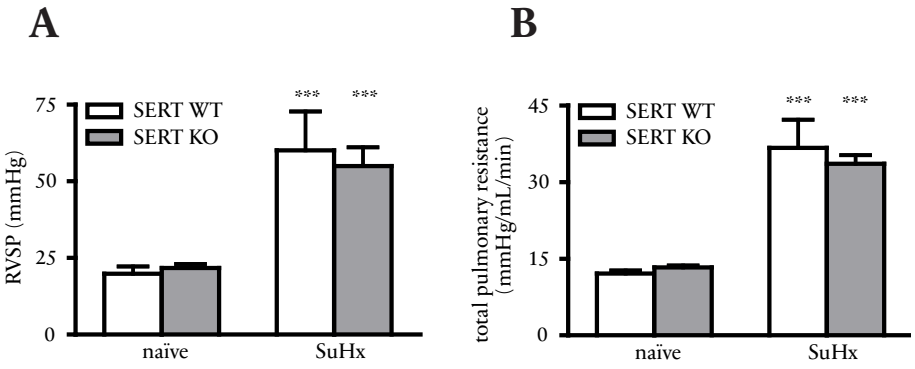

Figure 5: *Right Ventricular Systolic Pressure (RVSP, panel A) and Total Pulmonary Resistance (TPR, panel B) in wild type (WT) and knock-out (KO) rats, in naïve condition and after exposure to Sugen Hypoxia (SuHx). *** = p<0.001 for comparison between naïve vs. SuHx; n = 6/group.*

Pressure volume relationships

Ees and Ea (**Figure 6A-B**) were increased in the two SuHx groups, but not significantly different between WT and KO rats. Ees/Ea was not different between groups (**Figure 6C**).

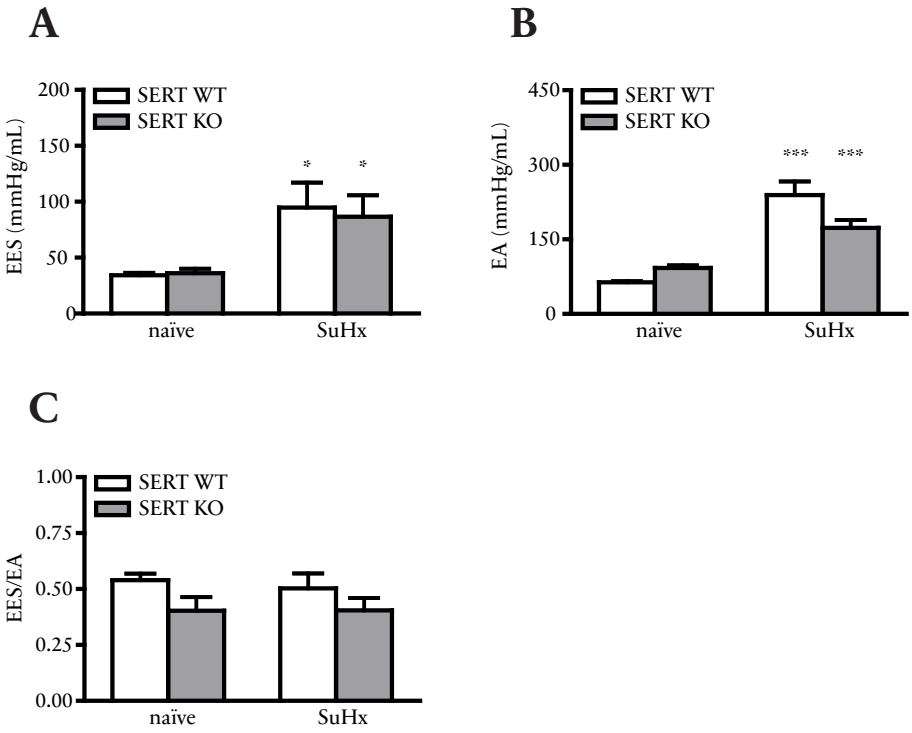

Figure 6: *End Systolic Elastance (EES, panel A), Arterial Elastance (EA, panel B) and arterial-ventricular coupling (EES/EA, panel C) in wild type (WT) and knock-out (KO) rats, in naïve condition and exposed to Sugen Hypoxia (SuHx). * = p<0.05 and *** = p<0.001 for comparison between naïve vs. SuHx; n = 6/group.*

Hematocrit and Fulton index

Hematocrit and Fulton index (RV/(LV+S)) were increased in SuHx rats, but not different between SERT WT and KO rats (**Figure 7**).

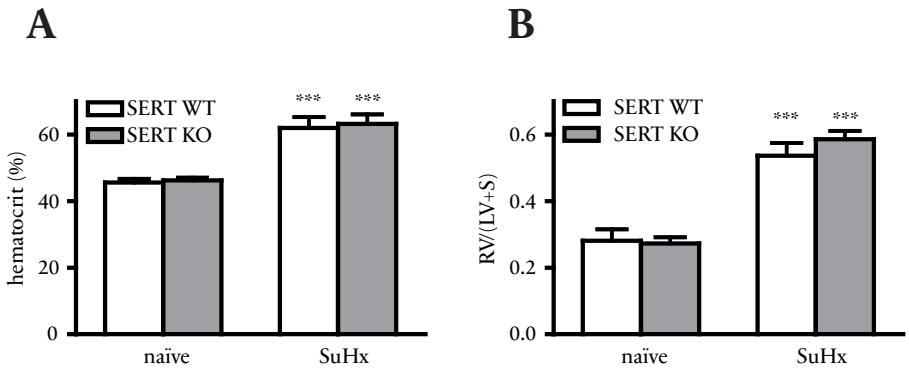

Figure 7: *Hematocrit (panel A) and fulton index (RV/LV+S, panel B) of wild type (WT) and knock-out (KO) rats, in naïve condition and after exposure to Sugen Hypoxia (SuHx). *** = p<0.001 in comparison between naïve vs. SuHx; n = 6/group.*

Pulmonary vascular remodeling

Vascular remodeling after SuHx exposure was similar in SERT WT and KO rats, with comparable degrees of medial wall and intima thickening and percent of obliteration in all vessel classes (**Figure 8A-C**). A representative overview (**Figure 8D**) and examples are shown of changes in 40µm vessels in SuHx-rats (**Figure 8C**). Western blot of proliferation marker PCNA showed no differences between WT and KO in naïve control and SuHx (**Figure 9**).

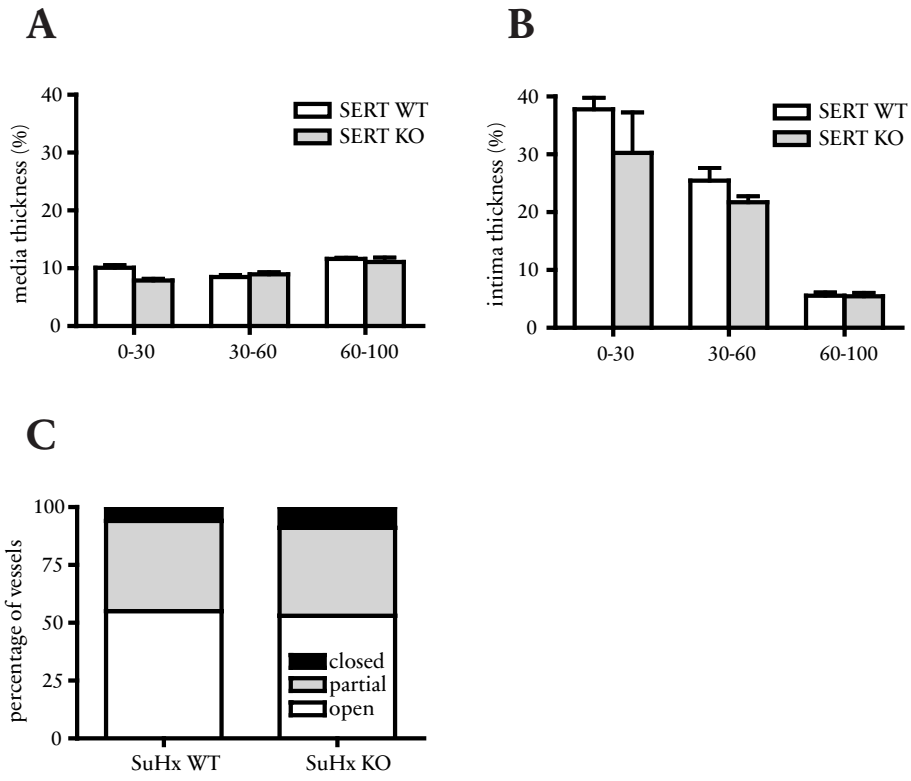
A
B
C
media thickness (%)
intima thickness (%)
SERT WT
SERT KO
0-30
30-60
60-100
percentage of vessels
closed
partial
open
SuHx WT
SuHx KO

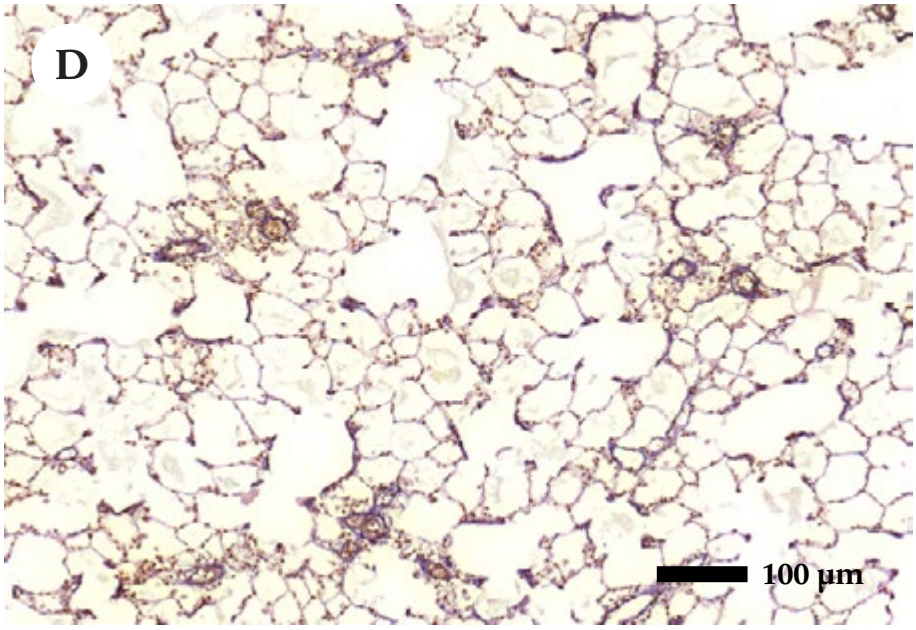
D
100 µm

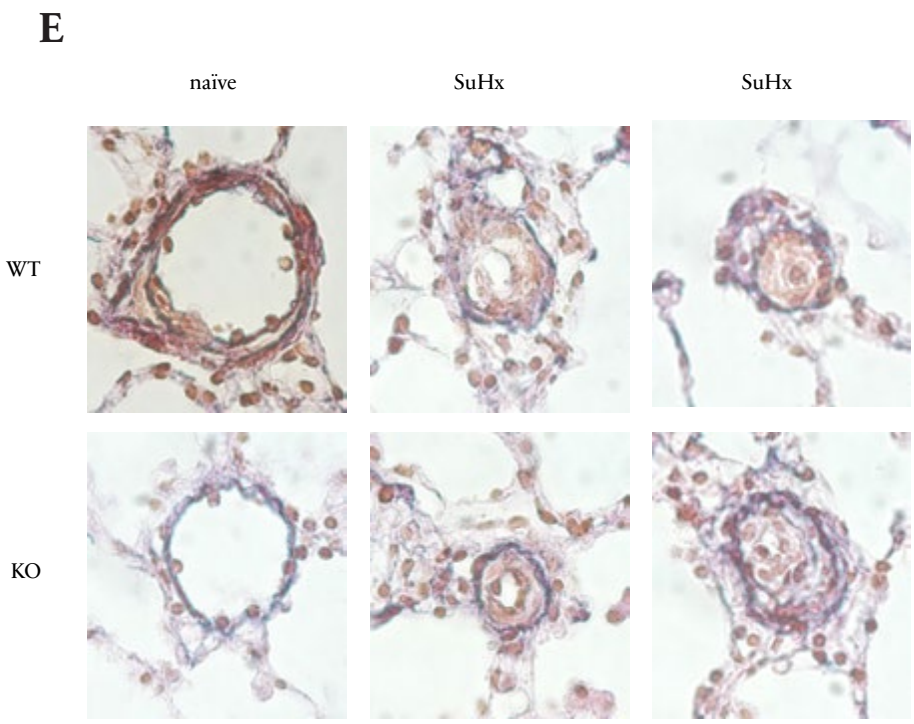

Figure 8: *Histology of medial wall thickness (panel A), intima thickness (panel B) and obliteration rate (panel C) in wild type (WT) and knock-out (KO) rats, in naïve condition and after exposure to Sugen Hypoxia (SuHx), in vessel classes 0-30 micron, 30-60 micron and 60-100 micron. Representative Elastica van Gieson stains of a SuHx lung tissue (panel D) and ~40 micron pulmonary vessels (panel E). No significant differences; n = 6/group.*

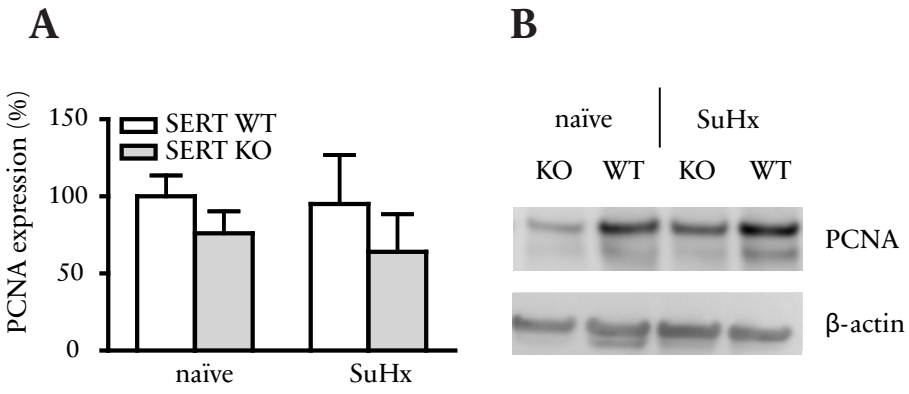

Figure 9: *Expression of the proliferation marker PCNA in wild type (WT) and knock-out (KO) rats, in naïve condition and after exposure to Sugen Hypoxia (SuHx).No significant differences; n = 6/group.*

Discussion

The main result of this study is that the absence SERT did not prevent the development of severe angioproliferative pulmonary hypertension in rats exposed to Sugen and hypoxia. SERT expression was not present in the lungs, indicating that a severely impaired serotonin system does not preclude the development of intima remodeling and vascular obliterations. A comparable increase in RVSP was found in WT and SERT KO SuHx rats, and this was reflected by similar changes in lung histology and functional cardiac measurements. A decrease in intima proliferation in SERT KO rats could have been postulated because serotonin is a known angiogenic factor [24, 51], but did not occur. In contrast to the SuHx study in TPH1 KO mice [24], the knock-out of SERT in the rat could not prevent the induction of vascular lesions and elevation of RVSP by SuHx. As a powerful regulator of vessel tone, "*a serum-tonis regulator*" [52], the effect of serotonin is directed towards the medial layer by vasoconstriction and its stimulation of smooth muscle cell proliferation [9]. It has been reported that in the mouse, the increase in RVSP upon exposure to hypoxia was partially prevented by knocking out SERT (**Table 1**) [25, 29]. The relative importance of intact serotonin signaling may even be greater in the monocrotaline model (MCT) of pulmonary hypertension, as MCT rats showed a profound up-regulation of SERT, and medial hyperplasia was fully inhibited in MCT rats treated with inhibitors of SERT and also with inhibitors of other components of the serotonin pathway (**Table 1**) [25, 32, 53]. In the SuHx model, intima remodeling plays a more dominant role in comparison to medial remodeling [17], which concentrates the desired effect on the intima solely. Here we show that SuHx induced intima remodeling and angio-obliteration is not impaired in SERT KO rats, which have a complete functional absence of SERT and undetectable levels of serotonin in plasma and lung tissue.

In the rat strain used in our study, SERT is lacking due to an impaired translation [22, 38, 39]. Because SERT is essential for transcellular transport of serotonin, platelets from SERT KO rats are serotonin free [40]. Here we confirm previous findings in mice that KO of SERT is also associated with undetectable levels of serotonin in the plasma [25]. This finding seems unrelated to altered synthesis, metabolism or degradation of serotonin because TPH1 expression and 5HIAA levels were unchanged, which is in line with the SERT KO mouse, published by Eddahibi et al. [25]. Using HPLC or ELISA, serotonin could not be detected in

the plasma of SERT KO rats, while ELISA and immunofluorescence did not show presence of serotonin nor SERT in lung tissue, respectively. Due to the protocol used, the plasma was probably not completely platelet free and the presence of ruptured platelets might have caused the increased level of serotonin in plasma of the WT rats. Because the platelets in the SERT KO rat were unable to take up serotonin, as was published previously [40], the serotonin level in plasma of KO rats was below the detectable level of 0.06 μmol/L. This result was already shown for this SERT KO rat, as in whole blood measurements the concentration of serotonin was about 1-6% of that compared to the SERT WT rat and was also reported earlier in SERT KO mice [25, 41]. Because 5-HIAA levels were not altered in KO rats, true platelet free serum concentrations of serotonin were probably normal in KO rats.Whereas undetectable plasma serotonin in SERT KO rodents remains unexplained, it does indicate a severely impaired serotonin system. The effect of SERT KO on circulating serotonin is opposite to what is observed after treatment with Selective Serotonin Re-uptake Inhibitors (SSRI's): by inhibiting SERT function in platelets SSRI's induce increased levels of circulatory serotonin [2]. It is possible that in our experimental set-up, very low concentrations of serotonin, although undetectable by HPLC, were still present and exerted vascular effects. 5HT1B expression was not altered in SERT KO rats, but it is possible that an increased sensitivity to receptor stimulation by serotonin could compensate for a loss of SERT. To fully address this question, future experiments using TPH1 inhibitors could be performed.

Our finding that the lack of SERT did not modify the hemodynamics or structural remodeling in the SuHx model, indicates that the pulmonary vascular changes in this rat model of severe PAH do not require a fully intact serotonin system. We have shown previously that changes in the medial layer in the SuHx-model are rather modest [17]. As such, the SuHx model mirrors findings in end stage PAH of major changes in the intima and not in the media of small pulmonary vessels [17, 54]. In our study, intima remodeling was present to the same degree in SuHx WT and SuHx KO rats, which implies that in this model an intact serotonin pathway does not play an essential role in the development of hyperproliferative angio-obliterative intimal lesions. We cannot exclude the possibility that this situation only applies to male rats, as we did not include female rats in our study. Recent publications have pointed to an increased sensitivity to alterations in the serotonin pathway in female compared to male mice [55–57]. Female smooth muscle cells have higher concentrations of serotonin and show higher prolifer-

ation in response to serotonin administration than male smooth muscle cells [58]. Estrogens are known to increase the protein expression of 5-HT1B receptor in smooth muscle cells [59] and therefore it has been suggested that serotonin based treatments are only, or at least more, effective in female patients [55, 58]. As indicated above, the major changes in the SuHx model take place in the vascular intima and sex differences in endothelial cell responses to serotonin signaling have not been explored. Although one could speculate that angioproliferative remodeling in the SuHx model is driven by serotonin independent mechanisms in male rats only, there is no evidence to support this hypothesis.

Serotonin has been attributed a positive inotropic action [60] and in chronic heart failure, the density of 5-HT2A and 5-HT4 receptors is increased [61, 62]. However, it is unclear whether the serotonin system directly affects cardiac function in pulmonary hypertension. The available data is inconclusive, because all studies in this context have been performed using interventions that primarily affect the pulmonary circulation. Experiments of pulmonary arterial banding would be better suitable to address cardiac specific effects of the serotonin system in a situation of pressure overload. We observed a lower CO in SERT KO SUHx rats, while all other parameters of cardiac function were not different between SERT WT and KO rats. The effect of SERT KO on CO was driven by a decrease in heart rate. Serotonin is known to regulate the autonomic regulation of heart rate [63], and although no differences in heart rate were observed in the naïve SERT KO rat, bradycardia was observed after exposure to the SuHx protocol. A mechanism to explain these findings is currently lacking. Paradoxically, the lack of SERT in the brain locally leads to increased concentrations of extracellular serotonin, which is produced by TPH2 [22]. Apparently this feedback mechanism is lacking outside the brain, as we found serotonin to be completely absent from the blood plasma and lungs.

Despite these new findings in SuHx rats, the fact that the serotonin pathway affects human PAH is well established [2]. In PAH patients, increased circulatory serotonin levels [8] were observed and increased SERT expression was measured in the lungs from PAH patients [5]. High intracellular serotonin levels trigger vasoconstriction and smooth muscle cell proliferation [64]. Increased serotonin signaling has been implicated in the development of PAH after use of serotonin re-uptake inhibitors or serotonin receptor agonists (the anorexigens dexfenfluramine and aminorex; antidepressants e.g. fluoxetine) and illicit drugs (for ex-

ample, amphetamines and cocaine) [65–68]). However, as only a fraction of the population taking these compounds will develop PAH, a second hit, in addition to excessive serotonin signaling, is apparently required. MacLean and Dempsie suggested combined inhibition of SERT and serotonin receptors as a new treatment option for PAH [2]. Our findings of unhindered angioproliferative remodeling even in absence of SERT and with undetectable levels circulatory serotonin question this therapeutic approach, within the limits of translating from animal models to the human disease. In conclusion: a fully intact serotonin system does not play an essential role in the pathobiology of severe angio-obliterative pulmonary hypertension in the rat SuHx model.

Acknowledgements

We would like to acknowledge Sjef van Hulten, Rick van der Doelen, Stefan Janssen, Dora Lopresto, Karin de Haas, (Radboud University medical center, Nijmegen, The Netherlands), Ingrid Schalij, Liza Botros (VU University medical center, Amsterdam, The Netherlands) and Manon de Raaf-Beekhuijzen for their contribution to this study by sharing their knowledge and expertise. The endocrine laboratory department (VU University medical center, Amsterdam) is acknowledged for the HPLC measurements of serotonin.

Support

Grant support was received from PAH patient association "Live Life Max" and the Dutch Lung Foundation (Longfonds #3.3.12.036). We acknowledge the support from the Netherlands CardioVascular Research Initiative: the Dutch Heart Foundation, Dutch Federation of University Medical Centers, the Netherlands Organisation for Health Research and Development, and the Royal Netherlands Academy of Sciences as well as the LeDucq foundation (PHAEDRA grant).

References

1. Simonneau G, Robbins IM, Beghetti M, Channick RN, Delcroix M, Denton CP, Elliott CG, Gaine SP, Gladwin MT, Jing Z-C, Krowka MJ, Langleben D, Nakanishi N, Souza R. Updated clinical classification of pulmonary hypertension. *J. Am. Coll. Cardiol.* 2009; 54: S43–S54.
2. Maclean MR, Dempsie Y. The serotonin hypothesis of pulmonary hypertension revisited. *Adv. Exp. Med. Biol.* 2010; 661: 309–322.
3. Souza R, Humbert M, Sztrymf B, Jaïs X, Yaïci A, Le Pavec J, Parent F, Hervé P, Soubrier F, Sitbon O, Simonneau G. Pulmonary arterial hypertension associated with fenfluramine exposure: report of 109 cases. *Eur. Respir. J.* 2008; 31: 343–348.
4. Thomas M, Ciuclan L, Hussey MJ, Press NJ. Targeting the serotonin pathway for the treatment of pulmonary arterial hypertension. *Pharmacol. Ther.* 2013; 138: 409–417.
5. Rothman RB, Ayestas MA, Dersch CM, Baumann MH. Aminorex, fenfluramine, and chlorphentermine are serotonin transporter substrates. Implications for primary pulmonary hypertension. *Circulation* 1999; 100: 869–875.
6. Launay J-M, Hervé P, Peoc'h K, Tournois C, Callebert J, Nebigil CG, Etienne N, Drouet L, Humbert M, Simonneau G, Maroteaux L. Function of the serotonin 5-hydroxytryptamine 2B receptor in pulmonary hypertension. *Nat. Med.* 2002; 8: 1129–1135.
7. Eddahibi S, Guignabert C, Barlier-Mur A-M, Dewachter L, Fadel E, Dartevelle P, Humbert M, Simonneau G, Hanoun N, Saurini F, Hamon M, Adnot S. Cross talk between endothelial and smooth muscle cells in pulmonary hypertension: critical role for serotonin-induced smooth muscle hyperplasia. *Circulation* 2006; 113: 1857–1864.
8. Hervé P, Launay JM, Scrobohaci ML, Brenot F, Simonneau G, Petitpretz P, Poubeau P, Cerrina J, Duroux P, Drouet L. Increased plasma serotonin in primary pulmonary hypertension. *Am. J. Med.* 1995; 99: 249–254.
9. Lawrie A, Spiekerkoetter E, Martinez EC, Ambartsumian N, Sheward WJ, MacLean MR, Harmar AJ, Schmidt A-M, Lukanidin E, Rabinovitch M. Interdependent serotonin transporter and receptor pathways regulate S100A4/Mts1, a gene associated with pulmonary vascular disease. *Circ. Res.* 2005; 97: 227–235.
10. Stenmark KR, Meyrick B, Galie N, Mooi WJ, McMurtry IF. Animal models of pulmonary arterial hypertension: the hope for etiological discovery and

pharmacological cure. *Am. J. Physiol. Lung Cell Mol. Physiol.* 2009; 297: L1013–L1032.
11. Hanahan D, Weinberg RA. The hallmarks of cancer. *Cell* 2000; 100: 57–70.
12. Hanahan D, Weinberg RA. Hallmarks of cancer: the next generation. *Cell* 2011; 144: 646–674.
13. Rai PR, Cool CD, King JAC, Stevens T, Burns N, Winn RA, Kasper M, Voelkel NF. The cancer paradigm of severe pulmonary arterial hypertension. *Am. J. Respir. Crit. Care Med.* 2008; 178: 558–564.
14. Guignabert C, Tu L, Le Hiress M, Ricard N, Sattler C, Seferian A, Huertas A, Humbert M, Montani D. Pathogenesis of pulmonary arterial hypertension: lessons from cancer. *Eur Respir Rev* 2013; 22: 543–551.
15. Taraseviciene-Stewart L, Kasahara Y, Alger L, Hirth P, Mc Mahon G, Waltenberger J, Voelkel NF, Tuder RM. Inhibition of the VEGF receptor 2 combined with chronic hypoxia causes cell death-dependent pulmonary endothelial cell proliferation and severe pulmonary hypertension. *FASEB J.* 2001; 15: 427–438.
16. Nicolls MR, Mizuno S, Taraseviciene-Stewart L, Farkas L, Drake JI, Husseini A Al, Gomez-Arroyo JG, Voelkel NF, Bogaard HJ. New models of pulmonary hypertension based on VEGF receptor blockade-induced endothelial cell apoptosis. *Pulm Circ* 2012; 2: 434–442.
17. de Raaf MA, Schalij I, Gomez-Arroyo JG, Rol N, Happé C, de Man FS, Vonk-Noordegraaf A, Westerhof N, Voelkel NF, Bogaard HJ. SuHx rat model: partly reversible pulmonary hypertension and progressive intima obstruction. *Eur. Respir. J.* 2014; .
18. Abe K, Toba M, Alzoubi A, Ito M, Fagan KA, Cool CD, Voelkel NF, McMurtry IF, Oka M. Formation of plexiform lesions in experimental severe pulmonary arterial hypertension. *Circulation* 2010; 121: 2747–2754.
19. Taraseviciene-Stewart L, Scerbavicius R, Choe K-H, Cool C, Wood K, Tuder RM, Burns N, Kasper M, Voelkel NF. Simvastatin causes endothelial cell apoptosis and attenuates severe pulmonary hypertension. *Am. J. Physiol. Lung Cell Mol. Physiol.* 2006; 291: L668–L676.
20. Bogaard HJ, Natarajan R, Mizuno S, Abbate A, Chang PJ, Chau VQ, Hoke NN, Kraskauskas D, Kasper M, Salloum FN, Voelkel NF. Adrenergic receptor blockade reverses right heart remodeling and dysfunction in pulmonary hypertensive rats. *Am. J. Respir. Crit. Care Med.* 2010; 182: 652–660.
21. Gomez-Arroyo J, Saleem SJ, Mizuno S, Syed AA, Bogaard HJ, Abbate A, Taraseviciene-Stewart L, Sung Y, Kraskauskas D, Farkas D, Conrad DH, Nicolls

MR, Voelkel NF. A brief overview of mouse models of pulmonary arterial hypertension: problems and prospects. *Am. J. Physiol. Lung Cell Mol. Physiol.* 2012; 302: L977–L991.

22. Homberg JR, Olivier JDA, Smits BMG, Mul JD, Mudde J, Verheul M, Nieuwenhuizen OFM, Cools AR, Ronken E, Cremers T, Schoffelmeer ANM, Ellenbroek BA, Cuppen E. Characterization of the serotonin transporter knockout rat: a selective change in the functioning of the serotonergic system. *Neuroscience* 2007; 146: 1662–1676.
23. Morecroft I, Dempsie Y, Bader M, Walther DJ, Kotnik K, Loughlin L, Nilsen M, MacLean MR. Effect of tryptophan hydroxylase 1 deficiency on the development of hypoxia-induced pulmonary hypertension. *Hypertension* 2007; 49: 232–236.
24. Ciuclan L, Hussey MJ, Burton V, Good R, Duggan N, Beach S, Jones P, Fox R, Clay I, Bonneau O, Konstantinova I, Pearce A, Rowlands DJ, Jarai G, Westwick J, MacLean MR, Thomas M. Imatinib attenuates hypoxia-induced pulmonary arterial hypertension pathology via reduction in 5-hydroxytryptamine through inhibition of tryptophan hydroxylase 1 expression. *Am. J. Respir. Crit. Care Med.* 2013; 187: 78–89.
25. Eddahibi S, Hanoun N, Lanfumey L, Lesch KP, Raffestin B, Hamon M, Adnot S. Attenuated hypoxic pulmonary hypertension in mice lacking the 5-hydroxytryptamine transporter gene. *J. Clin. Invest.* 2000; 105: 1555–1562.
26. Crona D, Harral J, Adnot S, Eddahibi S, West J. Gene expression in lungs of mice lacking the 5-hydroxytryptamine transporter gene. *BMC Pulm Med* 2009; 9: 19.
27. Abid S, Houssaini A, Chevarin C, Marcos E, Tissot C-M, Gary-Bobo G, Wan F, Mouraret N, Amsellem V, Dubois-Randé J-L, Hamon M, Adnot S. Inhibition of gut- and lung-derived serotonin attenuates pulmonary hypertension in mice. *Am. J. Physiol. Lung Cell Mol. Physiol.* 2012; 303: L500–L508.
28. Guignabert C, Izikki M, Tu LI, Li Z, Zadigue P, Barlier-Mur A-M, Hanoun N, Rodman D, Hamon M, Adnot S, Eddahibi S. Transgenic mice overexpressing the 5-hydroxytryptamine transporter gene in smooth muscle develop pulmonary hypertension. *Circ. Res.* 2006; 98: 1323–1330.
29. MacLean MR, Deuchar GA, Hicks MN, Morecroft I, Shen S, Sheward J, Colston J, Loughlin L, Nilsen M, Dempsie Y, Harmar A. Overexpression of the 5-hydroxytryptamine transporter gene: effect on pulmonary hemodynamics and hypoxia-induced pulmonary hypertension. *Circulation* 2004; 109: 2150–2155.

30. Marcos E, Adnot S, Pham MH, Nosjean A, Raffestin B, Hamon M, Eddahibi S. Serotonin transporter inhibitors protect against hypoxic pulmonary hypertension. *Am. J. Respir. Crit. Care Med.* 2003; 168: 487–493.
31. Keegan A, Morecroft I, Smillie D, Hicks MN, MacLean MR. Contribution of the 5-HT(1B) receptor to hypoxia-induced pulmonary hypertension: converging evidence using 5-HT(1B)-receptor knockout mice and the 5-HT(1B/1D)-receptor antagonist GR127935. *Circ. Res.* 2001; 89: 1231–1239.
32. Guignabert C, Raffestin B, Benferhat R, Raoul W, Zadigue P, Rideau D, Hamon M, Adnot S, Eddahibi S. Serotonin transporter inhibition prevents and reverses monocrotaline-induced pulmonary hypertension in rats. *Circulation* 2005; 111: 2812–2819.
33. Zopf DA, Neves LAA das, Nikula KJ, Huang J, Senese PB, Gralinski MR. C-122, a novel antagonist of serotonin receptor 5-HT2B, prevents monocrotaline-induced pulmonary arterial hypertension in rats. *Eur. J. Pharmacol.* 2011; 670: 195–203.
34. Hironaka E, Hongo M, Sakai A, Mawatari E, Terasawa F, Okumura N, Yamazaki A, Ushiyama Y, Yazaki Y, Kinoshita O. Serotonin receptor antagonist inhibits monocrotaline-induced pulmonary hypertension and prolongs survival in rats. *Cardiovasc. Res.* 2003; 60: 692–699.
35. Morecroft I, Loughlin L, Nilsen M, Colston J, Dempsie Y, Sheward J, Harmar A, MacLean MR. Functional interactions between 5-hydroxytryptamine receptors and the serotonin transporter in pulmonary arteries. *J. Pharmacol. Exp. Ther.* 2005; 313: 539–548.
36. Sato K, Webb S, Tucker A, Rabinovitch M, O'Brien RF, McMurtry IF, Stelzner TJ. Factors influencing the idiopathic development of pulmonary hypertension in the fawn hooded rat. *Am. Rev. Respir. Dis.* 1992; 145: 793–797.
37. Chemla D, Castelain V, Humbert M, Hébert J-L, Simonneau G, Lecarpentier Y, Hervé P. New formula for predicting mean pulmonary artery pressure using systolic pulmonary artery pressure. *Chest* 2004; 126: 1313–1317.
38. Smits BMG, Mudde JB, van de Belt J, Verheul M, Olivier J, Homberg J, Guryev V, Cools AR, Ellenbroek BA, Plasterk RHA, Cuppen E. Generation of gene knockouts and mutant models in the laboratory rat by ENU-driven target-selected mutagenesis. *Pharmacogenet. Genomics* 2006; 16: 159–169.
39. Smits BMG, Mudde J, Plasterk RHA, Cuppen E. Target-selected mutagenesis of the rat. *Genomics* 2004; 83: 332–334.
40. Homberg J, Mudde J, Braam B, Ellenbroek B, Cuppen E, Joles JA. Blood pressure in mutant rats lacking the 5-hydroxytryptamine transporter. *Hyper-*

tension 2006; 48: e115–e116; author reply e117.
41. Matondo RB, Punt C, Homberg J, Toussaint MJM, Kisjes R, Korporaal SJA, Akkerman JWN, Cuppen E, de Bruin A. Deletion of the serotonin transporter in rats disturbs serotonin homeostasis without impairing liver regeneration. *Am. J. Physiol. Gastrointest. Liver Physiol.* 2009; 296: G963–G968.
42. Olivier JDA, Jans LAW, Blokland A, Broers NJ, Homberg JR, Ellenbroek BA, Cools AR. Serotonin transporter deficiency in rats contributes to impaired object memory. *Genes Brain Behav.* 2009; 8: 829–834.
43. Homberg JR, la Fleur SE, Cuppen E. Serotonin transporter deficiency increases abdominal fat in female, but not male rats. *Obesity (Silver Spring)* 2010; 18: 137–145.
44. Bogaard HJ, Natarajan R, Henderson SC, Long CS, Kraskauskas D, Smithson L, Ockaili R, McCord JM, Voelkel NF. Chronic Pulmonary Artery Pressure Elevation Is Insufficient to Explain Right Heart Failure. *Circulation* 2009; 120: 1951–1960.
45. Husseini A Al, Bagnato G, Farkas L, Gomez-Arroyo J, Farkas D, Mizuno S, Kraskauskas D, Abbate A, Van Tassel B, Voelkel NF, Bogaard HJ. Thyroid hormone is highly permissive in angioproliferative pulmonary hypertension in rats. *Eur. Respir. J.* 2013; 41: 104–114.
46. Handoko ML, Schalij I, Kramer K, Sebkhi A, Postmus PE, van der Laarse WJ, Paulus WJ, Vonk-Noordegraaf A. A refined radio-telemetry technique to monitor right ventricle or pulmonary artery pressures in rats: a useful tool in pulmonary hypertension research. *Pflugers Arch.* 2008; 455: 951–959.
47. de Man FS, Handoko ML, van Ballegoij JJM, Schalij I, Bogaards SJP, Postmus PE, van der Velden J, Westerhof N, Paulus WJ, Vonk-Noordegraaf A. Bisoprolol delays progression towards right heart failure in experimental pulmonary hypertension. *Circ Heart Fail* 2012; 5: 97–105.
48. Hislop A, Reid L. Normal structure and dimensions of the pulmonary arteries in the rat. *J. Anat.* 1978; 125: 71–83.
49. Okada K, Tanaka Y, Bernstein M, Zhang W, Patterson GA, Botney MD. Pulmonary hemodynamics modify the rat pulmonary artery response to injury. A neointimal model of pulmonary hypertension. *Am. J. Pathol.* 1997; 151: 1019–1025.
50. Oka M, Homma N, Taraseviciene-Stewart L, Morris KG, Kraskauskas D, Burns N, Voelkel NF, McMurtry IF. Rho kinase-mediated vasoconstriction is important in severe occlusive pulmonary arterial hypertension in rats. *Circ. Res.* 2007; 100: 923–929.

51. Peters MAM, Walenkamp AME, Kema IP, Meijer C, de Vries EGE, Oosting SF. Dopamine and serotonin regulate tumor behavior by affecting angiogenesis. *Drug Resist. Updat.* 2014; 17: 96–104.
52. RAPPORT MM, GREEN AA, PAGE IH. Serum vasoconstrictor, serotonin; isolation and characterization. *J. Biol. Chem.* 1948; 176: 1243–1251.
53. Laudi S, Trump S, Schmitz V, West J, McMurtry IF, Mutlak H, Christians U, Weimann J, Kaisers U, Steudel W. Serotonin transporter protein in pulmonary hypertensive rats treated with atorvastatin. *Am. J. Physiol. Lung Cell Mol. Physiol.* 2007; 293: L630–L638.
54. Stacher E, Graham BB, Hunt JM, Gandjeva A, Groshong SD, McLaughlin VV, Jessup M, Grizzle WE, Aldred MA, Cool CD, Tuder RM. Modern age pathology of pulmonary arterial hypertension. *Am. J. Respir. Crit. Care Med.* 2012; 186: 261–272.
55. Mair KM, Johansen AKZ, Wright AF, Wallace E, MacLean MR. Pulmonary arterial hypertension: basis of sex differences in incidence and treatment response. *Br. J. Pharmacol.* 2014; 171: 567–579.
56. Wallace E, Morrell NW, Yang XD, Long L, Stevens H, Nilsen M, Loughlin L, Mair KM, Baker AH, MacLean MR. A Sex-specific MicroRNA-96/5HT1B Axis Influences Development of Pulmonary Hypertension. *Am. J. Respir. Crit. Care Med.* 2015; .
57. White K, Loughlin L, Maqbool Z, Nilsen M, McClure J, Dempsie Y, Baker AH, MacLean MR. Serotonin transporter, sex, and hypoxia: microarray analysis in the pulmonary arteries of mice identifies genes with relevance to human PAH. *Physiol. Genomics* 2011; 43: 417–437.
58. Mair KM, Yang XD, Long L, White K, Wallace E, Ewart M-A, Docherty CK, Morrell NW, MacLean MR. Sex affects bone morphogenetic protein type II receptor signaling in pulmonary artery smooth muscle cells. *Am. J. Respir. Crit. Care Med.* 2015; 191: 693–703.
59. Austin ED, Hamid R, Hemnes AR, Loyd JE, Blackwell T, Yu C, Phillips Iii JA, Gaddipati R, Gladson S, Gu E, West J, Lane KB. BMPR2 expression is suppressed by signaling through the estrogen receptor. *Biol Sex Differ* 2012; 3: 6.
60. Qvigstad E, Brattelid T, Sjaastad I, Andressen KW, Krobert KA, Birkeland JA, Sejersted OM, Kaumann AJ, Skomedal T, Osnes J-B, Levy FO. Appearance of a ventricular 5-HT4 receptor-mediated inotropic response to serotonin in heart failure. *Cardiovasc. Res.* 2005; 65: 869–878.
61. Qvigstad E, Sjaastad I, Brattelid T, Nunn C, Swift F, Birkeland JAK, Krobert KA, Andersen GØ, Sejersted OM, Osnes J-B, Levy FO, Skomedal T. Dual se-

rotonergic regulation of ventricular contractile force through 5-HT2A and 5-HT4 receptors induced in the acute failing heart. *Circ. Res.* 2005; 97: 268–276.

62. Levy FO, Qvigstad E, Krobert KA, Skomedal T, Osnes J-B. Effects of serotonin in failing cardiac ventricle: signalling mechanisms and potential therapeutic implications. *Neuropharmacology* 2008; 55: 1066–1071.
63. Pérgola PE, Alper RH. Effects of central serotonin on autonomic control of heart rate in intact and baroreceptor deficient rats. *Brain Res.* 1992; 582: 215–220.
64. Morecroft I, Heeley RP, Prentice HM, Kirk A, MacLean MR. 5-hydroxytryptamine receptors mediating contraction in human small muscular pulmonary arteries: importance of the 5-HT1B receptor. *Br. J. Pharmacol.* 1999; 128: 730–734.
65. Eddahibi S, Morrell N, d'Ortho MP, Naeije R, Adnot S. Pathobiology of pulmonary arterial hypertension. *Eur. Respir. J.* 2002; 20: 1559–1572.
66. Taraseviciute A, Voelkel NF. Severe pulmonary hypertension in postmenopausal obese women. *Eur. J. Med. Res.* 2006; 11: 198–202.
67. Chin KM, Channick RN, Rubin LJ. Is methamphetamine use associated with idiopathic pulmonary arterial hypertension? *Chest* 2006; 130: 1657–1663.
68. Chambers CD, Hernandez-Diaz S, Van Marter LJ, Werler MM, Louik C, Jones KL, Mitchell AA. Selective serotonin-reuptake inhibitors and risk of persistent pulmonary hypertension of the newborn. *N. Engl. J. Med.* 2006; 354: 579–587.

Chapter 4:
Pneumonectomy combined with SU5416 induces severe pulmonary hypertension in rats

C.M. Happé[1,2], M.A. de Raaf[1,2], D.Bos[1,2], N.Rol[1,2], I.Schalij[1,2] A. Vonk-Noordegraaf[2], N. Westerhof[1], N.F. Voelkel[3], F.S. de Man[2], H.J. Bogaard[2]

Adapted from the submitted manuscript

Affiliation: [1]Department of Physiology and [2]Pulmonology, Institute for Cardiovascular Research (ICaR-VU) / VU University Medical Center, Amsterdam, the Netherlands. [3]School of Pharmacy, Virginia Commonwealth University, Richmond, VA, USA

Abstract

The SU5416+Hypoxia (SuHx) is a now rather commonly used model of severe pulmonary arterial hypertension (PAH). Previous studies have suggested that pulmonary hypertension in this model is partly reversible after return to normoxia. We tested whether an increased blood flow to one (right) lung, after left pneumonectomy, combined with SU5416 (SuPNx), is sufficient to induce irreversible PH.

Sprague Dawley rats were subjected to either a SuHx or SuPNx protocol. Comparisons between models were made at week 2 and 6 utilizing echocardiography to determine cardiac morphometry and function, right ventricle (RV) catheterizations to determine RV blood pressure and RV-arterial coupling and tissue and molecular analysis to examine pulmonary vascular remodeling, proliferation, apoptosis and inflammation.

Both SuHx and SuPNx models displayed obliterative vascular remodeling leading to an increased right ventricular systolic pressure at week 6. Increased proliferative activity and rates of apoptosis were accompanied by inflammation in the lung vasculature in both models

The combination of SU5416 and PNx causes severe angio-obliterative pulmonary hypertension involving cell proliferation and apoptosis. This model features progressive and irreversible PAH at 6 weeks and is a suitable alternative to the SuHx model.

Introduction

Pulmonary Arterial Hypertension (PAH) is a group of progressive diseases, characterized by angio-obliterative lesions of the small precapillary resistance vessels resulting in increased pulmonary vascular resistance ultimately leading to right heart failure and death [1]. The arterial changes are based on pathobiological mechanisms that are to some degree shared with cancer including hyperproliferative angiogenesis and altered endothelial cell biology [2, 3]. At the same time it is well accepted that a disturbed blood flow may be important in the pathogenesis and pathobiology of PAH, in particular in those forms associated with congenital systemic to pulmonary shunts [4, 5] This concept is supported by animal studies based on disturbed blood flow, such as the monocrotaline (MCT) + pneumonectomy rat model [6, 7] and the MCT + aorta-caval shunt rat model [4, 8]. A 'wound healing gone awry' concept can connect the concepts of quasi-malignancy and flow–dependent alterations in the development of PAH [9].

Recently, we have characterized the Sugen-Hypoxia (SuHx) model by performing longitudinal histology and telemetric monitoring of the Right Ventricular Systolic Pressure (RVSP) [10, 11]. We showed partial reversibility of pulmonary hypertension and RV hypertrophy in this model after return to a normoxic environment and also that subsequent disease progression in the model was not dependent on remodeling of the lung vascular media. As such, hypoxia-induced changes in pulmonary artery smooth muscle cells seemed not required to maintain the obliterative vascular phenotype in rats with advanced SuHx induced PAH [11]. It can be hypothesized that the exuberant lumen obliterating cell growth in the SuHx lung vasculature is only partly and temporarily driven by hypoxic up regulation of HIF-1α protein expression. Changes in pulmonary blood flow velocity, first driven by hypoxic vasoconstriction and later by vascular obliteration, may play an additional causative role in the evolution of abnormal vascular cell phenotypes in the SuHx model.

The fact that hypoxia is not an obligatory secondary hit in SU5416 induced angio-obliterative PAH is exemplified by the development of other SU5416 mediated animal models that lack the stimulus of hypoxia, such as the Sugen Ovalbumin model [12]. The aim of the present study was to evaluate whether the combination of VEGF receptor blockade by SU5416 and an increase in pulmonary blood flow velocity, is sufficient to induce lung vascular cell proliferation and severe

angioobliterative pulmonary lesions. To achieve this, the hypoxic component of the SuHx model was substituted by a left pneumonectomy, to create a Sugen Pneumonectomy (SuPNx) model. In addition to disease progression, functional endpoints were monitored and compared with the SuHx model.

Materials and methods

Animals

All experiments were approved by the Institutional Animal Care and Use Committee of the VU University and were conducted in accordance with the European Convention for the Protection of Vertebrate Animals used for Experimental and Other Scientific Purposes, and the Dutch Animal Experimentation Act. Male Sprague Dawley rats (n= 60, 6-8 weeks, Charles River, Sulzfeld, Germany) were group housed (4/cage) under controlled conditions (22°C, 12:12 h light/dark cycle). Food and water were available ad libitum. All rats that developed signs of right heart failure (>15% loss of body mass in 2 days, lethargy, cyanosis and/or respiratory distress) were killed before the defined end of the protocol in accordance with the animal care committee protocol (FYS12-18, FYS-13-01).

Study design

Rats were randomly divided between five groups: Control (Con), SU5416 (SU), Pneumonectomy (PNx), SU5416 + hypoxia (SuHx) and SU5416 +PNx (SuPNx), (see (**Figure 1**) for an overview). The SuHx protocol was employed as previously described [11]. Briefly, animals were injected with SU5416 (25 mg/kg, Tocris Bioscience, #3037, Bristol, United Kingdom) dissolved in carboxymethycellulose (CMC) and exposed to hypoxia (10%) for four weeks followed by re-exposure to normoxia. PNx animals underwent a left pneumonectomy. Two days following PNx-surgery an injection of SU5416 was administered (25 mg/kg).The Con-group received only the solvent CMC.

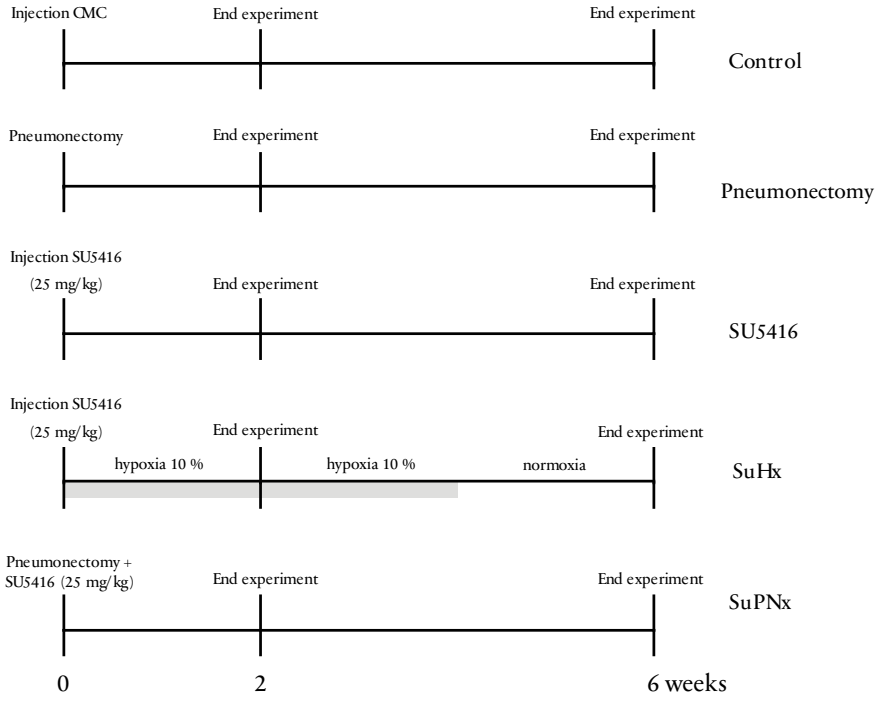

Figure 1: *Study design. 5 groups of N=12 (6 per time point). SuHx= SU5416+Hypoxia; SuPNx= SU5416+Pneumonectomy.*

Surgical Procedure

Thirty minutes prior to anaesthesia (Isoflurane; 4.0/2.5% induction/maintance; 1:1 O2/Air mix) and intubation (Teflon tube, 16 gauge) rats received an injection of buprenorphine analgesia (0,1 mg/kg). Rats were ventilated at a rate of 70/minute with a peak pressure of 10 cmH_2O and placed in half supine position on a heating pad. The surgical site was shaved and cleaned with chlorhexidine digluconate in 70% ethanol (Addedpharma, Oss, Netherlands). Heart rate, saturation, carbon dioxide levels and temperature were monitored at all times during the surgery. Thoracotomy was performed by opening the third intercostal space. Ventilation was briefly interrupted for a maximum of 30 seconds to fix the lung outside off the chest cavity with the use of Q-tips. Bronchus, artery and veins were ligated and the lung was removed. The thorax was closed by suturing of the muscular and dermal layers. After cessation of isoflurane administration animals

were extubated and received an additional injection of sterile saline (3 ml) and Carprofen (4.0 mg/kg) subcutaneous (Rimdadyl, Pfizer, Capelle aan den IJssel, the Netherlands).

Echocardiography

Echocardiography was utilized at baseline, week two and week six. Measurements (ProSound SSD-4000, 13-MHz linear transducer #UST-5542, Aloka, Tokyo, Japan) were performed on anesthetized rats (2,5% isoflurane, 1:1 O2/Air mix). Measured parameters were pulmonary artery acceleration time (PAAT), right ventricular wall thickness (RVWT) and end diastolic diameter (RVEDD), cycle length (CL) and tricuspid annular plane systolic excursion (TAPSE). Derived parameters were cardiac output, total pulmonary resistance (TPR), PAAT/CL, heart rate (HR) and stroke volume (SV). Analysis was performed offline (Tomtec Imaging systems, Unterschleisscheim, Germany).

Right ventricle pressure measurements

Two and six weeks post-surgery/post-hypoxia animals were anesthetized and right ventricle (RV) and left ventricle (LV) pressure measurements via catheterization were performed via an open-chest RV catheterization under general anesthesia in all animals (2.5% isoflurane, 1:1 O2/air mix). Before the procedure, rats were intubated (Teflon tube, 16 gauge) and attached to a mechanical ventilator (Micro-Ventilator, UNO, Zevenaar, the Netherlands; ventilator settings: breathing frequency, 70 breaths per minute; pressures, 12/0 cm H2O; inspiratory/expiratory ratio, 1:1). RV pressures were recorded by use of a microtip pressure-volume conductance catheter (Millar Instruments, Houston, TX). Analyses were performed when steady state was reached over an interval of at least 10 seconds. Animals were killed via exsanguination and organs were weighed and processed for analysis.

Histology and morphometry

Lungs were weighed and the airways of the right middle lobe were filled with 0.5% low-melt agarose in saline under constant pressure of 25 mmHg and stored in formaline (#4169-30, Klinipath BV, Duiven, The Netherlands). The remaining lobes were stored in liquid nitrogen for further processing. The heart was perfused with tyrode solution, weighed, dissected, snap-frozen in liquid nitrogen and stored in -80°C. Transversally cut lung sections (4µm) were stained with elastica van Gieson and hematoxylin - eosin (H&E) for analysis of vascular dimen-

sions for week two and six. Occlusion rate was determined by counting the presence of open, partially closed and fully closed vessels (total of 50) in randomly selected high power fields. For immunofluorescence staining, lung sections were deparaffinized and epitope retrieval was performed by immersing the slides in antigen unmasking solution (H3300, Vector Laboratories) for 40 minutes in a pressure cooker. Blocking steps with 1% bovine serum albumin were performed, before labeling with the primary antibody Von Willebrand Factor (VWF, ab8822, Abcam) O/N in 4°C, except for negative control. Subsequent labeling with appropriate secondary antibody, anti-actin α-smooth-muscle-actin – Cy3 (α-SMA, C6198, Sigma), and 4'6-diamidino-2-phenylindole (DAPI, H-1200, Vector Labs) counterstaining followed. Image acquisition was performed on a ZEISS Axiovert 200M Marianas inverted microscope.

Statistical Analysis

All analyses were performed in a blinded fashion. All data were verified for normal distribution. A p-value <0,05 was considered significant. All data are presented as mean ±SEM. Parameters were analysed by two-way ANOVA with Bonferroni post-hoc testing (GraphPad Prism for Windows 5.01, San Diego CA).

Results

Effect of SU5416- or pneumonecomty alone.

Results of the effects of SU5416- and pneumonectomy alone are summarized in tables I and II (**Table 1 and 2**). Right lung mass was found to be increased in the pneumonectomy group compared to control both after 2 and 6 weeks of initiation experiment. CD68 (macrophage) was found to be increased in the SU-group compared to control at week 2.

Table 1: *overview of echocardiography, hemodynamics and pulmonary vascular remodeling in control situation and after 2 weeks of exposure to SU5416 or pneumonectomy alone.*

2 weeks				
	CON	SU	PNX	P-VALUE
PAAT/CL	13,7 ± 4,9	16,9 ± 4,4	13,1 ± 2,1	n.s.
RVWT (mm)	1,0 ± 0,3	1,0 ± 0,1	0,9 ± 0,4	n.s.
RVEDD (mm)	2,3 ± 0,4	3,0 ± 0,3	2,8 ± 0,2	n.s.
TAPSE (mm)	3,2 ± 0,2	3,2 ± 0,3	2,9 ± 0,5	n.s.
ESP (mmHg)	2,5 ± 2,5	23,5 ± 1,9	29,6 ± 8,2	n.s.
EES (mmHg/ml)	55,6 ± 22,2	52,3 ± 25,1	42,0 ± 17,3	n.s.
EED (mmHg/ml)	3,1 ± 0,9	2,1 ± 0,9	3,4 ± 3,1	n.s.
EA (mmHg/ml)	101,0 ± 33,0	143,0 ± 31,0	120,0 ± 32,5	n.s.
SV (ml)	0,2 ± 0,06	0,2 ± 0,03	0,2 ± 0,06	n.s.
HR (bpm)	409,0 ± 23,6	384,7 ± 21,5	370,9 ± 23,0	n.s.
CO (ml)	88,2 ± 20,2	64,4 ± 10,4	80,3 ± 18,4	n.s.
TPR (mmHg/ml.min)	0,3 ± 0,1	0,3 ± 0,1	0,3 ± 0,1	n.s.
Intima fraction (%)	7,9 ± 1,3	10,1 ± 2,8	8,8 ± 0,5	n.s.
Media fraction (%)	10,5 ± 1,5	12,8 ± 1,3	14,1 ± 2,0	n.s.
Right lung mass (gr)	24,2 ± 3,1	41,9 ± 8,4	54,1 ± 13,5	0,05
Fulton/RV/(LV+S)	0,3 ± 0,1	0,4 ± 0,2	0,4 ± 0,1	n.s.

Table 2: *overview of echocardiography, hemodynamics and pulmonary vascular remodeling in control situation and after 6 weeks of exposure to SU5416 or pneumonectomy alone.*

	6 weeks			
	CON	SU	PNX	P-VALUE
PAAT/CL	15,5 ± 3,5	11,8 ± 3,9	12,5 ± 2,2	n.s.
RVWT (mm)	1,1 ± 0,2	1,2 ± 0,3	1,4 ± 0,2	n.s.
RVEDD (mm)	3,9 ± 0,8	4,4 ± 0,9	4,9 ± 1,1	n.s.
TAPSE (mm)	2,6 ± 0,5	2,7 ± 0,6	2,7 ± 0,4	n.s.
ESP (mmHg)	22,9 ± 4,5	24,0 ± 6,3	25,2 ± 2,3	n.s.
EES (mmHg/ml)	30,4 ± 10,0	33,9 ± 11,0	31,0 ± 11,8	n.s.
EED (mmHg/ml)	2,3 ± 0,9	2,6 ± 0,8	1,8 ± 0,7	n.s.
EA (mmHg/ml)	94,4 ± 52,9	112,3 ± 47,7	101,5 ± 24,4	n.s.
SV (ml)	0,2 ± 0,05	0,2 ± 0,04	0,2 ± 0,03	n.s.
HR (bpm)	345,0 ± 8,0	333,0 ± 42,0	383,0 ± 23,0	n.s.
CO (ml)	80,9 ± 19,9	72,9 ± 15,6	69,7 ± 11,9	n.s.
TPR (mmHg/ml.min)	0,2 ± 0,1	0,3 ± 0,0	0,4 ± 0,1	n.s.
Intima fraction (%)	7,6 ± 0,1	12,0 ± 1,5	12,2 ± 1,6	n.s.
Media fraction (%)	12,0 ± 2,8	16,7 ± 2,4	21,2 ± 8,2	n.s.
Right lung mass (gr)	26,3 ± 2,2	30,5 ± 4,8	43,9 ± 12,5	0,05
Fulton/RV/(LV+S)	0,2 ± 0,0	0,2 ± 0,1	0,3 ± 0,1	n.s.

Progressive pulmonary hypertension in SuHx and SuPNx rats.

RVSP was significantly elevated after two weeks in the SuHx model compared to Con and SuPNx, whereas no differences in RVSP were observed between SuPNx and control animals. Six weeks after initiation of the protocol both SuHx and SuPNx demonstrated an increased RVSP when compared to Con (**Figure 2A**). RV afterload (Ea) was significantly increased in both SuHx and SuPNx after six weeks (**Figure 2B**). RV Contractility (Ees) significantly increased in SuHx at week two compared to Con and SuPNx. SuPNx Ees at six weeks was significantly higher than Con, while no significant differences between groups in RV stiffness (Eed) were observed (**Figure 2C-D**). Coupling (Ees/Ea) was not significantly different between groups.

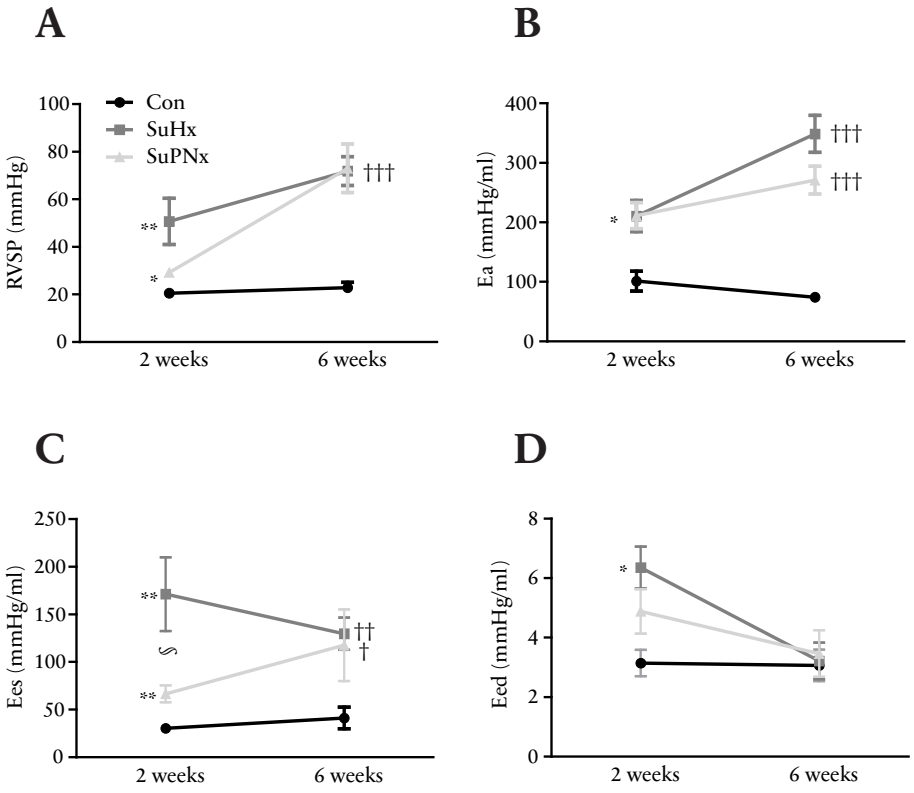

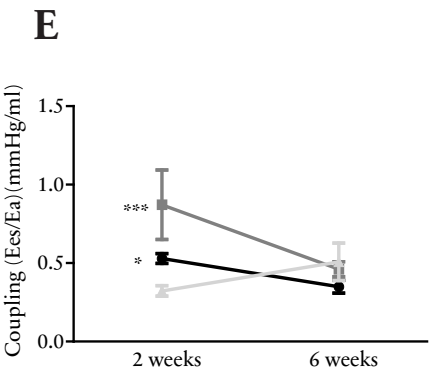

Figure 2: *Pressure-volume measurements. A: Right ventricle systolic pressure (RVSP); B: RV afterload (Ea); C:RV Contractility (end systolic elastance/Ees); D:RV stiffness (end diastolic stiffness/Eed) E: Coupling (Ees/Ea) ; Con= Control; SuHx= SU5416+Hypoxia ; SuPNx= SU5416+Pneumonectomy; * = p<0,05; *** = p<0,001; ††=p<0,01; †††=p<0,001; §= p<0.05; (*= SuHx/SuPNx vs. Con 2 weeks; †= Suhx/SuPNx vs. Con 6 weeks; §= SuHx vs. SuPNx)*

Total pulmonary resistance (TPR) was increased in SuHx and SuPNx rats after week six, which was in accordance with the increased Ea (**Figure 3A**). No differences in stroke volume index (SVI) were observed between groups (Figure 3B). The minor differences in heart rate at week two (**Figure 3C**) did not result in differences in cardiac index (Figure 3D). Pulmonary artery acceleration time / cycle length (PAAT/CL) was reduced in both SuHx and SuPNx at week six compared to Control animals (Figure 3E). RV wall thickness (RVWT) and end diastolic diameter (RVEDD) were increased at week two in SuHx rats when compared to both Controls and SuPNx, whilst after six weeks, RVWT and RVEDD were increased in SuHx and SuPNx rats alike (**Figure 3F-G**). Tricuspid annular plane excursion time (TAPSE) was decreased in SuHx at week two compared to Control animals. Both SuHx and SuPNx showed a further decline in TAPSE over time (**Figure 3H**)

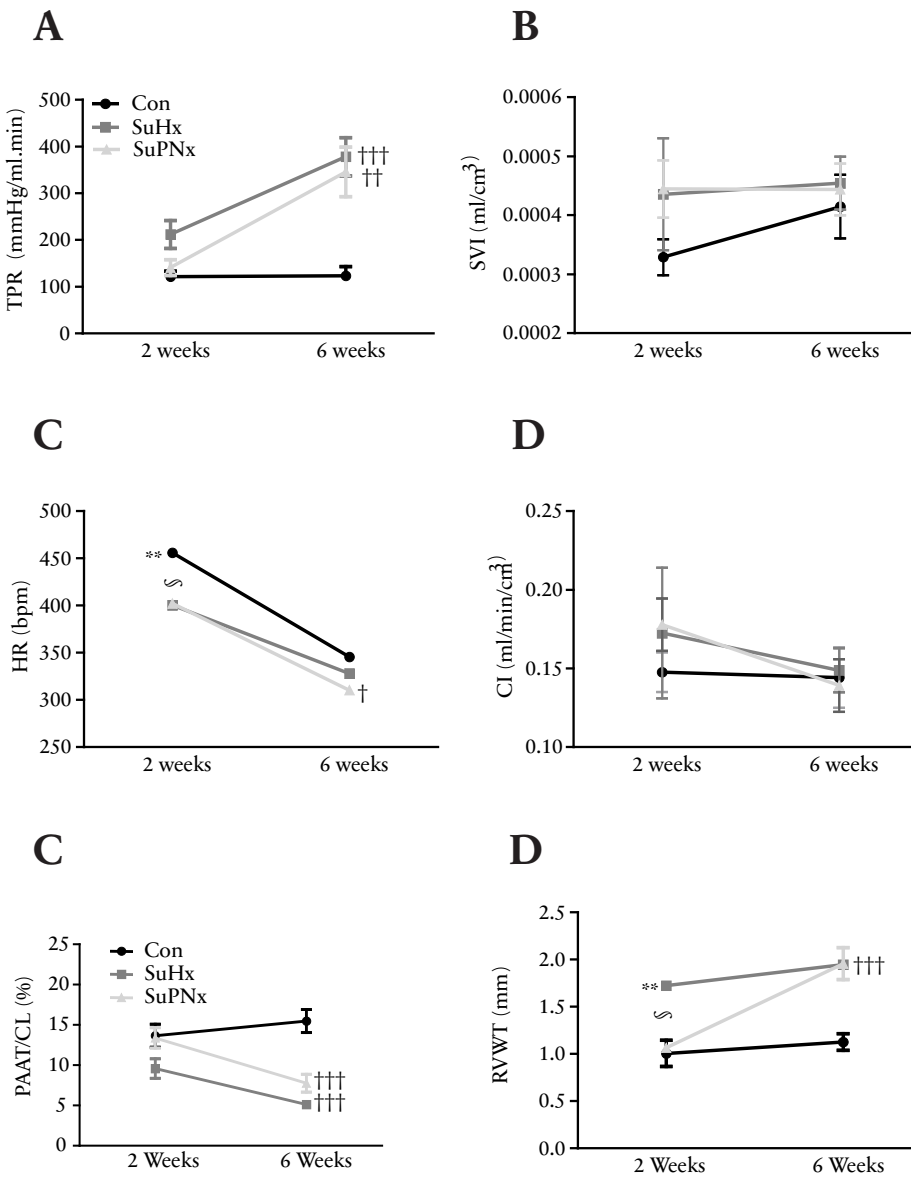
A
B
C
D
C
D
TPR (mmHg/ml.min)
Con
SuHx
SuPNx
2 weeks
6 weeks
SVI (ml/cm3)
HR (bpm)
CI (ml/min/cm3)
PAAT/CL (%)
2 Weeks
6 Weeks
RVWT (mm)

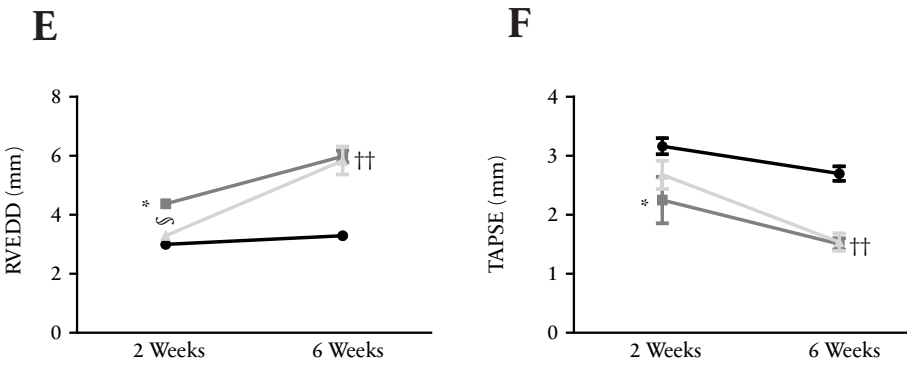

Figure 3: *Echocardiography parameters A: Total pulmonary resistance (TPR); B: Stroke volume index (SVI); C: Heart rate (HR); D: Cardiac index (CI); E: Pulmonary artery acceleration time / cycle length (PAAT/CL); F: Right ventricle wall thickness (RVWT); G: Right ventricle end diastolic diameter (RVEDD); H: Tricuspid annular plane systolic excursion (TAPSE); Con= Control; SuHx= SU5416+Hypoxia; SuPNx= SU5416+Pneumonectomy; * = p<0,05; ** = p<0,01; ††=p<0,01; †††=p<0,001; §= p<0.05; (*= SuHx/SuPNx vs. Con 2 weeks; †= Suhx/SuPNx vs. Con 6 weeks; §= SuHx vs. SuPNx)*

Right lung mass was increased at both time points in the SuPNx group, compared to Con and SuHx (**Figure 4A**). Suhx left lung mass was increased compare to Con at week two and six. At week two, the Fulton index in SuHx was higher when compared to Control and SuPNx animals. At week six both SuHx and SuPNx showed an increased Fulton index compared to Control animals (**Figure 4B**). The hematocrit levels were increased in the SuHx model at week two (hypoxic period) (**Figure 4C**). Bodymass of SuHx and SuPNx was significantly lower compared to Con at week two and six. SuHx bodymass mass at week two was lower compared to SuPNx (**Figure 4D**).

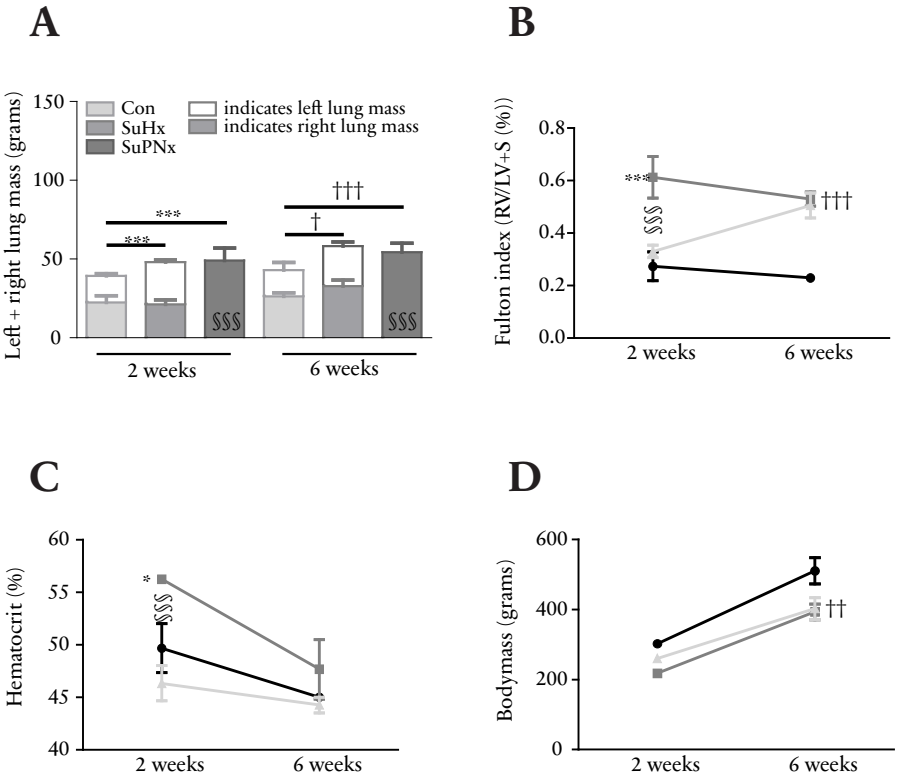

Figure 4: *Lung mass, Fulton index, Hematocrit and Body mass. A: Right and left lung mass. Left lung indicated by striped pattern; B: Fulton index (RV/LV+S)(%); C: Hematocrit (%); D: Bodymass (gr); Con= Control; SuHx= SU5416+Hypoxia; SuPNx= SU5416+Pneumonectomy; *= p<0,05; ***= p<0,001; †=p<0,05; ††=p<0,01; †††=p<0,001; §§§= p<0.001; (*= SuHx/SuPNx vs. Con 2 weeks; †= Suhx/SuPNx vs. Con 6 weeks; §= SuHx vs. SuPNx)*

Increased intimal fraction accompanied by obliterative lesions in SuHx and SuPNx

The vascular wall media fraction was already increased in SuPNx at week two, when compared to Con and SuHx, with similar elevated fractions of both SuHx and SuPNx at week six. By contrast, the intimal fraction increased earlier in the SuHx group, with equal fractions between SuHx and SuPNx at week six (**Figure 5A-C**). Overviews (10x magnification) of lung morphology reveal obliterative lesions in SuHx and SuPNx at week six (**Figure 5D-F**).

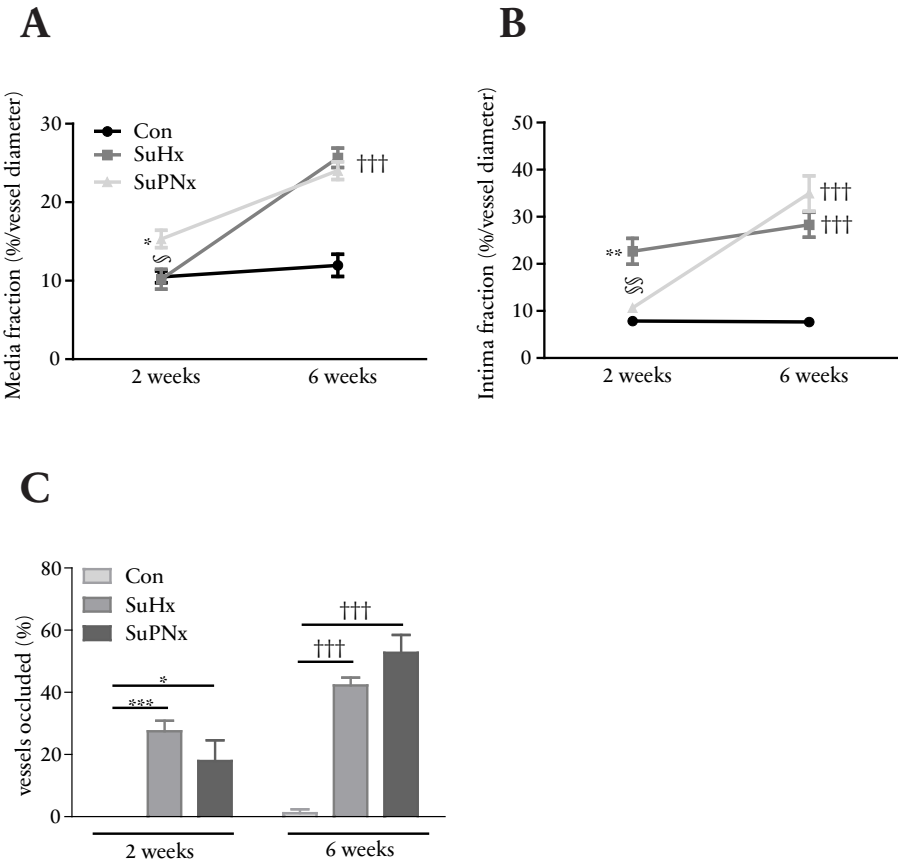
A
Media fraction (%/vessel diameter)
30
20
10
0
Con
SuHx
SuPNx
*
§§
†††
2 weeks
6 weeks
B
Intima fraction (%/vessel diameter)
50
40
30
20
10
0
**
§§
†††
†††
2 weeks
6 weeks
C
vessels occluded (%)
80
60
40
20
0
Con
SuHx
SuPNx
*
***
†††
†††
2 weeks
6 weeks

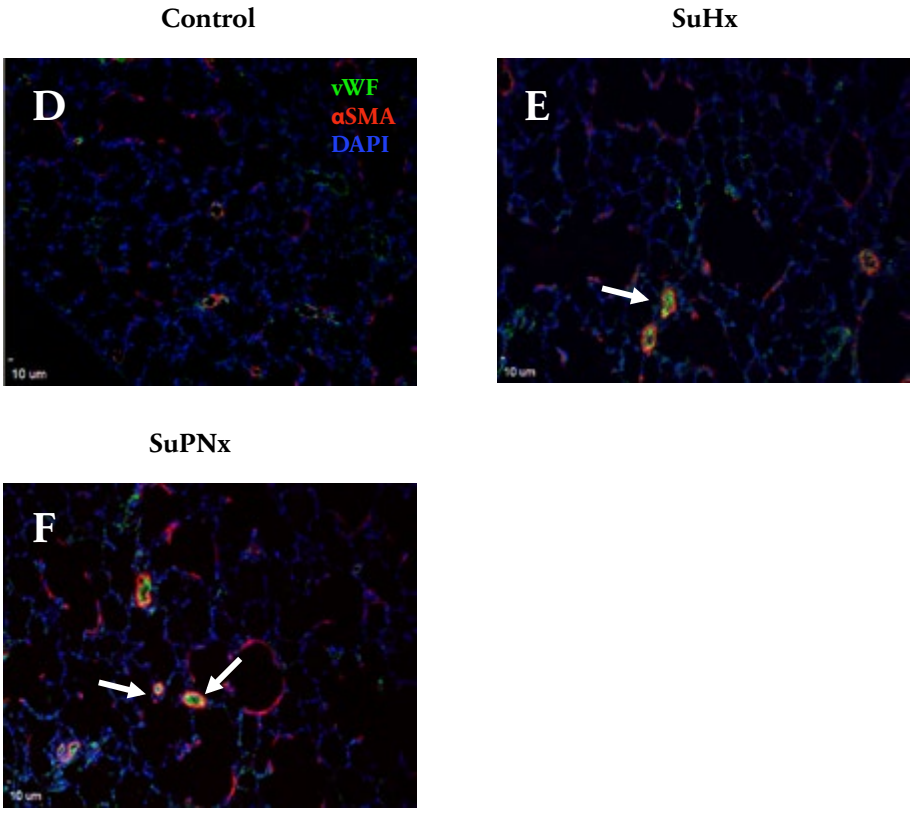

Figure 5: *Vascular remodeling A: Media fraction thickness; B: Intima fraction thickness; C: vessels occluded (%); Con= Control; SuHx= SU5416+Hypoxia; SuPNx= SU5416+Pneumonectomy; *= p<0,05; **= p<0,01; ***= p<0,001; †††=p<0,001; §= p<0.05; §§= p<0.01; n.s.= not significant (*= Suhx/SuPNx vs. Con 2 weeks; †= Suhx/SuPNx vs. Con 6 weeks; §= SuHx vs. SuPNx). Overview (magnification 100x) of lung vasculature Green = von-Willebrand Factor (ECs); Red = α-smooth-muscle-actin (SMC); Blue = DAPI (nuclei) in D: Control, E: SuHx and F: SuPNx. White arrows indicate occlusions.*

Discussion

To our knowledge this study is the first full report on the combined lung vascular effects of pneumonectomy and SU5416 in rats. In the current study, several important hallmarks of human PAH were detected in the rat model that combines PNx and one single injection of the VEGF receptor antagonist SU5416. These include severe pulmonary hypertension, angio-obliterative vascular lesions and increased rates of proliferation and pro-apoptotic signaling of lung endothelial and smooth muscle cells and RV dysfunction which shows many similarities to the SuHx model. The present study confirms that an increase in pulmonary blood flow velocity, combined with VEGF receptor blockade, is sufficient to establish PAH in rats. Additionally, our study supports the two-hit hypothesis of severe PAH, similar to previous studies in which PNx was paired with the administration of MCT [13, 14]. Other SU5416 based interventions that induce a similar vascular phenotype are the models of SU5416 plus chronic hypoxia (SuHx) [15–17] and SU5416 plus immune deregulation [12, 18].

SU5416 combined with pneumonectomy induces severe PH

As determined by echocardiography and pressure-volume analysis of the RV, the combination of SU5416 and PNx caused RV dysfunction as is frequently observed in severe PAH. Measurements of RVEDD and RVWT confirmed increased RV hypertrophy and dimensions, which findings were confirmed by an increase in RV/LV+S. In addition, the systolic function of the RV was affected as shown by a significant decrease in TAPSE. TPR was increased due to extensive pulmonary vascular changes. We found an increase in right lung mass in SuPNx which is possibly explained by compensatory lung growth and/or influx of inflammatory cells after pneumonectomy [19, 20].

The increase in TPR in SuPNx rats was associated with an increased pulmonary arteriolar mean wall thickness. Pneumonectomy combined with MCT[13, 16] induces neotintimal proliferation as does the combination of MCT with an abdominal aortacaval shunt [23]. Although MCT models are extensively used, concerns have been raised with regard to their translational value [24]. Besides the systemic side effects caused by the MCT as liver toxicity, the model shows a beneficial treatment response, while similar treatments are refractory in human disease. The vascular lesions observed in the SuPNx model show a great similarity with the characteristic lesions observed in the SuHx model. A hypothetical

explanation for the similarities between these models is that pneumonectomy (through a reduction in pulmonary vascular bed) and hypoxic exposure (through vasoconstriction) both exert their effects via an increased pulmonary blood flow velocity. We propose that the shear stress-induced activation and injury of lung vascular endothelial cells cannot be repaired when SU5416 impairs signaling via VEGF receptors, which is required for the homeostatic maintenance of lung vessels [25]. Since VEGFR2 and VEGFR3 are both part of a mechanosensory complex in endothelial cells it can be argued that SU5416 interferes with this complex, thereby hampering EC mechanosensing [26, 27]. A failure of normal adaptation to changes in shear stress may be crucial to the development of pulmonary vascular remodeling.

Comparison of SuHx and SuPNx

The SuHx model is a now frequently utilized model of severe angio-obliterative PAH[11]. In comparison to the SuHx-model, the combination of pneumonectomy with VEGF receptor blockade showed several important differences in disease progression. Although the vascular lesions in the SuPNx model are very similar to the SuHx-model, the hyperproliferation of endothelial cells and the resulting obliterative lesions as a consequence of high flow in the SuPNx model, indicate that the endothelial dysfunction and injury do not necessarily require metabolic pathways activated by hypoxia. This might suggest that the hypoxic exposure within the SuHx protocol is important for increasing the blood flow by its mechanical loss of vascular lumen and explains the efficacy of monocrotaline or SU5416 in hyper flow based animal models. SU5416, by itself, damages endothelial cells, but without a second hit SU5416 does not cause angio-obliterative luminal changes[15]. By design in the SuHx model, temporal exposure to hypoxia and reversal of hypoxic vasoconstriction and hemoconcentration upon return to normoxia results in a partial reversibility of pulmonary hypertension [11]. This aspect of reversibility is reflected by a decrease in RVSP and hypoxia after the hypoxic period and complicates drug treatment studies when using the SuHx model. Because the SuPNx model lacks elements of hypoxic vasoconstriction and hemoconcentration, the RVSP after pneumonectomy increases gradually over time, which may be a better representation of the human disease. The ultimate body mass is equally lowered in SuHx and SuPNx rats, although SuHx rats show a temporal more profound decline in bodymass in comparison to SuPNx rats in week two. This phenomenon is probably explained by a combination of hypoxia

induced diuresis and anorexia which lowers body mass [28].
A major advantage of the SuPNx model in comparison to the SuHx model is that the hematocrit in SuPNx rats is unaffected. In SuHx hematocrit increases during the hypoxic exposure and influences pulmonary vascular resistance and cardiac adaptation [11]. The normalization of hematocrit, in orchestra with the acute reversible hypoxic vasoconstriction, results in a partial decrease of RVSP upon normoxic re-exposure, while intimal wall thickening progressively increases. This means that within the time course of the SuHx protocol, the RV is not always reflecting the condition of pulmonary vascular remodeling and might question the efficacy of RV assessments, for example treatment studies, in the early phase upon normoxic re-exposure. In regard to cardiac remodeling, the SuPNx model has the advantage over the SuHx model, as pulmonary vascular remodeling is gradually progressive, as it is in the human condition. Within the time course chosen, the SuPNx study does not show signs of cardiac reversibility. Reversibility in a later phase of the model was not determined, but also not expected as the survival was affected upon 8 weeks after SU5416 injection.

The limitation of the SuPNx model is that a surgery is required, which may induce inflammatory processes. The mechanism of action of SU5416 is poorly understood, and might therefore complicate the interpretation of VEGF or tyrosine kinase mediated treatments.

In summary, we have shown that the combination of SU5416 and PNx causes severe angio-obliterative pulmonary hypertension, without the need of hypoxia. This SuPNx model can serve as an alternative model of severe angio-obliterative PAH when the equipment needed for chronic hypoxic exposure is not available. Our study together with previous studies on experimental models of pulmonary hypertension, shows that the typical histological findings of PAH, including obliterative lesions, inflammation and increased cell turnover, represent a final common pathway of a disease that can come about after a variety of insults to the lung vasculature. These insults may share increased shear stress and/or an impaired adaptive response to changes in shear stress as a common denominator.

Acknowledgements

This project was funded by Longfonds (grant number 3.3.12.036). In addition, we acknowledge the support from the Netherlands CardioVascular Research Initiative: the Dutch Heart Foundation, Dutch Federation of University Medical Centers, the Netherlands Organization for Health Research and Development and the Royal Netherlands Academy of Sciences

References

1. Simonneau G, Robbins IM, Beghetti M, Channick RN, Delcroix M, Denton CP, Elliott CG, Gaine SP, Gladwin MT, Jing Z-C, Krowka MJ, Langleben D, Nakanishi N, Souza R. Updated clinical classification of pulmonary hypertension. *J. Am. Coll. Cardiol.* 2009; 54: S43–S54.
2. Rai PR, Cool CD, King JAC, Stevens T, Burns N, Winn RA, Kasper M, Voelkel NF. The cancer paradigm of severe pulmonary arterial hypertension. *Am. J. Respir. Crit. Care Med.* 2008; 178: 558–564.
3. Guignabert C, Tu L, Le Hiress M, Ricard N, Sattler C, Seferian A, Huertas A, Humbert M, Montani D. Pathogenesis of pulmonary arterial hypertension: lessons from cancer. *Eur. Respir. Rev. Off. J. Eur. Respir. Soc.* 2013; 22: 543–551.
4. Dickinson MG, Bartelds B, Borgdorff MAJ, Berger RMF. The role of disturbed blood flow in the development of pulmonary arterial hypertension: lessons from preclinical animal models. *Am. J. Physiol. - Lung Cell. Mol. Physiol.* 2013; 305: L1–L14.
5. Chiu J-J, Chien S. Effects of disturbed flow on vascular endothelium: pathophysiological basis and clinical perspectives. *Physiol. Rev.* 2011; 91: 327–387.
6. Okada K, Tanaka Y, Bernstein M, Zhang W, Patterson GA, Botney MD. Pulmonary hemodynamics modify the rat pulmonary artery response to injury. A neointimal model of pulmonary hypertension. *Am. J. Pathol.* 1997; 151: 1019–1025.
7. White RJ, Meoli DF, Swarthout RF, Kallop DY, Galaria II, Harvey JL, Miller CM, Blaxall BC, Hall CM, Pierce RA, Cool CD, Taubman MB. Plexiform-like lesions and increased tissue factor expression in a rat model of severe pulmonary arterial hypertension. *Am. J. Physiol. Lung Cell. Mol. Physiol.* 2007; 293: L583–L590.
8. van Albada ME, Bartelds B, Wijnberg H, Mohaupt S, Dickinson MG, Schoemaker RG, Kooi K, Gerbens F, Berger RMF. Gene expression profile in flow-associated pulmonary arterial hypertension with neointimal lesions. *Am. J. Physiol. Lung Cell. Mol. Physiol.* 2010; 298: L483–L491.
9. Voelkel NF, Gomez-Arroyo J, Abbate A, Bogaard HJ, Nicolls MR. Pathobiology of pulmonary arterial hypertension and right ventricular failure. *Eur. Respir. J.* 2012; 40: 1555–1565.
10. Toba M, Alzoubi A, O'Neill KD, Gairhe S, Matsumoto Y, Oshima K, Abe K, Oka M, McMurtry IF. Temporal hemodynamic and histological progression in Sugen5416/hypoxia/normoxia-exposed pulmonary arterial hypertensive

rats. *Am. J. Physiol. Heart Circ. Physiol.* 2013; .

11. de Raaf MA, Schalij I, Gomez-Arroyo J, Rol N, Happé C, de Man FS, Vonk-Noordegraaf A, Westerhof N, Voelkel NF, Bogaard HJ. SuHx rat model: partly reversible pulmonary hypertension and progressive intima obstruction. *Eur. Respir. J.* 2014; 44: 160–168.
12. Nicolls MR, Mizuno S, Taraseviciene-Stewart L, Farkas L, Drake JI, Al Husseini A, Gomez-Arroyo JG, Voelkel NF, Bogaard HJ. New models of pulmonary hypertension based on VEGF receptor blockade-induced endothelial cell apoptosis. *Pulm. Circ.* 2012; 2: 434–442.
13. Dorfmüller P, Chaumais M-C, Giannakouli M, Durand-Gasselin I, Raymond N, Fadel E, Mercier O, Charlotte F, Montani D, Simonneau G, Humbert M, Perros F. Increased oxidative stress and severe arterial remodeling induced by permanent high-flow challenge in experimental pulmonary hypertension. *Respir. Res.* 2011; 12: 119.
14. White RJ, Meoli DF, Swarthout RF, Kallop DY, Galaria II, Harvey JL, Miller CM, Blaxall BC, Hall CM, Pierce RA, Cool CD, Taubman MB. Plexiform-like lesions and increased tissue factor expression in a rat model of severe pulmonary arterial hypertension. *Am. J. Physiol. - Lung Cell. Mol. Physiol.* 2007; 293: L583–L590.
15. Kasahara Y, Tuder RM, Taraseviciene-Stewart L, Le Cras TD, Abman S, Hirth PK, Waltenberger J, Voelkel NF. Inhibition of VEGF receptors causes lung cell apoptosis and emphysema. *J. Clin. Invest.* 2000; 106: 1311–1319.
16. Okada K, Tanaka Y, Bernstein M, Zhang W, Patterson GA, Botney MD. Pulmonary hemodynamics modify the rat pulmonary artery response to injury. A neointimal model of pulmonary hypertension. *Am. J. Pathol.* 1997; 151: 1019–1025.
17. Yuan JX-J, Rubin LJ. Pathogenesis of Pulmonary Arterial Hypertension The Need for Multiple Hits. *Circulation* 2005; 111: 534–538.
18. Mizuno S, Farkas L, Husseini AA, Farkas D, Gomez-Arroyo J, Kraskauskas D, Nicolls MR, Cool CD, Bogaard HJ, Voelkel NF. Severe Pulmonary Arterial Hypertension Induced by SU5416 and Ovalbumin Immunization. *Am. J. Respir. Cell Mol. Biol.* 2012; 47: 679–687.
19. Rannels DE, Rannels SR. Compensatory growth of the lung following partial pneumonectomy. *Exp. Lung Res.* 1988; 14: 157–182.
20. Ravikumar P, Yilmaz C, Bellotto DJ, Dane DM, Estrera AS, Hsia CCW. Separating in vivo mechanical stimuli for postpneumonectomy compensation: imaging and ultrastructural assessment. *J. Appl. Physiol.* 2013; 114: 961–970.

21. Taraseviciene-Stewart L, Kasahara Y, Alger L, Hirth P, Mc Mahon G, Waltenberger J, Voelkel NF, Tuder RM. Inhibition of the VEGF receptor 2 combined with chronic hypoxia causes cell death-dependent pulmonary endothelial cell proliferation and severe pulmonary hypertension. *FASEB J. Off. Publ. Fed. Am. Soc. Exp. Biol.* 2001; 15: 427–438.
22. Li F, Xia W, Li A, Zhao C, Sun R. Long-term inhibition of Rho kinase with fasudil attenuates high flow induced pulmonary artery remodeling in rats. *Pharmacol. Res.* 2007; 55: 64–71.
23. Dickinson MG, Bartelds B, Molema G, Borgdorff MA, Boersma B, Takens J, Weij M, Wichers P, Sietsma H, Berger RMF. Egr-1 Expression During Neointimal Development in Flow-Associated Pulmonary Hypertension. *Am. J. Pathol.* 2011; 179: 2199–2209.
24. Gomez-Arroyo JG, Farkas L, Alhussaini AA, Farkas D, Kraskauskas D, Voelkel NF, Bogaard HJ. The monocrotaline model of pulmonary hypertension in perspective. *AJP Lung Cell. Mol. Physiol.* 2011; 302: L363–L369.
25. Voelkel NF, Vandivier RW, Tuder RM. Vascular endothelial growth factor in the lung. *Am. J. Physiol. - Lung Cell. Mol. Physiol.* 2006; 290: L209–L221.
26. Coon BG, Baeyens N, Han J, Budatha M, Ross TD, Fang JS, Yun S, Thomas J-L, Schwartz MA. Intramembrane binding of VE-cadherin to VEGFR2 and VEGFR3 assembles the endothelial mechanosensory complex. *J. Cell Biol.* 2015; 208: 975–986.
27. Tzima E, Irani-Tehrani M, Kiosses WB, Dejana E, Schultz DA, Engelhardt B, Cao G, DeLisser H, Schwartz MA. A mechanosensory complex that mediates the endothelial cell response to fluid shear stress. *Nature* 2005; 437: 426–431.
28. Kim N, Voicu L, Hare GMT, Cheema-Dhadli S, Chong CK, Chan SKW, Bichet DG, Halperin ML, Mazer CD. Response of the renal inner medulla to hypoxia: possible defense mechanisms. *Nephron Physiol.* 2012; 121: p1–p7.
29. Taraseviciene-Stewart L, Nicolls MR, Kraskauskas D, Scerbavicius R, Burns N, Cool C, Wood K, Parr JE, Boackle SA, Voelkel NF. Absence of T Cells Confers Increased Pulmonary Arterial Hypertension and Vascular Remodeling. *Am. J. Respir. Crit. Care Med.* 2007; 175: 1280–1289.
30. Tamosiuniene R, Nicolls MR. Regulatory T cells and Pulmonary Hypertension. *Trends Cardiovasc. Med*. 2011; 21: 166–171

Chapter 5:
HDAC inhibition with Trichostatin A does not reverse severe angioproliferative pulmonary hypertension in rats.

Michiel Alexander de Raaf[1], Aysar Al Hussaini[2], Jose G. Gomez-Arroyo[2], Donatas Kraskaukas[2], Daniela Farkas[2], Chris Happé[1], Norbert F. Voelkel[2], Harm Jan Bogaard[1].

Adapted from Pulmonary Circulation, 2014 Jun;4(2):237-43.

[1]VU University Medical Center, Department of Pulmonology, Pulmonary Arterial Hypertension Knowledge Centre, Amsterdam, The Netherlands.
[2] Pulmonary and Critical Care Medicine Division, Virginia Commonwealth University, Richmond, Virginia, USA.

Abstract:

Pulmonary Arterial Hypertension (PAH) is a rapidly progressive and devastating disease characterized by remodeling of lung vessels, increased pulmonary vascular resistance and eventually right ventricular hypertrophy and failure. Because Histone deacetylase (HDAC) inhibitors are agents hampering tumor growth and cardiac hypertrophy, they have been attributed a therapeutic potential for patients with PAH. Outcomes of studies evaluating the use of HDAC inhibitors in models of PAH and right ventricular pressure overload have been equivocal, however. Here we describe the levels of HDAC activity in the lungs and hearts of rats with pulmonary hypertension and right heart hypertrophy or failure, experimentally induced by monocrotaline (MCT), the combined exposure to the VEGF-R inhibitor SU5416 and hypoxia (SuHx), and pulmonary artery banding (PAB). We show that HDAC activity levels are reduced in the lungs of rat with experimentally induced hypertension, whereas activity levels are increased in the hypertrophic hearts. In contrast to what was previously found in the MCT model, the HDAC-inhibitor trichostatin A had no effect on pulmonary vascular remodeling in the SuHx model. When our results and those in the published literature are taken together, it is suggested that the effects of HDAC inhibitors in humans with PAH and associated RV failure are, at best, unpredictable. Significant progress can perhaps be made by using more specific HDAC-inhibitors, but before clinical tests in human PAH can be undertaken, careful preclinical studies are required to determine potential cardiotoxicity.

Introduction

Pulmonary Arterial Hypertension (PAH) is a rapidly progressive and devastating disease, characterized by obstructive remodeling of lung vessels. If left untreated –and often despite treatment, the increased pulmonary vascular resistance eventually results in right ventricular (RV) dysfunction, heart failure and death [1]. After linking biological hallmarks of cancer [2, 3] with some of the abnormalities found in the PAH lung, the hypothetical etiological focus of PAH shifted from the concept of vasoconstriction to concepts of quasi-malignancy [4]. Endothelial cell proliferation is currently given a more prominent role in the pathogenesis of the disease and the view on vasodilators has changed, as these treatments are incapable of curing PAH [4–6]. Newer treatments are being developed which aim to reduce pulmonary vascular resistance by reversing the quasi-malignant behavior of cells in the pulmonary vascular wall of PAH patients [7]. Unfortunately, antiproliferative treatment of PAH with the tyrosine kinase inhibitor Imatinib was associated with adverse events in clinical trials (particularly subdural hematoma), despite very promising initial preclinical and clinical studies [8, 9].

As the insight developed that epigenetic modifications play a major role in the pathogenesis and behavior of several tumors [10, 11], Histone DeACetylases Inhibitors (HDACis) were shown to have therapeutic effects in malignant disease, including promotion of growth arrest, cell differentiation and apoptosis [12]. Although additional studies are necessary, HDACis were well tolerated by patients with urological cancers and were shown to have the potential to arrest tumor growth [10]. At the same time, it was discovered that class IIa Histone DeACetylases (HDACs) are involved in cardiac hypertrophy and that HDACis could regulate hypertrophic responses [13].

The combination of anti-malignant effects and suppressive effects on cardiac hypertrophy makes HDAC inhibitors attractive candidates for the treatment of PAH. Beneficial responses were observed in rats with monocrotaline (MCT) and chronic hypoxia induced pulmonary hypertension [14, 15]. Unlike human PAH, these experimental models do not exhibit endothelial hyperproliferation, however, which makes their use in the clinical situation unpredictable. Moreover, we have shown that HDAC inhibition induces a functional deterioration in the pressure overloaded right ventricle (RV), which was associated with the devel-

opment of fibrosis and capillary rarefaction [16]. Lungs and heart have different adaptation strategies and their own specific roles in the pathophysiology and outcome of PAH. While hampering remodeling in the lungs might be a beneficial effects of HDACis, they may also worsen the adaptive processes in the heart [14, 16, 15, 17].

To contribute to a better assessment of the therapeutic potential of HDACi in PAH, we determined HDAC activities in lung and right ventricular tissue derived from two models of experimental PH and one model of isolated RV pressure overload. In addition, to determine the effect of HDAC inhibition on lung endothelial hyperproliferation, the key hallmark of human PAH, we assessed the therapeutic efficacy of Trichostatin A in the Sugen/hypoxia (SuHx) model. This model is based on the combined exposure of rats to the VEGF-R inhibitor SU5416 and hypoxia and shows a striking hemodynamic and histological resemblance to human severe PAH.

Material and methods

Animal models

Male Sprague Dawley rats, weighing 180-200 grams at the start of the experiments, were exposed to MCT or Sugen plus 10% hypoxia, as described previously [18, 19] . MCT and SuHx rats were terminated after 28 days. To induce a fixed RV pressure overload insensitive to drug treatment, another group of rats underwent Pulmonary Artery Banding (PAB), as described earlier[18, 20]. Control animals were housed under similar conditions as the other groups and sacrificed after four weeks. Lungs and hearts were collected and immediately placed in liquid nitrogen to be stored at -80 degrees Celsius. The study was approved by the local Animal Welfare committee (VU Fys 11-11, Fys 11-16 & Fys 12-08).

HDAC activity

HDAC activity was determined by using the Fluor-de-Lys HDAC kit (Enzo Life Sciences, New York, USA), according to their instruction manual and recommendations.

Echocardiography, hemodynamics, fulton index and histology

Transthoracic echocardiography (Vevo770 imaging system, VisualSoncis, Toronto, ON, Canada) allowed assessment of Triscupid Annular Plane Systolic Excursion (TAPSE) and Right Ventricular Inner Diameter (RVID/d). Hemodynamics were measured invasively using a 4.5-mm Millar conductance catheter, which was inserted into the right ventricular outflow tract, in order to measure Right Ventricular Systolic Pressure (RVSP). After hemodynamic assessments, hearts were excised and after removal of atria and the great arteries, the right ventricle (RV) was separated from the residual left ventricle plus septum (LV+S). RV-weight and LV+S weights were both determined and the Fulton index (FI = RV/LV+S) was calculated. Lung tissue was fixated in formalin, processed and slides were stained with H&E.

TSA treatment study in Sugen hypoxia

Severe angioproliferative pulmonary hypertension was induced in two groups of four male Sprague Dawley rats by their combined exposure to a subcutaneous injection of SU5416 (20 mg/kg) suspended in CMC and subsequent housing in 10% oxygen, for the duration of four weeks [20, 21]. In one of the SuHx groups,

TSA was administered (450 mg/kg) for five times a week intraperitoneally starting on the day of sugen administration and lasting for four weeks; the other SuHx group received vehicle only. On the last day of hypoxia (study day 28), RV function was evaluated by transthoracic echocardiogram, hemodynamics and Fulton Index. A naïve control group, without induction of sugen hypoxia or TSA treatment, consisting of 4 animals, was included.

Statistical analyses

After confirmation that data were normally distributed, variables were compared between groups using two-way ANOVA with Bonferroni post-hoc tests.

Results

In comparison to normal rats, lung HDAC activity was significantly lower in the two models of experimental PH (**Figure 1**). All experimental models showed an increased HDAC activity in cardiac tissues in comparison to control rats.

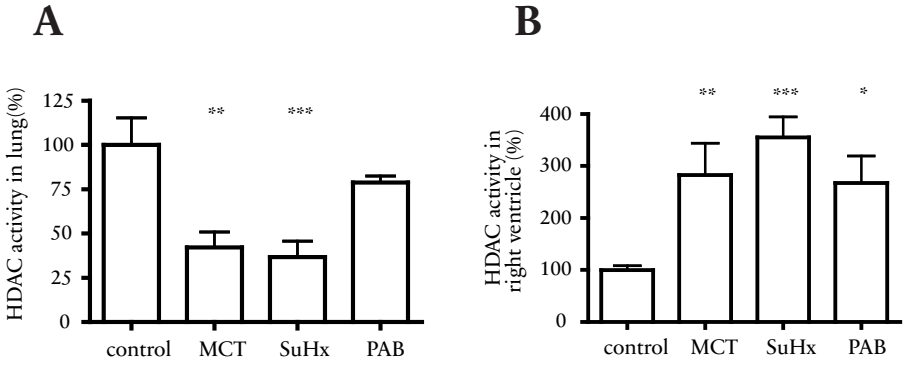

Figure 1: *HDAC activity was decreased in lung tissue (panel A) of monocrotaline and sugen hypoxia (SuHx) exposed rats. Lung tissue after pulmonary artery banding (PAB) was not affected. HDAC activity was increased in the pressure overloaded right ventricle of all experimental models used (panel B). Comparisons with controls are denoted by * ($p<0.05$), ** ($p<0.01$) and *** ($p<0.001$).*

RVSP and FI were significantly increased in SuHx-rats and unaffected by TSA administration. Echocardiography showed a decreased TAPSE and increased RVID/d in SuHx rats and, again, TSA treatment did not change these parameters (**Figure 2**). Likewise, lung histology of SuHx rats was unaltered after TSA treatment, with significant presence of occlusive vascular lesions and media hypertrophy (**Figure 3**).

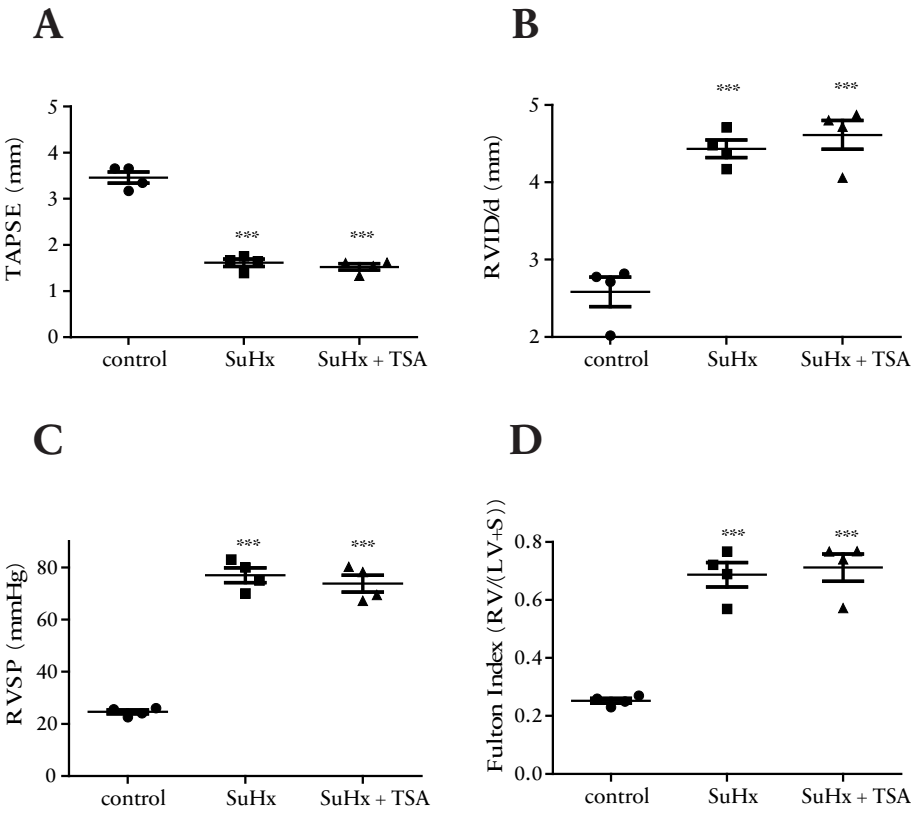

Figure 2: *Echocardiographic assessment and Fulton index of control rats and rats exposed to Sugen and hypoxia (SuHx), with or without treatment with trichostatin A (TSA). Tricuspid Annular Plane Systolic Excursion (TAPSE), Right Ventricular Inner Diameter (RVID/d) and Right Ventricular Systolic Pressure (RVSP) were altered due to the induction of experimental pulmonary hypertension by SuHx, but no differences were seen between the SuHx group and SuHx group with TSA treatment The Fulton*

*index showed similar results. Comparisons with controls are denoted by *($p<0.05$) and ** ($p<0.01$).*

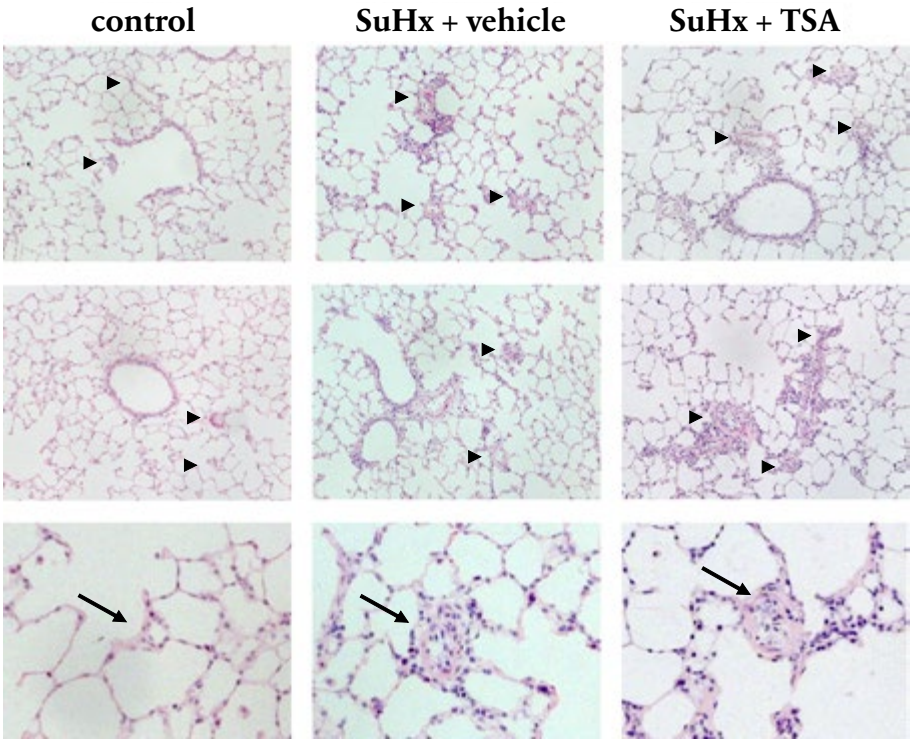

Figure 3: *Pulmonary vessel remodeling was seen in rats exposed to Sugen and hypoxia (SuHx) and consisted of medial hypertrophy and intima hyperproliferative lesions in small arteries (arrowheads and arrows). Trichostatin A (TSA) treatment in SuHx rats did not affect pulmonary vessel remodeling (column SuHx + TSA). H&E, magnification 40x, lowest panel 200x.*

Discussion

This study shows that HDAC activity is decreased in the lungs of rats with experimentally induced PH, whereas HDAC activity is increased in the pressure overloaded RV. Furthermore, we show that the pan-HDAC inhibitor TSA has no therapeutic or beneficial effects in SuHx induced PH, as it neither affected pulmonary vascular remodeling nor improved cardiac function.

Gene expression is regulated by folding and defolding of the DNA by histones. Defolding is controlled by Histone AcetylTransferases (HATs) and facilitates expression of specific genes [22]. Hampering of expression is caused by folding which is regulated by Histone DeACetylases (HDACs) [22]. In various cell types, HDACis exert therapeutic effects by direct suppression of overexpressed genes or, through the release from effects of suppressor genes, by increasing transcriptional activity of silenced genes. Additional effects of HDACis are related to acetylation of other substrates than histones, including proteins and enzymes [12, 23, 24]. Via these mechanisms, HDAC inhibitors affect proliferation, apoptosis and differentiation, as well as cardiac hypertrophy. This combination of effects makes HDAC inhibitors seemingly attractive candidate drugs for the treatment of PAH.

To study the preclinical efficacy of HDACis in PH, several experimental models are available [25, 26]. PH was reversed by the HDACis Valproic acid (VPA) and suberoylanilide hydroxamic acid (SAHA) in two of these models, namely the chronic hypoxia and MCT model[25, 27].) (**Figure 4**) [14, 28].

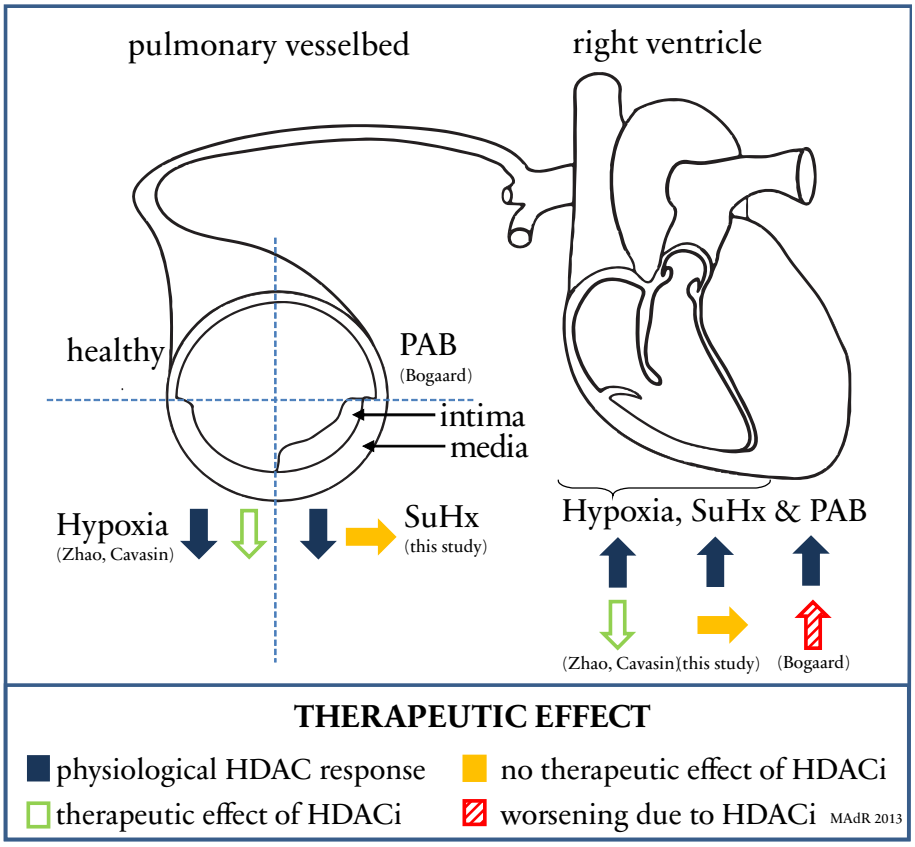

Figure 4: *Conclusive figure; whereas the physiological response on HDAC activity (blue) decreases in the lung, left panel, cardiac HDAC activity (right panel) increases (blue) upon different experimental PH exposures. Treatment of HDAC inhibitors was beneficial in hypoxia (and MCT) (green), was neither worsening nor beneficial in sugen hypoxia (orange) and detrimental for pulmonary artery banding in the heart (red).*

However, given the fact that HDAC activity was low in all PH models we tested, even without treatment, it seems unlikely that the therapeutic effect of SAHA and VPA were mediated by a further reduction in HDAC activity levels. The treatment effects of HDACis in chronically hypoxic and MCT rats may have resulted from the deacetylation of non-histone protein substrates, including those involved in hypoxic angiogenesis via Hypoxia Inducible Factor 1 alpha (HIF-1α) related signaling pathways[12]. Lung HIF-1α protein expression is increased in

MCT and chronically hypoxic rats and is thought to play a role in the vascular remodeling in these experimental models [29]. It has been suggested that TSA reduces the gene expression DNA-binding activity of HIF-1α in a non-histone related fashion, which would lead to a reduction in VEGF expression and inhibition of hypoxic angiogenesis [30]. The reduced overall HDAC activity we observed in the SuHx and MCT lung seems at odds with the previously reported increased protein expression of several specific HDACs in the lungs of MCT and chronically hypoxic rats [14]. Unfortunately, HDAC activity levels have never been determined in human PAH lung tissue. A discrepancy between human HDAC protein expression and activity could point to dysfunction of specific HDAC enzymes, which were not studied at this time. A limitation of the current study is that, using an activity kit, it remains unknown which specific HDACs are responsible for overall HDAC activity.

We chose to test TSA in the SuHx model, as this model features intima remodeling in the arterioles and pre-capillaries and thereby gives new insights into the pathobiology and treatment of PAH [21, 25, 31]. A therapeutic effect of TSA in this model was not observed (**Figure 2 & 3**). As the TSA dose level and dosing strategy used in this study caused detrimental cardiac effects in PA-banded rats[16], we can't attribute the absence of a treatment effect in SuHx rats to ineffective HDAC inhibition. This discrepancy with the therapeutic effects of HDAC inhibitors in other PH models is perhaps explained by the fact that the HIF-VEGF signaling pathway in this model is inhibited by SU5416, thereby rendering the model insensitive to further inhibition of HIF-1α related pathways [21].

Several investigators have shown that left ventricular hypertrophy, induced by stimuli varying from pressure overload to overexpression of pro-hypertrophic genes and continuous agonist infusion, is reduced or prevented by HDAC inhibitors [13, 14, 32–34]. In preclinical studies, it is clear that HDACis are actively lessening myocardial hypertrophy [14, 15]. HDACis were almost exclusively tested in preventive treatment strategies. Studying the effects of HDACis on RV function and hypertrophy in MCT or chronically hypoxic rats is problematic, as the treatment simultaneously changes RV afterload. To assess the therapeutic effect of HDACs on cardiac hypertrophy per se, PA-banding has shown to be an important tool [35], as this model only induces RV hypertrophy, without affecting the pulmonary vasculature [18, 20]. In PA-banded or aortic banded (TAC) animals, HDACis have resulted in controversial outcomes (**Figure 4**) [16, 17, 28].

We showed that the adaptive cardiac hypertrophy as induced by PAB, requires upregulation of HDAC activity and that TSA or VPA treatment leads to a deterioration of cardiac function [16].

When the RV is pushed towards hypertrophy, major shifts in fetal gene expression are taking place in order to remodel the ventricle into a high pressure pump [20, 34, 36, 37]. This compensatory gene response needs HDAC activity; blocking these fetal genes indirectly by HDACis prevent cardiac hypertrophy [38, 39]. In line with this hypothesis, we found an increased HDAC activity in RV tissue. Furthermore, Sano et al, observed a bimodal pattern in gene expression during the hypertrophic response; with an initial increase in HIF-1α expression early in the hypertrophic process, followed by a later decrease in HIF-1α expression due to p53 accumulation when hypertrophy is established [40]. The bimodal pattern has also been confirmed in monocrotaline induced RV hypertrophy [41]. The shift in expression during established hypertrophy hampers angiogenesis and the fetal remodeling program. Growth and maintenance of the capillary network are critical for the adaptation of the RV to pressure overload [18] and the inhibition of angiogenic pathways seems critical for the induction of RV failure by HDACis [16].

To date, preclinical work in models of pulmonary hypertension and RV pressure overload has relied on the exclusive use of rather unselective HDACis. Significant progress can perhaps be made by using more specific isoform-selective HDACis, which are currently under development[13] and have been used with success in left heart disease animal models[42]. When isoform-specific HDACis do not provoke failure of the pressure overloaded RV, they would be worth considering for the treatment of PAH.

Conclusions

Essential differences are found in HDAC activity between heart and lung. As lung HDAC activity is decreased in several experimental PH models, remodeling of the pulmonary vascular vessel seems not to require a continued increase in HDAC activity. In SuHx rats, HDAC inhibition by TSA did not lead to a reduction in pressure overload. RV HDAC activity was increased in several models of RV hypertrophy, which suggests that HDAC activity plays an important role in the compensation to pressure overload. The clinical implication of our findings

is that the effects of HDAC inhibitors in humans with PAH are unpredictable and may include RV functional deterioration, especially when a reduction in pulmonary vascular resistance is not feasible.

Acknowledgements

We would like to thank Silvia Rain, MD, VU University medical center, Amsterdam, The Netherlands, for her supportive hands-on assistance regarding protein analyses.

References

1. Simonneau G, Robbins IM, Beghetti M, Channick RN, Delcroix M, Denton CP, Elliott CG, Gaine SP, Gladwin MT, Jing Z-C, Krowka MJ, Langleben D, Nakanishi N, Souza R. Updated clinical classification of pulmonary hypertension. *J. Am. Coll. Cardiol.* 2009; 54: S43–S54.
2. Hanahan D, Weinberg RA. The hallmarks of cancer. *Cell* 2000; 100: 57–70.
3. Hanahan D, Weinberg RA. Hallmarks of cancer: the next generation. *Cell* 2011; 144: 646–674.
4. Rai PR, Cool CD, King JAC, Stevens T, Burns N, Winn RA, Kasper M, Voelkel NF. The Cancer Paradigm of Severe Pulmonary Arterial Hypertension. *American Journal of Respiratory and Critical Care Medicine* 2008; 178: 558–564.
5. Stacher E, Graham BB, Hunt JM, Gandjeva A, Groshong SD, McLaughlin VV, Jessup M, Grizzle WE, Aldred MA, Cool CD, Tuder RM. Modern age pathology of pulmonary arterial hypertension. *Am. J. Respir. Crit. Care Med.* 2012; 186: 261–272.
6. Morrell NW, Adnot S, Archer SL, Dupuis J, Jones PL, MacLean MR, McMurtry IF, Stenmark KR, Thistlethwaite PA, Weissmann N, Yuan JX-J, Weir EK. Cellular and molecular basis of pulmonary arterial hypertension. *J. Am. Coll. Cardiol.* 2009; 54: S20–S31.
7. Humbert M, Sitbon O, Simonneau G. Treatment of pulmonary arterial hypertension. *N. Engl. J. Med.* 2004; 351: 1425–1436.
8. Hoeper MM, Barst RJ, Bourge RC, Feldman J, Frost AE, Galié N, Gómez-Sánchez MA, Grimminger F, Grünig E, Hassoun PM, Morrell NW, Peacock AJ, Satoh T, Simonneau G, Tapson VF, Torres F, Lawrence D, Quinn DA, Ghofrani H-A. Imatinib mesylate as add-on therapy for pulmonary arterial hypertension: results of the randomized IMPRES study. *Circulation* 2013; 127: 1128–1138.
9. Ghofrani HA, Morrell NW, Hoeper MM, Olschewski H, Peacock AJ, Barst RJ, Shapiro S, Golpon H, Toshner M, Grimminger F, Pascoe S. Imatinib in pulmonary arterial hypertension patients with inadequate response to established therapy. *Am. J. Respir. Crit. Care Med.* 2010; 182: 1171–1177.
10. Sharma NL, Groselj B, Hamdy FC, Kiltie AE. The emerging role of histone deacetylase (HDAC) inhibitors in urological cancers. *BJU Int.* 2013; 111: 537–542.
11. Gallinari P, Di Marco S, Jones P, Pallaoro M, Steinkühler C. HDACs, histone deacetylation and gene transcription: from molecular biology to cancer ther-

apeutics. *Cell Res.* 2007; 17: 195–211.
12. Ververis K, Hiong A, Karagiannis TC, Licciardi PV. Histone deacetylase inhibitors (HDACIs): multitargeted anticancer agents. *Biologics* 2013; 7: 47–60.
13. McKinsey TA. Therapeutic potential for HDAC inhibitors in the heart. *Annu. Rev. Pharmacol. Toxicol.* 2012; 52: 303–319.
14. Zhao L, Chen C-N, Hajji N, Oliver E, Cotroneo E, Wharton J, Wang D, Li M, McKinsey TA, Stenmark KR, Wilkins MR. Histone deacetylation inhibition in pulmonary hypertension: therapeutic potential of valproic acid and suberoylanilide hydroxamic acid. *Circulation* 2012; 126: 455–467.
15. Cavasin MA, Demos-Davies K, Horn TR, Walker LA, Lemon DD, Birdsey N, Weiser-Evans MCM, Harral J, Irwin DC, Anwar A, Yeager ME, Li M, Watson PA, Nemenoff RA, Buttrick PM, Stenmark KR, McKinsey TA. Selective class I histone deacetylase inhibition suppresses hypoxia-induced cardiopulmonary remodeling through an antiproliferative mechanism. *Circ. Res.* 2012; 110: 739–748.
16. Bogaard HJ, Mizuno S, Hussaini AAA, Toldo S, Abbate A, Kraskauskas D, Kasper M, Natarajan R, Voelkel NF. Suppression of Histone Deacetylases Worsens Right Ventricular Dysfunction after Pulmonary Artery Banding in Rats. *American Journal of Respiratory and Critical Care Medicine* 2011; 183: 1402–1410.
17. Kong Y, Tannous P, Lu G, Berenji K, Rothermel BA, Olson EN, Hill JA. Suppression of class I and II histone deacetylases blunts pressure-overload cardiac hypertrophy. *Circulation* 2006; 113: 2579–2588.
18. Bogaard HJ, Natarajan R, Henderson SC, Long CS, Kraskauskas D, Smithson L, Ockaili R, McCord JM, Voelkel NF. Chronic Pulmonary Artery Pressure Elevation Is Insufficient to Explain Right Heart Failure. *Circulation* 2009; 120: 1951–1960.
19. Bogaard HJ, Natarajan R, Mizuno S, Abbate A, Chang PJ, Chau VQ, Hoke NN, Kraskauskas D, Kasper M, Salloum FN, Voelkel NF. Adrenergic receptor blockade reverses right heart remodeling and dysfunction in pulmonary hypertensive rats. *Am. J. Respir. Crit. Care Med.* 2010; 182: 652–660.
20. Bogaard HJ, Abe K, Vonk Noordegraaf A, Voelkel NF. The Right Ventricle Under Pressure: Cellular and Molecular Mechanisms of Right-Heart Failure in Pulmonary Hypertension. *Chest* 2009; 135: 794–804.
21. Taraseviciene-Stewart L, Kasahara Y, Alger L, Hirth P, Mc Mahon G, Waltenberger J, Voelkel NF, Tuder RM. Inhibition of the VEGF receptor 2 combined with chronic hypoxia causes cell death-dependent pulmonary endothelial

cell proliferation and severe pulmonary hypertension. *FASEB J.* 2001; 15: 427–438.
22. Bernstein BE, Meissner A, Lander ES. The mammalian epigenome. *Cell* 2007; 128: 669–681.
23. Ocker M. Deacetylase inhibitors - focus on non-histone targets and effects. *World J Biol Chem* 2010; 1: 55–61.
24. Dobaczewski M, Bujak M, Li N, Gonzalez-Quesada C, Mendoza LH, Wang X-F, Frangogiannis NG. Smad3 signaling critically regulates fibroblast phenotype and function in healing myocardial infarction. *Circ. Res.* 2010; 107: 418–428.
25. Nicolls MR, Mizuno S, Taraseviciene-Stewart L, Farkas L, Drake JI, Husseini A Al, Gomez-Arroyo JG, Voelkel NF, Bogaard HJ. New models of pulmonary hypertension based on VEGF receptor blockade-induced endothelial cell apoptosis. *Pulm Circ* 2012; 2: 434–442.
26. Ryan J, Bloch K, Archer SL. Rodent models of pulmonary hypertension: harmonisation with the world health organisation's categorisation of human PH. *Int J Clin Pract Suppl* 2011; : 15–34.
27. Stenmark KR, Meyrick B, Galie N, Mooi WJ, McMurtry IF. Animal models of pulmonary arterial hypertension: the hope for etiological discovery and pharmacological cure. *Am. J. Physiol. Lung Cell Mol. Physiol.* 2009; 297: L1013–L1032.
28. Cho YK, Eom GH, Kee HJ, Kim H-S, Choi W-Y, Nam K-I, Ma JS, Kook H. Sodium valproate, a histone deacetylase inhibitor, but not captopril, prevents right ventricular hypertrophy in rats. *Circ. J.* 2010; 74: 760–770.
29. Lai Y-L, Law TC. Chronic hypoxia- and monocrotaline-induced elevation of hypoxia-inducible factor-1 alpha levels and pulmonary hypertension. *J. Biomed. Sci.* 2004; 11: 315–321.
30. Kim MS, Kwon HJ, Lee YM, Baek JH, Jang JE, Lee SW, Moon EJ, Kim HS, Lee SK, Chung HY, Kim CW, Kim KW. Histone deacetylases induce angiogenesis by negative regulation of tumor suppressor genes. *Nat. Med.* 2001; 7: 437–443.
31. de Raaf MA, Schalij I, Gomez-Arroyo J, Rol N, de Man FS, Westerhof N, Voelkel NF, Vonk-Noordegraaf A, Bogaard HJ. Vasoreactivity and Persistent Vascular Remodeling in Experimental Pulmonary Hypertension. .
32. Kee HJ, Sohn IS, Nam KI, Park JE, Qian YR, Yin Z, Ahn Y, Jeong MH, Bang Y-J, Kim N, Kim J-K, Kim KK, Epstein JA, Kook H. Inhibition of histone deacetylation blocks cardiac hypertrophy induced by angiotensin II infusion

and aortic banding. *Circulation* 2006; 113: 51–59.
33. Kook H, Lepore JJ, Gitler AD, Lu MM, Wing-Man Yung W, Mackay J, Zhou R, Ferrari V, Gruber P, Epstein JA. Cardiac hypertrophy and histone deacetylase-dependent transcriptional repression mediated by the atypical homeodomain protein Hop. *J. Clin. Invest.* 2003; 112: 863–871.
34. Kee HJ, Kook H. Roles and targets of class I and IIa histone deacetylases in cardiac hypertrophy. *J. Biomed. Biotechnol.* 2011; 2011: 928326.
35. Voelkel NF. Pulmonary hypertension: the present and future. Shelton, Conn.: People's Medical Pub. House-USA; 2011.
36. Rajabi M, Kassiotis C, Razeghi P, Taegtmeyer H. Return to the fetal gene program protects the stressed heart: a strong hypothesis. *Heart Fail Rev* 2007; 12: 331–343.
37. Peacock AJ, Naeije R, Rubin LJ. Pulmonary Circulation, 3rd edition. 3rd ed. CRC Press; 2011.
38. Kee HJ, Kook H. Krüppel-like factor 4 mediates histone deacetylase inhibitor-induced prevention of cardiac hypertrophy. *J. Mol. Cell. Cardiol.* 2009; 47: 770–780.
39. Trivedi CM, Luo Y, Yin Z, Zhang M, Zhu W, Wang T, Floss T, Goettlicher M, Noppinger PR, Wurst W, Ferrari VA, Abrams CS, Gruber PJ, Epstein JA. Hdac2 regulates the cardiac hypertrophic response by modulating Gsk3 beta activity. *Nat. Med.* 2007; 13: 324–331.
40. Sano M, Minamino T, Toko H, Miyauchi H, Orimo M, Qin Y, Akazawa H, Tateno K, Kayama Y, Harada M, Shimizu I, Asahara T, Hamada H, Tomita S, Molkentin JD, Zou Y, Komuro I. p53-induced inhibition of Hif-1 causes cardiac dysfunction during pressure overload. *Nature* 2007; 446: 444–448.
41. Sutendra G, Dromparis P, Paulin R, Zervopoulos S, Haromy A, Nagendran J, Michelakis ED. A metabolic remodeling in right ventricular hypertrophy is associated with decreased angiogenesis and a transition from a compensated to a decompensated state in pulmonary hypertension. *J. Mol. Med.* 2013; .
42. McKinsey TA. Isoform-selective HDAC inhibitors: closing in on translational medicine for the heart. *J. Mol. Cell. Cardiol.* 2011; 51: 491–496.

Chapter 6:
Tyrosine Kinase Inhibitor BIBF1000 does not hamper right ventricular pressure adaptation in rats

Michiel Alexander de Raaf[1], Ingrid Schalij[1], Frances S. de Man[1], Anton Vonk Noordegraaf[1], Lutz Wollin[2], Harm Jan Bogaard[1].

Adapted from submitted manuscript (in revision AJP heart)

1= Departments of Pulmonology and Physiology, VU University Medical Center / Institute for Cardiovascular Research, Amsterdam, The Netherlands.
2= Boehringer Ingelheim Pharma GmbH & Co. KG, Dept. Respiratory Diseases Research . Birkendorfer Strasse 65, D-88397 Biberach, Germany

Abstract:

BIBF1000 is a small molecule tyrosine kinase inhibitor targeting Vascular Endothelial Growth Factor Receptor (VEGFR), Fibroblast Growth Factor Receptor (FGFR) and Platelet Derived Growth Factor Receptor (PDGFR) and a powerful inhibitor to treat fibrogenesis. BIBF1000 is very similar to BIBF1120 (Nintedanib) which was recently approved for the treatment of Idiopathic Pulmonary Fibrosis (IPF). A safety concern pertaining to VEGFR, FGFR and PDGFR inhibition is the possible interference with right ventricular (RV) responses to an increased afterload, which could adversely affect clinical outcome in IPF patients who developed pulmonary hypertension. We tested the effect of BIBF1000 on the adaptation of the RV in rats subjected to mechanical pressure overload.
BIBF1000 was administered for 35 days in pulmonary artery banded (PAB) rats. RV adaptation was assessed by echocardiography, pressure volume loop analysis, histology and determination of atrial natriuretic peptide (ANP) expression.
BIBF1000 treatment resulted in growth attenuation but had no effects on RV function after PAB, given absence of changes in cardiac index, end systolic elastance, connective tissue disposition and capillary density. We conclude that in this experimental model of increased afterload, VEGFR, FGFR and PDGFR inhibition does not hamper RV adaptation to pressure overload.

Introduction

Idiopathic Pulmonary Fibrosis (IPF) is characterized by progressive fibroblast/myofibroblast accumulation resulting in increased deposition of extracellular matrix components like collagen in the lungs. These pathogenic mechanisms are partly driven by growth factor signaling through Vascular Endothelial Growth Factor (VEGF), Platelet Derived Growth Factor (PDGF) and Fibroblast Growth Factor (FGF) receptors (2, 15, 38). BIBF1000, a potent tyrosine kinase inhibitor of VEGF, PDGF and FGF receptor signaling (6), attenuated pulmonary fibrosis in an animal model of lung fibrosis resembling aspects of IPF (11). Nintedanib (BIBF1120) and BIBF1000 are indolinone derivatives designed during the same chemical lead optimization program and are very similar with respect to the kinase specificity profile (6, 11). Nintedanib has anti-tumor activity and like BIBF1000 anti-fibrotic activity in animal models of IPF (14, 19, 36, 43). Because Nintedanib slows the decline in lung function in patients with IPF (34), the drug was recently approved for the treatment of IPF in the United States and Europe (44).

IPF is complicated by pulmonary hypertension (PH) in about 45% of patients (10, 37). To adapt to the increased pulmonary vascular pressures, the right ventricle (RV) undergoes progressive adaptation through increased contractility and hypertrophy, processes involving VEGF, PDGF and FGF signaling. Upregulation of VEGF in the pressure overloaded heart is required to maintain capillary density and systolic function (23, 35). Intact PDGF signaling contributes to cardiomyocyte survival and cardiac adaptation through activation of cardiomyocyte progenitor cells (5, 45). In models of acute myocardial infarction, enhanced PDGF signaling is cardioprotective (12, 20). FGF induces hypertrophic responses in cardiomyocytes, for example by activation of mitogen-activated protein kinase (MAPK) (22, 30). FGF-2 deficient mice develop dilated cardiomyopathy at normotension and do not show compensatory hypertrophy when hypertensive (30). Because cardiac remodeling involves VEGF, PDGF and FGF receptor signaling, the question may be raised whether BIBF1000 and nintedanib could hamper cardiac adaptation. This question is critically important because RV function is an important determinant of prognosis in IPF (16, 39, 42). The aim of this study was to assess the effect of VEGF, PDGF and FGF receptor inhibition on RV adaptation to pressure overload in rats subjected to Pulmonary Artery Banding (PAB).

Material and methods (467/500)

Animal model

Thirty-two male Sprague Dawley rats (Crl:CD(SD), Charles River, Sulzfeld, Germany), 180-200 grams body weight (BW) underwent PAB (n=16), or sham surgery (n=16) as described previously (8). Via a left thoracotomy, a silk suture was tied tightly around an 18-guage needle alongside the pulmonary artery. After subsequent rapid removal of the needle, a fixed constricted opening was created in the lumen equal to the diameter of the needle. One week after surgery, animals were randomized to vehicle or BIBF1000 treatment (n=8/group). Clinical signs and body weights were measured daily. The study was approved by the local Animal Welfare committee (VU-Fys 11-11).

Test substance formulation and dosing

The citrate salt of BIBF1000 (IUPAC-code 35113576) (Boehringer Ingelheim Pharma, Biberach Germany) was dissolved in deionized water (MilliQ, Millipore) to reach a concentration of 10 mg/mL (on basis of the free base) and stored at room temperature to a maximum of 7 days. BIBF1000 was administered at a dose of 50 mg/kg body weight once daily by oral gavage for 35 days. Dose calculation was adjusted to the individual body weights twice weekly.

Echocardiography

On the day of necropsy, animals underwent echocardiography using a ProSound system (Prosound SSD-4000) equipped with a 13-Mhz linear transducer (UST-5542, Aloka, Tokyo, Japan), as described previously (28). The following parameters were acquired: cardiac index (CI), tricuspid annular plane systolic excursion (TAPSE), RV wall thickness (RVWT) and RV end diastolic diameter (RVEDD).

Hemodynamics and pressure volume (PV)-loops

Just before necropsy, animals received isoflurane 2-3% in 1:1 O2/air mixture (60% oxygen) for anesthesia. Hematocrit was determined by centrifugation and fractional measurement. The chest was opened through the diaphragm. RV catheterization was performed using a Millar catheter (AD instruments, Bella Vista, Australia) for measuring right ventricular systolic pressure (RVSP) and pressure-volume measurements. For collecting end systolic elastance (EES), end diastolic elastance (EED) and arterial elastance (EA), the vena cava was occluded

with a tightened string placed around the abdominal vena cava, as described previously (28).

Histological and morphometric analyses

After necropsy, cardiac tissues and organs were weighed and processed for histology. Organ weights were corrected for tibia length. Tissues were fixed in formalin and embedded in paraffin. Four micron slices of heart tissue were prepared and stained. To assess the presence of connective tissue, a Masson's trichrome stain was performed. CD31 and CD45 immunohistochemical stains were performed to evaluate capillary density and inflammation, respectively.

Atrial natriuretic peptide (ANP) protein expression

According to the suppliers manual, a western blot on RV homogenizations was performed (ANP(N-20):sc-18811, 1:200 (Santa Cruz Biotechnology, inc., Dallas, Texas), 2nd antibody polyclonal Goat Anti-Rabbit immunoglobin E0432, 1:5000 (DAKO, Glostrup, Denmark). Novex ECL chemiluminescent (Invitrogen, Carlsbad, California) was used for protein detection. Optical densities were measured and standardized with β-actin.

Statistical analyses

All data are presented as mean ± S.E.M. of n animals. Parametric variables were compared between groups using appropriate ANOVA with Bonferroni post-hoc tests (GraphPad Prism, GraphPad Software Inc, La Jolla, CA USA.). A p value of less than 0.05 was considered significant.

RESULTS

Body weight gain and clinical signs

Increasing with time BIBF1000 treatment resulted in reduced body weight gain in sham treated (**Figure 1A**) and PAB-treated animals (**Figure 1B**). One BIBF1000-treated PAB-animal underwent necropsy one day before its scheduled necropsy due to significant weight loss and clinical signs.

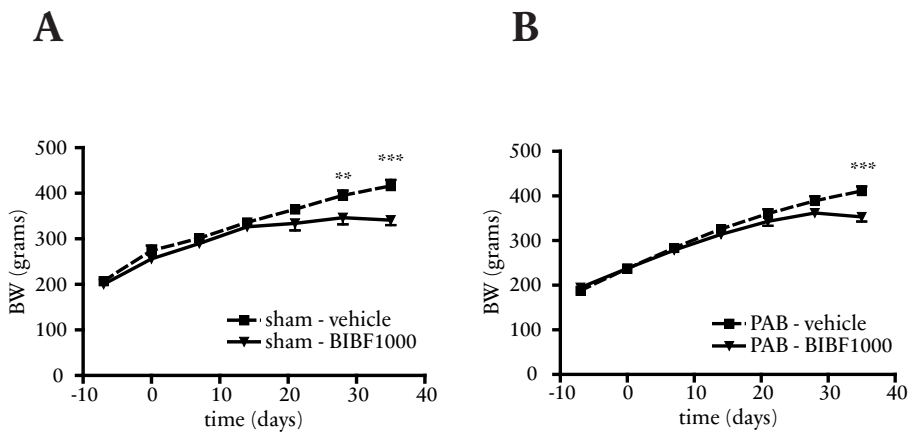

Figure 1: *Body weight gain in vehicle- and BIBF1000-treated groups of sham-operated (panel A) and Pulmonary Artery Banding (PAB)-operated (panel B) rats. Mean plus SEM, ** = p<0.01, *** = p<0.001.*

Echocardiography

PAB resulted in an increase of RVWT (**Figure 2A**) and RVEDD (**Figure 2B**) compared to sham treated animals. BIBF1000 did not significantly reduce the increased RVWT and RVEDD but effectuated a trend toward a reduction. No differences were found between the different treatment groups in TAPSE (**Figure 2C**) or CI (**Figure 2D**).

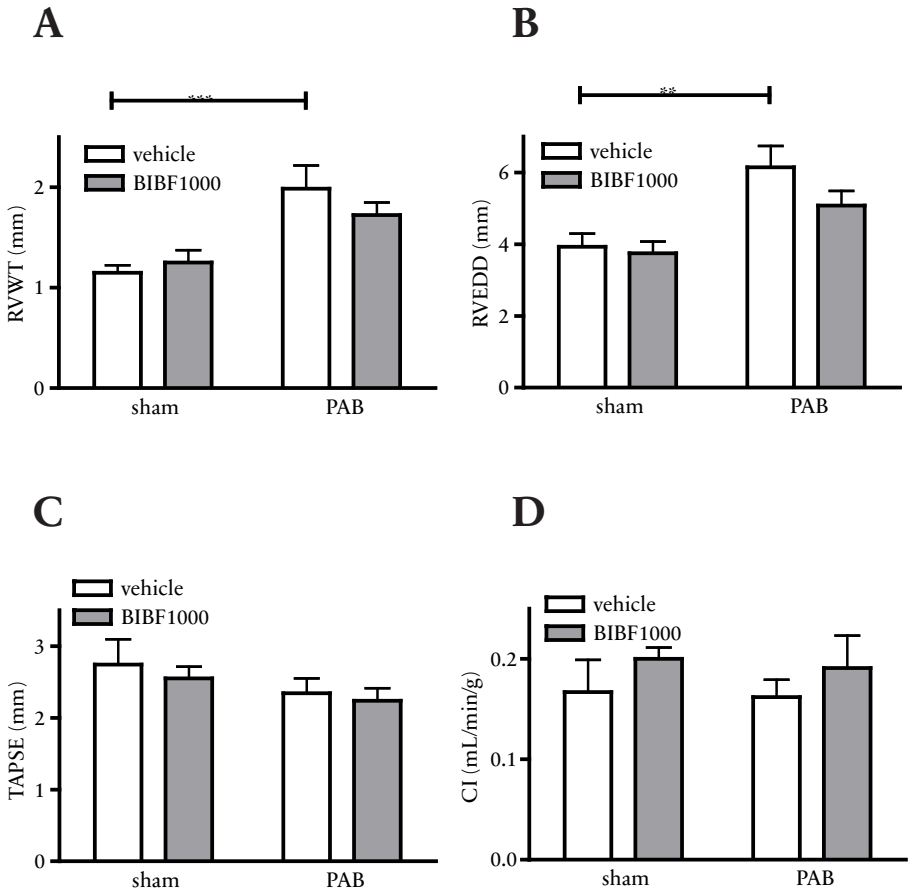

Figure 2: *Echocardiographic parameters in vehicle- and BIBF1000-treated groups of sham-operated and Pulmonary Artery Banding (PAB)-operated rats; Right Ventricular Wall Thickness (RVWT, panel A) and Right Ventricular End Diastolic Diameter (RVEDD, panel B), Tricuspid Annular Plane Systolic Excursion (TAPSE, panel C) and Cardiac Index (CI, panel D). Mean plus SEM, ** = p<0.01, *** = p<0.001.*

Hemodynamics and pressure volume (PV)-loops

RVSP, EES and EA (**Figure 3A-C**) were significantly increased in the PAB-treated animals. BIBF1000 did not significantly change the increase in RVSP, EES and EA. Ventriculo-arterial coupling (EES/EA), EED and stroke volume index (SVI) (**Figure 3D-F**) were not affected by either PAB or BIBF1000 treatment.

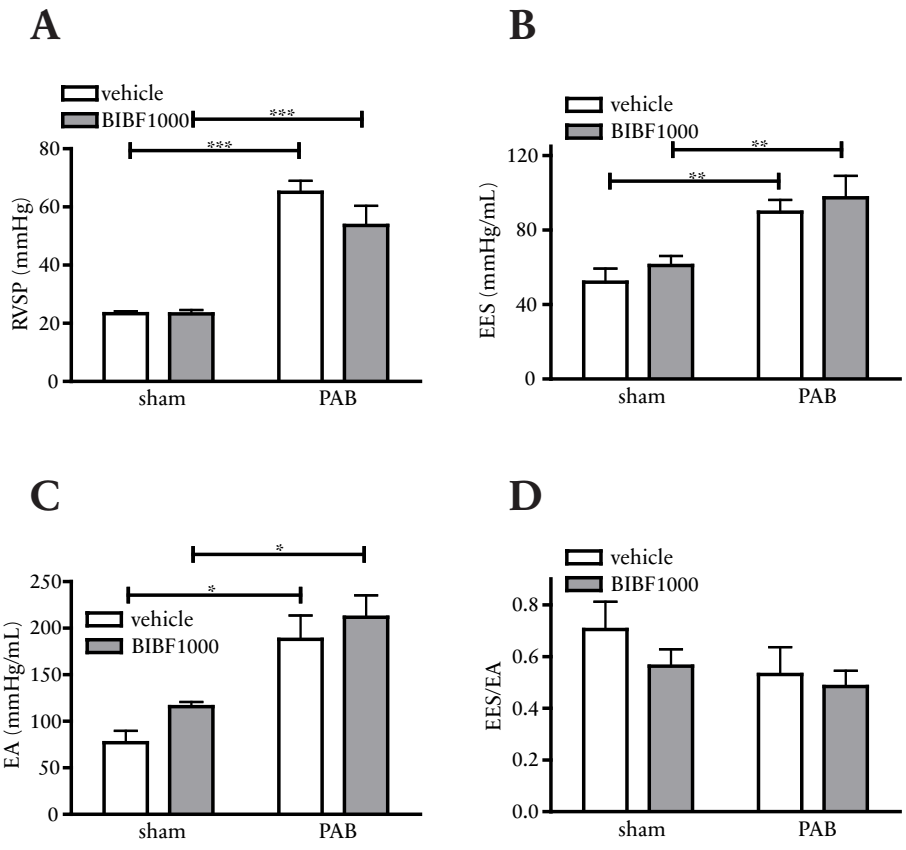

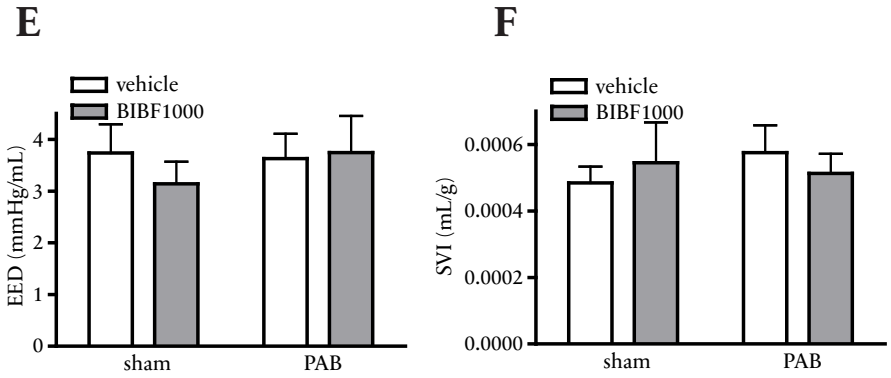

Figure 3: *Right Ventricular Systolic Pressure (RVSP, panel A), End Systolic Elastance (EES, panel B), Aterial Elastance (EA, panel C), ventriculo-arterial coupling; (EES/EA, panel D), End Diastolic Elastance (EED, panel E) and Stroke Volume Index (SVI, panel F) in vehicle- and BIBF1000-treated animals of sham-operated and Pulmonary Artery Banding (PAB)-operated rats. Mean plus SEM, *** = p<0.001.*

Necropsy

The hematocrit remained within physiological ranges (**Figure 4A**). Heart weight was increased in the PAB-treated animals, due to an increase of both right ventricular weight (RV/tibia) (**Figure 4B**) and, to lesser extent, left ventricular plus septum weight ((LV+S)/tibia) (**Figure 4C**). Heart weights were normalized with the tibia length to account for growth retardation. The ratio in RV/(LV+S) increased dramatically in the PAB-treated animals describing severe right ventricular hypertrophy (**Figure 4D**). In sham-treated as well as PAB-treated animals BIBF1000 induced a trend towards a decrease in RV/(LV+S) ratio indicating a possible reduction in right heart hypertrophy.

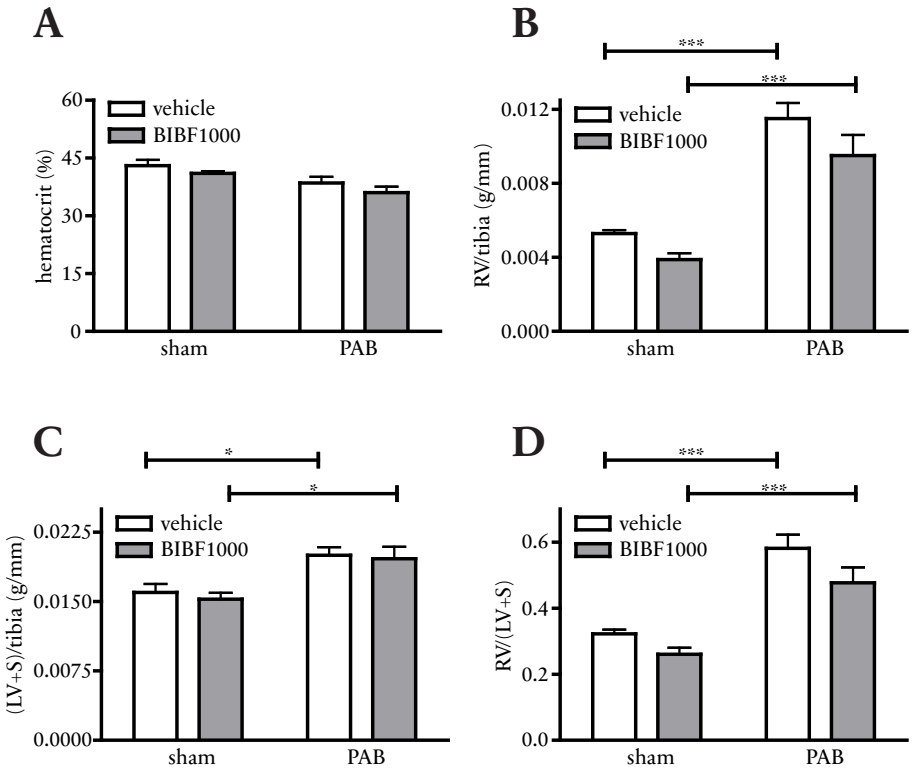

Figure 4: *Hematocrit (panel A) and organ weights in vehicle- and BIBF1000-treated animals of sham-operated and Pulmonary Artery Banding (PAB)-operated rats. RV weight was corrected by tibia length regarding growth retardation (RV/tibia, panel B), as well the Left Ventricle ((LV+S)/tibia, panel C). RV weight divided by left ventricle*

*plus septum weight based on the tibia corrected values (RV/(LV+S), panel D). Mean plus SEM, * = p<0.05, ** = p<0.01, *** = p<0.001.*

Histological and morphometric analyses of the heart

PAB induced an increase in cardiomyocyte cross sectional area (CSA), indicating hypertrophy. BIBF1000 treatment significantly prevented the increase in CSA (**Figure 5A**). The number of capillaries per cardiomyocyte was increased after PAB in vehicle-treated rats, but not in BIBF1000-treated rats (**Figure 5B**). In comparison to the vehicle-treated animals with PAB the BIBF1000 treatment did not significantly reduce the number of capillaries per mm2 (**Figure 5C**). No differences were seen among groups regarding amounts of connective tissue (**Figure 5D**) or inflammation (**Figure 5E**).

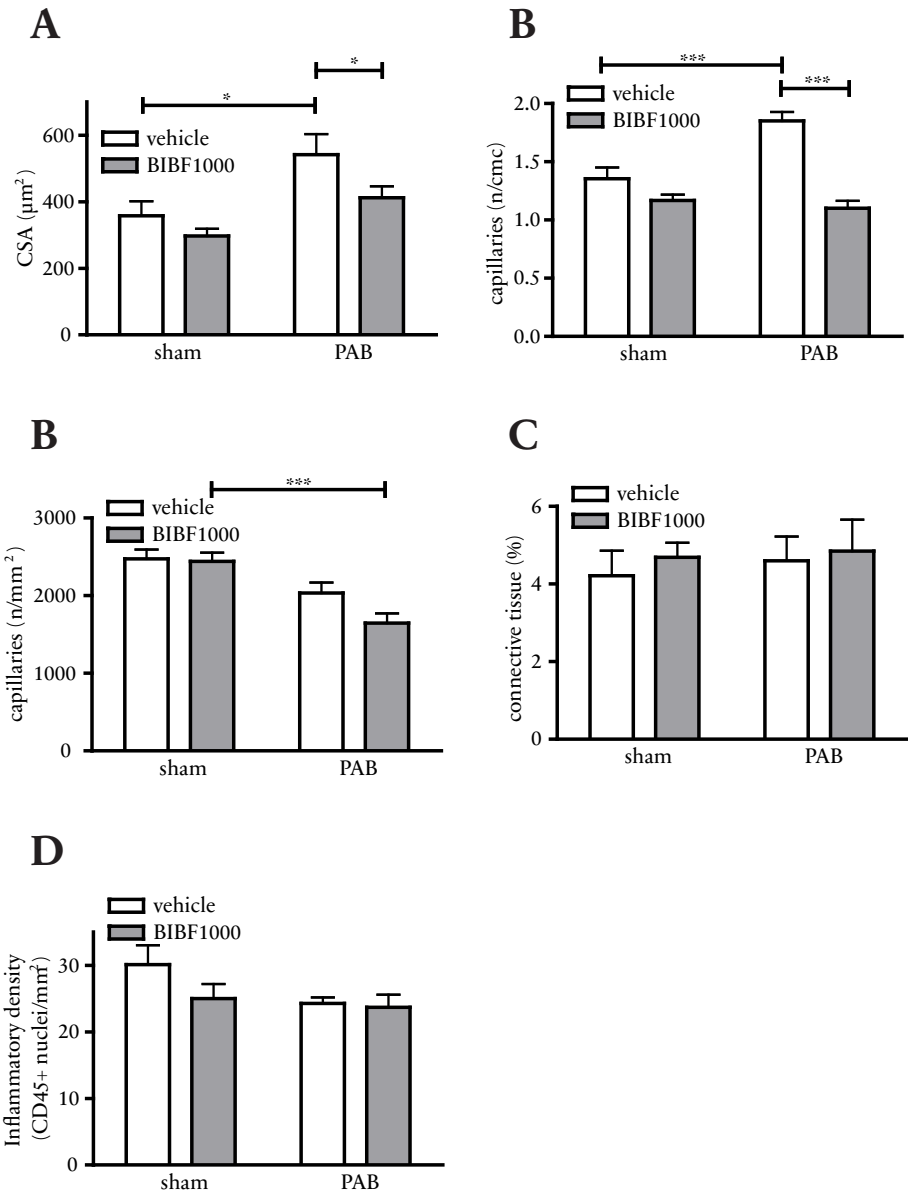

Figure 5: *Histological analyses in vehicle- and BIBF1000-treated animals of sham-operated and Pulmonary Artery Banding (PAB)-operated rats; Cross Sectional Area (CSA, panel A), capillaries (CD31⁺ cells per cardiomyocyte, panel B), capillaries (CD31+ cells*

*per mm², panel C), collagen tissue (panel D) and Inflammatory density (CD45⁺ nuclei per mm², panel E). Mean plus SEM, * = p<0.05, *** = p<0.001.*

ANP protein expression

PAB resulted in a non-significant increase in ANP protein expression in vehicle treated rats, but not in BIBF1000-treated rats (**Figure 6**).

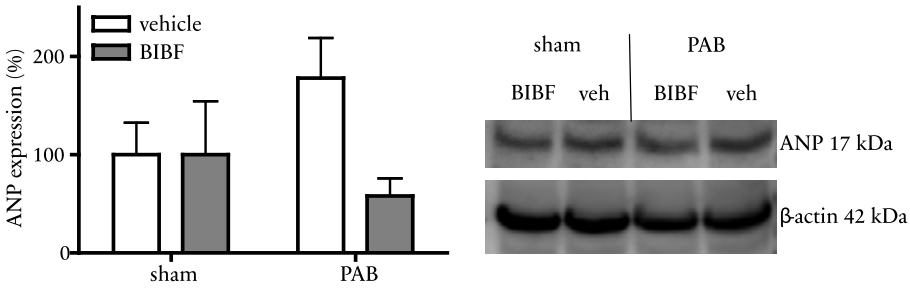

Figure 6: *ANP-protein expression measured by Western blot in vehicle- and BIBF1000-treated animals of sham-operated and Pulmonary Artery Banding (PAB)-operated rats. Mean plus SEM, * = p<0.05.*

Discussion

Our study shows that VEGF, FGF and PDGF receptor inhibition by BIBF1000 does not adversely affect the morphology or RV function of rats subjected to PAB. TAPSE, ESP, EES and CI were not different between groups. The load independent index of RV function EES/EA was not significantly different between groups. BIBF1000 treatment of PAB rats resulted in a trend toward less RV dilatation and less RV hypertrophy. Despite a decrease in number of capillaries per cardiomyocyte, the number of capillaries per surface area -which is most representative for myocardial oxygen transport- was not altered. As a marker for cardiac stress, ANP was increased in PAB-animals, but this increase was attenuated after administration of BIBF1000. No alteration in connective tissue disposition was observed after BIBF1000 administration in PAB rats, which finding was probably due to the fact that collagen disposition is minimal in this experimental model of adaptive RV hypertrophy (8). In summary, these findings suggest that it would be unlikely that inhibition of VEGFR, FGFR and PDGFR, either by BIBF1000 or by the very similar indolinone derivative nintedanib, result in a deterioration of RV function in IPF patients with secondary pulmonary hypertension. However, a clinical study to confirm these effects in human IPF with PH is warranted.

IPF is a progressive disease characterized by marked, patchy fibrosis in the lung parenchyma and loss of pulmonary function (31). In the pathophysiology of the disease, increased expression of FGF, PDGF and VEGF have been implicated (9, 21, 44). PH develops in approximately 45% of IPF patients and severely impacts functional status (10, 37). For example, the need for additional oxygen (L/min) was increased by 26% of the patients with PH in IPF and the cardiac index was decreased when mean pulmonary artery pressure exceeded 40 mmHg (37). Importantly, RV function is the most conclusive determinant of prognosis in IPF patients with secondary PH (42). The existence of PH in patients with IPF increases the 1-year mortality to 28% compared to 5.5% in IPF patients without PH (26, 37). Currently no treatment targeting PH in patients with IPF is approved (10). Hence, it is of paramount importance that treatment options approved for patients with IPF have no detrimental effects on RV function. This safety concern could particular apply to nintedanib, which was recently approved for the treatment of IPF.

At the start of our study a dosing rationale was available for BIBF1000 in rats (6)

but not for the very similar BIBF1120 (nintedanib) which is now approved for the treatment of IPF in US and the EU (34). BIBF1000 at 50 mg/kg attenuated the deposition of collagen and the expression of pro-fibrotic genes in an animal model of bleomycin-induced lung fibrosis (6). Nintedanib and BIBF1000 are very similar with respect to their kinase specificity and potency (4, 5). The combined inhibitory activity of FGFR, PDGFR and VEGFR by both compounds is assumed to target lung fibrosis (5, 9, 11). FGFR1 and 2 are expressed on various cells in the lungs of patients with IPF (21), and FGF-2 stimulates proliferation of lung fibroblasts from patients with IPF (18). *In vivo* abrogation of FGF signaling reduces bleomycin-induced pulmonary fibrosis and improves survival in bleomycin-treated mice (46). PDGF was shown to have an important role in fibroblast/myofibroblasts proliferation, migration and survival and acts as a stimulator of collagen synthesis (3, 9, 24, 29). Inhibition of PDGFR with specific compounds reduced pulmonary fibrosis in various animal models of lung fibrosis (1, 4, 27, 33, 41). VEGFR was assumed to be implicated in aberrant neovascularization (13, 32) and anti-VEGF gene therapy was shown to attenuate bleomycin-induced fibrosis in mice (17). In the heart, the same growth factors play a key role in cardiac adaptation and remodeling (14, 19, 22, 30). Inhibition of VEGF and PDGF signaling could lead to vascular rarefaction (7, 12, 20, 23, 35), while PDGF and FGF inhibition could theoretically lead to an insufficient RV hypertrophic response (7, 22, 30). As such, the use of nintedanib in patients with IPF complicated by PH could be potentially detrimental to RV function. At the time of our study, we had no access to nintedanib because the drug was still being evaluated in the registration process for the treatment of IPF. As first pre-clinical evidence, our translational study shows no cardiac dysfunction in PAB rats after treatment with BIBF1000.

A few previous studies addressed the effects of tyrosine kinase inhibitor (TKI)s on RV adaptation to pressure overload. Kojonazarov et al. (25), showed in monocrotaline treated and PAB rats that the multi kinase inhibitors Sunitib (PDGFR, VEGFR and c-Kit inhibition) and Sorafenib (raf, VEGFR and PDGFR inhibition) reduced RV hypertrophy, fibrosis and vascular remodeling. Importantly, the degree of pressure overload in these studies was diminished after TKI treatment, while a load independent assessment of RV function was not made. As such firm conclusions pertaining to the effects of these TKIs on cardiac adaptation cannot be made. A decrease in RVSP after PAB is most likely explained by growth inhibition, as the pressure gradient over a stenosis with a fixed diameter is determined by blood flow. In the normal and well-adapted heart, cardiac output is

strongly related to body weight. In fact, we observed that treatment with 50 mg/kg BIBF1000 hampered body weight gain which also decreased cardiac output, whereas CI was unchanged. This finding indicates that our dosing strategy was sufficiently rigorous, and that the absence of cardiac side effects was not due to under-dosing. Additionally, the finding stresses the fact that a proper evaluation of RV function in a PAB study should include load-independent parameters of RV function. Although no significant differences in RVSP were observed between treated and non-treated PAB rats, it can be speculated that the diminished RV hypertrophy and ANP expression after BIBF1000 treatment was not a direct pharmacological effect, but rather due to a relatively lower load due to the impaired body weight gain. Because we also show that the EES/EA ratio (a load independent indicator of RV function) was unaffected by BIBF1000 treatment, we can conclude that the drug does not adversely affect RV function, even in the presence of pulmonary hypertension. Within the limits of this animal model, a trend towards decreased capillary density (n/mm2) was noted. In a potential confirmatory clinical trial in patients with IPF and concomitant PH the determination of RV capillary flow reserve would be the best prognostic measurement if RV deterioration is suspected (40).

Conclusion

Given the absence of differences in cardiac index, RV arterial coupling, connective tissue disposition and capillary density, BIBF1000 treatment has no effects on the pressure overloaded RV. We conclude that in this experimental model, concomitant inhibition of VEGFR, FGFR and PDGFR does not hamper cardiac adaptation to pressure overload.

Acknowledgements

We would like to acknowledge A.J. Bak (AMC, Amsterdam, The Netherlands), N. Westerhof, N.Rol, C.M.Happé, R. Schutte (VU/VUMC, Amsterdam, The Netherlands) and M.E.W. de Raaf-Beekhuijzen for their contribution to this study by sharing their knowledge and expertise.

Grants

Financial support was received from Boehringer Ingelheim, Biberach, Germany.

Disclosures

The authors from VU University medical center received financial support from Boehringer Ingelheim to conduct this study. Author Lutz Wollin is an employee of Boehringer Ingelheim, the company who manufactured BIBF1000.

References

1. Abdollahi A, Li M, Ping G, Plathow C, Domhan S, Kiessling F, Lee LB, McMahon G, Gröne H-J, Lipson KE, Huber PE. Inhibition of platelet-derived growth factor signaling attenuates pulmonary fibrosis. *J Exp Med* 201: 925–935, 2005.
2. American Thoracic Society, European Respiratory Society. American Thoracic Society/European Respiratory Society International Multidisciplinary Consensus Classification of the Idiopathic Interstitial Pneumonias. This joint statement of the American Thoracic Society (ATS), and the European Respiratory Society (ERS) was adopted by the ATS board of directors, June 2001 and by the ERS Executive Committee, June 2001. *Am J Respir Crit Care Med* 165: 277–304, 2002.
3. Antoniades HN, Bravo MA, Avila RE, Galanopoulos T, Neville-Golden J, Maxwell M, Selman M. Platelet-derived growth factor in idiopathic pulmonary fibrosis. *J Clin Invest* 86: 1055–1064, 1990.
4. Aono Y, Nishioka Y, Inayama M, Ugai M, Kishi J, Uehara H, Izumi K, Sone S. Imatinib as a novel antifibrotic agent in bleomycin-induced pulmonary fibrosis in mice. *Am J Respir Crit Care Med* 171: 1279–1285, 2005.
5. Beltrami AP, Barlucchi L, Torella D, Baker M, Limana F, Chimenti S, Kasahara H, Rota M, Musso E, Urbanek K, Leri A, Kajstura J, Nadal-Ginard B, Anversa P. Adult cardiac stem cells are multipotent and support myocardial regeneration. *Cell* 114: 763–776, 2003.
6. Bisping G, Kropff M, Wenning D, Dreyer B, Bessonov S, Hilberg F, Roth GJ, Munzert G, Stefanic M, Stelljes M, Scheffold C, Müller-Tidow C, Liebisch P, Lang N, Tchinda J, Serve HL, Mesters RM, Berdel WE, Kienast J. Targeting receptor kinases by a novel indolinone derivative in multiple myeloma: abrogation of stroma-derived interleukin-6 secretion and induction of apoptosis in cytogenetically defined subgroups. *Blood* 107: 2079–2089, 2006.
7. Bogaard HJ, Abe K, Vonk Noordegraaf A, Voelkel NF. The Right Ventricle Under Pressure: Cellular and Molecular Mechanisms of Right-Heart Failure in Pulmonary Hypertension. *Chest* 135: 794–804, 2009.
8. Bogaard HJ, Natarajan R, Henderson SC, Long CS, Kraskauskas D, Smithson L, Ockaili R, McCord JM, Voelkel NF. Chronic Pulmonary Artery Pressure Elevation Is Insufficient to Explain Right Heart Failure. *Circulation* 120: 1951–1960, 2009.
9. Bonner JC. Regulation of PDGF and its receptors in fibrotic diseases. *Cyto-*

kine Growth Factor Rev 15: 255–273, 2004.
10. Caminati A, Cassandro R, Harari S. Pulmonary hypertension in chronic interstitial lung diseases. *Eur Respir Rev* 22: 292–301, 2013.
11. Chaudhary NI, Roth GJ, Hilberg F, Müller-Quernheim J, Prasse A, Zissel G, Schnapp A, Park JE. Inhibition of PDGF, VEGF and FGF signalling attenuates fibrosis. *Eur Respir J* 29: 976–985, 2007.
12. Edelberg JM, Lee SH, Kaur M, Tang L, Feirt NM, McCabe S, Bramwell O, Wong SC, Hong MK. Platelet-derived growth factor-AB limits the extent of myocardial infarction in a rat model: feasibility of restoring impaired angiogenic capacity in the aging heart. *Circulation* 105: 608–613, 2002.
13. Farkas L, Farkas D, Ask K, Möller A, Gauldie J, Margetts P, Inman M, Kolb M. VEGF ameliorates pulmonary hypertension through inhibition of endothelial apoptosis in experimental lung fibrosis in rats. *J Clin Invest* 119: 1298–1311, 2009.
14. Grimminger F, Schermuly RT, Ghofrani HA. Targeting non-malignant disorders with tyrosine kinase inhibitors. *Nat Rev Drug Discov* 9: 956–970, 2010.
15. Günther A, Korfei M, Mahavadi P, Beck D von der, Ruppert C, Markart P. Unravelling the progressive pathophysiology of idiopathic pulmonary fibrosis. *Eur Respir Rev* 21: 152–160, 2012.
16. Haddad F, Hunt SA, Rosenthal DN, Murphy DJ. Right ventricular function in cardiovascular disease, part I: Anatomy, physiology, aging, and functional assessment of the right ventricle. *Circulation* 117: 1436–1448, 2008.
17. Hamada N, Kuwano K, Yamada M, Hagimoto N, Hiasa K, Egashira K, Nakashima N, Maeyama T, Yoshimi M, Nakanishi Y. Anti-vascular endothelial growth factor gene therapy attenuates lung injury and fibrosis in mice. *J Immunol* 175: 1224–1231, 2005.
18. Hetzel M, Bachem M, Anders D, Trischler G, Faehling M. Different effects of growth factors on proliferation and matrix production of normal and fibrotic human lung fibroblasts. *Lung* 183: 225–237, 2005.
19. Hilberg F, Roth GJ, Krssak M, Kautschitsch S, Sommergruber W, Tontsch-Grunt U, Garin-Chesa P, Bader G, Zoephel A, Quant J, Heckel A, Rettig WJ. BIBF 1120: triple angiokinase inhibitor with sustained receptor blockade and good antitumor efficacy. *Cancer Res* 68: 4774–4782, 2008.
20. Hsieh PCH, Segers VFM, Davis ME, MacGillivray C, Gannon J, Molkentin JD, Robbins J, Lee RT. Evidence from a genetic fate-mapping study that stem cells refresh adult mammalian cardiomyocytes after injury. *Nat Med* 13: 970–974, 2007.

21. Inoue Y, King TE, Barker E, Daniloff E, Newman LS. Basic fibroblast growth factor and its receptors in idiopathic pulmonary fibrosis and lymphangioleiomyomatosis. *Am J Respir Crit Care Med* 166: 765–773, 2002.
22. Itoh N, Ohta H. Pathophysiological roles of FGF signaling in the heart. *Front Physiol* 4: 247, 2013.
23. Izumiya Y, Shiojima I, Sato K, Sawyer DB, Colucci WS, Walsh K. Vascular endothelial growth factor blockade promotes the transition from compensatory cardiac hypertrophy to failure in response to pressure overload. *Hypertension* 47: 887–893, 2006.
24. Khalil N, O'Connor RN, Unruh HW, Warren PW, Flanders KC, Kemp A, Bereznay OH, Greenberg AH. Increased production and immunohistochemical localization of transforming growth factor-beta in idiopathic pulmonary fibrosis. *Am J Respir Cell Mol Biol* 5: 155–162, 1991.
25. Kojonazarov B, Sydykov A, Pullamsetti SS, Luitel H, Dahal BK, Kosanovic D, Tian X, Majewski M, Baumann C, Evans S, Phillips P, Fairman D, Davie N, Wayman C, Kilty I, Weissmann N, Grimminger F, Seeger W, Ghofrani HA, Schermuly RT. Effects of multikinase inhibitors on pressure overload-induced right ventricular remodeling. *Int J Cardiol* 167: 2630–2637, 2013.
26. Lettieri CJ, Nathan SD, Barnett SD, Ahmad S, Shorr AF. Prevalence and outcomes of pulmonary arterial hypertension in advanced idiopathic pulmonary fibrosis. *Chest* 129: 746–752, 2006.
27. Li M, Abdollahi A, Gröne H-J, Lipson KE, Belka C, Huber PE. Late treatment with imatinib mesylate ameliorates radiation-induced lung fibrosis in a mouse model. *Radiat Oncol* 4: 66, 2009.
28. de Man FS, Handoko ML, van Ballegoij JJM, Schalij I, Bogaards SJP, Postmus PE, van der Velden J, Westerhof N, Paulus WJ, Vonk-Noordegraaf A. Bisoprolol delays progression towards right heart failure in experimental pulmonary hypertension. *Circ Heart Fail* 5: 97–105, 2012.
29. Pan LH, Yamauchi K, Uzuki M, Nakanishi T, Takigawa M, Inoue H, Sawai T. Type II alveolar epithelial cells and interstitial fibroblasts express connective tissue growth factor in IPF. *Eur Respir J* 17: 1220–1227, 2001.
30. Pellieux C, Foletti A, Peduto G, Aubert J-F, Nussberger J, Beermann F, Brunner H-R, Pedrazzini T. Dilated cardiomyopathy and impaired cardiac hypertrophic response to angiotensin II in mice lacking FGF-2. *J Clin Invest* 108: 1843–1851, 2001.
31. Raghu G, Collard HR, Egan JJ, Martinez FJ, Behr J, Brown KK, Colby TV, Cordier J-F, Flaherty KR, Lasky JA, Lynch DA, Ryu JH, Swigris JJ, Wells AU,

Ancochea J, Bouros D, Carvalho C, Costabel U, Ebina M, Hansell DM, Johkoh T, Kim DS, King TE, Kondoh Y, Myers J, Müller NL, Nicholson AG, Richeldi L, Selman M, Dudden RF, Griss BS, Protzko SL, Schünemann HJ, ATS/ERS/JRS/ALAT Committee on Idiopathic Pulmonary Fibrosis. An official ATS/ERS/JRS/ALAT statement: idiopathic pulmonary fibrosis: evidence-based guidelines for diagnosis and management. *Am J Respir Crit Care Med* 183: 788–824, 2011.

32. Renzoni EA, Walsh DA, Salmon M, Wells AU, Sestini P, Nicholson AG, Veeraraghavan S, Bishop AE, Romanska HM, Pantelidis P, Black CM, Bois RM Du. Interstitial vascularity in fibrosing alveolitis. *Am J Respir Crit Care Med* 167: 438–443, 2003.
33. Rice AB, Moomaw CR, Morgan DL, Bonner JC. Specific inhibitors of platelet-derived growth factor or epidermal growth factor receptor tyrosine kinase reduce pulmonary fibrosis in rats. *Am J Pathol* 155: 213–221, 1999.
34. Richeldi L, Costabel U, Selman M, Kim DS, Hansell DM, Nicholson AG, Brown KK, Flaherty KR, Noble PW, Raghu G, Brun M, Gupta A, Juhel N, Klüglich M, Bois RM du. Efficacy of a tyrosine kinase inhibitor in idiopathic pulmonary fibrosis. *N Engl J Med* 365: 1079–1087, 2011.
35. Sano M, Minamino T, Toko H, Miyauchi H, Orimo M, Qin Y, Akazawa H, Tateno K, Kayama Y, Harada M, Shimizu I, Asahara T, Hamada H, Tomita S, Molkentin JD, Zou Y, Komuro I. p53-induced inhibition of Hif-1 causes cardiac dysfunction during pressure overload. *Nature* 446: 444–448, 2007.
36. Santos ES, Gomez JE, Raez LE. Targeting angiogenesis from multiple pathways simultaneously: BIBF 1120, an investigational novel triple angiokinase inhibitor. *Invest New Drugs* 30: 1261–1269, 2012.
37. Shorr AF, Wainright JL, Cors CS, Lettieri CJ, Nathan SD. Pulmonary hypertension in patients with pulmonary fibrosis awaiting lung transplant. *Eur Respir J* 30: 715–721, 2007.
38. Voelkel NF. *Pulmonary hypertension: the present and future*. Shelton, Conn.: People's Medical Pub. House-USA, 2011.
39. Voelkel NF, Gomez-Arroyo J, Abbate A, Bogaard HJ, Nicolls MR. Pathobiology of pulmonary arterial hypertension and right ventricular failure. *Eur Respir J* 40: 1555–1565, 2012.
40. Vogel-Claussen J, Skrok J, Shehata ML, Singh S, Sibley CT, Boyce DM, Lechtzin N, Girgis RE, Mathai SC, Goldstein TA, Zheng J, Lima JAC, Bluemke DA, Hassoun PM. Right and left ventricular myocardial perfusion reserves correlate with right ventricular function and pulmonary hemodynamics in pa-

tients with pulmonary arterial hypertension. *Radiology* 258: 119–127, 2011.
41. Vuorinen K, Gao F, Oury TD, Kinnula VL, Myllärniemi M. Imatinib mesylate inhibits fibrogenesis in asbestos-induced interstitial pneumonia. *Exp Lung Res* 33: 357–373, 2007.
42. van Wolferen SA, Marcus JT, Boonstra A, Marques KMJ, Bronzwaer JGF, Spreeuwenberg MD, Postmus PE, Vonk-Noordegraaf A. Prognostic value of right ventricular mass, volume, and function in idiopathic pulmonary arterial hypertension. *Eur Heart J* 28: 1250–1257, 2007.
43. Wollin L, Maillet I, Quesniaux V, Holweg A, Ryffel B. Antifibrotic and anti-inflammatory activity of the tyrosine kinase inhibitor nintedanib in experimental models of lung fibrosis. *J Pharmacol Exp Ther* 349: 209–220, 2014.
44. Wollin L, Wex E, Pautsch A, Schnapp G, Hostettler KE, Stowasser S, Kolb M. Mode of action of nintedanib in the treatment of idiopathic pulmonary fibrosis. *Eur Respir J* 45: 1434–1445, 2015.
45. Xaymardan M, Tang L, Zagreda L, Pallante B, Zheng J, Chazen JL, Chin A, Duignan I, Nahirney P, Rafii S, Mikawa T, Edelberg JM. Platelet-derived growth factor-AB promotes the generation of adult bone marrow-derived cardiac myocytes. *Circ Res* 94: E39–45, 2004.
46. Yu Z, Wang D, Zhou Z, He S, Chen A, Wang J. Mutant soluble ectodomain of fibroblast growth factor receptor-2 IIIc attenuates bleomycin-induced pulmonary fibrosis in mice. *Biol Pharm Bull* 35: 731–736, 2012.

Chapter 7:
The activity of Nintedanib in a Rat Model of Sugen/hypoxia-induced pulmonary arterial hypertension

Michiel Alexander de Raaf[1], Nina Rol[1], V.P. Kuiper [1], Chris Happé[1], Ingrid Schalij [1], P. Koolwijk[2], Frances S. de Man[1], Nico Westerhof[1], Anton Vonk Noordegraaf[1], Stefan Lutz Wollin[3], Harm Jan Bogaard[1]

Adapted from to be submitted manuscript.

Affiliation: *[1] Department of Pulmonology, VU University Medical Center, Amsterdam, The Netherlands. [2] Department of Physiology, ICaR Research Institute, VU University Medical Center, Amsterdam, the Netherlands.[3] Boehringer Ingelheim Pharma GmbH & Co. KG, Department of Respiratory Diseases Research, Biberach, Germany.*

Abstract:

Deregulated growth factors, such as fibroblast growth factor (FGF), platelet derived growth factor (PDGF) and vascular endothelial growth factor (VEGF), contribute to the pulmonary vascular remodeling in Pulmonary Arterial Hypertension (PAH). Nintedanib is a tyrosine kinase inhibitor targeting primarily the receptors for FGF, PDGF and VEGF and is approved for the treatment of patients with idiopathic pulmonary fibrosis (IPF). The aim of this study was to examine the treatment efficacy in a rat model of pulmonary arterial hypertension (PAH).

PAH was induced in male Sprague Dawley rats by subcutaneous injection of sugen (SU5416) and subsequent exposure to 10% hypoxia for 4 weeks (SuHx model). After hypoxia, animals were re-exposed to normoxia for 7 weeks (n=8/group). Nintedanib (50 mg/kg p.o.) or vehicle was administered once daily during weeks 8-11.

Nintedanib treatment decreased the intimal thickness of pulmonary vessels (in vivo). Nintedanib improved the right arterial ventricular coupling significantly, which finding was in line with improved histology and reduced protein expression of ANP and collagen IV.

Nintedanib treatment resulted in a mild but beneficial attenuation of pulmonary intima remodeling and improved right ventricular adaptation to pressure overload. A clinical study might confirm the therapeutic potential of nintedanib in PAH.

Introduction

Pulmonary arterial hypertension (PAH) is a rare disease characterized by uncontrolled growth of endothelial cells, smooth muscle cells and fibroblasts located in the pulmonary vascular wall [1]. This uncontrolled growth leads to obliterative lesions in pre-capillary arterioles, an increase in pulmonary vascular resistance and, ultimately, right heart failure and death [2]. Today, PAH is still incurable despite treatment with vasodilating drugs, such as prostacyclins, endothelin receptor antagonists and phosphodiesterase type 5 (PDE) 5 inhibitors [2]. None of these medications directly inhibit the mitotic activities of the cell populations in the pulmonary vascular wall and mortality rates are only partially decreased by these drug classes. There is an ongoing search for novel medications which directly inhibit or reverse abnormal cell growth, for example by inhibiting growth factor receptors. Vascular endothelial growth factor (VEGF), platelet-derived growth factor (PDGF) and fibroblast growth factor (FGF) pathways are known to be upregulated in human PAH [3], and based on positive results in PAH animal models, a number of phase 2 and 3 trials are currently performed to evaluate different tyrosine kinase inhibitors (TKIs) in PAH. The PDGF-R inhibitor imatinib was not effective in all PAH patients, which may have been related to ongoing signaling through the VEGF and FGF receptors [4]. Because nintedanib inhibits all three kinase receptors, a higher treatment efficacy may be expected. Importantly, nintedanib has only low affinity to inhibit Src, which is one of the main targets of dasatinib: a drug known to be able to provoke PAH [5]. A general concern with all growth factor receptor inhibitors is that although these drugs may appear to be effective in reducing pulmonary vascular remodeling, they may also push the right ventricle towards failure by inhibiting myocardial adaptive hypertrophy and angiogenesis [6–9]. In a previous study, we show that nintedanib's sister compound BIBF1000 does not interfere with right ventricular adaptation to pressure overload (see chapter 6).

Material and methods

Animal model

Progressive pressure-overload *in conjunction with* angioproliferative pulmonary vascular remodeling was induced by the combined exposure to the tyrosine kinase inhibitor SU5416 and hypoxia. This SuHx model is characterized by pulmonary vascular lesions which resemble those found in human PAH and the model was described in detail by our group previously [10]. Briefly, male Sprague-Dawley rats weighing 200 g received a single injection of SU5416 (25 mg/kg s.c.) and were exposed to a simulated altitude of 5000 m in a nitrogen dilution chamber for 4 weeks; thereafter the animals were kept at the sea level for another 7 weeks [10]. Clinical signs and body weights were measured daily. Eight animals were dosed with nintedanib for 3 weeks, starting in week 8. The study was approved by the local Animal Welfare committee (VU-Fys 13-14).

Test substance formulation and dosing

The ethanesulfonate of nintedanib (Methyl (3Z)-3-{[(4-{methyl[(4-methylpiperazin-1-yl)acetyl]amino}phenyl)amino](phenyl)methylidene}-2-oxo-2,3-dihydro-1H-indole-6-carboxylate) (Boehringer Ingelheim Pharma, Biberach Germany) was dissolved in deionized water (MilliQ, Millipore) to reach a concentration of 2.8 mg/mL (on basis of the free base) and stored at room temperature to a maximum of 7 days. Nintedanib was administered at a dose of 41.5 mg/kg (50.0 mg/kg with ethanesulfonate) body weight once daily by oral gavage for 21 days, at a safe dose level based on the available results of 28-day or 90-day repeated dose toxicity studies (according ICH guidelines). Dose calculation was adjusted to the individual body weights twice weekly.

Echocardiography

On the day of necropsy, animals underwent echocardiography using a ProSound system (Prosound SSD-4000) equipped with a 13-Mhz linear transducer (UST-5542, Aloka, Tokyo, Japan), as described previously [10–12]. The following parameters were acquired; cardiac output, tricuspid annular plane systolic excursion (TAPSE), RV wall thickness (RVWT) and RV end diastolic diameter (RVEDD) and functional parameters such as cardiac output (CO), pulmonary artery acceleration time divided by cycle length (PAAT/cl) and stroke volume (SV) were measured. TAPSE was measured during systole in the four chamber view of the heart

and expresses the displacement of the lateral tricuspid annulus towards the apex.

Hemodynamics and pressure volume (PV)-loops

Just before necropsy, animals received isoflurane 2-3% in 1:1 O2/air mixture (60% oxygen) for anesthesia. Hematocrit was determined by centrifugation and fractional measurement. The chest was opened through the diaphragm. RV catheterization was performed using a Millar catheter (AD instruments, Bella Vista, Australia) for measuring right ventricular systolic pressure (RVSP) and pressure-volume measurements. For collecting end systolic elastance (EES), end diastolic elastance (EED) and arterial elastance (EA), the vena cava was occluded with a tightened string placed around the abdominal vena cava, as described previously [10–12]. Total pulmonary resistance (TPR) was calculated by dividing RVSP by CO.

Histological and morphometric analyses

After necropsy, lungs and cardiac tissues were weighed and processed for histology. Organ weights were corrected for tibia length. Tissues were fixed in formalin and embedded in paraffin. Four µm slides of lung tissue were prepared and stained with Elastica van Gieson, for specific coloration of the elastic laminae, and scanned (3DHISTECH, Budapest, Hungary). As described previously [10], only small arteries and arterioles with an approximate circular profile were included and divided into three classes based on external diameters, to distinguish: pre-capillaries, alveolar duct or respiratory bronchiole arteries and terminal bronchiole arteries. Averaged media and intima wall thickness were measured as described previously [10, 12, 13]. Completely obliterated vessels (>80% occlusion) and partially occluded vessels (0<x<80% occlusion) were included. Regarding the heart, four micron slices of tissue were prepared and stained. To assess the presence of connective tissue, a Masson's trichrome stain was performed. TIE2 (G-17, Santa Cruz, Dallas, TX,USA) and CD45 (550566, BD Pharmingen, San Jose, CA, USA) immunohistochemical stains were performed to evaluate capillary density and inflammation, respectively.

Protein expression

According to the suppliers manual, a western blot on RV homogenizations was performed (ANP(N-20):sc-18811, 1:200 (Santa Cruz Biotechnology, inc., Dallas, TX USA) and collagen 4 (COLIV, Rockland, inc. Limerick, PA USA), 2nd antibody

polyclonal Goat Anti-Rabbit immunoglobin E0432, 1:5000 (DAKO, Glostrup, Denmark). Novex ECL chemiluminescent (Invitrogen, Carlsbad, California) was used for protein detection. Optical densities were measured and standardized with β-actin.

Statistical analyses

All data are presented as mean ± S.E.M. of *n* animals. Parametric variables were compared between groups using appropriate ANOVA with Bonferroni post-hoc tests (GraphPad Prism, GraphPad Software Inc, La Jolla, CA USA.). A p value of less than 0.05 was considered significant.

Results

Clinical signs and body weight

In the nintedanib treated group, 3 animals showed reduced body weight gain, one animal showed pilo erection, ungroomed fur and paleness. In the vehicle treated group also reduced body weight gain was observed in 3 animals (**Table 1**). One animal died due to a technical dosing failure.

Echocardiography

A trend towards an increase in cardiac output was seen in the nintedanib group. Two dimensional parameters as tricuspid annular plane systolic excursion (TAPSE), RV wall thickness (RVWT) and RV end diastolic diameter (RVEDD) were not changed. Pulmonary artery acceleration time corrected for cycle length (PAAT/cl) and stroke volume (SV) were not different. A small trend towards a reduction of the TPR was observed in the nintedanib treated group.

Pressure Volume loops:

RV systolic pressure (end systole) was not different between vehicle and nintedanib treated animals. Nintedanib treatment resulted in an increase in the End Systolic Elastance (EES) which nearly reached statistical significance. As Arterial Elastance (EA) showed also a trend towards a small decrease in the nintedanib group, arterial ventricular coupling (EES/EA) was significantly increased in the nintedanib group (**Table 1**). Total pulmonary resistance (TPR) was not different between vehicle and nintedanib treated animals.

Ex-vivo measurements

The hematocrit was not different in comparison between vehicle treated and nintedanib treated animals (**Table 1**). Heart weight, RV weight, LV weight and fulton index (RV/(LV ± S), were not different between vehicle and nintedanib treated animals (**Table 1**). The Fulton index showed a trend towards an increase in the nintedanib group, but without reaching statistical significance (**Table 1**).

Parameter		vehicle treated	nintedanib treated	Significance
	terminal body weight (g)	440 ± 12..	403 ± 16..	ns
echocardiography	TAPSE (mm)	2.8 ± 0.1	2.5 ± 0.2	ns
	RVWT (mm)	2.1 ± 0.5	2.0 ± 0.1	ns
	RVEDD (mm)	4.4 ± 0.3	5.9 ± 0.3	ns
	PAAT/cl (%)	7.9 ± 0.5	7.8 ± 0.6	ns
	TPR (mmHg/mL/min)	0.4 ± 0.1	0.4 ± 0.1	ns
	SV (mL)	0.3 ± 0.1	0.4 ± 0.1	ns
pressure volume loops	RVSP (mmHg)	61.4 ± 8.03	66.4 ± 5.60	ns
	EES (mmHg/mL)	74.8 ± 19.7	126 ± 18..	ns (p = 0.076)
	EA (mmHg/mL)	227 ± 66..	205 ± 30..	ns
	EES/EA (fraction)	0.34 ± 0.05	0.80 ± 0.15	* (p = 0.0129)
	EED (mmHg/mL)	2.44 ± 0.54	2.78 ± 0.76	ns
ex-vivo measurements	Hematocrit (%)	44.2 ± 1.32	39.7 ± 2.56	ns
	Heart (grams)	2.42 ± 0.13	2.24 ± 0.19	ns
	RV (grams)	0.47 ± 0.11	0.50 ± 0.15	ns
	LV (grams)	0.98 ± 0.02	0.87 ± 0.05	ns
	Fulton index (RV/(LV+S))	0.48 ± 0.04	0.58 ± 0.06	ns

Table 1: *overview of body weight, echocardiographic, pressure volume loops and ex-vivo measurements in comparison between vehicle treated and nintedanib treated animals exposed to the Sugen hypoxia model.*

Lung histology

Medial and intimal thickness in all vessel classes was not different between vehicle and nintedanib treated animals (**Figure 1AB**). Regarding the occlusion rate, in the nintedanib group more open (O) vessels and less partially (P) or fully closed (C) were found in comparison to the vehicle group (**Figure 1C**).

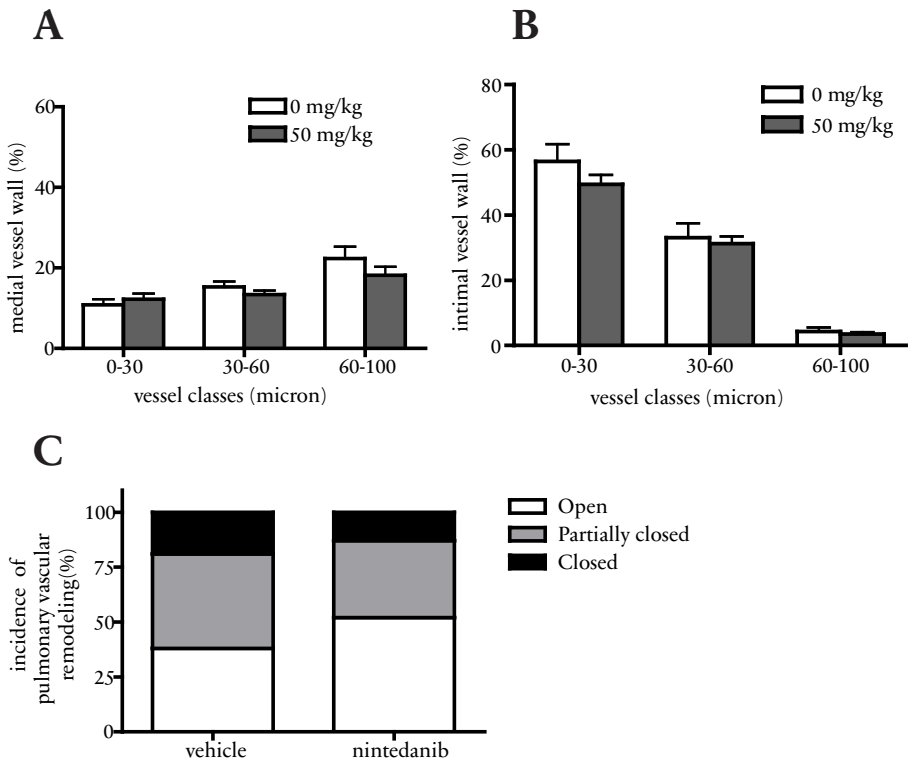

Figure 1: *Medial wall thickness (panel A), intimal wall thickness (panel B), in different vessel classes of 0-30, 30-60 and 60-100 micron in outer diameter, and occlusion rate (panel C) in vehicle treated and nintedanib treated animals. Mean plus SEM.*

Right ventricular histology and protein expression

RV capillary density was not altered between vehicle and nintedanib treated animals (**Figure 2A**). Masson trichrome staining showed that the presence of collagen was significantly decreased in the nintedanib group, in comparison to the vehicle group (**Figure 2B-C**). Inflammation, CD45, was not different between the vehicle treated and nintedanib treated group (**Figure 2D**). Western blots for Collagen IV and Atrial Naturetic Peptide (ANP) were performed. Both analyses show no differences between the nintedanib and vehicle group (**Figure 2E**).

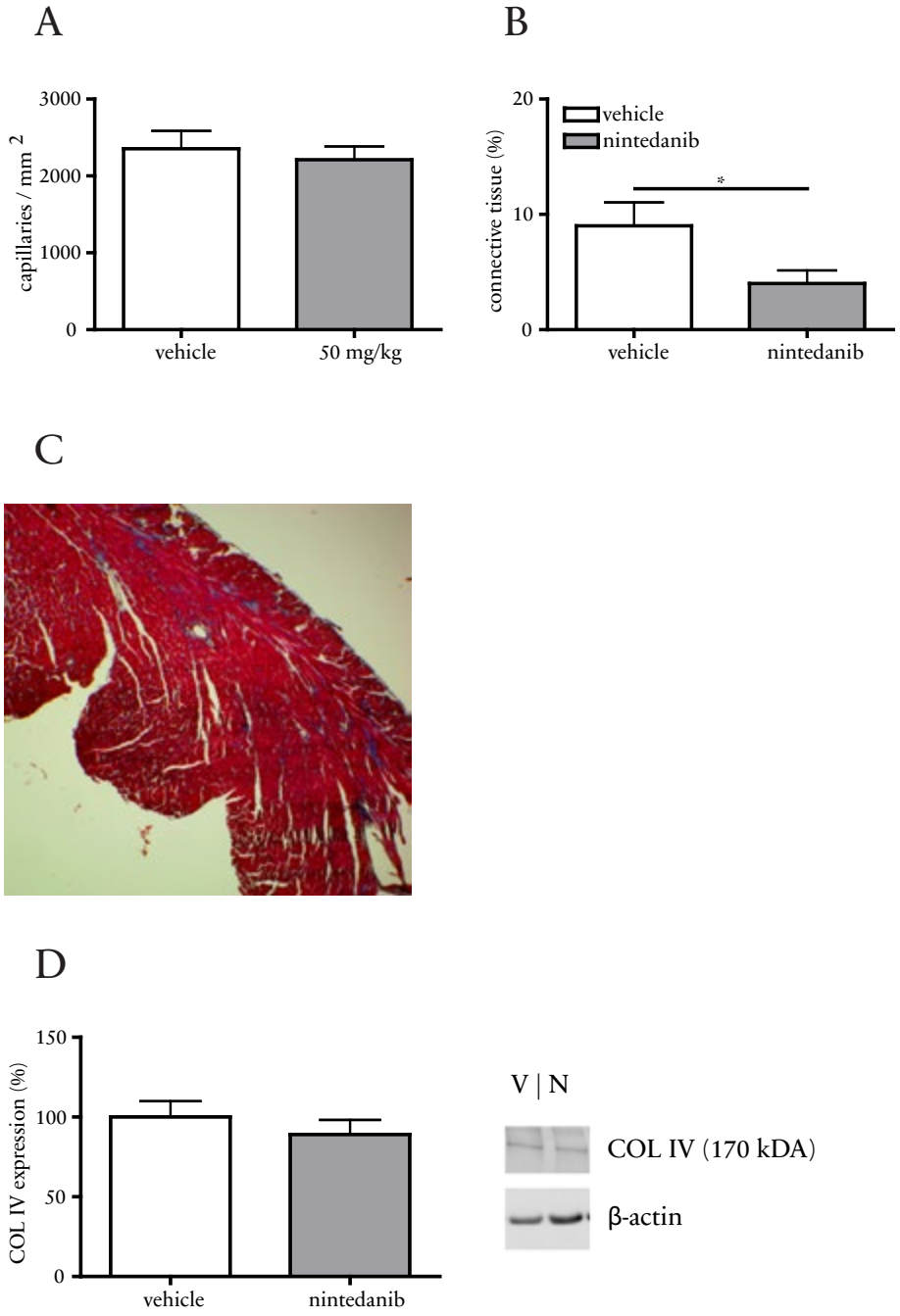
A
3000
2000
1000
0
capillaries / mm 2
vehicle
50 mg/kg
B
20
10
0
connective tissue (%)
vehicle
nintedanib
*
vehicle
nintedanib
C
D
150
100
50
0
COL IV expression (%)
vehicle
nintedanib
V | N
COL IV (170 kDA)
β-actin

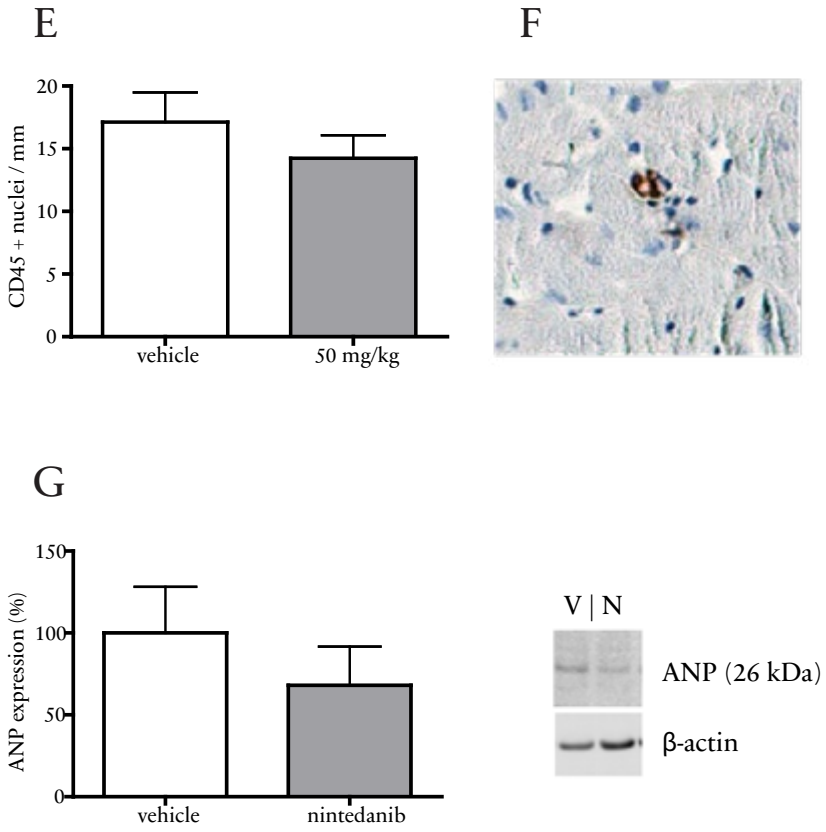

Figure 2: *Histological and protein analyses in vehicle- and nintedanib-treated animals in SuHx; Capillary density (endothelial cells per mm2, panel A), collagen tissue (panel B-D), Inflammatory density (CD45+ nuclei per mm2, panel E-F) and ANP expression (panel G). Mean plus SEM, * = p<0.05.*

Discussion

In the current study, we show that a 21-day repeated dosage of nintedanib in the advanced stage of the SuHx-model resulted in a mild decrease of the intima in the pulmonary vasculature. This finding was reflected in a decreased presence of partially and fully closed lung vessels in the range up to 40 micron. The treatment effect was, however, not prominently reflected in a change in TPR or EA. In respect to the literature regarding assessment of TKI's in experimental PH-models

[14–16, 16–19], the mild effect might be due to the fact that in this advanced stage of our SuHx-model, the medial thickness is completely normalized and beneficial treatment effects to the media are therefore limited [10].

The mild treatment effect in the lungs was reflected by a small (but not significant) improvement in cardiac output, and in improved arterial-ventricular coupling. These findings however, were not associated with improvements in RV hypertrophy, dilatation or inflammatory infiltration. Also, the cardiac stress marker ANP was similarly expressed in the nintedanib and vehicle groups. Histology showed a significant reduction in degree of RV fibrosis. Hematocrit and other parameters as for example body weight, clinical symptoms, are confirmative that no side effects have influenced the outcome of the cardiopulmonary results.

Nintedanib is a small molecule tyrosine kinase inhibitor targeting also PDGFR, FGFR and VEGFR and might have potential as a therapy for patients with PAH by its anti-tumor activity, anti-proliferative, and anti-fibrotic activity in animal models of IPF [20–24]. Nintedanib have showed to hamper the decline in lung function in patients with IPF [25], resulting in the approval of nintedanib as treatment of IPF in the United States and Europe [24].

Nintedanib treatment resulted in a mild beneficial attenuation of occlusion rate and in functional improvement of the right ventricle by increased cardiac output, contractility and arterial ventricular coupling. Nintedanib supported right ventricular adaptation to pressure overload by decreasing fibrosis. To assess if this mild treatment potential of nintedanib is of sufficient efficacy in PAH, further research is warrant, prior to perform clinical studies in order to confirm the therapeutic potential of nintedanib for PAH treatment.

References

1. Simonneau G, Gatzoulis MA, Adatia I, Celermajer D, Denton C, Ghofrani A, Gomez Sanchez MA, Krishna Kumar R, Landzberg M, Machado RF, Olschewski H, Robbins IM, Souza R. Updated clinical classification of pulmonary hypertension. *J. Am. Coll. Cardiol.* 2013; 62: D34–D41.
2. Humbert M, Sitbon O, Simonneau G. Treatment of pulmonary arterial hypertension. *N. Engl. J. Med.* 2004; 351: 1425–1436.
3. Selimovic N, Bergh C-H, Andersson B, Sakiniene E, Carlsten H, Rundqvist B. Growth factors and interleukin-6 across the lung circulation in pulmonary hypertension. *Eur. Respir. J.* 2009; 34: 662–668.
4. Ghofrani HA, Morrell NW, Hoeper MM, Olschewski H, Peacock AJ, Barst RJ, Shapiro S, Golpon H, Toshner M, Grimminger F, Pascoe S. Imatinib in pulmonary arterial hypertension patients with inadequate response to established therapy. *Am. J. Respir. Crit. Care Med.* 2010; 182: 1171–1177.
5. Montani D, Bergot E, Günther S, Savale L, Bergeron A, Bourdin A, Bouvaist H, Canuet M, Pison C, Macro M, Poubeau P, Girerd B, Natali D, Guignabert C, Perros F, O'Callaghan DS, Jaïs X, Tubert-Bitter P, Zalcman G, Sitbon O, Simonneau G, Humbert M. Pulmonary arterial hypertension in patients treated by dasatinib. *Circulation* 2012; 125: 2128–2137.
6. Bogaard HJ, Abe K, Vonk Noordegraaf A, Voelkel NF. The Right Ventricle Under Pressure: Cellular and Molecular Mechanisms of Right-Heart Failure in Pulmonary Hypertension. *Chest* 2009; 135: 794–804.
7. de Raaf MA, Beekhuijzen M, Guignabert C, Vonk Noordegraaf A, Bogaard HJ. Endothelin-1 receptor antagonists in fetal development and pulmonary arterial hypertension. *Reprod. Toxicol. Elmsford N* 2015; .
8. Bogaard HJ, Mizuno S, Hussaini AAA, Toldo S, Abbate A, Kraskauskas D, Kasper M, Natarajan R, Voelkel NF. Suppression of Histone Deacetylases Worsens Right Ventricular Dysfunction after Pulmonary Artery Banding in Rats. *Am. J. Respir. Crit. Care Med.* 2011; 183: 1402–1410.
9. De Raaf MA, Hussaini AA, Gomez-Arroyo J, Kraskaukas D, Farkas D, Happé C, Voelkel NF, Bogaard HJ. Histone deacetylase inhibition with trichostatin A does not reverse severe angioproliferative pulmonary hypertension in rats (2013 Grover Conference series). *Pulm. Circ.* 2014; 4: 237–243.
10. de Raaf MA, Schalij I, Gomez-Arroyo J, Rol N, Happé C, de Man FS, Vonk-Noordegraaf A, Westerhof N, Voelkel NF, Bogaard HJ. SuHx rat model: partly reversible pulmonary hypertension and progressive intima obstruction. *Eur. Respir. J.* 2014; 44: 160–168.

11. de Man FS, Handoko ML, van Ballegoij JJM, Schalij I, Bogaards SJP, Postmus PE, van der Velden J, Westerhof N, Paulus WJ, Vonk-Noordegraaf A. Bisoprolol delays progression towards right heart failure in experimental pulmonary hypertension. *Circ. Heart Fail.* 2012; 5: 97–105.
12. De Raaf MA, Kroeze Y, Middelman A, de Man FS, de Jong H, Vonk Noordegraaf A, de Korte C, Voelkel NF, Homberg J, Bogaard HJ. Serotonin transporter is not required for the development of severe pulmonary hypertension in the Sugen hypoxia rat model. *Am. J. Physiol. Lung Cell. Mol. Physiol.* 2015; : ajplung.00127.2015.
13. Okada K, Tanaka Y, Bernstein M, Zhang W, Patterson GA, Botney MD. Pulmonary hemodynamics modify the rat pulmonary artery response to injury. A neointimal model of pulmonary hypertension. *Am. J. Pathol.* 1997; 151: 1019–1025.
14. Aono Y, Nishioka Y, Inayama M, Ugai M, Kishi J, Uehara H, Izumi K, Sone S. Imatinib as a novel antifibrotic agent in bleomycin-induced pulmonary fibrosis in mice. *Am. J. Respir. Crit. Care Med.* 2005; 171: 1279–1285.
15. Kojonazarov B, Sydykov A, Pullamsetti SS, Luitel H, Dahal BK, Kosanovic D, Tian X, Majewski M, Baumann C, Evans S, Phillips P, Fairman D, Davie N, Wayman C, Kilty I, Weissmann N, Grimminger F, Seeger W, Ghofrani HA, Schermuly RT. Effects of multikinase inhibitors on pressure overload-induced right ventricular remodeling. *Int. J. Cardiol.* 2013; 167: 2630–2637.
16. Akagi S, Nakamura K, Miura D, Saito Y, Matsubara H, Ogawa A, Matoba T, Egashira K, Ito H. Delivery of imatinib-incorporated nanoparticles into lungs suppresses the development of monocrotaline-induced pulmonary arterial hypertension. *Int. Heart. J.* 2015; 56: 354–359.
17. Pankey EA, Thammasiboon S, Lasker GF, Baber S, Lasky JA, Kadowitz PJ. Imatinib attenuates monocrotaline pulmonary hypertension and has potent vasodilator activity in pulmonary and systemic vascular beds in the rat. *Am. J. Physiol. Heart Circ. Physiol.* 2013; 305: H1288–H1296.
18. Schermuly RT, Dony E, Ghofrani HA, Pullamsetti S, Savai R, Roth M, Sydykov A, Lai YJ, Weissmann N, Seeger W, Grimminger F. Reversal of experimental pulmonary hypertension by PDGF inhibition. *J. Clin. Invest.* 2005; 115: 2811–2821.
19. Jasińska-Stroschein M, Owczarek J, Łuczak A, Orszulak-Michalak D. The beneficial impact of fasudil and sildenafil on monocrotaline-induced pulmonary hypertension in rats: a hemodynamic and biochemical study. *Pharmacology* 2013; 91: 178–184.

20. Hilberg F, Roth GJ, Krssak M, Kautschitsch S, Sommergruber W, Tontsch-Grunt U, Garin-Chesa P, Bader G, Zoephel A, Quant J, Heckel A, Rettig WJ. BIBF 1120: triple angiokinase inhibitor with sustained receptor blockade and good antitumor efficacy. *Cancer Res.* 2008; 68: 4774–4782.
21. Santos ES, Gomez JE, Raez LE. Targeting angiogenesis from multiple pathways simultaneously: BIBF 1120, an investigational novel triple angiokinase inhibitor. *Invest. New Drugs* 2012; 30: 1261–1269.
22. Grimminger F, Schermuly RT, Ghofrani HA. Targeting non-malignant disorders with tyrosine kinase inhibitors. *Nat. Rev. Drug Discov.* 2010; 9: 956–970.
23. Wollin L, Maillet I, Quesniaux V, Holweg A, Ryffel B. Antifibrotic and anti-inflammatory activity of the tyrosine kinase inhibitor nintedanib in experimental models of lung fibrosis. *J. Pharmacol. Exp. Ther.* 2014; 349: 209–220.
24. Wollin L, Wex E, Pautsch A, Schnapp G, Hostettler KE, Stowasser S, Kolb M. Mode of action of nintedanib in the treatment of idiopathic pulmonary fibrosis. *Eur. Respir. J.* 2015; 45: 1434–1445.
25. Richeldi L, Costabel U, Selman M, Kim DS, Hansell DM, Nicholson AG, Brown KK, Flaherty KR, Noble PW, Raghu G, Brun M, Gupta A, Juhel N, Klüglich M, du Bois RM. Efficacy of a tyrosine kinase inhibitor in idiopathic pulmonary fibrosis. *N. Engl. J. Med.* 2011; 365: 1079–1087.
26. Bisping G, Kropff M, Wenning D, Dreyer B, Bessonov S, Hilberg F, Roth GJ, Munzert G, Stefanic M, Stelljes M, Scheffold C, Müller-Tidow C, Liebisch P, Lang N, Tchinda J, Serve HL, Mesters RM, Berdel WE, Kienast J. Targeting receptor kinases by a novel indolinone derivative in multiple myeloma: abrogation of stroma-derived interleukin-6 secretion and induction of apoptosis in cytogenetically defined subgroups. *Blood* 2006; 107: 2079–2089.
27. Chaudhary NI, Roth GJ, Hilberg F, Müller-Quernheim J, Prasse A, Zissel G, Schnapp A, Park JE. Inhibition of PDGF, VEGF and FGF signalling attenuates fibrosis. *Eur. Respir. J.* 2007; 29: 976–985.

Chapter 8:
Endothelin-1 receptor antagonists in fetal development and pulmonary arterial hypertension.

Michiel Alexander de Raaf[1], Manon Beekhuijzen[2], Christophe Guignabert[3,4], Anton Vonk Noordegraaf[1], Harm Jan Bogaard[1].

Adapted from Reproductive Toxicology. 2015 Aug 15;56:45-51.

Affiliation:
[1]Pulmonary Hypertension Knowledge Center, department of Pulmonology, VU University Medical Center / Institute for Cardiovascular Research, Amsterdam, The Netherlands. [2] WIL Research Europe B.V.,'s-Hertogenbosch, The Netherlands. [3]INSERM UMR_S 999, LabEx LERMIT, Centre Chirurgical Marie Lannelongue, Le Plessis-Robinson, France; [4]University of Paris-Sud, School of medicine, Kremlin-Bicêtre, France.

Abstract

The Pregnancy Prevention Program (PPP) is in place to prevent drug-induced developmental malformations. Remarkably, among the ten PPP-enlisted drugs are three endothelin-1 (ET-1) receptor antagonists (ERA's: ambrisentan, bosentan and macitentan), which are approved for the treatment of Pulmonary Arterial Hypertension (PAH). This review describes the effects of ERA's in PAH pathobiology and cardiopulmonary fetal development. While ERA's hamper pathological remodeling of the pulmonary vasculature and as such exert beneficial effects in PAH, they disturb fetal development of cardiopulmonary tissues. By blocking ET-1-mediated positive inotropic effects and myocardial fetal gene induction, ERA's may affect right ventricular adaptation to the increased pulmonary vascular resistance in both the fetus and the adult PAH patient.

Introduction

It is known that some medications induce severe fetal disorders when administered during pregnancy. The Pregnancy Prevention Program (PPP) was established to prevent these drug-induced developmental malformations by preventing the patient to become pregnant while using these medications. The program interdicts to start or continue a PPP-enlisted drug treatment in a pregnant patient and calls for adequate contraception in all female patients of reproductive age during treatment. Based on the patient information provided by the pharmaceutical companies, it is advised to use two forms of birth control concurrently and to perform pregnancy testing every month [1–3].

From the ten enlisted drugs in the PPP [4], three compounds are endothelin receptor antagonists (ERA's): ambrisentan, bosentan and macitentan. These ERA's are all approved for the treatment of Pulmonary Arterial Hypertension (PAH). PAH is a progressive and devastating disease, characterized by vasoconstriction, remodeling of the pulmonary vasculature and in situ thrombosis [5]. These pulmonary alterations lead to an increased vascular resistance and an increase in right ventricular (RV) pressure, demanding adaptive compensatory remodeling by RV hypertrophy [5, 6]. RV function is the most important prognostic determinant in pulmonary hypertension [7, 8]. In addition to ERA's, 3 other classes of medication are currently approved for PAH treatment: phosphodiesterase 5 inhibitors, soluble guanylate cyclase stimulators and prostacyclin analogues [9].

The purpose of this review is to describe the role of endothelin-1 (ET-1) in embryonic and fetal development and in the pathobiology of PAH. Parallels are drawn between the teratogenic effects of ERA's in utero and their therapeutic effect in adult PAH patients.

Endothelin-1 and endothelin-1 receptors

Endothelin is a peptide consisting of 3 isoforms, of which ET-1 is identified as an important player in cardiovascular homeostasis through strong vasoconstricting and positive inotropic effects [10]. ET-1 also has a mitogenic effect in the vascular wall which is important in angiogenesis and tissue repair [11]. Although endothelial cells are the predominant source of ET-1, pulmonary arterial smooth muscle cells and lung fibroblasts are additional potential producers of ET–1 [12, 13]. ET-1 responses are mediated by 2 receptor subtypes: ET-A and ET-B. Binding of ET-1 to ET-A and ET-B receptors on pulmonary artery smooth muscle cell promotes vasoconstriction, whereas activation of ET-B on pulmonary endothelial cells causes vasodilation [14] via increased endothelial secretion of prostacyclin and nitric oxide [10]. The endothelial ET-B receptor in the lungs is also responsible for the clearance of ET-1 [15, 16]. ET-1 and ET-A (but not ET-B) are both expressed in the healthy RV and even more so in patients with RV hypertrophy [17]. There are two classes of ERA's: selective antagonists of either the ET-A receptor or ET-B receptor and non-selective ERA's that inhibit both receptors [10, 16].

Endothelin-1 in embryonic and fetal development

ET-1 is important during early embryonic development. The neural crest is a transient embryonic structure unique to vertebrates that is generated at the lateral borders of the neural plate. The neural crest delaminates from the dorsal neural tube and subsets of neural crest cells migrate to various parts of the embryo, where they differentiate into a wide variety of cell types, including most of the craniofacial skeleton, cartilage, neurons and glia of the peripheral nervous system, connective tissue, neuroendocrine cells, and melanocytes [18]. The development of the neural crest is mediated by complex interactions of multiple signals and transcription factors. Bonano et al. [19], showed that early induction, migration and maintenance of neural crest specification require the ET-1/ET-A receptor signaling pathway. Thus, when endothelins and/or their receptors are affected, this will affect normal embyo-fetal development (**see Figure 1 for an overview**). Mice carrying targeted homozygous mutations for the ET-A receptor or ET-1 were viable to term but died shortly after birth due to severe defects in the formation of neural crest derivatives [20–22]. Malformations mainly consisted of craniofacial deformities and defects in the cardiovascular outflow tract. Developmental toxicity studies with ERA's in the rat confirmed these malformations [23, 24]. The pattern of fetal cardiovascular malformations is caused by the effect of

ERA's on specific neural crest cells in pharyngeal arches 3, 4 and 6 that migrate to the cardiac outflow tract. These cells express ET-A receptors and are involved in maturation of the great arteries and of the outflow septation complex. The ET-1/ ET-A receptor system is essential for the correct development of cardiac neural crest cells by means of an endothelium-mesenchyme interaction [22]. Also, the impaired migration of neural crest cells leads to craniofacial malformations

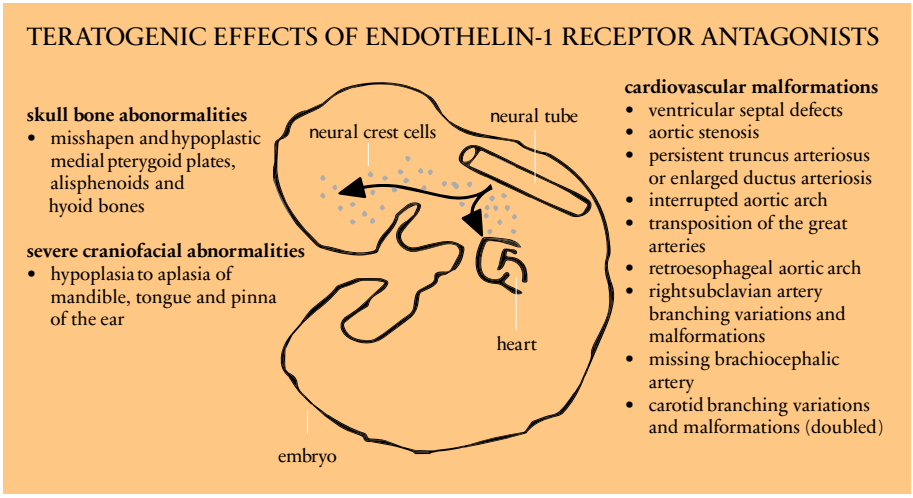

Figure 1: *Craniofacial and cardiac neural crest cells migrate from the neural tube to the craniofacial and cardiac region of the embryo. Considered as a class effect, Endothelin-1 receptor antagonists (ERA's)and homogenous mutations to Endothelin-1 or Endothelin-1 receptor A hamper the migration of these neural crest cells and lead to cardiovascular malformations and severe abnormalities of the skull bone or craniofacial region [23, 24]. Due to these preclinical teratogenic observations, both FDA and EMA strongly contraindicate the treatment of ERA's during pregnancy as the risk involved outweigh beneficial treatment effects.*

In the undeveloped fetal lung, ET-1 plays an important role in the maintenance of a high vascular resistance and a low blood flow. The fetal lung endothelium regulates pulmonary artery smooth muscle cell growth and proliferation via regulation of nitric oxide, prostacyclin and ETs [25]. Levy et al., showed an increase of ET-1 expression during gestation, which was decreased after birth [26]. This is probably due to the deployment of pulmonary tissue after birth, which at-

tenuates hypoxic pulmonary vasoconstriction. While ET-A receptor expression is strong both pre- and postnatally, expression of the ET-B receptor is low during early lung development, and increases and stabilizes in the last phases (saccular and alveolar stages) pre-natally and after birth [26]. By facilitating vasodilation and ET-1 clearance, the development of the ET-B receptor in the late fetal stage prevents muscularisation of the pulmonary pre-capillaries. ET-A receptor inhibition in the ovine fetus decreased pulmonary artery pressure, decreased right ventricular hypertrophy and attenuated the muscularization in small pulmonary arteries [27]. ET-B receptor inhibition increased pulmonary arterial pressure, increased pulmonary vascular resistance, increased right ventricular hypertrophy, increased muscularization of the small pulmonary arteries and maintained elevated ET-1 levels in the fetal lamb [28]. Indeed, impaired clearance of ET-1 in the early post-natal phase resulting in increased ET-1 plasma levels in humans is associated with Persistent Pulmonary Hypertension of the Newborn (PPHN) [25], characterized by a cardiac malformation which is caused by impaired closure of the cardiac septum resulting in a systemic-to-pulmonary shunt and high pressure in the pulmonary circulation. Animal studies showed that ET-B receptor stimulation prevents PPHN, while ET-A receptor stimulation provokes PPHN [29, 30]. This might suggest that normal RV development requires an ET-1 mediated high fetal pulmonary vascular resistance. Indeed, during fetal development the RV is relatively hypertrophic and undergoes major changes from the pre-natal to post-natal phase. After birth, when the lungs deploy and the pulmonary circulation becomes uncoupled from the systemic circulation, the RV is acting as a low pressure pump. After birth, the RV shows a lower weight increase compared to the left ventricle [31], which regresses the RV hypertrophy.

Pulmonary arterial hypertension and the pregnancy prevention program

Pregnancy is contraindicated in female PAH patients [32], because cardiopulmonary changes during pregnancy and around delivery are associated with significant rates of disease progression and maternal death in PAH [33]. During normal pregnancy, the cardiac output increases due to a 50% increase in circulatory blood volume and an increase in heart rate of about 10-20 beats per minute [33]. To accommodate this increase in cardiac output without an increase in pulmonary artery pressure, dilatation and recruitment of additional pulmonary vessels is needed. Failure of these mechanisms is thought to be responsible for the progression of PAH during pregnancy as well as for a perceived high frequency of new PAH cases becoming manifest during pregnancy.

ERA treatment during pregnancy is contraindicated by the PAH guideline, the PPP and the pharmaceutical companies [32, 34], and ERA's are indexed as category X in the FDA pregnancy labelling categories [35]. A category X label is given when animal or human studies showed evidence of fetal risk outweighing the potential benefits of the drug [35]. When pregnancy is not terminated, treatment needs to be switched to a PDE-5 inhibitor and/or prostacyclin analogues immediately [36]. Even on treatment, PAH pregnancies are associated with high rates of premature delivery and neonatal mortality [37].There have been no reports that the teratogenic character of ERA's found in animal studies [16, 38] translates to birth defects in children of mothers with PAH using ERA's in the first days of their pregancy.

Influences of Endothelin-1 on the pulmonary vasculature in Pulmonary Arterial Hypertension

ET-1 is a key contributor to the pathogenesis of PAH. Higher than normal plasma and lung ET-1 levels were reported in PAH patients [10] and these increased circulating ET-1 levels correlated with PAH severity and disease prognosis [39]. ET-1, ETA, and ET-B expressions are increased in the lungs of animals with experimental pulmonary hypertension [40–42]. It has also been demonstrated that administration of ERA's in several animal models resembling characteristic features of PAH prevents and reverses the elevated pulmonary artery pressure [43–47].

The three approved ERA's are the ET-A antagonist ambrisentan and the two dual ET-A and ET-B antagonists bosentan and macitentan [9, 16]. Because the ET-B

receptor on the endothelial cell induces vasodilation and ET-1 clearance, the beneficial treatment mechanism of ERA's inhibiting both ET-A and ET-B receptors, is more complex in comparison to the inhibition of ET-A receptor alone [48]. Clinical trials evaluating bosentan and ambrisentan showed functional improvements including decreases in pulmonary artery pressure and pulmonary resistance and an increase in cardiac output [9, 49–51]. Administration of ERA's can be associated with increased hepatic aminotransferase levels and these need to be monitored closely [9]. Sitaxsentan, a dual ERA, was withdrawn from the market in 2010 due to concerns of liver toxicity. Despite the suggested higher efficacy of non-selective ERA's [52, 53], there are no proven differences in clinical outcome when comparing selective ET-A inhibition (ambrisentan) with non-selective ET-A and ET-B inhibition (bosentan). In theory, inhibition of the ET-B receptor also hampers ET-1 clearance. This is seen in clinical studies, where ET-1 plasma levels increased significantly after bosentan administration [54]. Recently, macitentan, a new potent non-peptide non-selective ERA with a 50-fold higher affinity for ET-A than for ET-B receptors, was approved for the long-term treatment of PAH patients in WHO functional class II–III [55, 56].

Influence of ET-1 on the RV in PAH

In post-natal health, right ventricular pressures are one-fifth in comparison to the systemic circulation. In patients with pulmonary hypertension, the RV needs to remodel 'backwards' into a high pressure pump, and to accomplish this, the RV re-enters a fetal gene program [57, 58]. There is evidence to suggest that ET-1 plays a direct role in the regulation of a fetal gene program in cardiomyocytes [59]. PAH patients, as well as animals with experimental RV hypertrophy, show an upregulated ET-1 axis in the myocardium of the RV [17]. Because the fetal gene program is active in the developing fetal RV as well as in the adult RV adapting to an increased pulmonary vascular resistance, the use of ERA's could have similar effects in both situations. ET-1 is also known to directly affect cardiac contractility [10, 17, 57, 60]. Via the ET-A receptor on cardiomyocytes, ET-1 increases intracellular calcium and calcium influx [61]. In that respect, ERA's have been experimentally shown to induce a negative inotropic effect on the myocardium [17]. If these observations are relevant to patients with PAH remains unproven, but it is striking in this respect that ERA's worsened disease progression in patients with left heart failure [62, 63].

Based on clinical trial data, Nagendran et al. suggested that the observed reduc-

tion in vascular tone in patients treated with ERA's, are not always reflected in a proportional improvement in cardiac output [17, 64–68]. In animal models with RV hypertrophy, ERA's did not always improve RV function [69–71]. Nagendran et al. pointed to the negative inotropic effect of ERA's in the RV, which could potentially worsen disease progression in PAH patients with hypertrophied and compensated RV's [17]. The clinical relevance of these observations is unclear, however and further research is warranted. In most PAH patients, there is a delay between disease onset and diagnosis and therefore ERA treatment is usually only given after the process of RV adaptation to pressure overload has taken place. Upon ERA treatment, any negative effects on the RV could be negated by the beneficial decrease in pulmonary vascular resistance. Even if ERA's would worsen RV function, this effect may be easily overcome by using combination treatments, such as the PDE-5 inhibitor sildenafil and the ERA bosentan or tadalafil and the ERA ambrisentan, which showed improvement of cardiac index in experimental and human PAH [72, 73]. Treatment with the recently approved ERA macitentan showed a 30% decrease in pulmonary vascular resistance and an 11% increase in cardiac index, resulting in a decreased morbidity and mortality [55]. In comparison to other ERA's, it could be speculated that negative inotropic effect by macitentan is minor in comparison to the major beneficial decrease of pulmonary vascular resistance.

The use of ERA's in PAH post-partum

Hemodynamic normalization after an uncomplicated delivery takes approximately six weeks [33, 74, 75]. Post-partum fluid shifts and a temporary deterioration of myocardial function are particular risks to female PAH patients in the first days after delivery [33, 74]. If ERA's have a negative inotropic effect on the RV, this would be of particular importance during the post-partum period. There is no clinical data to guide optimal timing of (re-) starting ERA therapy after pregnancy in a PAH patient. It seems well-advised to carefully monitor post-partum hemodynamics and RV function prior to initiating ERA treatment.

Other parallels between vasoactive signals in fetal development and PAH pathophysiology

In addition to ET-1, other vasoactive signals play a mutual regulating role in the fetal circulation as well in the pathobiology of PAH. Bone marrow protein (BMP) is a key factor in pulmonary vasculogenesis and it has been suggested that dysfunctional BMP signaling due to a mutation of the BMP receptor II, leads to abnormal lung development which contribute to the pathogenesis of PAH [76]. An intact Rho kinase pathway is required for major morphogenetic events, also particularly in the heart, during embryonic development and teratogenicity was reported due to inhibition of Rho kinase[77, 78]. Prostaglandins, nitric oxide (NO), and endothelium derived NO (EDNO) play an important role in regulating vessel tone of the fetal pulmonary circulation and are of pivotal importance during the pre- to postnatal transition of lungs and heart [48, 79]. In PAH, the production of NO and prostacyclin is decreased and increasing the production by nitric oxide, phosphodiesterase 5 inhibitors or prostacyclin analogues beneficially affects vadodilatation and antiproliferation [9]. Fasudil is a Rho kinase inhibitor and regresses PAH disease progression in several animal models and has been proposed as PAH treatment [80–83]. Due to these many parallels and the safety labelling of these compounds, a safe PAH treatment for both mother as fetus during pregnancy cannot be assured. Also for non-vasoactive compounds which are associated as PAH treatment by hampering vessel remodeling, such as tyrosine kinase inhibitors of growth factors or histone deacetylase inhibitors, the possible teratogenicity should be considered. When a female PAH patient chooses to continue pregnancy, ERA treatment should be terminated immediately and attention to the recommendations in the review by Martínez and Rutherford is strongly advised [33]. They evaluated that most pregnant PAH patients receive prostacyclin analogues and summarized successful treatments in pregnant PAH patients [33].

Conclusion

The role of ET-1 in the pulmonary vasculature and in the RV in embryo-fetal life and in PAH shows many parallels (**Figure 2**), of which an increased pulmonary vascular resistance and an active state of the fetal gene program in the RV are the most prominent. Regarding embryo-fetal life, ERA's disturb the development of cardiopulmonary tissues and due to the induction of these severe malformations ERA treatment during pregnancy is strongly discouraged. The fetal parallels explain the beneficial treatment response of ERA's in the PAH lung, but could theoretically also translate into some degree of RV functional deterioration when a decrease in pulmonary vascular tone is not achieved. A high maternal mortality signifies that pregnancy in PAH is contraindicated, also without ERA treatment. When a female PAH patient nonetheless chooses to bring a pregnancy to full term, the use of ERA's is contraindicated due to the risk of fetal malformations and ERA treatment should be avoided or terminated immediately. More research is required to guide optimal timing of (re-) initiation of ERA treatment after delivery.

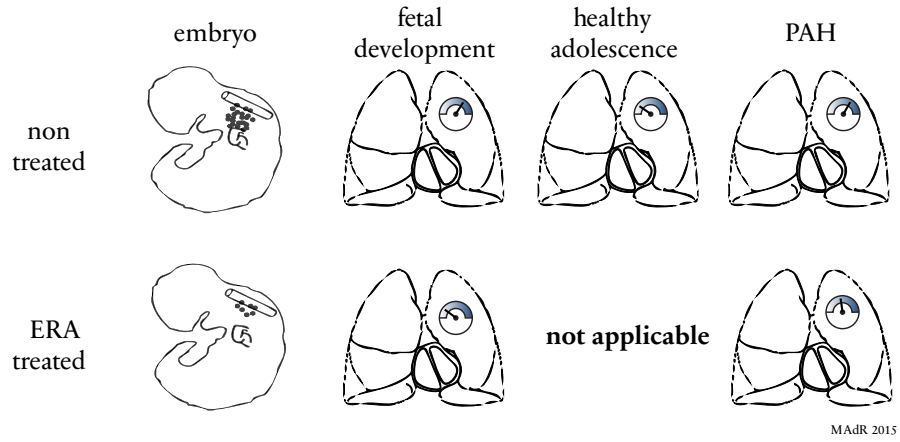

Figure 2: *Conclusive figure regarding the parallels in pre-natal development and Pulmonary Arterial Hypertension (PAH). In the embryo neuro crest cells migrate from the neural tube towards the cardiac region. Endothelin-1 Receptor Antagonists (ERA) hamper the migration of these neuro crest cells, resulting in cranio facial and cardiac malformations. During fetal development, the pulmonary vascular resistance (PVR) is increased by which the right ventricle (RV) can develop optimally. Administration*

of ERA's lower the PVR, which hampers RV development. In healthy adolescence the PVR is a 5-fold lower in comparison to the fetal PVR. The RV is now functioning as a low-pressure pump. In PAH the PVR increases to pathophysiological ranges. The demanded pressure-overload pushes the RV back into a fetal gene program for inducing hypertrophic adaptation. ERA's in PAH lower the PVR which lowers the needed RV systolic pressure. However, ERA's have also a direct negative inotropic effect on RV contractility and hamper the adaptive fetal gene program.

References

1. European Medicines Agency. EPAR summary for the public: Tracleer (bosentan). 2015; EMA/85270/2015 EMEA/H/C/000401.
2. European Medicines Agency. EPAR summary for the public Volibris (ambrisentan). 2013; EMA/783996/2012 EMEA/H/C/000839.
3. European Medicines Agency. EPAR summary for the public Opsumit (macitentan). 2014; EMA/670241/2013 EMEA/H/C/002697.
4. College ter Beoordeling van Geneesmiddelen | Medicines Evaluation Board. CBG-MED; Pregnancy Prevention Programme - http://www.cbg-meb.nl/CBG/en/human-medicines/pharmacovigilance/pregnancy-prevention-programme/default.htm. .
5. Simonneau G, Robbins IM, Beghetti M, Channick RN, Delcroix M, Denton CP, Elliott CG, Gaine SP, Gladwin MT, Jing Z-C, Krowka MJ, Langleben D, Nakanishi N, Souza R. Updated clinical classification of pulmonary hypertension. *J. Am. Coll. Cardiol.* 2009; 54: S43–S54.
6. Simonneau G, Gatzoulis MA, Adatia I, Celermajer D, Denton C, Ghofrani A, Gomez Sanchez MA, Krishna Kumar R, Landzberg M, Machado RF, Olschewski H, Robbins IM, Souza R. Updated clinical classification of pulmonary hypertension. *J. Am. Coll. Cardiol.* 2013; 62: D34–D41.
7. Mauritz G-J, Kind T, Marcus JT, Bogaard H-J, van de Veerdonk M, Postmus PE, Boonstra A, Westerhof N, Vonk-Noordegraaf A. Progressive changes in right ventricular geometric shortening and long-term survival in pulmonary arterial hypertension. *Chest* 2012; 141: 935–943.
8. D'Alonzo GE, Barst RJ, Ayres SM, Bergofsky EH, Brundage BH, Detre KM, Fishman AP, Goldring RM, Groves BM, Kernis JT, others. Survival in patients with primary pulmonary hypertension. *Ann. Intern. Med.* 1991; 115: 343–349.
9. Humbert M, Sitbon O, Simonneau G. Treatment of pulmonary arterial hypertension. *N. Engl. J. Med.* 2004; 351: 1425–1436.
10. Giannessi D, Del Ry S, Vitale RL. The role of endothelins and their receptors in heart failure. *Pharmacol. Res. Off. J. Ital. Pharmacol. Soc.* 2001; 43: 111–126.
11. Chen YF, Oparil S. Endothelial dysfunction in the pulmonary vascular bed. *Am. J. Med. Sci.* 2000; 320: 223–232.
12. Dingemanse J, van Giersbergen PLM. Clinical pharmacology of bosentan, a dual endothelin receptor antagonist. *Clin. Pharmacokinet.* 2004; 43: 1089–1115.
13. Shi-Wen X, Chen Y, Denton CP, Eastwood M, Renzoni EA, Bou-Gharios G,

Pearson JD, Dashwood M, du Bois RM, Black CM, Leask A, Abraham DJ. Endothelin-1 promotes myofibroblast induction through the ETA receptor via a rac/phosphoinositide 3-kinase/Akt-dependent pathway and is essential for the enhanced contractile phenotype of fibrotic fibroblasts. *Mol. Biol. Cell* 2004; 15: 2707–2719.

14. Simonson MS, Dunn MJ. Cellular signaling by peptides of the endothelin gene family. *FASEB J. Off. Publ. Fed. Am. Soc. Exp. Biol.* 1990; 4: 2989–3000.
15. Dupuis J, Goresky CA, Fournier A. Pulmonary clearance of circulating endothelin-1 in dogs in vivo: exclusive role of ETB receptors. *J. Appl. Physiol. Bethesda Md 1985* 1996; 81: 1510–1515.
16. Chaumais M-C, Guignabert C, Savale L, Jaïs X, Boucly A, Montani D, Simonneau G, Humbert M, Sitbon O. Clinical pharmacology of endothelin receptor antagonists used in the treatment of pulmonary arterial hypertension. *Am. J. Cardiovasc. Drugs Drugs Devices Interv.* 2015; 15: 13–26.
17. Nagendran J, Sutendra G, Paterson I, Champion HC, Webster L, Chiu B, Haromy A, Rebeyka IM, Ross DB, Michelakis ED. Endothelin axis is upregulated in human and rat right ventricular hypertrophy. *Circ. Res.* 2013; 112: 347–354.
18. Weston JA, Thiery JP. Pentimento: Neural Crest and the origin of mesectoderm. *Dev. Biol.* 2015; .
19. Bonano M, Tríbulo C, De Calisto J, Marchant L, Sánchez SS, Mayor R, Aybar MJ. A new role for the Endothelin-1/Endothelin-A receptor signaling during early neural crest specification. *Dev. Biol.* 2008; 323: 114–129.
20. Clouthier DE, Hosoda K, Richardson JA, Williams SC, Yanagisawa H, Kuwaki T, Kumada M, Hammer RE, Yanagisawa M. Cranial and cardiac neural crest defects in endothelin-A receptor-deficient mice. *Dev. Camb. Engl.* 1998; 125: 813–824.
21. Kurihara Y, Kurihara H, Oda H, Maemura K, Nagai R, Ishikawa T, Yazaki Y. Aortic arch malformations and ventricular septal defect in mice deficient in endothelin-1. *J. Clin. Invest.* 1995; 96: 293–300.
22. Pla P, Larue L. Involvement of endothelin receptors in normal and pathological development of neural crest cells. *Int. J. Dev. Biol.* 2003; 47: 315–325.
23. Treinen KA, Louden C, Dennis MJ, Wier PJ. Developmental toxicity and toxicokinetics of two endothelin receptor antagonists in rats and rabbits. *Teratology* 1999; 59: 51–59.
24. Spence S, Anderson C, Cukierski M, Patrick D. Teratogenic effects of the endothelin receptor antagonist L-753,037 in the rat. *Reprod. Toxicol. Elmsford*

N 1999; 13: 15–29.
25. Abman SH. Recent advances in the pathogenesis and treatment of persistent pulmonary hypertension of the newborn. *Neonatology* 2007; 91: 283–290.
26. Levy M, Maurey C, Chailley-Heu B, Martinovic J, Jaubert F, Israel-Biet D. Developmental changes in endothelial vasoactive and angiogenic growth factors in the human perinatal lung. *Pediatr. Res.* 2005; 57: 248–253.
27. Ivy DD, Parker TA, Ziegler JW, Galan HL, Kinsella JP, Tuder RM, Abman SH. Prolonged endothelin A receptor blockade attenuates chronic pulmonary hypertension in the ovine fetus. *J. Clin. Invest.* 1997; 99: 1179–1186.
28. Barman SA, Marrero MB. Mechanism of endothelin-1 activation of MAP kinases in neonatal pulmonary vascular smooth muscle. *Lung* 2005; 183: 425–439.
29. Ivy DD, Parker TA, Abman SH. Prolonged endothelin B receptor blockade causes pulmonary hypertension in the ovine fetus. *Am. J. Physiol. Lung Cell. Mol. Physiol.* 2000; 279: L758–L765.
30. Ivy DD, Yanagisawa M, Gariepy CE, Gebb SA, Colvin KL, McMurtry IF. Exaggerated hypoxic pulmonary hypertension in endothelin B receptor-deficient rats. *Am. J. Physiol. Lung Cell. Mol. Physiol.* 2002; 282: L703–L712.
31. Hew KW, Keller KA. Postnatal anatomical and functional development of the heart: a species comparison. *Birth Defects Res. B. Dev. Reprod. Toxicol.* 2003; 68: 309–320.
32. Taichman DB, Ornelas J, Chung L, Klinger JR, Lewis S, Mandel J, Palevsky HI, Rich S, Sood N, Rosenzweig EB, Trow TK, Yung R, Elliott CG, Badesch DB. Pharmacologic therapy for pulmonary arterial hypertension in adults: CHEST guideline and expert panel report. *Chest* 2014; 146: 449–475.
33. Martínez MV, Rutherford JD. Pulmonary hypertension in pregnancy. *Cardiol. Rev.* 2013; 21: 167–173.
34. Kenyon KW, Nappi JM. Bosentan for the treatment of pulmonary arterial hypertension. *Ann. Pharmacother.* 2003; 37: 1055–1062.
35. Food and Drug Administration, HHS. Content and format of labeling for human prescription drug and biological products; requirements for pregnancy and lactation labeling. Final rule. *Fed. Regist.* 2014; 79: 72063–72103.
36. Olsson KM, Jais X. Birth control and pregnancy management in pulmonary hypertension. *Semin. Respir. Crit. Care Med.* 2013; 34: 681–688.
37. Bédard E, Dimopoulos K, Gatzoulis MA. Has there been any progress made on pregnancy outcomes among women with pulmonary arterial hypertension? *Eur. Heart J.* 2009; 30: 256–265.

38. Dhillon S, Keating GM. Bosentan: a review of its use in the management of mildly symptomatic pulmonary arterial hypertension. *Am. J. Cardiovasc. Drugs Drugs Devices Interv.* 2009; 9: 331–350.
39. Giaid A, Yanagisawa M, Langleben D, Michel RP, Levy R, Shennib H, Kimura S, Masaki T, Duguid WP, Stewart DJ. Expression of endothelin-1 in the lungs of patients with pulmonary hypertension. *N. Engl. J. Med.* 1993; 328: 1732–1739.
40. Frasch HF, Marshall C, Marshall BE. Endothelin-1 is elevated in monocrotaline pulmonary hypertension. *Am. J. Physiol.* 1999; 276: L304–L310.
41. Sato K, Webb S, Tucker A, Rabinovitch M, O'Brien RF, McMurtry IF, Stelzner TJ. Factors influencing the idiopathic development of pulmonary hypertension in the fawn hooded rat. *Am. Rev. Respir. Dis.* 1992; 145: 793–797.
42. Miyauchi T, Yorikane R, Sakai S, Sakurai T, Okada M, Nishikibe M, Yano M, Yamaguchi I, Sugishita Y, Goto K. Contribution of endogenous endothelin-1 to the progression of cardiopulmonary alterations in rats with monocrotaline-induced pulmonary hypertension. *Circ. Res.* 1993; 73: 887–897.
43. Eddahibi S, Raffestin B, Clozel M, Levame M, Adnot S. Protection from pulmonary hypertension with an orally active endothelin receptor antagonist in hypoxic rats. *Am. J. Physiol.* 1995; 268: H828–H835.
44. Shinohara T, Sawada H, Otsuki S, Yodoya N, Kato T, Ohashi H, Zhang E, Saitoh S, Shimpo H, Maruyama K, Komada Y, Mitani Y. Macitentan reverses early obstructive pulmonary vasculopathy in rats: Early intervention in overcoming the survivin-mediated resistance to apoptosis. *Am. J. Physiol. Lung Cell. Mol. Physiol.* 2014; : ajplung.00129.2014.
45. Temple IP, Monfredi O, Quigley G, Schneider H, Zi M, Cartwright EJ, Boyett MR, Mahadevan VS, Hart G. Macitentan treatment retards the progression of established pulmonary arterial hypertension in an animal model. *Int. J. Cardiol.* 2014; 177: 423–428.
46. Pehlivan Y, Dokuyucu R, Demir T, Kaplan DS, Koc I, Orkmez M, Turkbeyler IH, Ceribasi AO, Tutar E, Taysi S, Kisacik B, Onat AM. Palosuran treatment effective as bosentan in the treatment model of pulmonary arterial hypertension. *Inflammation* 2014; 37: 1280–1288.
47. Clozel M, Hess P, Rey M, Iglarz M, Binkert C, Qiu C. Bosentan, sildenafil, and their combination in the monocrotaline model of pulmonary hypertension in rats. *Exp. Biol. Med. Maywood NJ* 2006; 231: 967–973.
48. Voelkel NF, Rounds, S. The Pulmonary Endothelium. 1rst ed. Wiley-Blackwell;

49. Rubin LJ, Badesch DB, Barst RJ, Galie N, Black CM, Keogh A, Pulido T, Frost A, Roux S, Leconte I, Landzberg M, Simonneau G. Bosentan therapy for pulmonary arterial hypertension. *N. Engl. J. Med.* 2002; 346: 896–903.
50. Galiè N, Hinderliter AL, Torbicki A, Fourme T, Simonneau G, Pulido T, Espinola-Zavaleta N, Rocchi G, Manes A, Frantz R, Kurzyna M, Nagueh SF, Barst R, Channick R, Dujardin K, Kronenberg A, Leconte I, Rainisio M, Rubin L. Effects of the oral endothelin-receptor antagonist bosentan on echocardiographic and doppler measures in patients with pulmonary arterial hypertension. *J. Am. Coll. Cardiol.* 2003; 41: 1380–1386.
51. D'Alto M. An update on the use of ambrisentan in pulmonary arterial hypertension. *Ther. Adv. Respir. Dis.* 2012; 6: 331–343.
52. Galié N, Manes A, Branzi A. The endothelin system in pulmonary arterial hypertension. *Cardiovasc. Res.* 2004; 61: 227–237.
53. Casserly B, Klinger JR. Ambrisentan for the treatment of pulmonary arterial hypertension. *Drug Des. Devel. Ther.* 2009; 2: 265–280.
54. Hiramoto Y, Shioyama W, Higuchi K, Arita Y, Kuroda T, Sakata Y, Nakaoka Y, Fujio Y, Yamauchi-Takihara K. Clinical significance of plasma endothelin-1 level after bosentan administration in pulmonary arterial hypertension. *J. Cardiol.* 2009; 53: 374–380.
55. Pulido T, Adzerikho I, Channick RN, Delcroix M, Galiè N, Ghofrani H-A, Jansa P, Jing Z-C, Le Brun F-O, Mehta S, Mittelholzer CM, Perchenet L, Sastry BKS, Sitbon O, Souza R, Torbicki A, Zeng X, Rubin LJ, Simonneau G, SERAPHIN Investigators. Macitentan and morbidity and mortality in pulmonary arterial hypertension. *N. Engl. J. Med.* 2013; 369: 809–818.
56. Channick RN, Delcroix M, Ghofrani H-A, Hunsche E, Jansa P, Le Brun F-O, Mehta S, Pulido T, Rubin LJ, Sastry BKS, Simonneau G, Sitbon O, Souza R, Torbicki A, Galiè N. Effect of macitentan on hospitalizations: results from the SERAPHIN trial. *JACC Heart Fail.* 2015; 3: 1–8.
57. Bogaard HJ, Abe K, Vonk Noordegraaf A, Voelkel NF. The Right Ventricle Under Pressure: Cellular and Molecular Mechanisms of Right-Heart Failure in Pulmonary Hypertension. *Chest* 2009; 135: 794–804.
58. Rajabi M, Kassiotis C, Razeghi P, Taegtmeyer H. Return to the fetal gene program protects the stressed heart: a strong hypothesis. *Heart Fail. Rev.* 2007; 12: 331–343.
59. Saito S, Aikawa R, Shiojima I, Nagai R, Yazaki Y, Komuro I. Endothelin-1 induces expression of fetal genes through the interleukin-6 family of cytokines in cardiac myocytes. *FEBS Lett.* 1999; 456: 103–107.

60. Sugden PH. An overview of endothelin signaling in the cardiac myocyte. *J. Mol. Cell. Cardiol.* 2003; 35: 871–886.
61. Nagasaka T, Izumi M, Hori M, Ozaki H, Karaki H. Positive inotropic effect of endothelin-1 in the neonatal mouse right ventricle. *Eur. J. Pharmacol.* 2003; 472: 197–204.
62. Anand I, McMurray J, Cohn JN, Konstam MA, Notter T, Quitzau K, Ruschitzka F, Lüscher TF, EARTH investigators. Long-term effects of darusentan on left-ventricular remodelling and clinical outcomes in the EndothelinA Receptor Antagonist Trial in Heart Failure (EARTH): randomised, double-blind, placebo-controlled trial. *Lancet* 2004; 364: 347–354.
63. Mylona P, Cleland JG. Update of REACH-1 and MERIT-HF clinical trials in heart failure. Cardio.net Editorial Team. *Eur. J. Heart Fail.* 1999; 1: 197–200.
64. Barst RJ, Rich S, Widlitz A, Horn EM, McLaughlin V, McFarlin J. Clinical efficacy of sitaxsentan, an endothelin-A receptor antagonist, in patients with pulmonary arterial hypertension: open-label pilot study. *Chest* 2002; 121: 1860–1868.
65. Galié N, Badesch D, Oudiz R, Simonneau G, McGoon MD, Keogh AM, Frost AE, Zwicke D, Naeije R, Shapiro S, Olschewski H, Rubin LJ. Ambrisentan therapy for pulmonary arterial hypertension. *J. Am. Coll. Cardiol.* 2005; 46: 529–535.
66. Galiè N, Olschewski H, Oudiz RJ, Torres F, Frost A, Ghofrani HA, Badesch DB, McGoon MD, McLaughlin VV, Roecker EB, Gerber MJ, Dufton C, Wiens BL, Rubin LJ, Ambrisentan in Pulmonary Arterial Hypertension, Randomized, Double-Blind, Placebo-Controlled, Multicenter, Efficacy Studies (ARIES) Group. Ambrisentan for the treatment of pulmonary arterial hypertension: results of the ambrisentan in pulmonary arterial hypertension, randomized, double-blind, placebo-controlled, multicenter, efficacy (ARIES) study 1 and 2. *Circulation* 2008; 117: 3010–3019.
67. Galiè N, Beghetti M, Gatzoulis MA, Granton J, Berger RMF, Lauer A, Chiossi E, Landzberg M, Bosentan Randomized Trial of Endothelin Antagonist Therapy-5 (BREATHE-5) Investigators. Bosentan therapy in patients with Eisenmenger syndrome: a multicenter, double-blind, randomized, placebo-controlled study. *Circulation* 2006; 114: 48–54.
68. Michelakis ED, Wilkins MR, Rabinovitch M. Emerging concepts and translational priorities in pulmonary arterial hypertension. *Circulation* 2008; 118: 1486–1495.
69. Hill NS, Warburton RR, Pietras L, Klinger JR. Nonspecific endothelin-re-

ceptor antagonist blunts monocrotaline-induced pulmonary hypertension in rats. *J. Appl. Physiol. Bethesda Md 1985* 1997; 83: 1209–1215.
70. Choudhary G, Troncales F, Martin D, Harrington EO, Klinger JR. Bosentan attenuates right ventricular hypertrophy and fibrosis in normobaric hypoxia model of pulmonary hypertension. *J. Heart Lung Transplant. Off. Publ. Int. Soc. Heart Transplant.* 2011; 30: 827–833.
71. Taguchi K, Hattori Y. Unlooked-for significance of cardiac versus vascular effects of endothelin-1 in the pathophysiology of pulmonary arterial hypertension. *Circ. Res.* 2013; 112: 227–229.
72. Wilkins MR, Paul GA, Strange JW, Tunariu N, Gin-Sing W, Banya WA, Westwood MA, Stefanidis A, Ng LL, Pennell DJ, Mohiaddin RH, Nihoyannopoulos P, Gibbs JSR. Sildenafil versus Endothelin Receptor Antagonist for Pulmonary Hypertension (SERAPH) study. *Am. J. Respir. Crit. Care Med.* 2005; 171: 1292–1297.
73. Cavasin MA, Demos-Davies KM, Schuetze KB, Blakeslee WW, Stratton MS, Tuder RM, McKinsey TA. Reversal of severe angioproliferative pulmonary arterial hypertension and right ventricular hypertrophy by combined phosphodiesterase-5 and endothelin receptor inhibition. *J. Transl. Med.* 2014; 12: 314.
74. Ruys TPE, Cornette J, Roos-Hesselink JW. Pregnancy and delivery in cardiac disease. *J. Cardiol.* 2013; 61: 107–112.
75. Robson SC, Hunter S, Moore M, Dunlop W. Haemodynamic changes during the puerperium: a Doppler and M-mode echocardiographic study. *Br. J. Obstet. Gynaecol.* 1987; 94: 1028–1039.
76. Southwood M, Jeffery TK, Yang X, Upton PD, Hall SM, Atkinson C, Haworth SG, Stewart S, Reynolds PN, Long L, Trembath RC, Morrell NW. Regulation of bone morphogenetic protein signalling in human pulmonary vascular development. *J. Pathol.* 2008; 214: 85–95.
77. Wei L, Roberts W, Wang L, Yamada M, Zhang S, Zhao Z, Rivkees SA, Schwartz RJ, Imanaka-Yoshida K. Rho kinases play an obligatory role in vertebrate embryonic organogenesis. *Dev. Camb. Engl.* 2001; 128: 2953–2962.
78. Zhao Z, Rivkees SA. Rho-associated kinases play an essential role in cardiac morphogenesis and cardiomyocyte proliferation. *Dev. Dyn. Off. Publ. Am. Assoc. Anat.* 2003; 226: 24–32.
79. Heymann MA. Control of the pulmonary circulation in the fetus and during the transitional period to air breathing. *Eur. J. Obstet. Gynecol. Reprod. Biol.* 1999; 84: 127–132.

80. Oka M, Homma N, Taraseviciene-Stewart L, Morris KG, Kraskauskas D, Burns N, Voelkel NF, McMurtry IF. Rho kinase-mediated vasoconstriction is important in severe occlusive pulmonary arterial hypertension in rats. *Circ. Res.* 2007; 100: 923–929.
81. Jasińska-Stroschein M, Owczarek J, Łuczak A, Orszulak-Michalak D. The beneficial impact of fasudil and sildenafil on monocrotaline-induced pulmonary hypertension in rats: a hemodynamic and biochemical study. *Pharmacology* 2013; 91: 178–184.
82. Jiang X, Wang Y-F, Zhao Q-H, Jiang R, Wu Y, Peng F-H, Xu X-Q, Wang L, He J, Jing Z-C. Acute hemodynamic response of infused fasudil in patients with pulmonary arterial hypertension: a randomized, controlled, crossover study. *Int. J. Cardiol.* 2014; 177: 61–65.
83. Doggrell SA. Rho-kinase inhibitors show promise in pulmonary hypertension. *Expert Opin. Investig. Drugs* 2005; 14: 1157–1159.

Chapter 9: Discussion

The aims of this thesis were to characterize the SuHx rat model and to evaluate in this model the effects of new treatments on remodeling of the lung vasculature, in particular the intimal layer.

Characterization of the Sugen Hypoxia model

The characterization of the SuHx model, (Chapter 2), led to several new insights into the specifics of this animal model. The hemodynamic changes in the SuHx model are partially reversible upon normoxic re-exposure, through immediate regression of hypoxic vasoconstriction and a gradual normalization of the hematocrit. However, intima remodeling is progressive in the model and culminates into the development of angio-obliterative lesions. Based on these findings, figure 1 shows a hypothetical overview of the evolution of disease in the SuHx model. The transient role of medial hypertrophy in the SuHx model is interesting, because in most other experimental models of pulmonary hypertension, such as the chronic hypoxia (CH) and monocrotaline (MCT) models, medial thickening is considered an important factor in the initiation and maintenance of the phenotype. Many interventions to prevent or reverse media remodeling have been shown effective in CH and MCT, in particular interruption of serotonin signaling. Serotonin has been thought to play a key role in the pathogenesis in PAH by regulating pulmonary vascular tone and the mitogenic properties of the medial layer. Genetic knock-down of serotonin signaling was shown to prevent hypoxic pulmonary vascular remodeling in mice. Altered serotonin signaling was implicated in two PAH outbreaks caused by the administration of serotonin re-uptake inhibitors Aminorex (Menocil©) and fenfluramine (Ponderal©) [1–3]. Surprisingly, in chapter 3 we showed that knock-out of the serotonin transporter did not prevent the induction of angio-obliterative intima remodeling in the SuHx model (Chapter 3). This finding suggests that while upregulated serotonin is perhaps sufficient, it is not required to induce pulmonary hypertension.

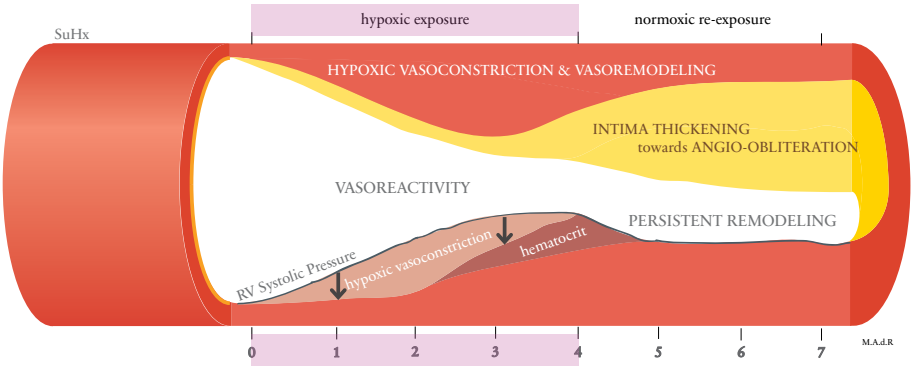

Figure 1: *The results of the characterization of the Sugen hypoxia (SuHx) protocol is visualized in this schematic overview. The 'vessel' shows both histological remodeling of the vessel wall (upper part) and Right Ventricular (RV) Systolic Pressure response, which is influenced by reversibility of acute hypoxic vasoconstriction and the normalization of hematocrit upon normoxic re-exposure [4].*

At this point, it is difficult to say whether or not media remodeling is required at all for the development of pulmonary hypertension in the SuHx model. It could be postulated that in the absence of the serotonin transporter, hypoxia exerts its effects on the vascular media via other mediators than serotonin. Alternatively, the role of hypoxia as a second hit in the SuHx model could involve other mechanisms than media remodeling. To further study the role of hypoxia in the SuHx model, we studied its substitution by increased blood flow/shear stress via a left pneumonectomy in Chapter 4, developing the so-called SuPNx model. A loss of vascular bed after pneumonectomy is assumed to result in an increase in blood flow velocity and elevated shear stress and this has been the rationale for developing experimental models combining pneumonectomy with subcutaneous administration of monocrotaline. This model, together with a model of combined aortocaval shunting and pneumonectomy, is sufficient to induce angio-obliterative intima remodeling [5–8]. Indeed, we were able to reproduce a similar model combining Sugen administration with pneumonectomy. It is possible that increased shear stress on endothelial cells is the common denominator in all these experimental PH models. The role of hypoxia in the SUHx model may be simply to reduce the inner diameter of the small pulmonary vessels (through hypoxic vasoconstriction), thereby forcing an unchanged flow through narrowed vessels

and increasing shear stress. High blood flow and shear stress make endothelial cells (EC) prone to endothelial dysfunction, hyperproliferation and disobedience to the "law of the monolayer" [9–12]. It can be hypothesized that increased blood flow velocity and shear stress are important mediators in the disease progression of experimental and human PAH.

The characterization of the SuHx model showed a central role of intimal remodeling, which is paralleled by descriptions of the hyperproliferative endothelial cell in human PAH [13]. Therefore, in the second part of this thesis, several compounds inhibiting endothelial proliferation were tested in the SuHx model. As these compounds may affect the remodeling of the lungs and heart simultaneously, I will also discuss a cardiopulmonary treatment paradox in PAH.

Targeting endothelial dysfunction in the SuHx model

Endothelial dysfunction in PAH leads to a hyperproliferative phenotype of the endothelium and characteristic angio-obliterative lesions in the pulmonary circulation. As the SuHx model features lesions that resemble the angio-obliterative lesions in PAH patients, this animal model is valuable for investigating the treatment effect of compounds inhibiting endothelial proliferation. We choose to hamper proliferation via a treatment acting on epigenetic gene regulation and growth factor receptor signaling. Dependent on the scientific question and the characteristics of the intervention to answer this question, minor adjustments to the SuHx protocol were made.

Gene regulation is regulated by folding and defolding of the DNA by histones [14]. Histone DeACetylase inhibitors (HDACis) are constitutional proteins that deacetylate histones and thereby regulate DNA transcription. Aberrant HDACs hamper cellular differentiation, leading in to proliferation. As these processes are important in hypertrophy and angiogenesis, HDACis are attractive for PAH as they are known to hamper the expression of proliferation, apoptosis and differentiation in several tumors [15–17]. In chapter 5, HDAC Trichostatin A (TSA) showed not to be successful in the SuHx model [18]. A possible explanation for this could be the fact that HDAC activity was already decreased in the MCT and SuHx lung, indicating that remodeling of the pulmonary vasculature does not seem to require a continued increase in HDAC activity [18]. Growth factors such as Vascular Endothelial Growth Factor (VEGF), Platelet Derived Growth Factor

(PDGF) and Fibroblast Growth Factor (FGF) are activating vascular remodeling and are known to be upregulated in human PAH [19]. Tyrosine Kinase Inhibitors (TKI) hampering these growth factor pathways have been a treatment candidate for PAH for several years. Nintedanib, a TKI inhibiting VEGF, PDGF and FGF, has potential as a PAH treatment for its anti-proliferative feature [20–24]. Therefore, in chapter 8, nintedanib was tested in the SuHx model. Treatment of nintedanib resulted in a mild but beneficial attenuation of pulmonary intima remodeling, by hampering the thickening of the pulmonary vascular intimal wall and showed functional improvement of the right ventricle by increased cardiac output, contractility and arterial ventricular coupling. From these two studies we can conclude that pulmonary vascular remodeling in the SuHx model is not regressed by gene regulation via HDACi TSA and mildly affected by inhibition of cell signaling via VEGF, PDGF and FGF receptor via TKI nintedanib. A better understanding of the pathways involved in endothelial dysfunction will lead to new and more effective approaches to treat PAH [25].

Considering lungs and heart as one functional unit; parallels and treatment paradoxes

The right ventricle in PAH is required to adapt to an increased pulmonary vascular resistance [26, 27]. Because cardiac function is the strongest prognostic parameter in PAH patients [28, 29], meticulous care should be given to improve, or at least conserve, cardiac function, when PAH patients are treated. Many of the signaling pathways that cause angio-obliterative vascular remodeling in the PAH lung, are also invoked in the adaptive response of the pressure overloaded right ventricle [25, 26, 30–33]. This brings the field to an important treatment paradox: drugs that are predicted to be beneficial to the lungs, might be harmful for the right ventricle. To assess the right ventricular in response to such a treatment in an animal model, right ventricular remodeling is preferably induced and maintained independently from any medication induced changes in pulmonary vascular resistance. If a treatment is beneficial in the lungs, mild cardiotoxicity in the heart could be overruled by the beneficial effects in the lungs which affect the heart indirectly [18, 34–36]. The pulmonary artery banding model is superior for right ventricular assessments as it features a mechanical stenosis which gradually increases related to body weight gain. The compounds investigated in this thesis are examples harboring such a treatment paradox. In chapter 5, the treatment paradox of HDACis was discussed [18]. HDACis were reported to be beneficial in the MCT and chronic hypoxia model [34, 37, 38], while in the pulmonary artery banding model, the same HDACis were previously shown to be detrimental to the right ventricle, with increased disposition of connective tissue and hypovascularization [18, 35, 36]. A similar treatment paradox may be at play when it comes to Endothelin-1 Receptor Antagonists (ERA's). ERA's are registered to treat human PAH [32, 39–41]. Despite the beneficial responses in the pulmonary vessel bed, ERA's also inhibit the positive inotropic effects of endothelin-1 and hamper the fetal gene programming of the right ventricle, which program seems required for adequate pressure adaptation. We discuss potential concerns about cardiac function during ERA treatment in chapter 8 [42, 43]. In the process to improve specificity and efficacy of new medications, the direct assessment of right ventricular adaptation in animal models is essential for the development of successful therapies for PAH. Therefore, we assessed in chapter 6 first the right ventricular adaptation during treatment with the TKI BIBF1000, a more toxic chemical analog of nintedanib, and evaluated the treatment potential

of nintedanib for the lungs in the SuHx model in chapter 7. We show that a mild regression of pulmonary vascular remodeling together with improved right ventricular function, which indicates that Nintedanib is safe and potentially effective in human PAH.

Conclusion

In conclusion, the SuHx model was demonstrated to exhibit a partial reversibility after re-exposure to normoxia, due to a normalization of acute reversible hypoxic vasoconstriction. Driven by the temporal response of the media in the evolution of the disease progression in SuHx rats, we explored the influence of the media in the disease progression in the SuHx model. The lack of the serotonin transporter, a key regulator for the pulmonary medial layer, did not influence vascular remodeling in the model. Also, exposure to hypoxia was successfully substituted by flow increasing pneumonectomy, which suggests that, in symphony with SU5416, the increase of blood flow and/or shear stress might be the initiation to pulmonary vascular remodeling.
The treatments tested and evaluated in this thesis are targeting endothelial hyperproliferation via gene regulation and cell signaling, both not leading to normalization of the pulmonary vasculature. Such treatments affect lungs but also the right ventricle. To maintain cardiac function under treatment, right ventricular adaptation should be assessed in animal models by which right ventricular remodeling is not derived from an increased pulmonary vascular resistance.

References:

1. Maclean MR, Dempsie Y. The serotonin hypothesis of pulmonary hypertension revisited. *Adv. Exp. Med. Biol.* 2010; 661: 309–322.
2. Souza R, Humbert M, Sztrymf B, Jaïs X, Yaïci A, Le Pavec J, Parent F, Hervé P, Soubrier F, Sitbon O, Simonneau G. Pulmonary arterial hypertension associated with fenfluramine exposure: report of 109 cases. *Eur. Respir. J.* 2008; 31: 343–348.
3. Thomas M, Ciuclan L, Hussey MJ, Press NJ. Targeting the serotonin pathway for the treatment of pulmonary arterial hypertension. *Pharmacol. Ther.* 2013; 138: 409–417.
4. de Raaf MA, Schalij I, Gomez-Arroyo J, Rol N, Happé C, de Man FS, Vonk-Noordegraaf A, Westerhof N, Voelkel NF, Bogaard HJ. SuHx rat model: partly reversible pulmonary hypertension and progressive intima obstruction. *Eur. Respir. J.* 2014; 44: 160–168.
5. Dorfmüller P, Chaumais M-C, Giannakouli M, Durand-Gasselin I, Raymond N, Fadel E, Mercier O, Charlotte F, Montani D, Simonneau G, Humbert M, Perros F. Increased oxidative stress and severe arterial remodeling induced by permanent high-flow challenge in experimental pulmonary hypertension. *Respir. Res.* 2011; 12: 119.
6. White RJ, Meoli DF, Swarthout RF, Kallop DY, Galaria II, Harvey JL, Miller CM, Blaxall BC, Hall CM, Pierce RA, Cool CD, Taubman MB. Plexiform-like lesions and increased tissue factor expression in a rat model of severe pulmonary arterial hypertension. *Am. J. Physiol. - Lung Cell. Mol. Physiol.* 2007; 293: L583–L590.
7. Dickinson MG, Bartelds B, Molema G, Borgdorff MA, Boersma B, Takens J, Weij M, Wichers P, Sietsma H, Berger RMF. Egr-1 expression during neointimal development in flow-associated pulmonary hypertension. *Am. J. Pathol.* 2011; 179: 2199–2209.
8. Dickinson MG, Bartelds B, Borgdorff MAJ, Berger RMF. The role of disturbed blood flow in the development of pulmonary arterial hypertension: lessons from preclinical animal models. *Am. J. Physiol. - Lung Cell. Mol. Physiol.* 2013; 305: L1–L14.
9. Sakao S, Taraseviciene-Stewart L, Lee JD, Wood K, Cool CD, Voelkel NF. Initial apoptosis is followed by increased proliferation of apoptosis-resistant endothelial cells. *FASEB J. Off. Publ. Fed. Am. Soc. Exp. Biol.* 2005; 19: 1178–1180.
10. Chaumais M-C, Guignabert C, Savale L, Jaïs X, Boucly A, Montani D, Simon-

neau G, Humbert M, Sitbon O. Clinical pharmacology of endothelin receptor antagonists used in the treatment of pulmonary arterial hypertension. *Am. J. Cardiovasc. Drugs Drugs Devices Interv.* 2015; 15: 13–26.
11. Tuder RM, Groves B, Badesch DB, Voelkel NF. Exuberant endothelial cell growth and elements of inflammation are present in plexiform lesions of pulmonary hypertension. *Am. J. Pathol.* 1994; 144: 275.
12. Voelkel NF, Cool C, Lee SD, Wright L, Geraci MW, Tuder RM. Primary pulmonary hypertension between inflammation and cancer. *Chest* 1998; 114: 225S – 230S.
13. Stacher E, Graham BB, Hunt JM, Gandjeva A, Groshong SD, McLaughlin VV, Jessup M, Grizzle WE, Aldred MA, Cool CD, Tuder RM. Modern age pathology of pulmonary arterial hypertension. *Am. J. Respir. Crit. Care Med.* 2012; 186: 261–272.
14. Bernstein BE, Meissner A, Lander ES. The mammalian epigenome. *Cell* 2007; 128: 669–681.
15. Ververis K, Hiong A, Karagiannis TC, Licciardi PV. Histone deacetylase inhibitors (HDACIs): multitargeted anticancer agents. *Biol. Targets Ther.* 2013; 7: 47–60.
16. Ocker M. Deacetylase inhibitors - focus on non-histone targets and effects. *World J. Biol. Chem.* 2010; 1: 55–61.
17. Dobaczewski M, Bujak M, Li N, Gonzalez-Quesada C, Mendoza LH, Wang X-F, Frangogiannis NG. Smad3 signaling critically regulates fibroblast phenotype and function in healing myocardial infarction. *Circ. Res.* 2010; 107: 418–428.
18. De Raaf MA, Hussaini AA, Gomez-Arroyo J, Kraskaukas D, Farkas D, Happé C, Voelkel NF, Bogaard HJ. Histone deacetylase inhibition with trichostatin A does not reverse severe angioproliferative pulmonary hypertension in rats (2013 Grover Conference series). *Pulm. Circ.* 2014; 4: 237–243.
19. Selimovic N, Bergh C-H, Andersson B, Sakiniene E, Carlsten H, Rundqvist B. Growth factors and interleukin-6 across the lung circulation in pulmonary hypertension. *Eur. Respir. J.* 2009; 34: 662–668.
20. Hilberg F, Roth GJ, Krssak M, Kautschitsch S, Sommergruber W, Tontsch-Grunt U, Garin-Chesa P, Bader G, Zoephel A, Quant J, Heckel A, Rettig WJ. BIBF 1120: triple angiokinase inhibitor with sustained receptor blockade and good antitumor efficacy. *Cancer Res.* 2008; 68: 4774–4782.
21. Santos ES, Gomez JE, Raez LE. Targeting angiogenesis from multiple pathways simultaneously: BIBF 1120, an investigational novel triple angiokinase

inhibitor. *Invest. New Drugs* 2012; 30: 1261–1269.
22. Grimminger F, Schermuly RT, Ghofrani HA. Targeting non-malignant disorders with tyrosine kinase inhibitors. *Nat. Rev. Drug Discov.* 2010; 9: 956–970.
23. Wollin L, Maillet I, Quesniaux V, Holweg A, Ryffel B. Antifibrotic and anti-inflammatory activity of the tyrosine kinase inhibitor nintedanib in experimental models of lung fibrosis. *J. Pharmacol. Exp. Ther.* 2014; 349: 209–220.
24. Wollin L, Wex E, Pautsch A, Schnapp G, Hostettler KE, Stowasser S, Kolb M. Mode of action of nintedanib in the treatment of idiopathic pulmonary fibrosis. *Eur. Respir. J.* 2015; 45: 1434–1445.
25. Guignabert C, Tu L, Girerd B, Ricard N, Huertas A, Montani D, Humbert M. New molecular targets of pulmonary vascular remodeling in pulmonary arterial hypertension: importance of endothelial communication. *Chest* 2015; 147: 529–537.
26. Bogaard HJ, Abe K, Vonk Noordegraaf A, Voelkel NF. The Right Ventricle Under Pressure: Cellular and Molecular Mechanisms of Right-Heart Failure in Pulmonary Hypertension. *Chest* 2009; 135: 794–804.
27. Voelkel NF, Bogaard HJ, Gomez-Arroyo J. The need to recognize the pulmonary circulation and the right ventricle as an integrated functional unit: facts and hypotheses (2013 Grover Conference series). *Pulm. Circ.* 2015; 5: 81–89.
28. Mauritz G-J, Kind T, Marcus JT, Bogaard H-J, van de Veerdonk M, Postmus PE, Boonstra A, Westerhof N, Vonk-Noordegraaf A. Progressive changes in right ventricular geometric shortening and long-term survival in pulmonary arterial hypertension. *Chest* 2012; 141: 935–943.
29. D'Alonzo GE, Barst RJ, Ayres SM, Bergofsky EH, Brundage BH, Detre KM, Fishman AP, Goldring RM, Groves BM, Kernis JT, others. Survival in patients with primary pulmonary hypertension. *Ann. Intern. Med.* 1991; 115: 343–349.
30. Rajabi M, Kassiotis C, Razeghi P, Taegtmeyer H. Return to the fetal gene program protects the stressed heart: a strong hypothesis. *Heart Fail. Rev.* 2007; 12: 331–343.
31. Sano M, Minamino T, Toko H, Miyauchi H, Orimo M, Qin Y, Akazawa H, Tateno K, Kayama Y, Harada M, Shimizu I, Asahara T, Hamada H, Tomita S, Molkentin JD, Zou Y, Komuro I. p53-induced inhibition of Hif-1 causes cardiac dysfunction during pressure overload. *Nature* 2007; 446: 444–448.
32. Humbert M, Sitbon O, Simonneau G. Treatment of pulmonary arterial hypertension. *N. Engl. J. Med.* 2004; 351: 1425–1436.
33. Simonneau G, Gatzoulis MA, Adatia I, Celermajer D, Denton C, Ghofrani A, Gomez Sanchez MA, Krishna Kumar R, Landzberg M, Machado RF,

Olschewski H, Robbins IM, Souza R. Updated clinical classification of pulmonary hypertension. *J. Am. Coll. Cardiol.* 2013; 62: D34–D41.

34. Zhao L, Chen C-N, Hajji N, Oliver E, Cotroneo E, Wharton J, Wang D, Li M, McKinsey TA, Stenmark KR, Wilkins MR. Histone deacetylation inhibition in pulmonary hypertension: therapeutic potential of valproic acid and suberoylanilide hydroxamic acid. *Circulation* 2012; 126: 455–467.
35. Bogaard HJ, Mizuno S, Hussaini AAA, Toldo S, Abbate A, Kraskauskas D, Kasper M, Natarajan R, Voelkel NF. Suppression of Histone Deacetylases Worsens Right Ventricular Dysfunction after Pulmonary Artery Banding in Rats. *Am. J. Respir. Crit. Care Med.* 2011; 183: 1402–1410.
36. Bogaard HJ, Mizuno S, Voelkel NF. Letter by bogaard et Al regarding article, "histone deacetylation inhibition in pulmonary hypertension: therapeutic potential of valproic Acid and suberoylanilide hydroxamic Acid." *Circulation* 2013; 127: e539.
37. Cavasin MA, Demos-Davies K, Horn TR, Walker LA, Lemon DD, Birdsey N, Weiser-Evans MCM, Harral J, Irwin DC, Anwar A, Yeager ME, Li M, Watson PA, Nemenoff RA, Buttrick PM, Stenmark KR, McKinsey TA. Selective class I histone deacetylase inhibition suppresses hypoxia-induced cardiopulmonary remodeling through an antiproliferative mechanism. *Circ. Res.* 2012; 110: 739–748.
38. Cho YK, Eom GH, Kee HJ, Kim H-S, Choi W-Y, Nam K-I, Ma JS, Kook H. Sodium valproate, a histone deacetylase inhibitor, but not captopril, prevents right ventricular hypertrophy in rats. *Circ. J. Off. J. Jpn. Circ. Soc.* 2010; 74: 760–770.
39. Rubin LJ, Badesch DB, Barst RJ, Galie N, Black CM, Keogh A, Pulido T, Frost A, Roux S, Leconte I, Landzberg M, Simonneau G. Bosentan therapy for pulmonary arterial hypertension. *N. Engl. J. Med.* 2002; 346: 896–903.
40. Galiè N, Hinderliter AL, Torbicki A, Fourme T, Simonneau G, Pulido T, Espinola-Zavaleta N, Rocchi G, Manes A, Frantz R, Kurzyna M, Nagueh SF, Barst R, Channick R, Dujardin K, Kronenberg A, Leconte I, Rainisio M, Rubin L. Effects of the oral endothelin-receptor antagonist bosentan on echocardiographic and doppler measures in patients with pulmonary arterial hypertension. *J. Am. Coll. Cardiol.* 2003; 41: 1380–1386.
41. D'Alto M. An update on the use of ambrisentan in pulmonary arterial hypertension. *Ther. Adv. Respir. Dis.* 2012; 6: 331–343.
42. Nagendran J, Sutendra G, Paterson I, Champion HC, Webster L, Chiu B, Haromy A, Rebeyka IM, Ross DB, Michelakis ED. Endothelin axis is upreg-

ulated in human and rat right ventricular hypertrophy. *Circ. Res.* 2013; 112: 347–354.

43. de Raaf MA, Beekhuijzen M, Guignabert C, Vonk Noordegraaf A, Bogaard HJ. Endothelin-1 receptor antagonists in fetal development and pulmonary arterial hypertension. *Reprod. Toxicol. Elmsford N* 2015; .

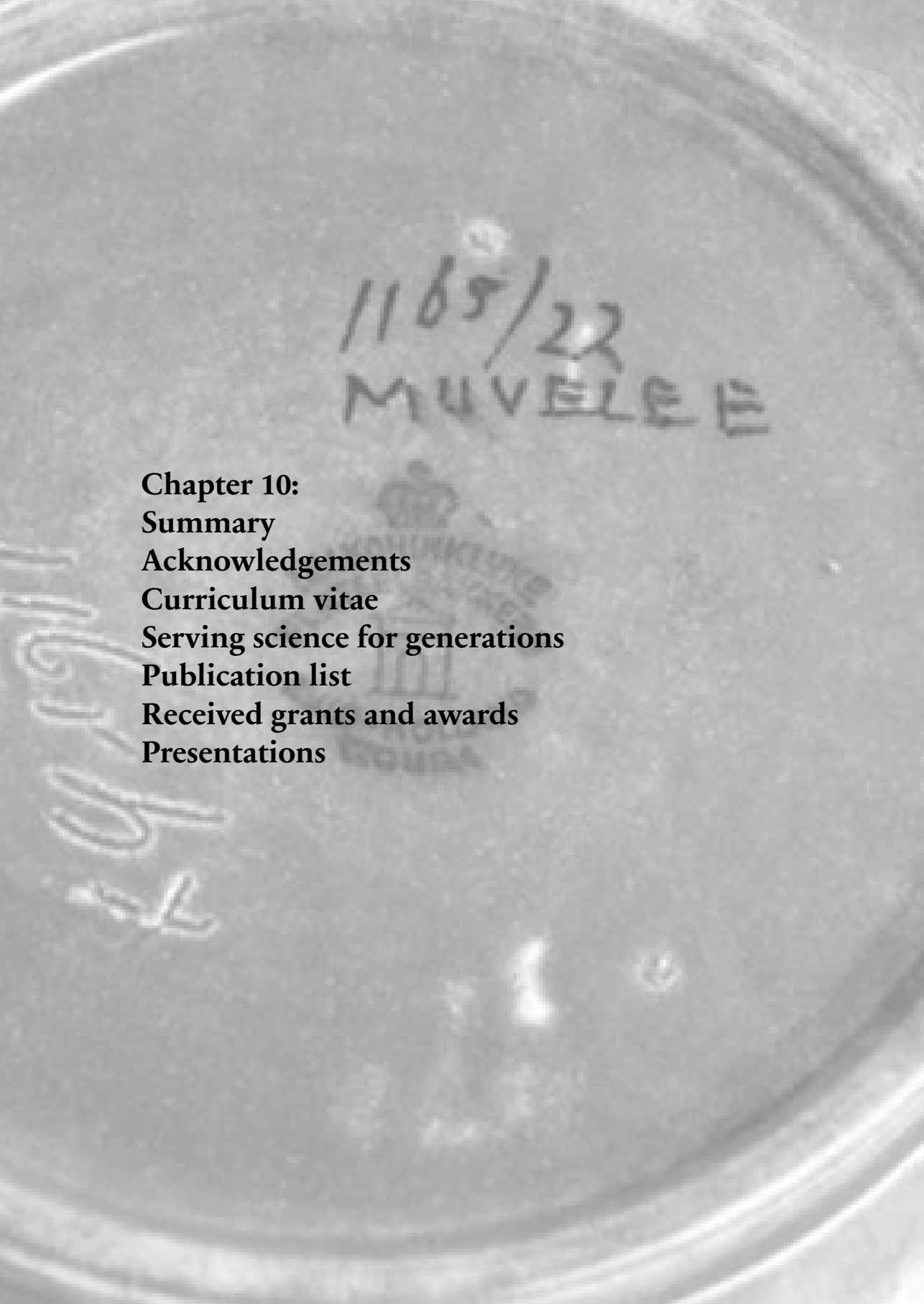

Chapter 10:
Summary
Acknowledgements
Curriculum vitae
Serving science for generations
Publication list
Received grants and awards
Presentations

Summary

Pulmonary Arterial Hypertension is a progressive and devastating disease characterized by dysfunction and remodeling of the pulmonary vasculature, leading to increased pulmonary vascular resistance, compensatory right ventricular remodeling and eventually dilatation and heart failure. To find an effective treatment for Pulmonary Arterial Hypertension, animal models are used to simulate the disease.

In this thesis, Michiel Alexander de Raaf and colleagues describe and characterize the disease progression of the Sugen Hypoxia model, an animal model that simulates Pulmonary Arterial Hypertension and is induced by exposure to VEGF-inhibition and chronic hypoxia. The dependence of an intact serotonin pathway in this animal model was tested and chronic hypoxia was substituted by pneumonectomy to understand the interchangeability of the methodology. Several treatments, as histone deacetylase inhibitors, tyrosine kinase inhibitors and endothelin-1 receptor antagonists were tested and evaluated on their efficacy. As both lungs and heart use mutual pathways for disease progression as well as for compensatory remodeling against the disease, the treatment paradox 'what might be beneficial for the lungs, could harm the right ventricle' was evaluated.

Acknowledgements:

The research that has been written in this thesis has been made possible with acknowledgements to:

to the ones who bring light in life:

Manon de Raaf - Beekhuijzen

Bas Alexander de Raaf

Roos Manon de Raaf

to the staff members of the VU University medical center – Amsterdam:

Harm Jan Bogaard
Anton Vonk Noordegraaf
Nico Westerhof
Frances de Man
Norbert F. Voelkel
Christophe Guignabert

to those who co-authored the publications in this thesis:

Ingrid Schalij
José (Pepe) Gomez-Arroyo
Nina Rol
Chris Happé
Yvette Kroeze
Anthonieke Middelman
Helma de Jong
Chris de Korte
Judith Homberg
Christophe Guignabert
Stefan-Lutz Wollin

to those from the Vrije Universiteit - UPC ;
with special acknowledgements to

Rika van der Laan
Carla Prins
Jerry Middelberg

to those from the VU University medical center - Amsterdam, departments of physiology and pulmonology;
with special acknowledgements to

Emmy Manders
Silvia Rain
Wies Lommers
Willem van der Laarse
Femke Hoevenaars
Pieter Koolwijk
Coen Ottenheijm
Liza Botros

to those from the Virginia Commonwealth University - Richmond; *with special acknowledgements to*

Jose 'Pepe' Gomez Arroyo
Donatas Kraskauskas
Daniela Farkas
Norbert F. Voelkel

to those from the INSERM UMR_S999 - Paris;
with special acknowledgements to

Christophe Guignabert
Ly Tu
Raphael Tuilliet
Carole Phan
Jennifer Bordenave
Morane Le Hiress
Alice Huertas
Marc Humbert

to those from the Radboud University medical center - Nijmegen; *with special acknowledgements to*

Judith Homberg
Anthonieke Middelman
Sjef van Hulten
Rick van der Doelen
Yvet Kroeze
Stefan Janssen

to those who were internship students:

Rosa van Amerongen
Rindi Schutte

to those from the Pulmonary Vascular Research Institute - PVRI Young Council; *with special acknowledgements to*

Djuro Kosanovic
Michael Seimetz
Rebecca Vanderpool
Oleg Pak
Aaron Shefras
Nikki Krol
Ghazwan Butrous
Stephanie Barwick

to those who contributed by sharing knowledge and expertise; *with special acknowledgements to*

Albert Jan Bak
Elisa Meinster
Hans Niessen
Katrien Grünberg
Klaas Kramer
Jos Beekhuijzen
Geerling Langenbach
Henny Ketelaars
Asger Andersen
Andrew Peacock
Tim Lahm
Hilda Moucharrafieh
Joost Lensen
Jeroen van den Wijngaard
Eric Rieux
Stefano Gaburro

to those who supported by motivating and moral encouragement; *with special acknowledgements to*

Lucas Marijnissen
Robert Kreupeling
Esther de Wolff-Kreupeling
Peter Paul de Goeij
Benedetto Grimaldi
Claudia Grimaldi - de Mai
Henk Jan Aarts
Eva Zegger
Marieke van Meeteren
Hans van der Spek

Curriculum vitae

Michiel Alexander de Raaf was born on May 24th, 1984 in Breda, the Netherlands. He grew up in Rijsbergen and graduated as Bachelor in Applied Sciences at Hogeschool Brabant/Avans Hogeschool in 2006. Within that study he performed an internship at 'La Sapienza', university of Rome (Italy), under supervision of Prof. Dr. Paola Ballario, and at a contract research organization NOTOX B.V. in 's-Hertogenbosch (the Netherlands). After graduation Michiel Alexander started working at NOTOX B.V. in the function of data analyst telemetry for Safety Pharmacology and study director assistant focusing on validations and statistics. Being married with Manon de Raaf-Beekhuijzen and father of Bas and Roos, he changed gears in 2010 to perform his master at the University of Amsterdam, where graduated cum laude in 2011 as Master in Science.

Michiel Alexander started as PhD-student at the VU University medical center in 2011 under supervision of Dr. Harm Jan Bogaard, MD and Prof. Dr. Anton Vonk Noordegraaf, MD. The PhD research was based at the VU University (Amsterdam, the Netherlands), Virginia Commonwealth University (Richmond, VA, USA) and Radboud University medical center (Nijmegen, the Netherlands), focusing on the characterization of the Sugen Hypoxia model and assessing treatment potential in this animal model for Pulmonary Arterial Hypertension. As side activity, Michiel Alexander started in 2013 as guest lecturer at the Hogeschool Utrecht and as secretary of the Pulmonary Vascular Research Institute Committee of Young Clinicians and Scientists. He is board member of the telemetry workgroup in The Netherlands.

In 2015 Michiel Alexander received the European Respiratory Society Long Term Research Fellowship grant and started his post-doc at Hospital Marie Lannelongue (Le Plessis-Robinson, France) and University of Paris-Sud (Paris, France) under supervision of Dr. Christophe Guignabert and Prof. Dr. Marc Humbert, MD.

Serving science for generations

In October 1929, the disastrous Stock Market Crash took place. Consequences were also found in Gouda, a city in the region of The Netherlands well known for its Dutch pottery. The royal faience factory fired all its 150 pottery painting artists. To remain the production, and save the company, the new industrial technique of spraying enamel needed to be implemented. Herman Verlee, chemist and chief of the laboratory, implemented the technique and invented the stabilization of new colors in the enamel, as lava red, celadon green and sky blue. With this effort and perseverance, he pushed the company successfully through the Great Depression, and soon thereafter they were able to hire their painting artists again.

79 years later, the economical world collapsed in a new global financial crisis. Inspired by the innovation capacity of his grandfather, Michiel Alexander de Raaf changed gears and transformed from lab technician to medical biologist, whereafter he was able to start his PhD-program.

The chapter covers and lava red color shades used in this thesis are a dedication to Herman Verlee and the familial roots of laboratory profession.

The photos for the chapter covers are courtesy of – and cordially provided by - Bert-Jan Baas and Frits Muller.

PUBLICATION LIST

PEER-REVIEWED PUBLICATIONS

de Raaf MA, Kroeze Y, Middelman A, de Man FS, de Jong H, Vonk-Noordegraaf A, de Korte C, Voelkel NF, Homberg J, Bogaard HJ. Serotonin transporter is not required for the development of severe pulmonary hypertension in the Sugen hypoxia rat model. Am J Physiol Lung Cell Mol Physiol. 2015 Nov 15;309(10):L1164-73. doi: 10.1152/ajplung.00127.2015. Epub 2015 Sep 18.

de Raaf MA, Beekhuijzen M, Guignabert C, Vonk Noordegraaf A, Bogaard HJ. Endothelin-1 receptor antagonists in fetal development and pulmonary arterial hypertension. Reprod Toxicol. 2015 Aug 15;56:45-51.

Gomez-Arroyo J, **de Raaf MA**, Bogaard HJ, Voelkel NF. Chapter 22: Animal Models of Chronic Right Ventricular Stress and Failure The Right Ventricle in Health and Disease, 1 edited by Norbert F. Voelkel, Dietmar Schranz, 09/2014: chapter chapter 22: pages 455-469; Springer New York., ISBN: 978-1-4939-1064-9

De Raaf MA, Schalij I, Gomez-Arroyo J, Rol N, Happé C, de Man FS, e.a. SuHx rat model: partly reversible pulmonary hypertension and progressive intima obstruction. Eur Respir J. july 2014;44(1):160–8.

De Raaf MA, Hussaini AA, Gomez-Arroyo J, Kraskaukas D, Farkas D, Happé C, e.a. Histone deacetylase inhibition with trichostatin A does not reverse severe angioproliferative pulmonary hypertension in rats (2013 Grover Conference series). Pulm Circ. june 2014;4(2):237–43.

Beekhuijzen M, **de Raaf MA**, Zmarowski A, van Otterdijk F, Peter B, Emmen H. The underestimated value of OECD 421 and 422 repro screening studies: Putting it in the right perspective. Reprod Toxicol Elmsford N. september 2014;48:81–7.

Grimaldi B, de Raaf MA, Filetici P, Ottonello S, Ballario P. Agrobacterium mediated gene transfer and enhanced green fluorescent protein visualization in the mycorrhizal ascomycete Tuber borchii: a first step towards truffle genetics. Curr Genet. juli 2005;48(1):69–74. (joined first authorship from bachelor internship)

NON-PEER REVIEWED PUBLICATION

De Raaf MA, Voelkel NF, Bogaard HJ. Advances in understanding of pulmonary arterial hypertension and the evolution of Experimental pulmonary hypertension models. PVRI Chronicle. 02/2015; 2(1):55-61.

Seimetz M, Kosanovic D, Luitel H, Schermuly RT, **de Raaf MA**, Bogaard HJ, Baumgart-Vogt E, Weissmann N, Karnati S. The two faces of antioxidants in pulmonary vascular disease: Focus on COPD PVRI Chronicle. 01/2015; 2(1):18-21.

Received grants and awards:

Pulmonary Vascular Research Institute Committee
of Young Clinicians and Scientists:
certificate of achievement & travel award
as PVRI CYCS secretary & very active membership 2015
travel award to PVRI annual meeting 2016, Roma, Italy

European Respiratory Society:
Long Term Research Fellowship 2015
post-doc at INSERM UMR_S999 – Paris, France

Pulmonary Vascular Research Institute Committee
of Young Clinicians and Scientists:
award in recognition of their outstanding contribution to the PVRI Chronicle and PVRI educational activities in 2015
Guangzhou, China

Pulmonary Vascular Research Institute Committee
of Young Clinicians and Scientists:
certificate of recognition & travel award
as PVRI CYCS secretary & very active membership 2014
travel award to PVRI annual meeting 2015, Guangzhou, China

Bayer cardiovascular pharmacology
travel grant
to Grover conference 2013 - Sedalia, Colorado, USA

Presentations:

Oral presentations:

Workgroup Telemetry of the Netherlands – Wageningen, The Netherlands – 2016
European Teratology Society Annual Meeting – Amsterdam, The Netherlands - 2015
DSI user group meeting – Berlin, Germany - 2013
European Respiratory Society – Munich, Germany - 2014
Thalys meeting – Paris, France - 2014
DSI user group meeting – Berlin, Germany - 2013
Biotechnische dagen – Noordwijk, The Netherlands - 2012

Poster presentations

American Thoracic Society – San Diego, California, USA 2014
PVRI Annual Meeting – Giessen, Germany 2014
Grover Meeting 2013 – Sedalia, Denver, Colorado, USA 2013
American Thoracic Society -Philadelphia, Pennsylvania, USA - 2013
Rembrandt Meeting – Noordwijkerhout, The Netherlands - 2012
Netherlands Respiratory Society – Amsterdam, The Netherlands - 2012
American Heart Scientific Sessions – Los Angeles, California, USA - 2012
American Thoracic Society – San Francisco, California, USA - 2012

Guest lectures:

WIL Research – 's-Hertogenbosch, The Netherlands 2014
Vienna Campus Science Support Facilities – Vienna, Austria - 2014
Radboud University medical center – Nijmegen, The Netherlands - 2014
Radboud University medical center, MUSIC department (Medical UltraSound Imaging Center) – Nijmegen, The Netherlands - 2014
Virginia Commonwealth University – Richmond, Virginia, USA - 2013
Hogeschool Utrecht – Utrecht, The Netherlands - 2013,2014,2015,2016
Boehringer Ingelheim – Bibberach am Rhein, Germany - 2013
Academic Medical Center / University of Amsterdam -Amsterdam, The Netherlands - 2013
Bayer pharma -Wuppertal, Germany – 2013
University Medical Center Groningen, Groningen, The Netherlands - 2012
Hogeschool Avans – Breda, The Netherlands – 2012

Chaired sessions:

Workgroup Telemetry of the Netherlands – Wageningen,
The Netherlands – 2016
PVRI Annual Meeting – Rome, Italy – 2016
(as secretary of the PVRI Committee of Young Clinicians and Scientists)
European Teratology Society Annual Meeting – Amsterdam,
The Netherlands – 2015
DSI usergroup meeting – Leeds, United Kingdom – 2015
PVRI Annual Meeting – Guangzhou, China – 2015
(as secretary of the PVRI Committee of Young Clinicians and Scientists)